Alqahtani, Fulwah Yahya Saleh (2012) Investigation of Galectin-3 interaction with N. meningitidis and its dimerization with laminin receptor. PhD thesis, University of Nottingham.

Investigation of Galectin-3 interaction with N. meningitidis and its dimerization with laminin receptor

Fulwah Yahya Saleh Alqahtani
B.Sc., M.Sc.

Thesis submitted to the University of Nottingham for the degree of Doctor of Philosophy

2012

Molecular Bacteriology and Immunology Group
Institute of Infection, Immunity and Inflammation
Centre for Bimolecular Sciences
School of Molecular Medical Sciences
University of Nottingham

Declaration

With the exception of references to other people's work, which have been duly acknowledged, I do hereby declare that all the work described in this thesis is the result of my own research, and has not been submitted in any form for the award of a higher degree elsewhere.

(.../11/2012)
Fulwah Yahya Saleh Alqahtani
PhD Student
Molecular Bacteriology and Immunology Group
University of Nottingham

Acknowledgements

First of all, thanks to **ALLAH**, the most graceful and most merciful for giving me the great opportunity, strength, patience and guidance to complete this degree despite all difficulties and challenges.

I would like to express my gratitude to my principal supervisor, Prof. Dlawer Ala'Aldeen for giving me this invaluable opportunity to carry out my PhD study in the Molecular Bacteriology and Immunology Group (MBIG) at the University of Nottingham. I do really appreciate Del's outstandable understanding of my needs, careful listening, continuous advice and excellent encouragement, in both group and individual meetings. It inspires me how he clarifies most sophisticated microbiological issues in simple cartoons and scenarios.

It is difficult to overstate my deep and sincere gratitude to my co-supervisor Dr. Jafar Mahdavi, who is most responsible for helping me complete the writing of this thesis as well as the challenging research that lies behind it, for his confidence in me, his endless enthusiasm and his immense patience. Thank you so much Jafar for opening your heart, mind and door for me at any time. It was not only pure science that he taught me; he was a lifetime mentor who widened my scope of knowledge to different aspects of life. Without Jafar's support and active participation in every step in this process, this thesis would not have reached completion.

Del and Jafar gave me generously of their experiences and expertise which will have great impact on my future academic career. Thank you both for all the time

Lastly, but not least, I express my deepest gratitude to my family for the support they provided me throughout this journey. A very special thank you goes out to my father Yahya, my mother Norah, my sister Hajer, my brothers Ibrahim, and Mohammed, my dearest uncle Yahya and the rest of my family members, for whom I dedicate this thesis to. Your unquestionable trust, unconditional love, support, patience, and encouragement have been the driving force behind my hard work throughout my research.

To my grandfather (Saleh), grandmother (Salehah), my aunties (Shareefah and the two Mounirahs) and my cousin (Mohammed) who all died during my staying in Nottingham and they were always with me.

Table of Contents

List of Figures

List of Tables

Abbreviations

AM	Astrocyte medium	**ECM**	Endothelial cell medium
AGC	Astrocyte glial supplement	**EMEM**	Eagle's Minimum Essential Medium
BBB	Blood brain barrier	**FCS**	Foetal calf serum
BHI	Brain heart infusion medium	**gm/mg/μg/ng**	Gram/milligram/microgram/ nanogram
BiFC	Bimolecular fluorescence complementation	**Gal-3**	Galectin-3
BSA	Bovine serum albumin	**GNA**	Genome-derived neisserial antigen
CNS	Central nervous system	**h/min**	Hour/ minute
COS7	Fibroblast-like cell line derived from monkey kidney tissue	**HBMECs**	Human brain microvascular endothelial cells
CO₂	Carbon Dioxide	**His**	Histidine
CRD	Carbohydrate recognition domain	**Ig**	Immunoglobulin
CSF	Cerebrospinal fluid	**IL**	Interleukin
CT	Cycle threshold	**IPTG**	Isopropyl β-D-1 thiogalactopyranoside
Da/kDa	Dalton/kilodalton	**IU/ U/ mU**	International units/ units/milli-units
dH₂O	Distilled water	**l/ml/μl/nl**	Litre/millilitre/microliter/ nanoliter
DNA	Deoxyribonucleic acid	**LB**	Luria broth
DIG-NHS	Digoxigenin-3-0-succinyl-ε-aminocaproic acid-N-hydroxy-succinimide ester	**LOS**	Lipooligosaccharides
DMEM	Dulbecco's modified Eagle's medium	**LPS**	Lipopolysaccharides
dNTP	Deoxyribonucleoside triphosphate	**67 LR**	67 kDa laminin receptor
E. coli	Escherichia coli	**37 LRP**	37 kDa laminin receptor precursor
EcoRI	Restriction enzyme isolated from E. coli	**MC58**	A meningococcal strain belonging to the serogroup B
EDTA	Ethylenediaminetetraacetic acid	**NaCL**	Sodium chloride
ELISA	Enzyme linked immunosorbant assay	**NadA**	Neisseria adhesion A
ECGS	Endothelial cell glial supplement	**NspA**	Neisserial surface protein A

N2a	Neuroblastoma cell lines	**Sec**	The general secretion pathway (Sec pathway) of bacteria
OD	Optical density at specific wavelength	**SOC**	Super optimal broth with catabolite
OMV	Outer membrane vesicle	**SSM**	Slipped strand mispairing
Opa	Colony opacity-associated protein A	**Ser**	Serine
Opc	Opacity protein C	**TBS**	Tris buffered saline
p	Probability value	**TBST**	Tris buffered saline with Tween
PFA	paraformaldehyde	**T4P**	Type 4 pili
PCR	Polymerase chain reaction	**Thr**	Threonine
pH	Unit of acidity/alkalinity	**Tyr**	Tyrosine
PorA	Porin A	**TLR**	Toll-like receptor
PorB	Porin B	**TNF-α**	Tumour necrosis factor-α
PBS	Phosphate buffered saline	**× g**	The centrifugal force applied as multiples of the earth's gravitation
PBS-T	Phosphate buffered saline-Tween	**°C**	Degrees Celsius
pNPP	p-nitrophenyl phosphate	**ΔΔCT method**	Delta delta cycle threshold method
rpm	Revolutions per minute	**ΔCT**	Cycle threshold of target gene –cycle threshold of endogenous gene
SDS-PAGE	Sodium dodecyl sulphate- polyacrylamide gel electrophores	**XhoI**	Restriction enzyme
Ser	Serine		

List of Conference / Oral and poster presentation

Fulwah Alqahtani, **Jafar Mahdavi, Lee Wheldon, Jeroen Stoof, Ann-Beth Jonsson, Hong Sjölinder and DAA Ala'Aldeen (2012).** Host Galectin-3 binds meningococcal PilE and PilQ, and promotes bacterial invasion. Submitted to 18th International Pathogenic Neisseria Conference (IPNC 2012) 9th to 14th September, 2012- Würzburg, Germany.

Fulwah Alqahatni, Jafar Mahdavi and DAA Ala'Aldeen (2011). Heterodimerization of Galectin-3 and laminin receptor; A role in meningococcal infection. Presented as oral presentation at Annual Postgraduate Research Day on 23rd June 2011, organized by School of Molecular Medical Sciences, University of Nottingham, UK.

Fulwah Alqahatni, Jafar Mahdavi and DAA Ala'Aldeen (2011). Meningococcal outer membrane proteins PorA and PilQ induces 67kDa laminin receptor expression in human brain microvascular endothelial cells (HBMECs).Presented as poster at Annual Postgraduate Research Day on 23rd June 2010, organized by School of Molecular Medical Sciences, University of Nottingham, UK.

Abstract

Meningococcal meningitis from the causative organism Neisseria meningitidis is the leading cause of meningitis globally. This bacterium is among a limited number of pathogens that have the propensity to cross the blood brain barrier (BBB) vasculature causing meningitis. It has been recently demonstrated that Neisseria meningitidis targets the laminin receptor (37 LRP/67 LR) on the surface of human brain microvascular endothelial cells, and two meningococcal outer membrane proteins, PorA and PilQ, have been identified as bacterial ligands. Interestingly, this interaction is hypothesized to underlie meningococcal tropism for the central nervous system (CNS). There are two isoforms of laminin receptor; monomeric 37 kDa laminin receptor precursor (37 LRP) and mature 67 kDa laminin receptor (67 LR). The relationship between the 67 LR and its precursor 37 LRP is not completely understood, but previous observations have suggested that 37 LRP can undergo homo- and/or hetero- dimerization with Galectin-3 (Gal-3) to form mature 67 LR. Gal-3 is the only member of the chimera-type group of galectins, and has one C-terminal carbohydrate recognition domain (CRD) that is responsible for binding the ß-galactoside moieties of mono- or oligosaccharides on several host and bacterial molecules, including neisserial lipooligosaccharide (LOS).

To identify the LOS-independent meningococcal ligands that bind Gal-3, binding of lactose liganded Gal-3 and CRD with meningococci was investigated using ELISA assay. Neisseria meningitidis bound lactose liganded Gal-3 significantly more than H. pylori, which is known to bind Gal-3 via LPS. This binding was not inhibited by increasing concentrations of lactose. Also the lactose liganded CRD

of Gal-3 bound meningococci but to a lesser extent than full molecule. Importantly, binding of Gal-3 was conserved among 25 meningococcal clinical isolates tested in the current study. A meningococcal mutant lacking the glycosyltransferase required for chain elongation from the core lipid A-(KDO)2-Hep2 showed reduced binding to lactose-liganded Gal-3, but binding was not abolished indicating that the meningococcal-Gal-3 binding was not entirely LOS-dependant.

Using a re-tagging approach, meningococcal PilQ and PilE proteins were identified as Gal-3 binding ligands. Mutation of the genes encoding either of these two molecules in strain MC58 led to a significant reduction in Gal-3 binding. PilQ is not known to be glycosylated, therefore its interaction with Gal-3 is likely to be protein-mediated. PilE is post-translationally glycosylated and deletion of the pilin glycosylation genes pglC and/or pglL dramatically reduced bacterial-Gal-3 binding.

Given the binding of meningococcal PilQ to 37 LRP/67 LR and Gal-3, this study sought to investigate possible dimerization between 37 LRP and Gal-3 to form 67 LR. Double immunofluorescence staining of endogenous receptors revealed colocalization of 67 LR with its precursor and both of them with Gal-3 in HBMECs, astrocyte and COS7 cells. Moreover, co-expression of 37 LRP and Gal-3 fused to different fluorescent proteins indicated colocalization of these receptors in COS7 cells. Using bimolecular fluorescence complementation (BiFC) assays, the presence of 67 LR in homo- and hetero-dimer forms with Gal-3 has been confirmed in different cell lines. In addition, the recombinant laminin receptor bound Gal-3 and its CRD to comparable level. Further investigation for

Gal-3 and 37 LRP dimerization mechanism revealed that the conserved cysteine (C173A) within the CRD of human Gal-3, which is known to abolish disulphide-mediated dimerization of murine Gal-3, is critical for Gal-3 homo- and hetero-dimerization with 37 LRP, whereas neither of the two cysteines on 37LR (cys148 and cys163) are required for dimerization.

To examine the role of Gal-3 in meningococcal interaction with host cells, the adhesive and invasive capacities of meningococci were compared between Gal-3 transfected and non-transfected neuroblastoma cell line (N2a) cells. Transient expression of Gal-3 in mouse N2a cells significantly enhanced meningococcal invasion when compared with non-transfected cells. Moreover, infection of CD46-expressing transgenic mice with meningococcal strain MC58 significantly increased the expression of Gal-3 and 37 LRP in the brain.

This work also attempts to study whether the 37 LRP/67 LR meningococcal ligands (rPorA, loop 4 of PorA and rPilQ) have any influence on the surface level of 67 LR and Gal-3. As indicated by flow cytometry analysis, recruitments of 67 LR and Gal-3 to the surface of HBMECs were increased in cells incubated with rPilQ, Loop 4 of PorA and more prominently rPorA. To examine these results in more detail, effect of each of these ligands on 37 LRP expression was investigated using qPCR. Loop4 of PorA and rPilQ induced 37 LRP expression significantly more than PBS. Although there was a trend for an increase in 37 LRP expression with treatment with rPorA, the difference was not statistically significant (p = 0.1507). Further investigation in future study for the effect of these bacterial adhesins on Gal-3 gene expression will be of great value.

Collectively, these data revealed the capacity of Gal-3 to target meningococcal PilQ and PilE, as well as the previously known LOS and showed the importance of Gal-3 in the meningococcal-host cell interaction. This interaction may be part of host-cell defence against the organism, and/or, conversely, it may be part of a strategy adopted by the organism to modulate the host response and facilitate its invasion. Remarkably, the current findings also demonstrated the existence of 67 LR as homo- and hetero- dimer with Gal-3. This dimerization of two meningococcal host receptors may help to extend spectrum of their bacterial adhesins which may act cooperatively or synergistically at different stages of infection. Besides, the expression pattern of these receptors may suggest specific receptor repertoire in the BBB which might contribute in meningococcal tropism for the CNS.

1. Chapter 1: General introduction

1.1. Bacterial meningitis

Bacterial meningitis is the most common type of bacterial infection in the central nervous system (CNS) and one of the top ten infectious causes of death worldwide (WHO, 2004).

1.2. Definition

Bacterial meningitis is defined as an inflammation of the meninges, the membranes surrounding the brain and spinal cord. It causes an infection of the pia, the arachnoid and the CSF (cerebro spinal fluid), which results in leptomeningeal inflammation.

1.3. Aetiology

The majority of cases are caused by Streptococcus pneumoniae, Haemophilus influenzae and Neisseria meningitidis (Somand & Meurer, 2009). Other bacteria, such as E. coli K1, group B streptococci and Listeria monocytogenes, can also cause meningitis. Importantly, Neisseria meningitidis is known to be the leading cause of meningitis globally (Kim, 2008).

1.4. Historical background of meningococcal disease

Meningococcal disease, which is known as cerebrospinal fever, was first reported by Vieusseux in 1805 in the city of Geneva (de Souza & Seguro, 2008). After this, several outbreaks of a similar disease were reported in different countries (de Souza & Seguro, 2008). However, it was not until 1887 that the Austrian pathologist Anton Weichselbaum elucidated the aetiological nature of meningococcal disease by demonstrating for the first time that there was a connection between bacteria (at that time it was known as Diplococcus intracellularis meningitidis) and epidemic cerebrospinal meningitidis (de Souza &

Seguro, 2008). Eventually, the name of the bacteria was changed to N. meningitidis, after the German scientist and clinician Alberet Neisser, who discovered the related bacteria, Neisseria gonorrhoeae (the gonococcus) (Ala'Aldeen, 2006).

1.5. Cultural and biochemical characteristics of N. meningitidis

N. meningitidis (meningococcus) is a Gram-negative, oxidase and catalase positive, non-sporing, aflagellate, aerobic diplococcus of approximately 0.8 µm in diameter. Meningococci belong to the genus Neisseria in the family Neisseriaceae. This genus consists of 19 species of commensal Gram-negative bacteria that colonize the mucous membranes of many mammals. 15 of these are human originated species and only two are pathogenic: Neisseria meningitidis and Neisseria gonorrhoeae (Ala'Aldeen, 2006; Lee et al., 2010). The rest of the Neisseria species, such as N. lactamica and N. polysaccharea, are commensal bacteria that may cause disease in immunocompromized patients (Ala'Aldeen, 2006).

N. meningitidis is a fastidious microorganism that requires enriched media to grow in, including blood, chocolate, the modified New York City medium and Muller-Hinton agar (Ala'Aldeen, 2006). Colonies of N. meningitidis are transparent, non-haemolytic, non-pigmented and convex. Optimally, meningococcus grows at 35-37°C in a moist environment containing 5-10% CO_2 at pH 7.0-7.4 (Ala'Aldeen, 2006).

1.6. Genetic characteristics of N. meningitidis

Up to now, the complete genome sequence of N. meningitidis serogroup A (strain Z2491), B (strain MC58) and C (strains FAM18 and 053442) has been reported

(Bentley et al., 2007; Parkhill et al., 2000; Tettelin et al., 2000). An analysis of the sequence has revealed that the average genome size for these strains is 2.2 megabase pair (Mbp) with an average G + C content of 51% (Tettelin et al., 2000).

Meningococcal genomes have several distinguishing characteristics, including the presence of the repetitive DNA element, a high level of genome fluidity and a high capacity for phase variation. Regarding the first characteristic, the repetitive DNA sequences within the meningococcal genome range in size from short (10bp) sequences, which are involved in DNA uptake, to large (39 kb) gene duplications and prophage sequences (Ala'Aldeen, 2006). In addition, the neisserial genome possesses highly repetitive small nucleotide sequences, known as Correia elements, which have transposon-like properties (Siddique et al., 2011).

The second characteristic of the meningococcal genome is its high fluidity, which results from different mechanisms involving natural transformation, horizontal gene transfer, recombination and spontaneous mutation (Schoen et al., 2007). This characteristic enables the bacteria to adapt to different environmental changes. In this context, the chromosomal DNA of MC58 is larger than that of strains Z2491 and FAM18 by almost 100 kb (Schoen et al., 2007). This is due to the acquirement of two horizontal genomic islands of 17.1 kb and 32.6 kb and the duplication of the 30 kb coding sequence (Schoen et al., 2007).

Finally, many of the N. meningitidis genes (more than 60) are subject to a phase variation process (Ala'Aldeen, 2006). In this process, the translational or transcriptional control of the expression reversibly switches the gene expression

on and off or changes the level of gene expression, respectively (Virji, 2009). Phase variation is considered to be one of the mechanisms that is used by meningococcus to evade the immune system (Virji, 2009).

1.7. Epidemiology of meningococcal disease

Despite the availability of effective vaccines, therapeutic choices and the sensitivity of the N. meningitidis to several antibiotics, a significant number of patients either die of the disease or suffer long-term neurological complications such as epilepsy, neurological damage and deafness (Dawson et al., 1999; Grimwood et al., 2000). Out of the estimated 500,000 cases, 50,000 deaths are thought to occur annually worldwide (Girard et al., 2006). N. meningitidis is classified into 13 serogroups based on immune specificity and the structure of capsular polysaccharide; however, only six of them cause invasive disease (serogroups A, B, C, W-135, X and Y) (Stephens et al., 2007). It is also classified into 20 serotypes and 10 serosubtypes based on the outer membrane porins (PorB and PorA), respectively, and into different immunotypes depending on its LPS (lipopolysaccharide) (Frasch et al., 1985). In addition, variations in seven housekeeping genes are used to classify the meningococcal strain into STs (sequence types) using MLST (multi-locus sequence typing) (Brehony et al., 2007).
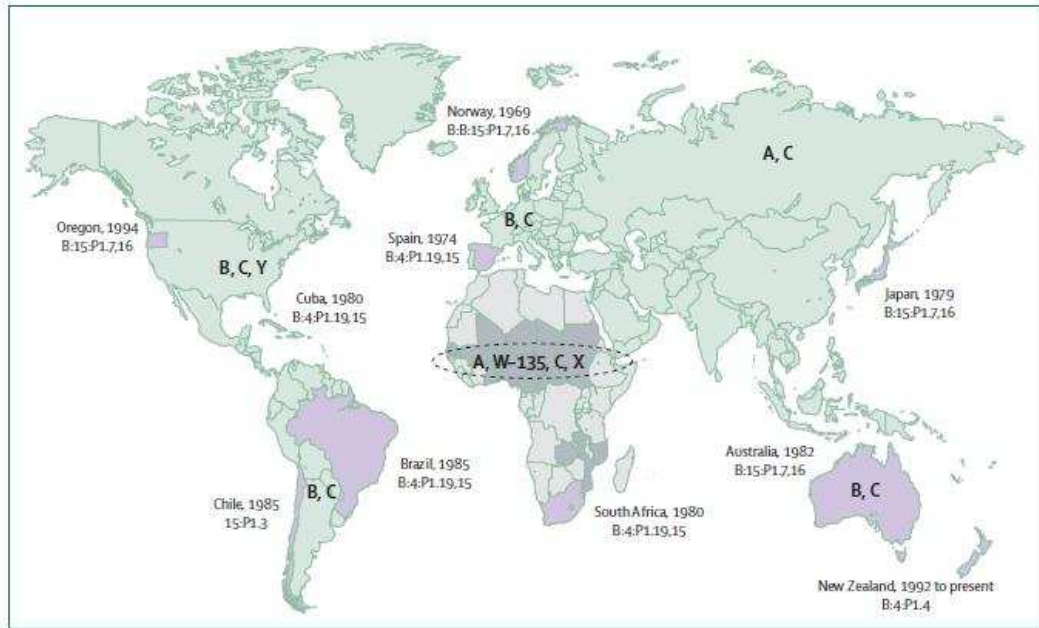
Figure 1.1: Worldwide distribution of invasive meningococcal disease.
Worldwide distribution of major meningococcal serogroups and outbreaks of serogroup B by serotype (shaded in purple). The meningitis belt (dotted line) of Sub-Saharan Africa and other areas of substantial meningococcal disease in Africa are shown. Reproduced from (Stephens et al., 2007).

N. meningitidis serogroup A is the most common cause of meningococcal disease in what is known as the African Meningitis Belt and some areas of Asia (Schoen et al., 2007). The African Meningitis Belt is a region in Africa that expands from Senegal to Ethiopia and it has a high rate of meningococcal disease (Figure 1.1), while the meningococci serogroups B and C are responsible for the majority of cases in Europe and the United States (Stephens et al., 2007). Meningococcal disease caused by serogroup Y has emerged recently in the United States (Schoen et al., 2007). Meningococcal serogroup W135 accounted for large outbreaks among Hajj pilgrims in Saudi Arabia in 2000 and 2001 and also in Burkina Faso in 2002 (Schoen et al., 2007).

1.8. Virulence factors of N. meningitidis

In this section, the most important meningococcal virulence factors that have been utilized by bacteria to develop the infection or evade the immune system will be highlighted and illustrated in a schematic presentation (Figure 1.2).
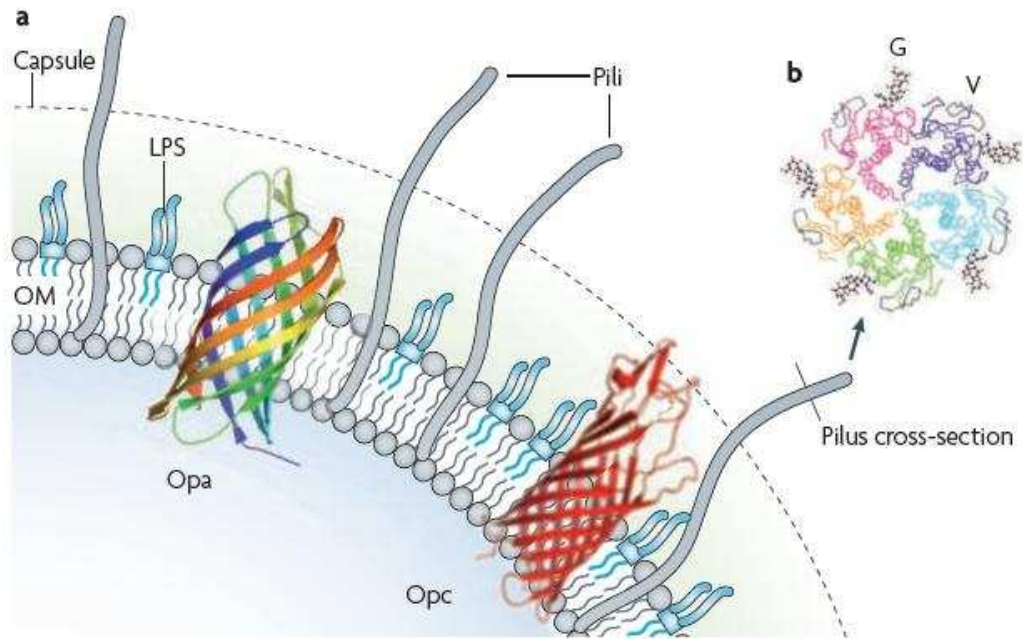
Figure 1.2: Prominent outer membrane components of N. meningitidis that influence bacterial interaction with host cells. (A) Pili traverse the capsule and are the most prominent adhesions of encapsulated N. meningitidis. In addition, the integral outer membrane (OM) adhesions, Opa and Opc, are also known to mediate interactions with specific host cell receptors. LPS may interfere with the adhesion functions of OM proteins, but can also contribute to cellular interactions by interacting with various cellular receptors. (B) A cross-section of a pilus fibre showing that variable domains (V) and glycans (G) as well as other substitutions (not shown) are located externally, whereas the constant domains are buried within the fibre and protected from the host environment. Reproduced from (Virji, 2009).

1.8.1.   Capsule

The polysaccharide capsule is considered to be one of the major virulence factors for N. meningitidis, as the majority of meningococci isolated from patients infected by invasive meningococcal disease are capsulated and express capsules belonging to serogroups A, B, C, Y and W-135 (Stephens et al., 2007). In serogroups B, C, Y and W-135, the capsules' structures are composed of polymers of sialic acid (N-acetylneuraminic acid, NANA) derivatives (Ala'Aldeen, 2006). The composition of sialic acid in meningococcal capsules differs among serogroups; the serogroup B capsule consists of ($\alpha2\rightarrow8$)-linked NANA, the serogroup C capsule consists of ($\alpha2\rightarrow9$)-linked NANA, the serogroup Y capsule consists of alternating D-glucose and NANA and the serogroup W-135 capsule consists of D-galactose and NANA (Ala'Aldeen, 2006). On the other hand, the serogroup A capsule is non-sialyated and consists of N-acetyl mannosamine residues (Ala'Aldeen, 2006). Sialylation of meningococcus capsules provides a protective mechanism for the bacteria against the host immune system, since sialic acid exists on the host cell surface (Hill et al., 2010). In the context of molecular mimicry, only the serogroup B capsule of N. meningitidis is similar in structure to a component of the human NCAM (neural cell-adhesion molecule). Because of this similarity, the meningococcal serogroup B capsule is poorly immunogenic and this is considered to be one of the obstacles for vaccine development (Diaz Romero & Outschoorn, 1994). The meningococcal capsule also has anti-phagocytic and anti-bacteriiadal activities through the prevention of complement activation and antibody recognition, which enables bacterial survival in the blood stream and CSF (Nassif, 1999). It is not only the infection process that the meningococcal capsule is involved in; it also promotes meningococcal

transmission by hindering bacterial attachment to the respiratory mucus membrane, facilitating bacterial spreading from one person to another. It also acts as a hydrating shield that protects bacteria from environmental factors such as desiccation during transmission (Diaz Romero & Outschoorn, 1994).

The cps locus is responsible for meningococcal capsular expression, which consists of the genes required for the biosynthesis and polymerization of the polysaccharide, and surface translocation (Frosch et al., 1989). N. meningitidis has the ability to switch capsule type through the horizontal transfer of the siaD gene in the cps region. This phenomenon has been reported by previous studies where meningococci switch capsules from serogroups B to C, Y to B and C to W-135 (Beddek et al., 2009; Tsang et al., 2005). In addition, meningococcal capsular expression is subject to reversible on/off phase variation. This results from slipped strand mispairing (SSM) and the reversible insertion of mobile elements (Hammerschmidt et al., 1996; Hill et al., 2010).

1.8.2. Lipooligosaccharide (LOS)

As opposed to other Gram-negative bacteria, meningococcal LPS lacks an O-antigen repeating unit; thus it is known as an LOS (Kahler & Stephens, 1998). It is composed of inner and outer oligosaccharide cores attached to lipid A (Figure 1.3) (Jennings et al., 1999). As demonstrated in Figure 1.3, the inner core comprises two heptoses (HepI and HepII) linked to lipid A by one of the two KDOs (2-keto-3-deoxy-d-manno-2-octulosonic acids), and the outer core consists of variable lengths of oligosaccharides extending from the HepI residue to form α and ß chains (Jennings et al., 1999). The outer core extension of meningococcal LOS is regulated by glycosyltransferases that are encoded by lgt genes (Figure

1.3) (Jennings et al., 1999). Meningococcal lipid A and the inner core are embedded in the cell membrane while variable oligosaccharide chains are surface exposed.
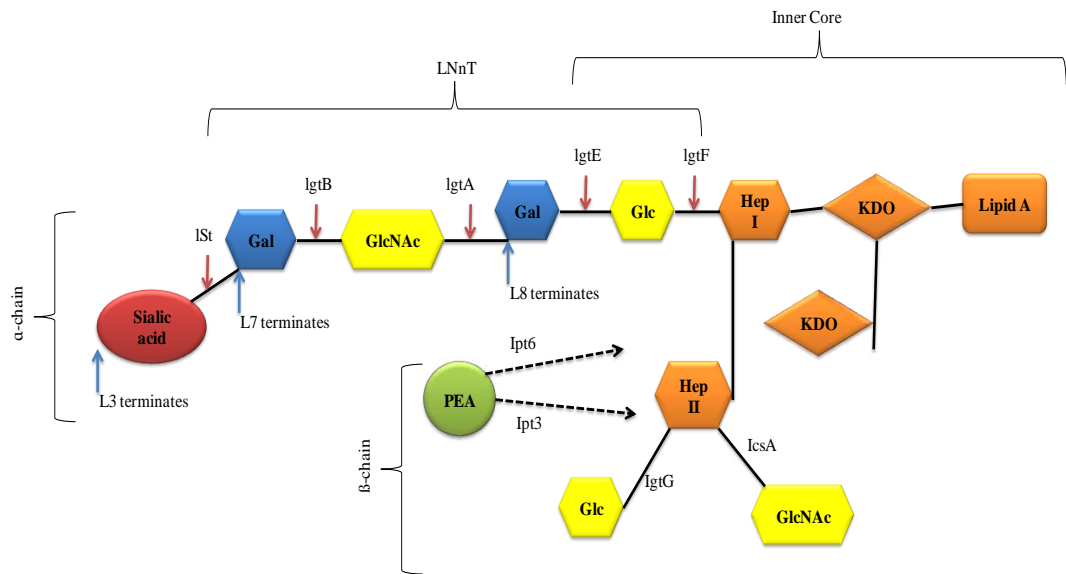
Figure 1.3: Representation of the structure of N. meningitidis LOS. The meningococcal LOS consists of lipid A and inner and outer cores. Variations in both the HepI α-chain extensions (Glc, Gal, GlcNAc, Gal and sialic acid) and the HepII β-chain extensions (GlcNAc, PEA and Glc) determine the different immunotypes of LOS. The α-chain structures of the L3, L7 and L8 immunotypes are shown. The genes encoding the glycosyltransferases responsible for outer core extension are indicated as lgt A, B, E and F (Jennings et al., 1999). The addition of PEA in the indicated position of Hep II is mediated by enzymes encoded by lpt3 and lpt6. Sialylation of terminal galactose in LNnT residue is mediated by the product of the lst gene, the α-2,3-sialyltransferase. The α-chain structures of the L3, L7 and L8 immunotypes are indicated. The residues are as follows: Kdo is 2-keto-3-deoxy octulosonic acid, Hep is L-glycero-D-manno heptose, Glc is glucose, Gal is galactose, GlcNAc is 2-acetamido-2-deoxy-glucose and PEA is phosphoethanolamine. Reproduced from (Hill et al., 2010).

According to the composition of the outer core oligosaccharides, meningococci are classified into 12 immunotypes, designated by L1-L12 (Mandrell & Zollinger, 1977). Some of these immunotypes, such as L2-5, L7 and L9, have a lacto-N-neotetraose motif (LNnT: galactose, N-acetylglucosamine, galactose and glucose) in the chain of variable glycan moiety linked to the Hep I residue (Figure 1.3) (Jennings et al., 1995). LNnT mimics human antigens expressed on human erythrocytes, thus facilitating bacterial evasion from the immune system. Interestingly, invasive meningococcal isolates have LNnT in their LOS but not carriage isolates (Scholten et al., 1994). In addition, LNnT acts as an acceptor for sialic acid; thus some meningococci bearing LNnT in their LOS are subjected to sialylation addition of sialic acid to the terminal galactose residue of LNnT (Gilbert et al., 1996). Importantly, the sialylation of meningococcal LOS enhances bacterial resistance to the complement-mediated bactericidal activity and to opsonophagocytosis by means of human neutrophils (Estabrook et al., 1997; Vogel et al., 1997).

Like the meningococcal capsule, LOS is also subject to phase variation, mainly in the gene encoded enzymes responsible for the extension of sugar chains. For example, immunotype L8 results from phase variation in the lgtA gene (Figure 1.3) (Jennings et al., 1999). Such variations change the antigenic properties of the LOS and allow switching between immunotypes (Hill et al., 2010; Jennings et al., 1999).

Lipid A of meningococcal LOS is responsible for the stimulation of inflammatory cytokine release during sepsis (Brandtzaeg et al., 2001). In addition, an in vitro study has found that LOS is toxic for human endothelial cells (Dunn et al., 1995).

Of interest, the observed LOS toxicity is enhanced by the pili, revealing a cooperative mechanism between the LOS and pili to induce signalling in endothelial cells (Dunn et al., 1995).

1.8.3. Type 4 pili

Neisseria meningitidis has hair-like projections that extend beyond the capsule, known as pili (Strom & Lory, 1993). Meningococcal pili belong to the Type 4 pili (T4p) family that undergo a rapid cycle of extension and retraction. They are thin (4-6 nm in diameter) and flexible and can extend several micrometres in length from the bacterial surface and can also aggregate laterally to form bundles of pili (Mattick, 2002).

Meningococcal pili initiate bacterial adhesion to epithelial and endothelial cells (Pujol et al., 1997). It has been suggested (Kallstrom et al., 1997) that CD46, a membrane bound complement (C') regulator, is the host cell receptor for T4p. However, another study (Kirchner et al., 2005) has reported CD46-independent adhesion , which necessitates further investigation of T4p initial adhesion to the host cell.

There are other multiple functions mediated by neisserial T4p, including twitching motility and DNA uptake during transformation (Mattick, 2002). In addition, it has been shown that the interaction of N. meningitidis T4p with the host cell leads to an induction of the signal transduction pathway, and increases the calcium level (Kallstrom et al., 1998).

Recently, 15 proteins, designated pilC-pilX and ComP, have been identified as being involved in the pilus biogenesis through systemic genetic analyses (Virji,

2009). The structural model of meningococcal pili is based on the reported crystal structure of the related gonococcal (GC) pilus filament (Craig et al., 2006). The biogenesis of the T4p is resolved in four steps: assembly, functional maturation, emergence on the cell surface and counter-retraction (Figure 1.4). In this review, pilus biogenesis will be described briefly (Figure 1.4), and the focus will be on Type IV pili components, which have been reported to be involved in meningococcal-host interaction.
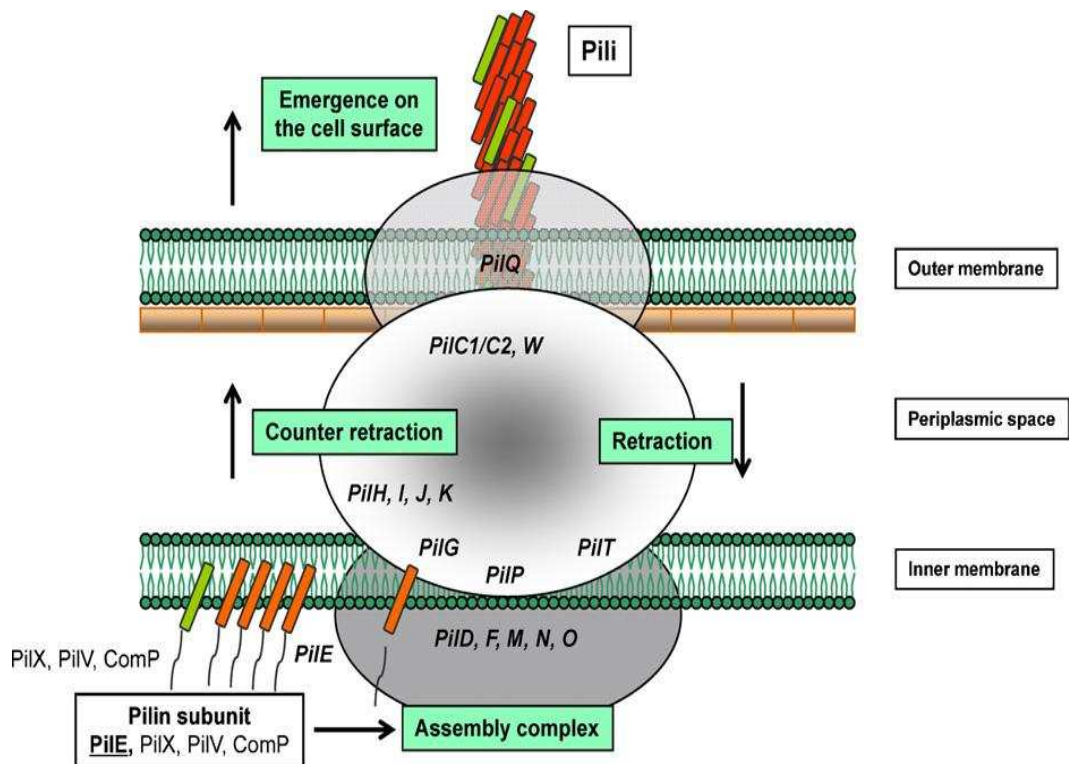
Figure 1.4: Implication of the N. meningitidis pili components in the different steps of T4p biogenesis fibre assembly, functional maturation and counter retraction of fibres, retraction powered by the PilT protein and emergence of the fibres on the cell surface. At the inner membrane-periplasm interface, the pilin subunits (PilE) are assembled from a platform complex (PilD, PilF, PilM, PilN, PilO and PilP) and the growing fibre is translocated to the cell surface via the secretin (PilQ). It has been recently demonstrated that PilP, which co-purifies with the inner membrane,

interacts with PilQ. Two inner membrane ATPases, PilF and PilT, promote pilus elongation and pilus retraction, respectively. Different components are required to counteract pilus retraction (PilC1/C2, PilG, PilH, PilI, PilJ, PilK and PilW). PilC1/C2 and PilW are located in the outer membrane whereas PilG is in the inner membrane. Some components are important for pilus function (PilC1, PilW, PilI, PilJ, PilK, PilX, PilV and ComP). Among the minor pilin components (PilH, PilI, PilJ, PilV, PilX and ComP), PilV, X and ComP are incorporated into the fibre. Adapted from (Carbonnelle et al., 2009).

1.8.3.1.   PilE

PilE is the major pilus subunit, the pilin, which is arranged in a helical configuration to form pilus fibre (Craig et al., 2006). Neisserial pilins are encoded by the pilE gene, which is subject to antigenic variation as a result of a genetic recombination with one or more of the truncated silent pilin genes (pilS) (Segal et al., 1986).

First, pilin is synthesized as a precursor (prepilin) in the cytoplasm, which is inserted into the inner membrane by the Sec machinery. The N-terminal leader sequence (first seven amino acids) is cleaved by the inner membrane prepilin peptidase (PilD) in order to generate the mature pilin (Strom & Lory, 1993) (Figure 1.4). The resulting mature pilin, which is approximately145-160 amino acids in length, is also methylated at the N-terminal phenylalanine by PilD; however, a lack of methylation does not appear to have a dramatic effect on the pilus assembly (Pepe & Lory, 1998). At the inner membrane, the processed PilE subunits are assembled into a helical filament by complex machinery consisting of PilM, PilN, PilO and PilP and extruded from the membrane by the cytoplasmic

ATPase PilF (Carbonnelle et al., 2006). T4p emerge at the surface via outer membrane secretin PilQ. Another cytoplasmic ATPase protein called PilT powers pilus retraction (disassembly) to counteract the pilus extension (assembly) mediated by PilF (Wolfgang et al., 1998) (Figure 1.4). The remainder of the 15 proteins mentioned earlier as being involved in pilus biogenesis play a role after pilus assembly by antagonizing pilus retraction (Carbonnelle et al., 2006).

The crystal structure of highly homologous PilE from N. gonorrhoeae (Figure 1.5) has been resolved (Craig et al., 2006); therefore, it has been predicted that all T4p pilins, including meningococcal pilin, have fairly similar structures. Based on a crystal structure study of GC pilin, PilE protein is elongated and is ladle shaped (Figure 1.4A) (Craig et al., 2006). The PilE structure is composed of a conserved N-terminal α-helix surrounded by β sheets and a hypervariable C-terminal (blue in Figure 1.5). The helix, known as α1, is divided into two parts: the hydrophobic N-terminal half (α1-N) protrudes from the protein and the C-terminal half (α1-C). The α1-C has two faces: a hydrophobic face, which is surrounded by four anti-parallel stranded β sheets to form the globular domain, and a hydrophilic face, which is embedded in the assembled pilus (Craig et al., 2006). The globular head domain is conserved and flanked by two variable regions that are exposed at the surface: the αβ loop connects α1 with the β sheets, and the D-region contains two conserved cysteine residues, which form a disulphide bond, linking the C-terminal to the β sheets. Two post-translational modifications, a phosphethanolamine and a disaccharide, can be seen in the αβ loop of PilE, which will be described below. The disulfide bridge in the D-region is involved in the formation of the surface accessible, variable and immune dominant part of the pilus (Craig et al., 2006; Philippe C morand, 2006; Schaechter, 2009).

It is worth noting that N. meningitidis produces two types of pilins, known as class I and class II pilins (Virji et al., 1989). Class I pilins are recognized by their immunoreactivity to the monoclonal antibody SM1, which is specific for epitopes 49-53 of N. gonorrhoea strain MS11 pilin, whereas Class II pilins are not (Virji et al., 1989).
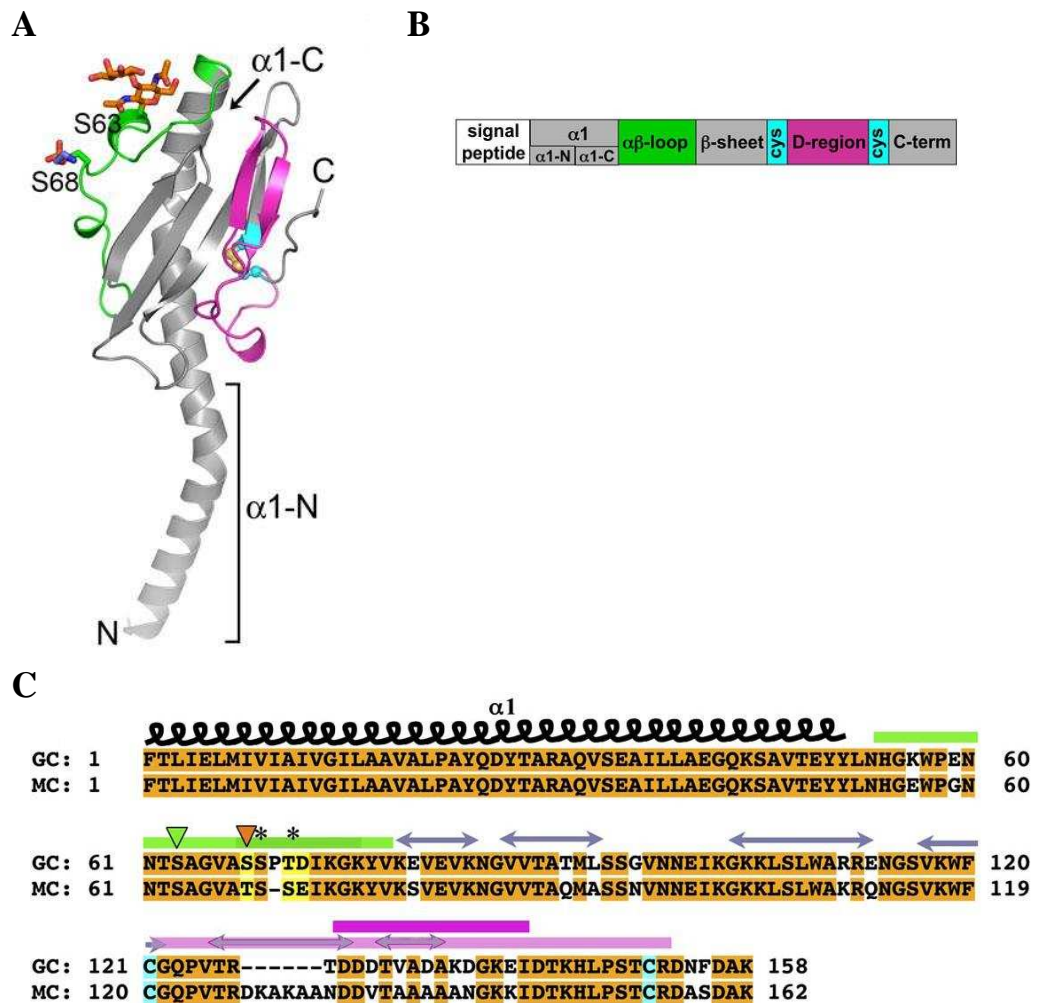
Figure 1.5: Full-length gonococcal (GC) pilin crystal structure and sequence alignment with MC pilin. (A) X-ray crystal structures of full-length N. gonorrhoeae GC pilin. The αß-loops are coloured green and the D-regions are coloured magenta. The conserved regions among the type IV pilins (grey), including the extended N-terminal α-helix α1 (comprised of α1-N and α1-C), the ß sheet and the disulfide-bonded cysteines

(cyan), plus the structurally variable D region (pink) and the αß-loops (green) with the disaccharide Gal-DADDGlc at Ser63 and phosphoethanolamine (PE) at Ser68. (B) Schematic representation of the pilins, indicating the relevant regions and residues. (C) Sequence alignment of GC (N. gonorrhoeae strain C30) and MC (N. meningitidis MC58) pilin with the identical (orange) and conserved (yellow) residues highlighted. The structural features of GC pilin are shown as follows: disulfide cysteines, cyan; Ser63 disaccharide, green arrowhead; Ser68 phosphoethanolamine, orange arrowhead; Ser69 and Thr71 sequence differences from the previous structure, asterisks; ß strands, arrows; αß loop, green bar; and D region with hypervariable loop (pink and magenta bars, respectively). Reproduced from (Craig et al., 2006; Craig & Li, 2008).

Post translational modification of PilE

Meningococcal PilE is known to be post-translationally modified at several serine residues by O-linked glycosylation at position 63 and α-glycerophosphate at position 93 (Stimson et al., 1995; Virji et al., 1993b; Virji, 1997). In addition, substitutions of residue at position 68 with phosphate, phosphoethanolamine or phosphorylcholine have been reported (Hegge et al., 2004; Weiser et al., 1998). Previous studies have suggested that pilin glycosylation is involved in influencing bacterial cellular interaction, perhaps by affecting the agglutination of bacterial pili (Stimson et al., 1995; Virji et al., 1993b). It has also been suggested that pilin glycosylation might promote the secretion of the soluble pilin, called S pilins, since no production of S pilins was observed with the meningococcal strain producing non-glycosylated pilin (Marceau et al., 1998). Secreted pilins are not assembled into pili and could have functions in immune diversion and/or adhesion (Marceau et al., 1998). Glycosylation also can be involved in the interaction of the bacteria with the immune system, as suggested by a previous study (Hamadeh

et al., 1995), where complement mediated lysis was shown to be interfered by a naturally occurring antibody directed against the terminal galactose of meningococcal PilE.

The modification of meningococcal pilin with glycans is regulated by a pgl (6-phosphogluconolactonase) gene cluster, which is initially identified by sequence homology searches (described in Chapter 3). Although the genetics of glycan biosynthesis, modification and transfer to protein have been described, polymorphisms and the phase variation of protein glycosylation enzymes contribute to the observed variations in the glycan structure of PilE (Power et al., 2003).

Over and above the glycosylation at position 63, meningococcal pilin is modified by phosphorylcholine or phosphoethanolamine at position 68. Such modifications have the potential to affect cellular interactions and immune recognition owing to their alteration of the charge in the substituted position of PilE (Virji, 2009). The presence of phosphorylcholine on the bacterial surface may lead to bacterial clearance by promoting their targeting by CRP (C-reactive protein) and anti-phosphorylcholine antibodies. In addition, phosphorylcholine resembles the platelet activating factor, which might enhance bacterial adhesion by binding to the PAF (platelet-activating factor) receptor and neutralizing the host antimicrobial peptide in the nasopharynx (Lysenko et al., 2000). It is interesting to note that, in commensal Neisseria species and H. influenzae, phosphorylcholine is attached to the LPS not the pili (Serino & Virji, 2002; Weiser et al., 1997). Both phosphorylcholine and phosphoethanolamine are added to the Neisserial pilins by a single pilin phosphor-form transferase enzyme (PptA).

Recently, the enzyme responsible for the addition of phosphoglycerol to the meningococcal pilin at serine 93 has been identified, which is the pilin phosphotransferase B (PptB) (Chamot-Rooke et al., 2011). Interestingly, the expression of PptB is found to be upregulated during the attachment of meningococci to the host cells, which increases the addition of phosphoglycerol to PilE and leads to the separation of the bundled pili into single strands (Chamot-Rooke et al., 2011). Such an increase in pilin modifications results in a loss of bacterial aggregation and allows bacterial migration across the host cells and dissemination to other hosts (Chamot-Rooke et al., 2011).

1.8.3.2.   PilQ

The PilQ secretin is required for the extrusion and retraction of N. meningitidis T4p (Carbonnelle et al., 2006; Drake & Koomey, 1995). It is a member of the secretin family of outer membrane proteins with conserved C-terminals that are involved in type II secretion, including type IV pilus biogenesis and type III secretion (Genin & Boucher, 1994). PilQ forms a multimeric ring-like structure as revealed by the transmission electron microscopy (TEM) examination of purified protein (Collins et al., 2004; Frye et al., 2006). PilQ secretin oligmer is composed of 12 identical monomers, forming pores through which pilus are extruded (Collins et al., 2004; Frye et al., 2006). Three features distinguish meningococcal PilQ from other bacterial secretins: its abundance in the outer membrane, the sole secretin in N. meningitidis and the presence of an octapeptide repeat PAKQQAAA, called a small basic repeat (SBR), in its N- terminal (Tonjum et al., 1998).

In a recent study, meningococcal PilQ has been identified as an adhesin for laminin receptor 37 LRP/67 LR (Orihuela et al., 2009).

1.8.3.3. PilC

It has been suggested that meningococcal PilC is located at the tip of T4p (Rudel et al., 1995). The PilC protein plays a crucial role in pilus expression on the bacterial surface, transformation competence and adhesion to human cells (Nassif et al., 1994). Two PilC variants, known as $PilC_1$ and $PilC_2$, have been found to be expressed by meningococci (Jonsson et al., 1995). Although both variants of PilC mediate bacterial piliation and transformation competence only $PilC_1$ is found to be involved in bacterial adhesion to endothelial and epithelial cells (Nassif et al., 1994; Ryll et al., 1997). In contrast, a recent study reported by Morand et al. (2009) showed that $PilC_2$ also mediates meningococcal adhesion; however, both versions of PilC display different effects on the host cells (Morand et al., 2009).

1.8.3.4. Prepilin-like proteins

The major subunit of T4p, PilE, has a hydrophobic N-terminal, which is involved in the polymerization of the pilin subunit to form T4p fibre, as mentioned earlier. There are seven proteins in pathogenic Neisseria, which share the same N-terminal domain of PilE and are termed prepilin-like proteins: PilH, PilI, PilJ, PilK, ComP, PilV and PilX (Koomey, 1995). Among the prepilin-like proteins' ComP, PilV and PilX, which have canonical PilD cleavage motifs and mature lengths similar to PilE, play a role in T4p related function but not directly in pilus biogenesis. ComP was the first pre-pilin protein to be identified and it is important for DNA transformation (Wolfgang et al., 1999). PilV is involved in the modulation of bacterial adhesion to epithelial cells (Winther-Larsen et al.,

2001). Based on the fact that both PilC and PilV can be copurified with T4p and that purified T4p from the PilV null mutant reduces the level of PilC, it has been suggested that the role of PilV in adhesion is mediated via the functional display of PilC in the pilus (Philippe C morand, 2006; Winther-Larsen et al., 2001). Recently, PilV has been shown to be involved in meningococcal resistance to shear stress forces through the induction of cholesterol recruitment to form cortical plaques in the endothelial cells (Mikaty et al., 2009). PilV also antagonizes ComP transformation competence and modulates the level of phosphorylcholine or phosphoethanolamine in the pili (Aas et al., 2002; Hegge et al., 2004).

Meningococcal PilX is necessary for bacterial aggregation and adhesion (Helaine et al., 2005). The abolition of PilX leads to a loss of bacterial autoaggregation ability, which subsequently affects bacterial adhesion to the host cell.

1.8.4. Major outer membrane proteins

1.8.4.1. PorA and PorB

Two distinct porins, PorA (class 1 protein) and PorB (class 2 or class 3 protein) are expressed by N. meningitidis. Porins are β-barrel proteins that assemble into trimer forming pores in the bacterial outer membrane. These pores regulate the exchange of ions between the bacteria and the surrounding environment. PorA is approximately a 45 kDa protein, highly cation-selective and composed of 16 transmembrane β-strands and 8 surface-exposed loops (van der Ley et al., 1991). Some variability of PorA sequence has been shown among meningococcal strains, mainly owing to the surface-exposed loops 1 and 4 (variable regions) (van der Ley et al., 1991). PorB is expressed as PorB1 (~41 kDa) or PorB2 (~38 kDa), the

expression of which is mutually exclusive and anion-selective and has a similar transmembrame loop structure to that of PorA (Minetti et al., 1997; Minetti et al., 1998). Meningococcal PorB2 and PorB3 show sequence similarity with N. gonorrhoeae Por1B and Por1A, respectively (Derrick et al., 1999). Unlike PorB, there is no homology of PorA expressed in gonococci (Feavers & Maiden, 1998).

Meningococcal PorA has been shown to interact with the complement regulator C4b-binding protein (C4bp), inhibiting complement activation, which subsequently enhances meningococcal serum resistance (Jarva et al., 2005). However, poly sialic acid capsules reduce the C4bp-PorA binding by 50% (Jarva et al., 2005). In addition, the involvement of PorA and PorB in bacterial entry has been suggested through the rearrangement of the cytoskeleton (Nassif et al., 1999). Neisserial porins also are able to stimulate B-cells through TLR2 (toll-like receptor 2) in a MyD88 dependent pattern (Massari et al., 2002). Moreover, meningococcal PorB has been shown to interact with mitochondria and protect host cells from apoptotic stimuli (Massari et al., 2000). Interestingly, laminin receptor 37 LRP/67 LR has been shown to target meningococcal PorA (Orihuela et al., 2009).

1.8.4.2. Opacity proteins

Two types of meningococcal outer-membrane proteins, Opa and Opc, impart an opaque phenotype to agar-grown colonies (Hill et al., 2010). Opa and Opc, initially known as class 5 proteins, have similar molecular weights (27-31 kDa) but share a very limited sequence homology. Meningococci express three to four Opa proteins, while gonococci possess up to 12 Opa genes (Aho et al., 1991). Opa protein has eight transmembrane domains arranged in β-parallel strands and

four surface-exposed loops. Three of these loops are highly variable within and among different N. meningitidis strains (Malorny et al., 1998). The gene encoding Opa is subjected to phase variation via different mechanisms: SSM, point mutations, insertion and deletion (Aho et al., 1991; Hill et al., 2010; Malorny et al., 1998).

Opc expression only occurs in meningococci and Opc is encoded by a single opcA gene (Zhu et al., 1999). The expression of Opc is phase variable through transcriptional regulation (Sarkari et al., 1994). Structurally, Opc is also a b-barallel protein that consists of 10 transmembrane domains producing five surface exposed loops (Zhu et al., 1999).

It is worth noting that the opacity proteins play an important role in meningococcal–host interaction (Hill et al., 2010; Virji, 2009). In this context, Opa binds carcinoembryonic antigen-related cell-adhesion molecules (CEACAMs) family and heparan sulfate proteoglycans (HSPGs) (Virji et al., 1996; Virji et al., 1999). Like Opa proteins, Opc interacts with HSPGs and it also binds the extracellular matrix (ECM), such as fibronectin, vitronectin and integrin (Unkmeir et al., 2002; Virji et al., 1994; Virji et al., 1995).

1.8.5. Minor adhesins of N. meningitidis

There are other minor adhesins that have been recently identified as a result of N. meningitidis genome sequencing, including NadA (Neisserial adhesinA), NhhA (Neisseria hia homologue A), App (adhesion and penetration protein) and MspA (meningococcal serine protease A). NadA belongs to the oligomeric coiled-coil adhesin (OCA) family of adhesins and interacts with human epithelial cells using an as yet unknown receptor (Capecchi et al., 2005). Interestingly, approximately

50% of disease isolates express NadA compared with ∼5% of carriage isolates (Comanducci et al., 2004).

Both NhhA and App are homologous to the autotransporter proteins Hsf/Hia and Hap of H. influenzae, respectively. NhhA is expressed in most meningococcal disease isolates (Pizza et al., 2000). It has been reported that the NhhA mediates a low level of adhesion to epithelial cells, HspGs and laminin (Scarselli et al., 2006). Both pathogenic and commensal Neisseria spp. express App (Serruto et al., 2003). Before App autocleavage, it helps in bacterial colonization and, after cleavage, in bacterial detachment and subsequent spreading (Serruto et al., 2003). MspA is homologous to App, which is expressed by several but not all virulent meningococcal strains, and it is reported to support bacterial adhesion and invasion into epithelial and endothelial cells (Turner et al., 2006).

1.9. Pathogenesis

Various steps in bacteria−host interaction are involved in the development of bacterial meningitis. These consist of adhesion to the host, mucosal colonization of the upper respiratory tract, bacterial invasion of the intravascular space and survival/multiplication in the blood stream, resulting in bacteraemia (Hill et al., 2010; Somand & Meurer, 2009). Pathogens then cross the blood brain barrier (BBB), survive and multiply in the subarachnoid space, which induces host inflammatory responses and pathophysiological changes such as pleocytosis and BBB disruption (Kim, 2008).

1.9.1. Colonization and penetration of the respiratory mucosa

N. meningitidis lives commensally in the nasopharynx, which serves as a reservoir for and source of meningococcal infection. The transmission of meningococci

from one person to another can occur by direct contact or respiratory droplets (Stephens & Farley, 1991). Virtually, meningococci are transmitted as encapsulated bacteria in order to enhance the bacteria's ability to survive outside the host (Diaz Romero & Outschoorn, 1994). Colonization of the upper respiratory mucosal surface by N. meningitidis is the first step in the establishment of a human carrier state and invasive meningococcal disease (Stephens, 2009). To avoid the bacteria being washed by mucous, the firm and fast adhesion of bacteria to mucosal epithelial cells is assumed to be crucial (Hill et al., 2010). Type IV pili (T4p), which extend beyond the capsule, initiate the binding of encapsulated meningococci to non-ciliated epithelial cells (Scheuerpflug et al., 1999). It has been suggested that this initial attachment is mediated by the recognition of PilC by the CD46 receptor on the epithelial cells (Kallstrom et al., 1997). However, CD46-independent adhesion has been reported by another study (Kirchner et al., 2005). For efficient initial attachment, meningococci multiply and auto-aggregate with each other through pilus–pilus (PilX-PilX) interactions on the cell surface, forming tightly associated microcolonies (Merz & So, 2000). After the initial attachment, downregulation of T4p, dispersion of microcolonies and spreading of bacteria on the cell surface as a monolayer take place to initiate closer adhesion (Pujol et al., 1997). Both T4p downregulation and microcolony dispersal have been attributed to ATPase PilT (Pujol et al., 1999). Moreover, the expression of meningococcal capsules is downregulated (Deghmane et al., 2002), allowing intimate adhesion via opacity proteins (Opa and Opc) (Virji, 2009). In addition to opacity proteins, the engagement of other meningococcal adhesins, such as NhhA, App and NadA, may support bacterial colonization and the invasion of a mucosal barrier.

Meningococcal adhesins target host receptors, and Opa interacts with CEACAMs and HSPGs (Virji et al., 1996; Virji et al., 1999); Opc interacts with fibronectin, vitronectin and endothelial integrins (Unkmeir et al., 2002; Virji et al., 1994; Virji et al., 1995); and the receptors of recently identified meningococcal adhesins are not yet determined except for NhhA, which targets laminin and HSPGs (Scarselli et al., 2006). Such intimate adhesion mediated by the interaction of meningococcal adhesins with receptors in epithelial cells can trigger cell-signalling events that lead to meningococcal internalization (Hill et al., 2010; Virji et al., 1994) (Figure 1.6).

Both the antigenic variation of meningococcal surface proteins and invasion of meningococci into the epithelial cells enable the bacteria to evade the host immune system (Hill et al., 2010).
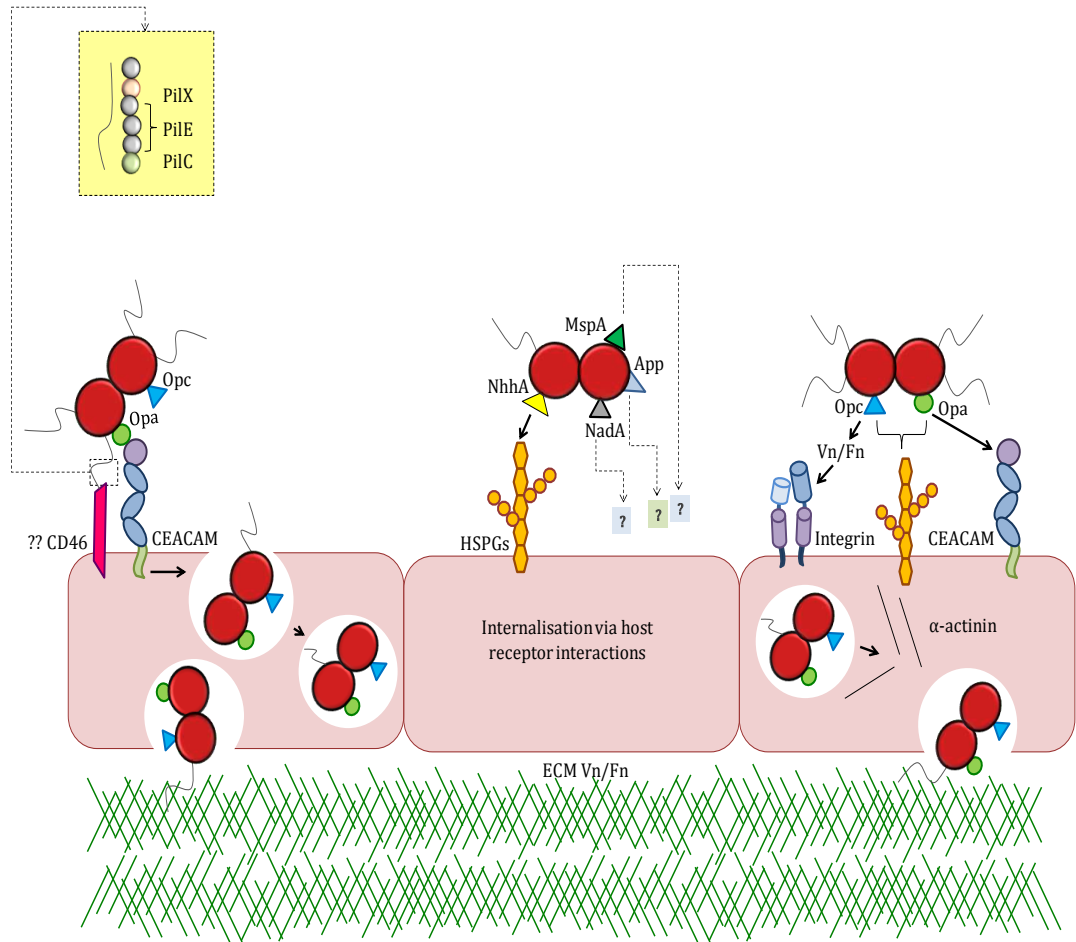
Figure 1.6: Overview of meningococcal interactions at the epithelial barrier of the nasopharynx. T4p mediates the initial attachment with epithelial cells via the interaction of PilC, which is located at the tip of pilus, with CD46. Intimate adhesion is mediated by the interaction of other non-pilus adhesins with their cognate receptors; for example, Opa proteins may bind CEACAM and HSPGs, and Opc proteins can target HSPGs and, via vitronectin and fibronectin, with their integrin receptor. Although some minor adhesins such as NhhA have been shown to interact with HSPGs, the receptors targeted by MspA, App and NadA have not yet been determined. Receptor-adhesin interactions result in meningococcal internalization into epithelial cells by triggering a variety of host cell-signalling mechanisms. Reproduced from (Hill et al., 2010; Trivedi et al., 2011).

1.9.2.   Spread in the bloodstream

After crossing the nasopharyngeal mucosa, meningococci can occasionally enter the blood stream, leading to a strong inflammatory response and activation of the complement and the coagulation cascade (Hill et al., 2010). Meningococcal LOS plays a vital role in the induction of inflammatory responses that lead to sepsis (Braun et al., 2002). A correlation between the amount of circulating LOS with the rate of morbidity and mortality associated with meningococcal bacteremia and meningitis has been shown (Brandtzaeg et al., 1989).

The lipid A portion of meningococcal LOS is the moiety that induces the inflammatory response associated with meningococcal sepsis. Different inflammatory cytokines, including IL-6 and TNF-α (tumour necrosis factor-α), and chemkines such as ROS (reactive oxygen species) and NO are released in response to meningococcal LOS. This induction results in part from the interaction of lipid A moiety with TLR 4 (toll-like receptor 4) (Chow et al., 1999).

In the blood, meningococci adopt different mechanisms to resist being killed by antibodies, complement-mediated lysis and opsonophagocytosis in the blood stream. Two important mechanisms are the N. meningitidis capsule and LOS, since disruption of the genes is involved in LOS and capsule synthesis increases meningococcal sensitivity to serum killing (Chow et al., 1999). Another mechanism is the negative regulation of the complement system, which enhances bacterial survival. In this context, meningococcal fHbp (factor H-binding protein) and PorA have been shown to bind factor H and C4bp, respectively, influencing bacterial resistance in the blood (Jarva et al., 2005; Madico et al., 2006). In

addition, the binding of meningococcal Opc to vitronectin, which inhibits the formation and insertion of a MAC (membrane attack complex) into bacterial membranes, increases bacterial resistance to serum-mediated killing (Virji, 2008). Meningococcal porins may act as an adjuvant, resulting in the stimulation of B-cells through the interaction with TLR2 (toll-like receptor 2) (Massari et al., 2002). Out of the minor adhesins, NadA, has been shown to induce high levels of IL-8 and TNF-α production from human monocytes and macrophages (Franzoso et al., 2008). As a result it is not only meningococcal LOS and capsules but also several proteinaceous adhesins that can modulate the immune response (Hill et al., 2010).

1.9.3.   Traversal of the BBB and meninges invasion

Many pathogens can survive and multiply in the blood stream but only certain bacteria, including Neisseria meningitidis, are able to traverse the BBB (Kim, 2008; Somand & Meurer, 2009). The BBB is a highly specialized structure and acts as a barrier to protect the brain from any microbes and toxins and it controls the passage of molecules into and out of the brain (Kim, 2008). Different cell types that constitute the BBB, among them brain microvascular endothelial cells, represent the first line of defence against pathogens in the CNS. These brain endothelial cells are characterized by their tight junctions and low rates of pinocytosis. The interaction of N. meningitidis with endothelial cells is a crucial step for meningeal invasion. This step is greatly affected by the blood flow rate and shear stress. Post-mortem histological examination of meningitis patients has shown that meningococci adhere to capillaries with a low rate of cerebral blood flow (Mairey et al., 2006). To investigate this in vitro, Mairey, Genovesia et al.

(2006) used a model for meningococcal binding with brain endothelial cells in the presence of shear stress, mimicking the blood stream. The study revealed that meningococcal T4p plays an important role in maintaining bacterial adhesion under a high flow rate. Following bacterial adhesion, N. meningitidis induces the formation of membrane protrusion, filopodia-like structures that help to protect the bacteria against shear stress (Eugene et al., 2002). The development of a cellular projection after the attachment of meningococci to the host cell via T4p stems from the organization of a honeycomb lattice structure underneath the bacterial microcolonies, called the "cortical plaque" (Merz et al., 1999).The formation of the cortical plaque, which contains different structural proteins and membrane receptors, is a two-step process. First, there is the initial recruitment of one or several receptors following T4p mediated adhesion (Coureuil et al., 2012). Second, the activation of these receptors leads to the recruitment of other transmembrane components and the modification of the host cell cytoskeleton, which is also mediated by T4p (Coureuil et al., 2012).

In the context of receptor recruitment or clustering, it has been suggested that the adhesion receptor for meningococci is CD46, as mentioned earlier (Kallstrom et al., 1997). However, subsequent studies have reported CD46-independent adhesion. Therefore, it is possible that one or several cellular receptors in addition to CD46 is/are responsible for the meningococcal T4p interaction with brain endothelial cells (Join-Lambert et al., 2010). Recently, 37 LRP/67 LR has been found to be an adhesion receptor for N. meningitidis (Orihuela et al., 2009). PorA and PilQ have been identified as meningococcal-laminin receptor ligands. In addition, the invasion of uncapsulated N. meningitidis into endothelial cells has been shown to be mediated by the interaction of Opc with integrin via fibronectin

(Unkmeir et al., 2002). However, meningococci are encapsulated in the blood stream; thus the relevance of such a binding in vivo is unclear (Kim, 2008). A recent study (Coureuil et al., 2010) has shown that the β2-adrenergic receptor is recruited after the initial adhesion of N. meningitides to brain endothelial cells. Two meningococcal ligands have been reported for the β2-adrenergic receptor, the major and minor pilin PilE and PilV, respectively (Coureuil et al., 2010). Interestingly, the involvement of the PilV in meningococcal resistance against shear stress has been reported recently. This effect results from the PilV induction of cholesterol recruitment to the cortical plaque in endothelial cells, protecting bacterial microcolonies from the shear stress of the blood stream (Mikaty et al., 2009) (Figure 1.7).

Turning to the second step of the cortical plaque formation, there are several cytoplasmic proteins that have been recruited to this niche, which will be illustrated briefly below. Ezrin and moeisn, members of the ERM (ezrin-radixin-moesin) protein family, are key components in the formation of membrane protrusion (Doulet et al., 2006; Eugene et al., 2002; Lambotin et al., 2005). These proteins control the organization of the cortical actin cytoskeleton via their carboxy terminal F-actin binding sites. Furthermore, ERM proteins bind the cytoplasmic domain of numerous ERM binding transmembrane receptors such as CD44 and ICAM-1 and -2, acting as a linker between the actin cytoskeleton and the plasma membrane. In addition, the activation of cortical actin polymerization has been shown to be associated with cortical plaque formation, resulting in the elongation of membrane protrusions (Coureuil et al., 2012). This stimulation of cortical actin polymerization is due to the activation of RhoA and Cdc42 GTPases and PI3-K/Rac1signalling pathways involved in cortactin recruitment to the

membrane protrusions (Eugene et al., 2002; Lambotin et al., 2005). Cortactin (cortical actin binding protein) is a perinuclear cytoplasmic protein involved in the reorganization of the cell's cortical actin cytoskeleton. Not only is cortactin recruitment required for the formation of membrane protrusions at the meningococcal adhesion site but also its activation by phosphorylation (Coureuil et al., 2012; Join-Lambert et al., 2010). Phosphorylation of the cortactin in meningococcal infection has shown to be mediated by the activation of the host cell tyrosine kinase receptor ErbB2, which subsequently activates src kinase activity (Hoffmann et al., 2001). In addition, activation of the tyrosine kinase Src by direct interaction with βarrestin, which accumulated in the cortical plaque in response to the activation of the β2-adrenergic receptor, also leads to the phosphorylation of cortactin (Coureuil et al., 2010) (Figure 1.7).

It is important to note that it has been reported by Coureuil et al. (2009) that the adhesion of N. meningitidis to endothelial cells recruits several proteins involved in the formation and stabilization of adherens and tight junctions, to the cortical plaque. This effect is attributable to the recruitment of polarity complex proteins, namely PAR3, PAR6 and PKC, in response to meningococcal T4P binding to endothelial cells (Coureuil et al., 2009). Such recruitment of polarity complex proteins leads to the formation of ectopic domain, which has filopodia-like structures and is enriched with several junctional proteins; it is called the ectopic intracellular junctional domain (Coureuil et al., 2009). Several junctional proteins, such as V-cadherin, ZO-1 or claudin-5, are depleted from tight junctions and redistributed underneath bacterial microcolonies, leading to the disruption of the intercellular junctions and enabling meningococcal entry (Coureuil et al., 2009). In addition, the possibility that meningococci can cross the BBB through the

transcytosis route cannot be excluded (Hill et al., 2010). Alternately, damage to the endothelial cells caused by the cytotoxic effect of LOS may facilitate the meningococcal crossing of the BBB (Dunn et al., 1995). Other routes, such as direct inoculation into the cerebrospinal fluid and mechanical spread from the contagious source of infection, are less frequently attributed to microbial entry into the central nervous system (Kim, 2006) (Figure 1.7).

A

1. Paracellular route
   (Opening tight junctions)

Cortical plague

2. Trancytosis ?

B

P120-catenin

PI3K
Rac1

Cdc42
Par3/par6/aPKC

P120-catenin

P120-catenin

? ? ? Adhesion receptor   CD44 ICAM-1, ICAM-2   Tyrosine kinase Src

β2-adrenoreceptor   ErbB2   βarr βarrestin   C Cortactin

P Phosphatase   Adherence junction proteins   Tight junction proteins

P120-catenin   Ezrin   F-actin   P120-catenin
B catenin
ZO-1/2

PI(4,5)P2

Figure 1.7: Formation of the cortical plaque and transmigration of Neisseria meningitidis. (A) Meningococcal T4p mediate the bacterial adhesion to the brain's microvascular endothelial cells using an unknown adhesion receptor. Following the initial bacterial adhesion, T4p lead to the formation of membrane protrusions that result from the organization of a specific cytoplasmic molecular complex called the cortical plaque. The formation of the cortical plaque involves the clustering and activation of different receptors, such as the β2-adrenergic receptor, and triggers their subsequent signalling events. The consequences of these events enable meningococcal transmigration between endothelial cells as result of the damaged barrier or it may also enable bacteria to transmigrate by endocytosis, which is something that is still unknown. (B) Signalling pathways induced by N. meningitidis lead to the formation of the cortical plaque and disruption of the junctional adhesion molecules. T4p mediated adhesion of N. meningitidis to the endothelial cells, including the β2-adrenergic receptor, leads to the formation of membrane protrusions that result from the organization of a specific cytoplasmic molecular complex called the cortical plaque. (1) Endothelial cell protrusions are enriched in ezrin and ezrin binding receptors (CD44, ICAM-1 and -2), which are recruited in a phosphatidylinositol-4, 5-bisphosphate (PI(4,5)P2) dependent manner. (2) Actin polymerization requires the recruitment and phosphorylation of cortactin. The recruitment of cortactin is mediated by the activation of two signalling pathways: the PI3-Kinase/Rac1 GTPase signalling pathway and the Cdc42 GTPases that recruit the Par6/aPKC polarity complex and allow the recruitment of the p120-catenin/Cortactin/Arp2/3 complex beneath the bacterial colonies. N. meningitidis induces phosphorylation of the cortactin by activating the host cell tyrosine kinase receptor ErbB2, which activates downstream the src kinase and β2-adrenergic receptor /β arrestin activated src. (3) Cdc42 mediated activation of Par3/Par6/aPKC elicits the recruitment of adherens and tight junction proteins from pre-existing junctional complexes. Reproduced from (Coureuil et al., 2012; Join-Lambert et al., 2010).

1.10. Clinical manifestations of meningococcal disease

N. meningitidis causes a diverse disease spectrum, which usually occurs within the first week after acquisition (Stephens et al., 2007). The most common types of meningococcal disease are meningitis and septicaemia, which may co-exist (Kirsch et al., 1996).

The progression of meningococcal disease from an initial mild clinical presentation to fulminant disease, multi-organ failure and death may occur within hours (Pace & Pollard, 2012; Stephens et al., 2007). The main factor contributing to the clinical manifestations of meningococcal disease is the extent of the activation of the host immune response, which is affected by bacterial factors such as the level of circulating endotoxin and the bacterial load (Darton et al., 2009), and genetic variation in microbial recognition genes, such as the complement system and inflammatory response (Figure 1.8) (Brouwer et al., 2010; Pace & Pollard, 2012; Wright et al., 2009).
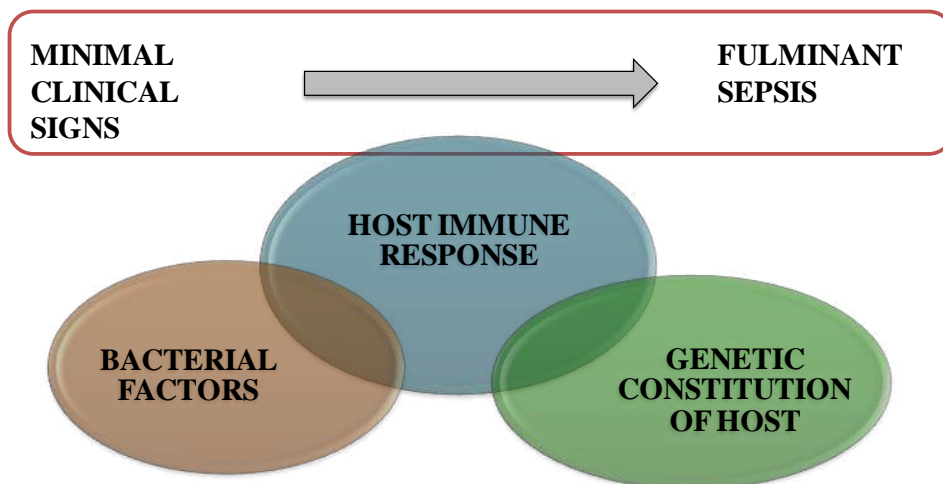
Figure 1.8: Interplay of factors contributing to the manifestations of meningococcal disease. Reproduced from (Pace & Pollard, 2012).

The initial symptoms of meningococcal disease are similar to the symptoms of upper respiratory tract infection, such as pharyngitis, fever, loss of appetite, nausea and vomiting (Thompson et al., 2006). Thus the early symptoms are non-specific and usually misdiagnosed by the clinician. However, late manifestations are specific and suggestive of the development of meningitis or septicaemia (Pace & Pollard, 2012).

Meningitis affects 30-60% of infected individuals and is commonly associated with the following symptoms: severe headache, fever, nausea, vomiting, stiff neck, lethargy, loss of consciousness and photophobia (CDC, 2009; Stephens et al., 2007). The resulting manifestation of meningitis is due to the inflammatory response triggered within the subarachnoid space in response to the meningococcal invasion (Brandtzaeg et al., 1992a).

However, septicaemia represents 20-30% of meningococcal disease and is characterized by lower limb pain, cold peripheries and the appearance of a petechial or purpuric rash (CDC, 2009; Thompson et al., 2006). The release of large amounts of meningococcal LOS in the blood stream activates a massive immune response, leading to damage to the microvascular endothelium (Pathan et al., 2003). In severe cases, microvascular thrombosis, hypoperfusion, ischemia, multiple tissue injury and death might occur (Pathan et al., 2003).

In rare cases meningococci infect other anatomical sites in addition to the meninges and blood stream, causing pneumonia, conjunctivitis, arthritis, pericarditis and myocarditis (Hart & Thomson, 2006; Pace & Pollard, 2012).

1.11. Diagnosis of meningococcal disease

After the initial recognition of the above-mentioned clinical features, a confirmed diagnosis of meningococcal disease is achieved through microbiological testing (Stephens et al., 2007). These microbiological tests rely on obtaining samples of meningococci from the blood, CSF, nasopharyngeal throat, skin lesion and synovial fluid of infected patients (Cartwright & Ala'Aldeen, 1997; Nadel & Kroll, 2007). Cultured bacteria can be further characterized by Gram staining and antibiotic sensitivity tests. Among these diagnostic methods, the determination of CSF protein, glucose and the white cell count (WCC) through a lumbar puncture (if not contraindicated) is the method of choice for the diagnosis of meningococcal disease (Fitch & van de Beek, 2007; Somand & Meurer, 2009). Recently, PCR has been used extensively for the detection of meningococcal DNA in clinical samples (Carrol et al., 2000). Other non-specific laboratory tests, such as WCC and CRP, are commonly used in febrile children to distinguish between invasive bacterial infection from self-limiting viral infection (Bourke et al., 2010).

1.12. Management of meningococcal disease

Parenteral administration of β-lactam antibiotics, such as cephalosporins and penicillins, is the drug treatment of choice for meningococcal disease (Chaudhuri et al., 2008). It is worth noting that the mortality rate from invasive meningococcal disease has been shown to decrease by the prehospital administration of antibiotics in suspected patients (Perea-Milla et al., 2009).

Once a case of meningococcal disease has been confirmed, antibiotic treatment should be given to anyone in close contact with the patient to eradicate the

potential colonization of N. meningitidis (Gardner, 2006). In addition to the effective eradication of the meningococcal carriage, the administration of prophylactic antibiotics has shown to decrease secondary cases among close contacts (Bilukha & Rosenstein, 2005). Antibiotic regimens for prophylaxis against meningococcal disease include rifampin, ciprofloxacin and ceftriaxone (Gardner, 2006).

1.13. Meningococcal vaccine

1.13.1. Capsular polysaccharide vaccine

The meningococcal polysaccharide capsule is an important virulence factor, which renders the bacteria serum resistance, and it is located in the surface of the bacteria. Therefore, capsule based vaccines have been used for the prevention of meningococcal disease caused by serogroups A, C, W-135 and Y for considerable periods of time (Gold et al., 1977). However, although these vaccines produce protective antibody responses against meningococcal disease, they have some limitations. First, these vaccines are poorly immunogenic in children younger than two years of age (Bilukha & Rosenstein, 2005). Second, they do not induce long-term memory (Gotschlich et al., 1969). Third, owing to their short-memory protection repeated doses of capsule based vaccines every three to five years are required, which may attenuate the serum bactericidal antibody response to N. meningitidis, known as hyporesponsiveness (Pollard et al., 2009). More importantly, there is no vaccine against the meningococcal serogroup B capsule, which is the most common serogroup in developed countries, because of its poor immunogenicity.

1.13.2.   Meningococcal conjugate vaccines

The short-lived memory problem of capsule based vaccines necessitates the consideration of other approaches to produce long-term protection against meningococcal disease (Pollard et al., 2009). One of the approaches that have been used in the Haemophilus vaccine, which has shown great efficacy and is based on the conjugation of capsular polysaccharides to a protein carrier to produce what is known as a conjugate vaccine (Stein, 1992). Such conjugation converts polysaccharide from the T-cell independent antigen into a T-cell dependent antigen, resulting in longer memory protection (Bilukha & Rosenstein, 2005). There are several immunogenic protein carriers that have been linked to meningococcal polysaccharides, including tetanus or diphtheria toxoid and CRM 197 (a non-toxin variant of the diphtheria toxin) (Granoff MD, 2008).

In 1999, a conjugate vaccine against serogroup C polysaccharide (MenC) was first introduced into schedules for routine infant immunization in the United Kingdom, leading to a significant reduction in the disease and carriage cases caused by this serogroup (Maiden et al., 2008; Miller et al., 2001). Another conjugate vaccine against serogroup A (MenAfriVac) has been introduced in Africa (Moszynski, 2010). Recently, in the United States of America (USA) and the European Union (EU) two tetravalent conjugate vaccines (A/C/Y/1-135) have been licensed for use; these are called Menactra and Menveo, respectively (Bilukha & Rosenstein, 2005; Gasparini & Panatto, 2011). However, this approach cannot be implicated in the development of a vaccine against N. meningitidis serogroup B (Gasparini & Panatto, 2011).

1.13.3.   Vaccines against meningococcal serogroup B

The similarity between the meningococcal serogoup B capsule and host glycan hinders the generation of a capsule based vaccine as such a similarity may lead to a severe autoimmune disease. Thus other approaches have been adopted to develop vaccines to combat meningococcal serogroup B using non-capsular surface structures. In this context, several licensed non-capsular group B vaccines are based on detergent extracted OMV (outer membrane vesicle) preparation. The OMV is composed of a mixture of LOS and outer membrane proteins, which can be separated from meningococci or isolated as a membrane bleb that is released into the media during bacterial growth (Holst et al., 2009). It is necessary to treat the OMV with detergent in order to extract the LOS and decrease the endotoxin level (Holst et al., 2009). Although meningococcal OMV vaccines are safe and effective, they generate a strain-specific immune response to the protein PorA (Tappero et al., 1999). PorA is the immunodominant antigen in these vesicles and it is highly variable in different strains of N. meningitidis serogroup B (Tappero et al., 1999). This limitation renders meningococcal B OMV vaccines effective only in epidemics caused by a single PorA expressing strain (Tan et al., 2010). In an attempt to increase their limited coverage, OMV vaccines have been prepared from more than one strain (Sandbu et al., 2007). Another approach is to prepare OMV from mutants where the PorA gene is inactivated and other minor outer membrane proteins are overexpressed (Weynants et al., 2007). These minor proteins are usually expressed in low levels, such as transferrin-binding protein A, neisserial surface protein A (NspA) and outer membrane protein 85.

In 2000, a genome based method called "reverse technology" was used to identify the potential novel meningococcal vaccine candidate (Pizza et al., 2000). More

than 600 potential meningococcal antigens have been identified based on the prediction that they will be recognized by a component of the immune system, and only 350 of them can be expressed in E. coli (Rappuoli & Covacci, 2003). These expressed proteins were injected into mice and their ability to produce bactericidal antibodies were evaluated (Rappuoli & Covacci, 2003). Of these proteins, the most promising five proteins, known as genome-derived neisserial antigens (GNAs), were selected for use in the formulation of a multivalent vaccine named rMenB. These GNAs are N. meningitidis adhesin A (NadA, or GNA1994), the factor H-binding protein (GNA1870), GNA2091, GNA2132 (recently renamed the neisserial heparin binding antigen) and GNA1030. This vaccine has been shown to elicit murine bactericidal antibodies against 78% of the selected group B meningococcal strains (Giuliani et al., 2006; Tan et al., 2010). Therefore, the reverse technology concept has been implicated in the current development of a universal vaccine against meningococcal serogroup B, and two promising vaccines are under study at the present time. One of these vaccines, known as Bexsero (4CMenB), is a multicomponent vaccine combined with OMV and is produced by Novartis (Tan et al., 2010). The other vaccine has been developed by Wyeth and contains two protein variants of fHbps (Tan et al., 2010).

1.14. Laminin receptor

In 1983, three different laboratories identified and isolated the laminin binding receptor from different cell lines (Lesot et al., 1983; Nelson et al., 2008; Rao et al., 1983; Terranova et al., 1983). Laminin affinity chromatography was used to extract and purify 67 LR from the cell membrane. The isolated receptor displayed a single protein with an apparent molecular mass of approximately 67 kDa, as

estimated by SDS/PAGE. The receptor binds to laminin with specificity and high affinity; thus it is referred to as the 67 kDa laminin receptor (67 LR) (Malinoff & Wicha, 1983; Rao et al., 1983).

Microsequencing analysis of the peptide obtained from the cyanogen bromide digestion of the purified 67 LR has revealed a unique octapeptide with the sequence MLAREVLR (Wewer et al., 1986). These octapeptides have enabled the identification and isolation of a cDNA clone encoding the protein since the direct sequence of the protein has not been determined, probably due to its blocked N-terminus (Wewer et al., 1986). Northern blot analysis has revealed that the mRNA encoding 67 LR is approximately 1700bp and contains an open reading frame of 888bp (Wewer et al., 1986). The resulting open reading frame encodes a protein of 295 amino acids in length and a calculated molecular mass of approximately 32 kDa. In a western blot, this protein is detected at approximately 37 kDa and is considered to be the precursor for 67 LR; therefore, it is referred to as the 37 kDa laminin receptor precursor (37 LRP) (Nelson et al., 2008).

Homologues of 37 LRP/67 LR are found in all five kingdoms (archaebacteria, eubacteria, fungi, plants and animals). The amino acid sequence of 37 LRP is highly conserved, with at least 98.3% similarity between mouse, bovine and human sequences, and 99% similarity between rat and human sequences (Menard et al., 1997; Nelson et al., 2008). The formation of 67 LR from its precursor 37 LRP has only been described in vertebrates. However, the mechanism by which 37 LRP is converted to 67 LR is not yet understood (described below). It is worth noting that the C-terminal of 37 LRP is highly conserved among vertebrates but very divergent in other organisms (Menard et al., 1997). Therefore, it has been

suggested that the C-terminal of 37 LRP might be involved in the biosynthesis of 67 LR (Menard et al., 1997).

1.14.1. Molecular structure and function

The separation of 67 LR protein from the cell onto the denaturing polyacrylamide gel reveals that it is 67 kDa in size; however, the cDNA of this receptor encodes a protein that is transferred at approximately 37 kDa on SDS/PAGE and this is known as the laminin receptor precursor (37 LRP) (Wewer et al., 1986). The most common reason for such a difference in the molecular mass between 67 LR and 37 LRP might be a posttranslational modification or the formation of homo- and/or heterodimers (Nelson et al., 2008).

The translational protein resulting from 37 LRP cDNA does not have an N-linked glycosylation site or transmembrane domain, which is revealed through the absence of a recognizable signal sequence, at the N-terminus. On the other hand, there is a hydrophobic domain between amino acids 86-101 in the N-terminal region that has been proposed as a transmembrane domain (Rao et al., 1989) (Figure 1.9). This prediction for the transmembrane domain position is consistent with the immunofluorescence staining pattern of 67 LR using a panel of antibodies directed to various parts of the receptor (Castronovo et al., 1991b). However, the recent crystal structure of 37 LRP has suggested that this domain is an integral part of the protein fold and is unlikely to serve as an transmembrane helix (Jamieson et al., 2008). It should be noted that the published crystal structure of the 37 LRP represents amino acid residues from 1 to 220 (Jamieson et al., 2008) (Figure 1.9).

The extracellular C-terminal region contains 70 amino acid segments, which have five repeats of the (D/E)W(S/T) sequence and are characterized by their resistance to trypsin and a high negative charge (Nelson et al., 2008; Sylvie et al., 1997) (Figure 1.9).
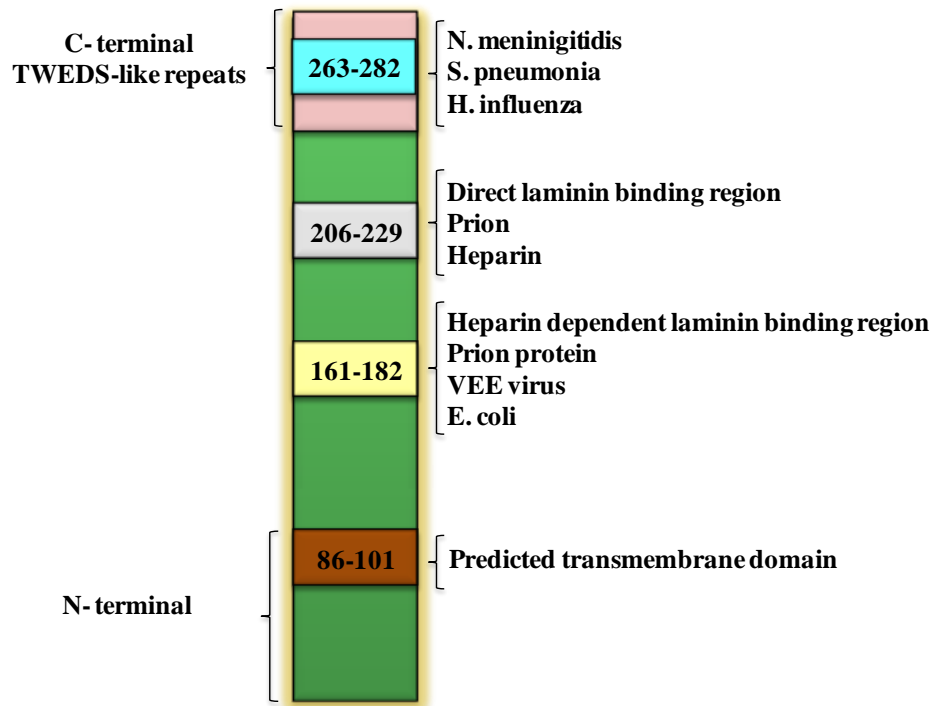
Figure 1.9: Schematic representation of 37 LRP. The 37 LRP is 295 amino acids in length and three functional domains within its C-terminal are exposed to extracellular space. The transmembrane domain is located between amino acids 86 and 101. The binding sites of laminin, heparin, prion, VEE virus and bacteria causing meningitis, including N. meningitidis, are located in the C-terminal of 37 LRP.

The 67 LR is considered to be the mature form of the receptor, which it has been suggested to originate from homo- or heterodimerization of its precursor 37 LRP (Nelson et al., 2008; Sylvie et al., 1997). This receptor-precursor relationship has been revealed by the cross-reactivity of some antibodies raisied against 37 LRP

with the mature form, 67 LR, using the western blot (Rao et al., 1989). In addition, a pulse chase experiment has shown that the radiolabeled 37 LRP is initially detected, followed by the appearance of a similarly labelled 67 kDa protein, which also supports the receptor–precursor relationship (Rao et al., 1989).

The reason for the observed variation in size between the mature (67 LR) and the precursor (37 LRP) forms is not fully understood. Many hypotheses attribute this to the post-translational covalent modification or dimerization of the precursor protein into the homo- or heteroform (Nelson et al., 2008). It has been shown that 37 LRP is modified by post- translational acylation to form the surface exposed form of the receptor (67 LR) (Landowski et al., 1995; Simona Butò, 1998). The involvement of acylation has been revealed by the accumulation of the 37 LRP and either the inhibition or decrease in the formation of the 67 LR after using of fatty acid synthase inhibitor such as cerulenin (Simona Butò, 1998). In addition, the 67 LR has been subjected to methyl-transesterification and GC-MS (gas chromatography-MS) recognizes three covalently bound acylated fatty acids: palmitate, oleate and stearate in the 67 LR (Landowski et al., 1995).

Moreover, there is no effect on the size of protein after O-glycanase, neuraminidase or Endo-F glycosidase treatments (Landowski et al., 1995; Nelson et al., 2008). This indicates that 67 LR maturation involves acylation but not the glycosylation process.

The 37 LRP has been found to be associated with the 40S ribosome and bound to the nucleus; in addition, its function has been found to be a precursor for the cell surface laminin binding receptor 67 LR (Nelson et al., 2008; Sylvie et al., 1997).

In conclusion, lipid modification of the protein through fatty acid acylation might help to stabilize the two dimers of 37 LRP and target them as a 67 LR to surface of the cell membrane (Landowski et al., 1995; Nelson et al., 2008; Simona Butò, 1998). On the other hand, lipids can participate in the conformational changes of the protein or enable protein binding with other components (Landowski et al., 1995).

1.14.2. Dimerization

Several studies have suggested homo- or hetero- dimerization of 67 LR. The evidence supporting each hypothesis will be presented below.

1.14.2.1. Heterodimerization

It has been predicted that 67 LR is a heterodimer that results from dimerization between 37 LRP and the β-galactoside binding lectin known as Galectin-3 (Gal-3) (which is described in detail later on) (Castronovo, 1993). This model was first proposed by Castronovo in 1993 (Figure 1.10). Both Galectin-3 and 67 LR are non-integrin laminin binding proteins. Galectin-3, previously known as HLBP31 (a 31 kDa human laminin-binding protein), binds to the poly-N-acetyl-lactosamine residues of laminin (Castronovo, 1993; Nelson et al., 2008), while the binding of 37 LRP/67 LR to laminin involves the YIGSR, a short sequence from the β1 chain of laminin (Nelson et al., 2008).
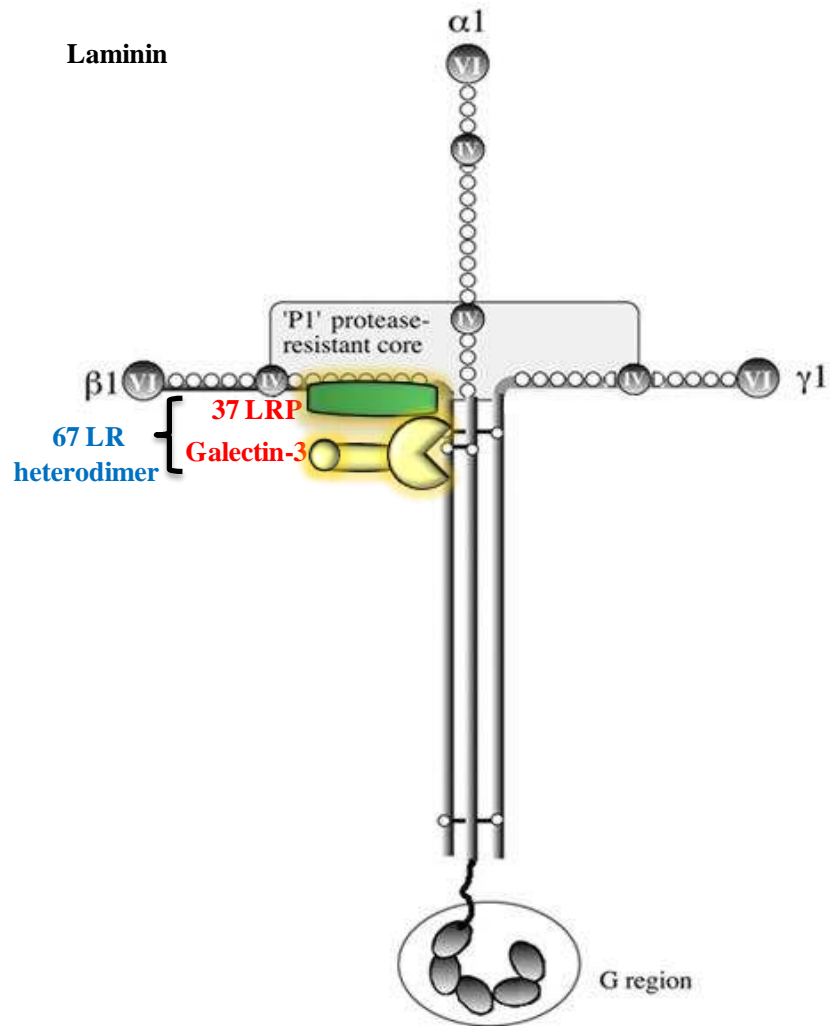
Figure 1.10: Speculative model for the 67 LR. In the proposed model, the 67 LR would be obtained through the association between the 37 LRP and Galectin-3. Laminin is a heterotrimer protein and is composed of three subunits: α-chain, β-chain and γ-chain, found in five, four and three genetic variants, respectively. These chains assemble in various combinations to form at least 15 laminin isoforms. The laminin molecule has a cross-like structure with three short arms and one long arm. Galectin-3 binds the poly-N-acetyl-lactosamine moiety of laminin. Residues 205-229 of 37 LRP/67 LR interact with nanopeptide from the β1 chain of laminin (CDPGYIGSR). In addition, residues 161-180 of 37LRP/ 67 LR (called peptide G) bind laminin.

A proposed heterodimerization model between 37 LRP and Gal-3 is based on several findings. First, it has been shown that both Gal-3 and 67 LR can be eluted from the laminin affinity column by lactose, galactose and N-acetyllactoseamine (Castronovo et al., 1992). Second, antibodies generated against another lectin, known as HLBP14 (human laminin binding protein 14), also immunoreacted with lactose eluted 67 LR and Gal-3 in the western blot (Castronovo et al., 1992). Third, treating laminin with endo-β-galactosidase, an enzyme that disrupts linear type 2 poly-N-acetyllactoseamine, abolishes its binding with 67 LR and Gal-3 (Castronovo et al., 1992). As a result, it has been suggested that the recognition of laminin by 67 LR is dependent on the N-acetyllactoseamine moiety (Castronovo et al., 1992) (Figure 1.10). In 1998, further evidence backing up the 67 LR heterodimer model was reported by Butó et al. In their study the immunoblotting of a detergent-soluble extract from a human carcinoma cell, which has been proved to express 67 LR and 37 LRP, using a polyclonal antibody directed against Galectin-3 recognized a band at 67kDa, which is the same size as the mature 67 LR, but not at 37 kDa (Buto et al., 1998). In conclusion, all these findings indicate that 37 LRP might be associated with Gal-3 to form the 67 LR.

1.14.2.2. Homodimerization

In contrast to the heterodimerization hypothesis, it has been shown that the amino acid composition of 67 LR is found to be identical to that of 37 LRP (Landowski et al., 1995). Another study (Gauczynski et al., 2006) reported that both 67 LR and 37 LRP co-exist on the surface of N2a cells, cells that do not express Gal-3, based on the immunoblotting of the membrane fraction. These studies revealed that Gal-3 or any other lectin is not obligated to surface expression of 67 LR (Nelson et al., 2008).

1.14.3. Function of the laminin receptor

1.14.3.1. Interactions with laminin

It binds extracellular matrix glycoprotein laminin, collagen and elastin, which mediate the receptor role in cell differentiation, movement and growth. The expression of 67 LR is high in cancer and indicates an invasive and aggressive phenotype of tumour (Sylvie et al., 1997).

1.14.3.2. Pathogen receptor

In addition to its role as a membrane receptor for the adhesive basement-membrane protein laminin, 37 LRP/67 LR has been targeted by many pathogens. These infectious agents, including viruses, bacteria, protozoa, cellular proteins and toxins, mainly infect the central nervous system. The Sindbis virus (Wang et al., 1992), Dengue virus (Thepparit & Smith, 2004), adeno-associated virus (Akache et al., 2006), tick-borne encephalitis virus and Venezuelan equine encephalitis virus (Ludwig et al., 1996) have all been found to bind with the 37 LRP/67 LR of the host cell. Moreover, the prion protein PrP that causes prion disease uses 37 LRP/67 LR in its internalization pathway (Gauczynski et al., 2006).

Importantly, bacteria causing meningitis, including E. coli K1, S. pneumonia, H. influenza and N. meningitidis, have been reported to target 37 LRP/67 LR on the surface of HBMECs. All these bacteria interact with specific domains within 37 LRP/67 LR, as shown in Figure 1.9. Interestingly, the binding of the three commonest bacteria causing meningitis, S. pneumonia, H. influenza and N. meningitidis, is thought to be within 263-282 domain, as the adhesion of these pathogens to the host cell is decreased by the antibody targeting this region

(Orihuela et al., 2009). As mentioned earlier, 37 LRP/67 LR helps to initiate bacterial adhesion to the BBB, which is a crucial step in meninges infection. The following bacterial adhesins, pneumococcal CbpA, meningococcal PilQ and PorA and OmpP2 of H. influenzae, are identified as bacterial ligands for 37 LRP/67 LR. Furthermore, E. coli K1 targets the same receptor via its cytotoxic necrotizing factor 1 (CNF1) (Kim et al., 2005). The interaction of CNF1 with 37/67-kDa LR provokes the enrolment of focal adhesion kinase (FAK) and paxillin into the 67LR, leading to bacterial invasion into HBMECs (Kim et al., 2005).

In conclusion, there are various ranges of ligands that share the common feature of infecting the CNS and utilize 37 LRP/67 LR to mediate their pathogenesis. This specific ligand-receptor interaction potentiates 37 LRP/67 LR to become a novel therapeutic target, particularly in the case of limited treatment or a prevention option for such as, bacterial meningitis.

1.15. Galectin-3

Galectins are a group of β-galactoside-binding lectins that share a conserved carbohydrate recognition domain (CRD) (Barondes et al., 1994a). Lectins are glycan binding proteins, in which galectins represent the most widely expressed type of lectins. Fifteen mammalian galectins have been described in the literature so far, 11 of which are expressed in humans (Cooper, 2002). According to the number of CRDs and structural differences, mammalian galectins are classified into three subgroups: proto, chimera and tandem repeat types (Barondes et al., 1994b; Cooper, 2002) (Figure 1.11). Proto-type galectins (galectins 1, 2, 5, 7, 10, 11, 13, 14 and 15) have one CRD while tandem repeat galectins (galectins 4, 6, 8, 9 and 12) consist of two CRDs that are joined by a linker peptide. In the chimera-

type galectins, one CRD is connected by a collagenase-sensitive domain, a region rich in proline, glycine and tyrosine, to the N-terminal. Galectin-3 is the only chimeric member of the family of galectins, and will be the focus of this review.

Prototype galectin
e.g. Galectin-1

Chimera type
Galectin-3

Tandem repeat
e.g. Galectin-9
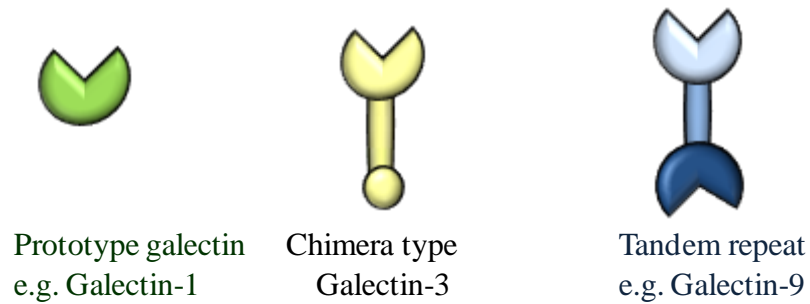
Figure 1.11: Subtypes of the galectin family. Galectins can be divided into three subtypes based on their structure. Schematic examples of prototype galectins: Gal-1 has one carbohydrate recognition domain (CRD); Gal-3 is the only chimeric galectin with one CRD and it is a proline-, glycine- and tyrosine-rich repeating domain and the N-terminus and tandem-repeat galectins (for example, Gal-9) consist of two CRDs joined by a short peptide. Reproduced from (Barondes et al., 1994b).

1.15.1. Discovery

Initially, Galectin-3 was identified as a Mac-2 antigen on the surface of murine macrophage (Ho & Springer, 1982). Later, Galectin-3 was described as CBP-35, a galactoside binding protein in mouse fibroblasts (Roff & Wang, 1983); L-34, a tumour surface lectin in oncogene-transfected rat embryonal fibroblasts (Raz et al., 1987); RL-29 or HL-29, lectins identified in the rat or human lung, respectively (Cerra et al., 1985; Sparrow et al., 1987); IgE-binding protein in rat basophilic leukaemia cells (Liu & Orida, 1984); and LBP, a laminin binding protein in macrophages (Woo et al., 1990). In 1994, all of these proteins were

termed Galectin-3 (Gal-3) with the establishment of the nomenclature of galectins (Barondes et al., 1994a).

1.15.2.   Structure and specificity

Galectin-3 is made up of three distinct structural domains: a short N-terminal domain, a repetitive collagen-like sequence and one CRD at the C-terminal (Barondes et al., 1994b).

The N-terminal domain of Galectin-3 consists of 110-130 amino acids based on the species. It contains multiple homologues repeats of nine amino acids (Pro-Gly-Ala-Tyr-Pro-Gly-X-XX). The N-terminal domain mediates Galectin-3 multimerization and it is sensitive to proteolysis by certain matrix metalloproteinases, MMP-2 and MMP-9 (Ochieng et al., 1998). It has been shown that the first 12 amino acids of Galectin-3 N-terminal, also called the small N-terminal domain, are essential for Galectin-3 secretion and nuclear localization (Gong et al., 1999; Menon & Hughes, 1999). Within the small N-terminal domain, the highly conserved Ser6 residue has been shown to be involved in the anti-apoptotic activity of Galectin-3 (Seetharaman et al., 1998). The N-terminal domain of Galectin-3 lacks glycan binding activity; hence, it is referred to as the non-lectin domain. However, a modelling and mutagenesis analysis study has shown that the N-terminal domain Tyr102 residue is also attributed to the glycan binding activity of Galectin-3 (Barboni et al., 2000).

The C-terminal domain of Galectin-3 is composed of approximately 130 amino acids. This domain is called the lectin-domain since it contains the glycan binding sites and is, therefore, responsible for the glycan binding activity of Galectin-3. The crystal structure of Gal-3 CRD has revealed five and six stranded β sheets

arranged in a β-sandwich (Seetharaman et al., 1998). One of the characteristic features of the Gal-3 CRD sequence is the presence of the NWGR (Asp-Trp-Gly-Arg) motif, which is important for galectin-3 binding to β-galactoside (Akahani et al., 1997). Interestingly, this motif also exists in the B-cell lymphoma 2 Bcl-2 family proteins, and is found to be responsible for the anti-apoptotic activity of Bcl-2 and Galectin-3 (Yang et al., 1996). In addition to glycan binding and anti-apoptotic activities, the NWGR motif participates in the self-association of Gal-3 through the CRD in the absence of carbohydrate ligands (Yang et al., 1998). Close to the NWGR motif, there is a single cysteine residue (Cys 186) that has been shown to be required for the dimerization of murine Gal-3 (Woo et al., 1991).

Galectin-3 binds β-galactoside containing glycan, preferably to galactose terminated glycans rather than to simple galactose (Agrwal et al., 1993; Sato & Hughes, 1992). For instance, lactose and N-acetyllactosamine (LacNac) bind Galectin-3 more strongly than galactose (Agrwal et al., 1993; Sato & Hughes, 1992). The CRD of Galectin-3 has an extended binding site for glycan as revealed by crystal structure analysis when compared with other galectins (Seetharaman et al., 1998). This results in the increased affinity of Gal-3 for glycans with multiple lactoseamines and the substitution of the non-reducing terminal galactose moiety with ABH blood group oligosaccharides (Fucα1,2, GalNAcα1,3 (Fucα1,2) and Galα1,3 (Fucα1,2) (Seetharaman et al., 1998).

Galectin-3 can form a homodimer and/or pentamer through intermolecular interactions involving the N-terminal domain, leaving the CRD free to interact with different glycans (Ahmad et al., 2004; Nieminen et al., 2007). The

multimerization of Galectin-3 leads to the crosslinking of different glycoconjugates. In the absence of glycan ligands, Galectin-3 can also form homodimer via CRD (Woo et al., 1991; Yang et al., 1998).

1.15.3.   Cellular localization and functions

Galectin-3 presents in the cytosol, nucleus and cell surface but they are also excreted extracellulary by an unknown mechanism (Dagher et al., 1995; Hughes, 1999; Sato & Hughes, 1994).

The cellular localization of Gal-3 determines its biological activities. In cytoplasm, Galectin-3 interacts with several cytosolic proteins and is involved in a diverse range of intracellular events (Dumic et al., 2006). Among these binding proteins, apoptosis repressor Bcl-2 binds Galectin-3 and this binding mediates the anti-apoptotic effect of Gal-3 (Yang et al., 1996). Other binding proteins include CD95 (APO-1/Fas), Nucling and Alix/AIP1, GTP-bound K-Ras and Akt-protein, which are involved in the role of Gal-3 in apoptosis, proliferation and differentiation (Elad-Sfadia et al., 2004; Fukumori et al., 2004; Liu et al., 2004). Nuclear Galectin-3 acts as a pre-mRNA splicing factor through interacting with the nuclear protein Gemin4 (Dagher et al., 1995; Park et al., 2001). In addition, nuclear Galectin-3 is involved in the regulation of the gene transcription via enhancing the transcription factor binding with CRE and Sp1, the promoters for the cell cycle regulating gene cyclin D1 (Lin et al., 2002).

Extracellularly, Galectin-3 plays a role in cell-cell adhesion and in adhesion to the extracellular matrix through binding with cell surface glycoproteins and the glycosyalted components of extracellular matrix (Dumic et al., 2006; Ochieng et al., 2004). In contrast to intracellular Galectin-3, extracellular Galectin-3 induces

apoptosis in activated T cells (Fukumori et al., 2003). In addition, extracellular Galectin-3 mediates cell activation by crosslinking its cell surface glycoconjugate ligands, leading to the formation of a lattice-like structure and induces cell signalling (Ahmad et al., 2004; Ochieng et al., 2004). It also acts as a chemoattractant and promotes the migration of monocytes and macrophages (Sano et al., 2000).

The majority of interactions between Galectin-3 and intracellular host proteins are glycan independent (protein-protein interaction) (Dumic et al., 2006), while extracellular Galectin-3 binds a diverse range of glycosylated molecules on the cell surface in a glycan dependent pattern (Dumic et al., 2006).

1.15.4.   Galectins-3 in host-pathogen interactions

Host defence against pathogens is achieved by two types of immune response: the innate and adaptive immune systems. Pathogens that invade the human host are initially recognized by their innate immunity. This recognition is accomplished by germline encoded pattern recognition receptors (PRRs). These receptors can recognize the microbial components, termed pathogen-associated molecular patterns (PAMPs), and subsequently activate the immune system (Akira et al., 2006; Cerliani et al., 2011). Out of these receptors, members of the host C-type lectin family are used by the innate immune system as PRRs to recognize pathogens. Such recognition is mediated by binding the host C-type lectin to pathogen glycans, such as the multiple terminal mannose cluster or β-glucan, inducing the release of inflammatory cytokines and reactive oxygen intermediates (Cerliani et al., 2011; van Kooyk & Rabinovich, 2008). Other host lectins, such as DC-SIGN, selectins and siglecs, bind microorganisms carrying host-like glycans

(Cerliani et al., 2011). For instance, DC-SIGN and the mannose receptor bind to the ManLAM of Mycobacterium tuberculosis, N-linked high mannose-type glycans attached to HIV-1 gp120, and Lewis$_x$ and Lewis$_y$ on H. pylori (Cerliani et al., 2011; Sato et al., 2009; van Kooyk & Rabinovich, 2008). Sialic acid-binding lectins, siglecs, also recognize sialic acid expressing pathogens and regulate the immune response (Crocker & Redelinghuys, 2008; Sato et al., 2009). In this context, Galectin-3 recognizes a diverse range of surface glycans of many pathogens, such as Neisseria gonorrhoeae, Leishmania major, Schistosoma mansoni, Candida albicans and Trypanosoma cruzi (John et al., 2002; Kleshchenko et al., 2004; Kohatsu et al., 2006; Pelletier & Sato, 2002). Therefore, it has been suggested that galectins, including Galectin-3, act as PRRs (Cerliani et al., 2011; Sato & Nieminen, 2004; Sato et al., 2009). The recognition of these pathogens by Galectin-3 can initiate an immune response, which subsequently leads to the clearance of microorganisms or instead may promote infection (Sato et al., 2009) (Figure 1.10). In addition, Galectin-3 is known to be released from the epithelium, endothelium and professional immune cells, such as inflammatory activated macrophages, as a result of bacterial infection, which further supports the consideration of Galectin-3 as PRRs (Almkvist & Karlsson, 2004; Sato et al., 2009). An example of the latter has been reported by a recent study where the binding of Galectin-3 to Toxoplasma gondii glycosylphosphatidylinositols in macrophages was found to be essential for parasite recognition and TNF production (Cerliani et al., 2011; Debierre-Grockiego et al., 2010).

In addition, instead of activating the immune system Galectin-3 may confer a direct immune function. This is best exemplified by the binding of the α1-2-type

mannans of Candida albicans with Galectin-3, which results in a loss of fungal viability (Cerliani et al., 2011; Kohatsu et al., 2006).

On the other hand, several studies have suggested that Galectin-3-pathogen interactions may promote infection. In this context, Galectin-3 may facilitate H. pylori infection through allowing bacterial adhesion to the gastric epithelium (Cerliani et al., 2011; Fowler et al., 2006) (Figure 1.12).
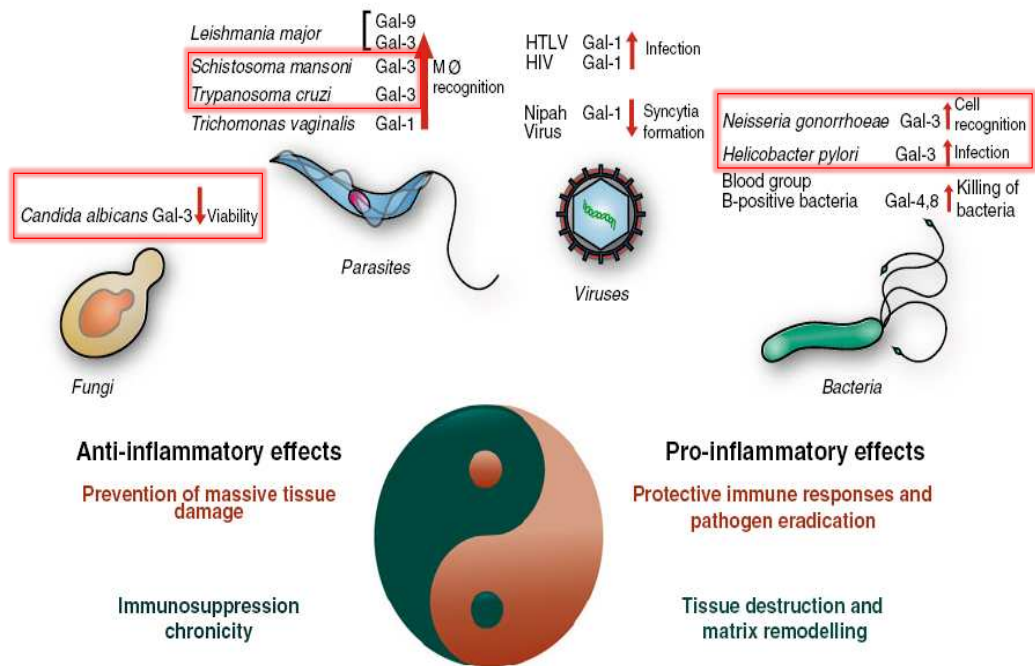
Figure 1.12: Role of galectins, including Gal-3, in host–pathogen interactions and innate immunity. The recognition of specific glycans by galectins can lead to pro-inflammatory responses and pathogen clearance or favour immune suppressive microenvironments that promote chronic infection. For example, the recognition of the α1-2-type mannans of Candida albicans by Galectin-3 lead to fungal killing. However, in parasitic infection such as Schistosoma mansoni and Trypanosoma cruzi, Galectin-3 helps in the recognition of these pathogens by macrophages, which subsequently leads to pathogen eradication. On the other hand, Galectin-3 can promote the infections of H. pylori and Neisseria gonorrhoeae by enabling bacterial adhesion and bacterial host cell recognition, respectively. Reproduced from (Cerliani et al., 2011).

A brief overview of Galectin-3's role as PRRs has been given first in this review in order to understand the subsequent illustration of Galectin-3 interactions with different pathogens and the consequences of these interactions (described below).

1.15.4.1. Bacteria

Galectin-3 recognizes the N-acetyllactosamine (LacNac) Galβ1-4GlcNAc residue of bacterial lipooligo(poly)saccharides. This interaction of Gal-3 has been suggested by several reports, including different bacteria, such as H. pylori, Neisseria gonorrhoeae, E. coli and Klebsiella pneumonia (John et al., 2002; Li et al., 2008; Mey et al., 1996). Galectin-3 seems to be involved in Pseudomonas aeruginosa binding with the corneal epithelium via LPS (Gupta et al., 1997). Up to now, two independent sites of Galectin-3 have been suggested to mediate the binding with bacterial LPS. First, the binding site represents the CRD of Gal-3 (lectin domain), which binds β-galactosides containing LPS from Klebsiella pneumonia (Mey et al., 1996). The second site is the N-terminal part of Gal-3 (Non-lectin domain), which binds the lipid A moiety of LPS. LPS from S. minnesota, which is devoid of β-galactosides, only binds the N-terminal domain of Gal-3 (Mey et al., 1996), while LPS from E. coli binds both the CRD and N-terminal domain of Gal-3 (Li et al., 2008). It has been suggested by Li et al (2008) study, that the Galectin-3 acts as a negative regulator of LPS. This was evident by elevated cytokine production from macrophages of Galectin-3 deficient mice when challenged with LPS, which was suppressed by the addition of exogenous Gal-3 (Li et al., 2008).

It has been demonstrated that Galectin-3 accumulates in alveolar space after the induction of pneumonia with S. pneumonia, which correlates with neutrophil extravasation (Sato et al., 2002). It is worth noting that the recruitment of neutrophil from blood vessels to the infection site (neutrophil extravasation) is considered to be one of the most important components of innate immunity (Sato et al., 2002). Such recruitment requires the neutrophil to be firmly attached to the

endothelial wall of blood vessels, which is mediated in part by two types of adhesion molecules, beta (2) integrins and selectins (Sato et al., 2002), taking into consideration that, in vitro, Galectin-3 has been shown to promote neutrophil adhesion to the endothelium owing to the direct crosslinking between the neutrophil and the N-terminal aggregating domain of Galectin-3 (Almkvist & Karlsson, 2004). Returning to the previous point, during streptococcal pneumonia it has been suggested that Galectin-3 plays a role in beta (2) integrin-independent neutrophil extravasation (Sato et al., 2002). In contrast, Galectin-3 does not accumulate during neutrophil emigration in the alveoli induced by E. coli infection since the majority of neutrophil emigration is known to be beta (2) integrin-dependent (Sato et al., 2002). This has been further supported by a recent study (Farnworth et al., 2008), which showed that the migration of neutrophils to the S. pneumoniae-infected alveoli is reduced dramatically in Galectin-3 deficient mice. The development of more severe pneumonia with increased bacteremia and lung damage following infection with S. pneumonia is observed in Galectin-3 null mice when compared with wild-type mice (Farnworth et al., 2008). A reduction in the severity of pneumococcal pneumonia has been attributed in part to Galectin-3 via its augmentation of neutrophil function (Farnworth et al., 2008). In addition, exogenous Galectin-3 induces the neutrophil phagocytosis of bacteria and delayed neutrophil apoptosis (Farnworth et al., 2008). It has also been shown that Galectin-3 has a bacteriostatic effect on S. pneumonia in vitro (Farnworth et al., 2008). The addition of recombinant Gal-3 in vivo helps to protect Galectin-3 deficient mice from developing severe pneumococcal pneumonia (Farnworth et al., 2008).

Galectin-3 expression has been shown to be upregulated in several infections, including pneumococcal meningitis (PM) (Bellac et al., 2007; Coimbra et al., 2006).

1.15.4.2. Parasites

Not only lactosamine containing glycans have been shown to interact with Gal-3 but also other types of ß-galactoside on the parasite surface, including (Galß1-3)n and (GalNacß1-4GlcNac) (Sato et al., 2009). For example, Galectin-3 binds the polygalactosyl repeat residue (Galß1-3)n of Leishmania major lipophosphoglycans (LPGs) (Pelletier & Sato, 2002). This binding leads to the cleavage of Galectin-3, producing truncated Galectin-3 that has the CRD but lack the N-terminal domain (Pelletier & Sato, 2002). Truncated Gal-3 lacks the ability to oligmerize or to form a stable association on the cell surface, which is required for Gal-3 innate immune modulation. Thus it has been suggested that this truncation of Gal-3 in response to Leishmania major may play a role in species-specific immune responses (Pelletier & Sato, 2002). In addition, Galectin-3 binds T. cruzi and enhances its adhesion to the smooth muscle cells of coronary arteries (Kleshchenko et al., 2004). The silencing of Galectin-3 in these cells leads to a reduction in T. cruzi adhesion, which is restored by adding exogenous Gal-3 (Kleshchenko et al., 2004). This provides evidence for the involvement of endogenous Galectin-3 in host–parasite interaction (Sato et al., 2009). Another unique β-galactoside (GalNacß1-4GlcNac), known as LacdiNAc, is expressed by parasitic worms or helminths and is recognized by Galectin-3 (van den Berg et al., 2004). This recognition increases the phagocytosis of LacdiNAc coated beads by macrophages (van den Berg et al., 2004).

1.15.4.3. Fungi

Galectin-3 can differentiate between pathogenic fungal species, such as Candida albicans and non-pathogenic S. cerevisiae (Kohatsu et al., 2006). Such recognition is mediated by Gal-3 binding to the ß-1,2-oligomannosides (Manβ1–2)$_n$ of Candida albicans, which are present in the cell wall glycolipid (Kohatsu et al., 2006). This glycan is specifically expressed by Candida albicans and is involved in the binding with the macrophage membrane, resulting in TLR2-dependent NF-$_K$B activation and tumour necrosis factor-a (TNF-a) (Fradin et al., 1996). Interestingly, Galectin-3-Candida albicans binding leads to fungi being killed, indicating the fungicidal effect of Gal-3 (Kohatsu et al., 2006).

1.16. Aims of the study

The aim of this study was to characterize the role of Gal-3 in meningococcal-host cell interaction and identify the non-LOS meningococcal molecules that bind Gal-3. It was also our aim to investigate the dimerization of Galectin-3 with 67 LR/37 LRP, and to study the effect of meningococcal 67 LR/37 LRP adhesins on receptor gene expression.

2.1. Bacterial strains, growth conditions and media

N. meningitidis serogroup B, strain MC58 wild type (B:15:P1.7.16b) (Tettelin et al., 2000). Different meningococcal mutants (Table 2.1) were produced in the laboratory. Clinical isolates used are listed in Table 2.2. All Neisseria strains were cultured on chocolated horse blood agar (Oxoid) at 37°C in an atmosphere of 5% CO_2. When grown in suspension, all meningococcal strains were grown in brain-heart infusion (BHI) broth (Oxoid) at 37°C with agitation. H. pylori 26695 strain was used and grown on blood agar plate (Oxoid) at 37°C under microaerobic conditions.

Strains	Description	Source or references
MC58	wild-type serogroup B strain	(Tettelin et al., 2000)
MC58ΔPilQ	PilQ deletion and replaced with omega cassette	(Orihuela et al., 2009)
MC58ΔPorA	PorA deletion and replaced with omega cassette	(Orihuela et al., 2009)
MC58ΔPilE	PilE deletion and replaced with kanamycin cassette	In house
MC58ΔPglL	PglL deletion and replaced with kanamycin cassette	In house
MC58ΔPglC	PglC deletion and replaced with omega cassette	In house
MC58ΔPglLC	PglC and PglL deletions and replaced with omega and kanamycin cassettes, respectively.	In house
MC58Δlgtf	Lgtf deletion and replaced with kanamycin cassette	In house

Table 2.1: List of meningococcal strain used in this project.

Strain[a]	Country of origin	Date of isolation	Disease	Serogroup
MC58[b]	UK		Invasive	B
z1503[c]	China	1984	Invasive	A
z1035[c]	Pakistan	1967	Invasive	A
z4662[c]	Netherlands	1967	Invasive	B
z4665[c]	Netherlands	1977	Invasive	B
z6413[c]	South Africa	1990	Invasive	C
z6414[c]	New Zealand	1994	Invasive	C
z6415[c]	England	1996	Invasive	C
z3515[c]	Saudi	1987	Carrier	A
z1392[c]	Greece	1968	Carrier	A
z4686[c]	Norway	1988	Carrier	B
z4685[c]	Norway	1988	Carrier	B
z23279[d]	UK	2009	Carrier	B
z23288[d]	UK	2009	Carrier	B
z23000[d]	UK	2009	Carrier	B
z23464[d]	UK	2009	Carrier	B
z22955[d]	UK	2009	Carrier	B
z22951[d]	UK	2009	Carrier	Y
z22972[d]	UK	2009	Carrier	Y
z23484[d]	UK	2009	Carrier	Y
z99615[d]	UK	2010	Carrier	Y
z22984[d]	UK	2009	Carrier	Y
z1506[c]	Brazil	1976	Unspecified	A
z4262[c]	USA	1964	Unspecified	B
z4765[c]	Brazil	1976	Unspecified	C
z5163[c]	Spain	1985	Unspecified	C

[a.] Further details of strains are available at **http://pubmlst.org/;**

[b.] Strain obtained from ATCC.

[c.] Strain obtained from Prof D. Caugant

[d.] Strains isolated in Nottingham, UK

Table 2.2: List of meningococcal clinical isolates used in this project.

2.2. Transformation of N. meningitidis

2.2.1. Chromosomal DNA extraction and purification from meningococcal cells

Genomic DNA was isolated using a DNeasy® tissue kit (Qiagen) according to manufacturers' instructions. In brief, the strains were grown overnight on chocolate agar then sub-cultured in 5 ml BHI. A maximum of 2×10^9 cells were harvested by centrifuging at $5,000 \times g$ for 5 min and the supernatant discarded. The pellet was re-suspended in 180 μl of buffer ATL (supplied in the kit). 20 μl proteinase K (20 mg /ml) were then added and incubated at 55ºC for 2 hr. 200 μl buffer AL (supplied with the kit) was added, mixed thoroughly by vortexing, and incubated at 70ºC for 10 min. To produce a homogeneous solution, 200 μl 100% ethanol was added and mixed thoroughly by vortexing. The mixture was then applied to the DNeasy® Mini spin column including any precipitate formed from the ethanol addition and centrifuged at $6,000 \times g$. The flow-through was discarded and 500 μl buffer AW1 (supplied with the kit) was added to the column and centrifuged for 1 min at $6,000 \times g$. The flow-through was again discarded and 500 μl buffer AW2 (supplied with the kit) was added and centrifuged for 3 min at $18,000 \times g$ to remove any residual ethanol. Finally the DNA was eluted using 100 μl nuclease free deionised water. Chromosomal DNA was stored at -20°C until required.

2.2.2. Natural transformation of N. meningitidis

N. meningitidis was grown in BHI broth to an optical density of 0.2 at 600nm and added to a 15 ml tube containing 1.5 ml of BHI agar. After incubation for 2 h at 37°C in 5% CO_2 250ng of the mutagenic plasmid DNA was added to the culture and incubation was continued overnight. The cells were then harvested and plated

on BHI agar plates supplemented with the appropriate antibiotic and incubated overnight at 37°C in 5% CO2. Colonies were observed after 24 and 48 h. Antibiotics used were kanamycin (Oxoid) (50μg/ml), streptomycin (Oxoid) (50μg/ml) and spectinomycin (Oxoid) (50μg/ml).

2.2.3.   Chemical transformation of N. meningitidis

Non piliated meningococci transformed by chemical transformation method (Bogdan et al., 2002). N. meningitidis was grown in BHI broth to an early exponential phase (OD600 0.5–0.6). The cells were harvested by centrifugation at 1000xg for 10 min at 4°C and gently resuspended in 1.0 ml of ice cold Transformation Solution (TS) (Appendix B). An aliquot of 190 µl of the cells resuspended in TS was transferred to a sterile 1.5 ml eppendorf tube. 100 ng of mutagenic plasmid or N. meningitidis chromosomal DNA was added to cells and mixed gently by stirring with a pipette tip. The cells were incubated on ice for 15 min. 1.3 ml of BHI broth was added to the cells and incubated at 37°C for 1 hr with shaking at 250 rpm. The culture was then centrifuged at 9000 rpm in a microfuge for 4 min, re-suspended in 200µl of BHI broth and spread on a BHI agar plates containing antibiotics and incubated at 37°C in 5% CO2 for 1–3 days or until colonies appeared.

2.2.4.   Electroporation of N. meningitidis cells

Electroporation method was used for meningococcal transformation as described before (Duenas S et al., 1998). The overnight growth from chocolated horse blood agar plate was harvested into 10 ml of BHI broth and centrifuged (4000 rpm, 10 min). The bacteria were then resuspended in 20 ml of ice-cold S&G buffer (272 mM sucrose, 15% glycerol) before being re-centrifuged. This washing procedure was repeated three times before the bacterial cells were finally resuspended in 1

ml S&G buffer and left on ice until required. Purified DNA (1 - 5 μg) was added to an electroporation cuvette (0.2 cm inter-electrode distance; Bio-Rad, UK) along with 40 μl of competent N. meningitidis cells and placed on ice for 10 min. This was then subjected to electroporation in a Bio-Rad Gene Pulser at a voltage of 2.5 kV, a resistance of 400 Ω and a capacitance of 25 μFD. The contents of the tube were then added to 2 ml of BHI and incubated at 37°C for 5 hr. Aliquots were plated out onto BHI plate containing any appropriate selective antibiotics and incubated for up to 2 days at 37°C in 5% CO_2.

2.3. Enzyme linked immunosorbant assay

2.3.1. Digoxigenin labeling of bacteria

Bacteria were harvested from an overnight plate culture and suspended in PBS-T, washed 3 times and suspended in PBS (PH 7.2). Optical density at 600 nm was adjusted to 1, and then digoxigenin-3-0-succinyl-ε-aminocaproic acid-N-hydroxy-succinimide ester (DIG-NHS; Roche) was added and incubated at room temperature for 2 hrs. Bacteria were then washed 3 times with PBS-T and suspended in PBS containing 1% bovine serum albumin. Optical density at 600 nm was adjusted to 0.02.

2.3.2. ELISA

Purified recombinant human rGalectin-3 full molecule or its C terminal (CRD) (Calbiochem) or recombinant laminin recptor (rLR) or BSA (5μg/ml) diluted in PBS was used to coat Covalink amino-reactive 96 well microtiter plates (Immoblizer Amino; Nunc) overnight at 4 °C. Wells were washed with PBS-T 3 times and blocked with 100 μl of 1% BSA for 1 hr at room temperature. Blocking buffer was decanted and 100μl of either DIG-labelled bacteria or purified proteins

(rLR, rPora, rPilQ and loop 4 synthetic peptide 5μg/ml in PBS) were added and incubated for 4 hours at room temperature, or at 4°C overnight. The plate was vigorously washed with PBS-T 5 times with 5 min soaking intervals and incubated with anti- digoxigenin alkaline phosphatase antibody (Roche, 1:5000) or polyclonal anti-37 LRP (1:1000); anti-PilQ (1:10000); anti-PorA(1:10000); anti-Loop4 (1:10000) in PBS/1% BSA at room temperature. Bacterial incubated plates were incubated at room temperature for an additional 1h and washed several times as described above. 100μl of alkaline phosphatase substrate (5mg/ml;Roche) were added to each well, and the absorbance was measured at 405nm after 15min using an ELISA plate reader. Purified protein plates were incubated with protein antibody at room temperature for an additional 2h and washed several times as described above. Plates were incubated with anti-rabbit alkaline phosphatase (1:12,000, Sigma) for 1h at room temperature followed by washing 3 times with PBS-T and 100μl of alkaline phosphatase substrate (5mg/ml; Roche) was added and absorbance measured at 405nm. Inhibition assays were performed as described above, except that bacteria were pre-incubated with lactose or sugars for 2h at room temperature before being added to the ELISA plates.

2.4. Expression and purification of recombinant proteins

2.4.1. Protein expression

E. coli BL21(DE3) and JM109, containing recombinant plasmids pET2837 LRP, PQE30PorA and PNJ072PilQ (courtesy of N. Abouseada and N. Oldfield) were cultured into 50ml LB broth (Fisher Scientific) containing (50μg/ml) of kanamycin or (100μg/ml) of ampicillin overnight at 37˚C. Cultures were then

transferred into 1L of LB (1:20 dilution) containing kanamycin or ampicillin, respectively and incubated for 2hr until the OD600 reached 0.6, at this point 1ml of culture was aliquoted and retained. Then 1mM of IPTG Isopropyl β-D-1-thiogalactopyranoside (Promega) was added to induce protein expression and cultures grown for an additional 3hr, and 1 ml of induced culture was aliquoted and retained. The cultures were harvested and the pellets were collected and stored in -20°C freezer. E. coli JM109 containing blank plasmid PQE70 and E. coli BL21 (DE3) containing blank plasmid pET28a were used as a negative control. Aliquoted samples were centrifuged at 13,000 x g for 1min. The cell pellet was re-suspended in the appropriate volume of 5 x SDS sample buffer using the following formula (volume in μl = O.D. × 800/3). The samples were boiled for 5 min at 95°C and then centrifuged again at 13,000 x g for 1min to be analyzed by SDS-PAGE (Section 2.5).

2.4.2. Purification of recombinant protein

Cells from 50ml culture were re-suspended in 5ml of buffer B (8M urea (Sigma), 0.1M NaH_2PO_4 (BDH) & 0.01M Tris.HCl (Sigma) pH 8.0) and then sonicated in an ice bath for 15 cycles of 10 sec with 5 sec of cooling between cycles. Lysate was centrifuged at 45000 rpm for 30-40min at 4°C to pellet cellular debris, followed by incubation of the supernatant with 20mM of imidazole (Qiagen) and cobalt resin (Fisher Scientific) overnight at 4C˚. Supernatant was passed through a gravity column and extensively washed with buffer C (8M urea, 0.1M NaH_2PO_4 & 0.01M Tris.HCl, pH 6.3) and incubated overnight at 4C° with buffer E (8M urea, 0.1M NaH_2PO_4 & 0.01M Tris.HCl, pH 4.5). Buffer exchange was performed using PD-10 desalting columns (Amersham Biosciences), replacing the acidic urea

buffer with PBS (pH 7.2). Protein concentration was measured using a Nanodrop ND-1000 spectrophotometer (NanoDrop Technologies) by measuring the absorbance at 280 nm and proteins were stored at – 20˚C.

2.5. Cloning of laminin receptor and Galectin-3

2.5.1. Bacterial strains, growth conditions and media

E. coli strains and plasmids used in this chapter are described in Table 2.3. E. coli strains were routinely grown at 37°C on Luria-Bertani (LB) agar or in LB broth (Fisher Scientific) containing ampicillin (100 µg /ml) where necessary. Where appropriate, blue/white selection of transformants in cloning experiments was achieved using IPTG (Roche) and X-gal at 0.5 mM and 80 µg/ml, respectively. All liquid cultures were aerated by agitation at 200 revolutions per minute (r p m) in a shaking incubator.

2.5.2. Extraction of plasmid DNA

E. coli JM109, harboring the desired plasmid, were streaked out from -80°C glycerol stock on to LB agar plates containing appropriate antibiotic and incubated overnight at 37°C . The following day, a single colony was used to inoculate a 10 ml of LB broth supplemented with 100 µg /ml ampicillin. The broth culture was incubated at 37°C overnight with shaking at 200 rpm. Purification of plasmids was achieved using 5 ml overnight cultures using a QIAprep spin kit (Qiagen) according to the manufacturer＇s instructions. In case of large-scale (70-100 µg) plasmid purification, GeneElute the Midi Prep kit (Sigma) was used according to manufacturer＇s recommendation.

2.5.3. Quantification of DNA and protein

The concentration of purified PCR products, plasmid, genomic DNA and purified proteins was quantified using a NanoDrop (ND-1000) spectrophotometer (Agilent Technologies).

2.5.4. Polymerase chain reaction (PCR)

All PCR reactions were performed in a 50 µl final volume using sterile 0.2 ml thin-walled PCR tubes and cycled using a C1000 model Thermal Cycler (BIO-RAD). A master mix containing all of the PCR components except template DNA was prepared in a pre-chilled, sterile microcentrifuge tube and thoroughly mixed by vortex. Following a brief centrifugation, a 50 µl aliquot of master mix was dispensed into chilled PCR tubes and 1 µl appropriate template DNA. The solution was mixed by gently stirring with a pipette tip and kept on ice prior to placement in the thermal cycler. Unless otherwise stated, all PCR mixtures contained: 100 ng of chromosomal DNA or 1-10 ng of Plasmid DNA; each of the respective primers to a final concentration of 300 nM; 5 µl of 10x Expand buffer (Roche); dNTPs (Roche) to a final concentration of 200 µM, Expand Hi Fidelity DNA polymerase 0.42 µl (3.5 U/ µl) (Roche) and the reaction mixture was made up to a final volume of 50 µl with dH2O. The PCR conditions were: initial template denaturation step of 3 min at 95°C, followed by 30 cycles of incubation, annealing at 55°C for 1 min, primer extension at 72°C for 3 min, and 95°C for 45s, with final extension at 68°C for 10 min.

2.5.5. Agarose gel electrophoresis

1% agarose gel electrophoresis was used to analyse the PCR and plasmid products. The prepared gel was stained with 10µg/ml ethidum bromide (Sigma)

and run in 1 x Tris Acetate EDTA buffer (TAE buffer, Sigma) at 5 V/cm for1 hr. The gel was visualized using an ultraviolet trans-illuminator to detect the ethidium bromide-labelled DNA. Quick load (100bp and 1kb) and 2-log (0.1-10.0 kb) DNA ladder mixes (New England Biolab) were used to estimate the size of PCR product and linearized plasmid.

2.5.6. Poly-A tailing

PCR products were subjected to A tailing procedure according to manufacturer instruction (Promega). In this procedure, 7µl of PCR product, Taq DNA polymerase, Polymerase 10X Reaction Buffer with $MgCl_2$, dATP to a final concentration of 0.2mM and de-ionized water (to a total volume 10µl) were added and incubated at 70˚C for 15-30min. As a result, this poly-A tailed PCR product was used in further cloning steps.

2.5.7. Purification of Gel-extracted DNA products

For gel extraction of DNA fragments amplified by PCR or generated by restriction digestion, samples were separated by agarose gel electrophoresis and the band of interest was excised with Gene catcher Tips (Web Scientific) and purified using a Gel extraction Kit (Qiagen) according to manufacturer's instructions.

Strains/plasmids	Description	Source or reference
E. coli strain		
JM109	endA1 recA1 gyrA96 thi hsdR17 (rK⁻ rK⁻) relA1 supE44 Δ(lac-proAB) [F'traD36 proAB laqIᵃZΔM15]	Promega
Plasmids		
pGEM-T easy	Cloning vector encoding resistance to ampicillin	Promega
pET2837 LRP	laminin receptor protein cloned in pET28 plasmid vector	(Orihuela et al., 2009)
pcDNA3.1zeo YFP	Mammalian expression vector encoding full length venus YFP	Kindly provided by Dr. N. Holliday (Kilpatrick et al.)
pcDNA3.1zeo YNL	Mammalian expression vector encoding N terminal of venus YFP	Kindly provided by Dr. N. Holliday (Kilpatrick et al.)
pcDNA3.1zeo YCL	Mammalian expression vector encoding C terminal of venus YFP	Kindly provided by Dr. N. Holliday (Kilpatrick et al.)

Table 2.3: List of bacteria strain and plasmids used in this project.

Primers	Sequence (5- 3)[a]	Restriction site
LRP-F1	gcgc**gaattc**gccatgtccggagcccttgat	EcoRI
LRP-R2	gcgc**ctcgag**agaccagtcagtggttgctcc	XhoI
Gal-3-F1	gcgc**gaattc**gccatggcagacaatttttcgct	EcoRI
Gal-3-R2	gcgc**ctcgag**tatcatggtatatgaagcactggtg	XhoI
mCherry-F	gcgc**ctcgag**gtgagcaagggcgaggagga	XhoI
mCherry-R	gcgc**tctaga**ttacttgtacagctcgtccatgc	XbaI

[a]Sequences in bold identify restriction enzyme sites and the kozak consensus sequence is underlined.

Table 2.4: Primers used for cloning of laminin receptor and Galectin-3.

2.5.8. Cloning of laminin receptor and Galectin-3 in pGEM-T easy vector

A 888bp DNA fragments corresponding to laminin receptor (37 LRP) coding sequences was amplified by PCR using pre existing vector (pET2837 LRP) (Orihuela et al., 2009) and the pair primers 37 LRPP-F1 and 37 LRPP-R2 (Table 2.4). A 725bp DNA fragments corresponding to Galectin-3 coding sequences was amplified by PCR using cDNA sequences of human galectin-3 and the pair primer Gal-3-F1and Gal-3-R2 (Table 2.4). The forward and reverse primers have EcoRI containing Kozak sequence and XhoI restriction sites, respectively, as shown in Table 2.4. The PCR reaction was performed as described in Section 2.3.4. The amplified PCR products of both receptors were extracted from the gel and underwent poly A tailing as described in Section 2.2.5 and 2.5.6, respectively. Then, digested with EcoRI and XhoI as described in Section 2.5.4 and and ligated to pGEM-T easy vector (Promega) according to the manufacturer's instructions. The ligated product was transformed into E. coli JM109 according to the manufacturer's instructions. Screening for a successful clone was performed by colony PCR amplification of the desired DNA fragment and subsequent DNA sequencing.

2.5.9. Cloning of laminin receptor and Galectin-3 in pcDNA3.1zeo containing vYFP, vYNL and vYCL

37 LRP and Gal-3 cloned into pGEM-T easy vector were digested with EcoRI and XhoI. The digested receptors were extracted from the gel and ligated into pcDNA3.1zeo containing either full length or the C or N terminal regions of venus YFP (kindly provided by Dr. N. Holliday, Cell signalling Institution) (Kilpatrick et al.). The vector pcDNA3.1zeo containing either full length or the C

or N terminal regions of venus YFP were pre digested with the same enzymes to be prepared for subsequent ligation with 37 LRP and galectin-3. Then, ligated product was transformed into E. coli JM109 according to the manufacturer's instructions. Screening for a successful clone was performed by colony PCR amplification of the desired DNA fragment and subsequent DNA sequencing. The resulting plasmids were designated 37 LRP and Gal-3.vYFP, vYNL and vYCL (Table 2.7, Figure 2.1).
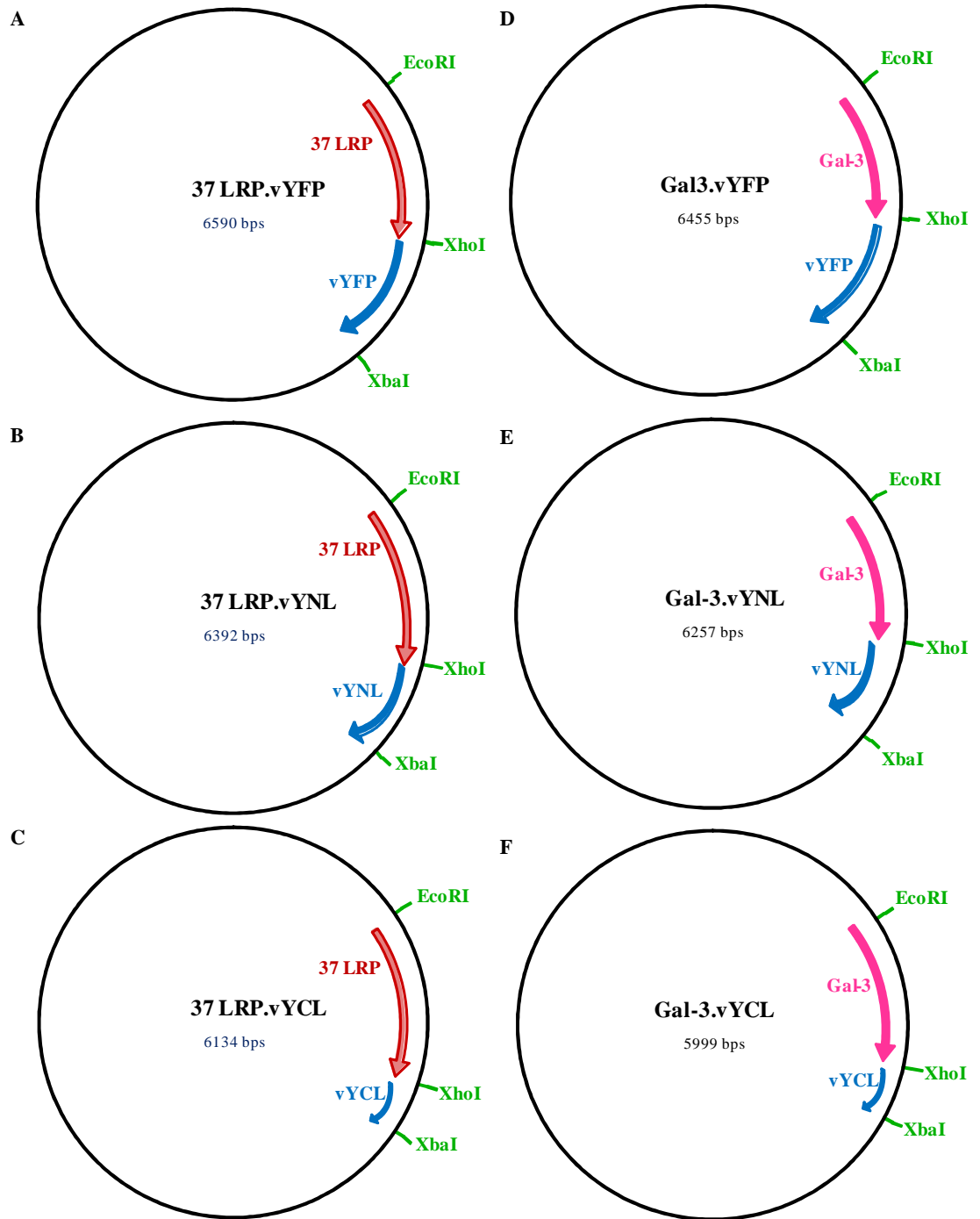
Figure 2.1: **A map of the 37 LRP and Gal-3.vYFP, vYNL and vYCL constructed by cloning 37 LRP and Gal-3. into pcDNA3.1zeo containing full length (vYFP), N-terminal (vYNL) and C-terminal (vYCL) of venus yellow fluorescence protein.** The plasmids contain ampicillin resistance gene.

2.5.10. Cloning of laminin receptor and Galectin-3 in pcDNA3.1zeo containing mCherry

A 711bp DNA fragments corresponding to mCherry coding sequences was amplified from a pre-existing vector (Shaner et al., 2004) (kindly provided by Dr. Shaista Bano , Center for Biomolecular Science, University of Nottingham, UK) using PCR and the pair primers mCherry-F and mCherry-R (Table 2.4), removing the start methionine and including a stop codon. The forward and reverse primers have XhoI and XbaI restriction sites, respectively, as shown in Table 2.3. The PCR reaction was performed as described in Section 2.3.4. 37 LRP.vYFP and Gal-3.vYFP vectors were linearized by digestion (Section 2.3.12) with XhoI and XbaI removing vYFP. The plasmids 37 LRP.mCherry and Gal-3.mCherry were constructed by ligating XhoI and XbaI digested, gel-purified mCherry PCR product with 37 LRP.pcDNA3.1zeo and Gal-3.pcDNA3.1zeo, respectively. Then, ligated product was transformed into E. coli JM109 according to the manufacturer's instructions. Screening for a successful clone was performed by colony PCR amplification of the desired DNA fragment and subsequent DNA sequencing. The resulting plasmids were designated 37 LRP.mCherry and Gal-3.mCherry (Table 2.7, Figure 2.2).
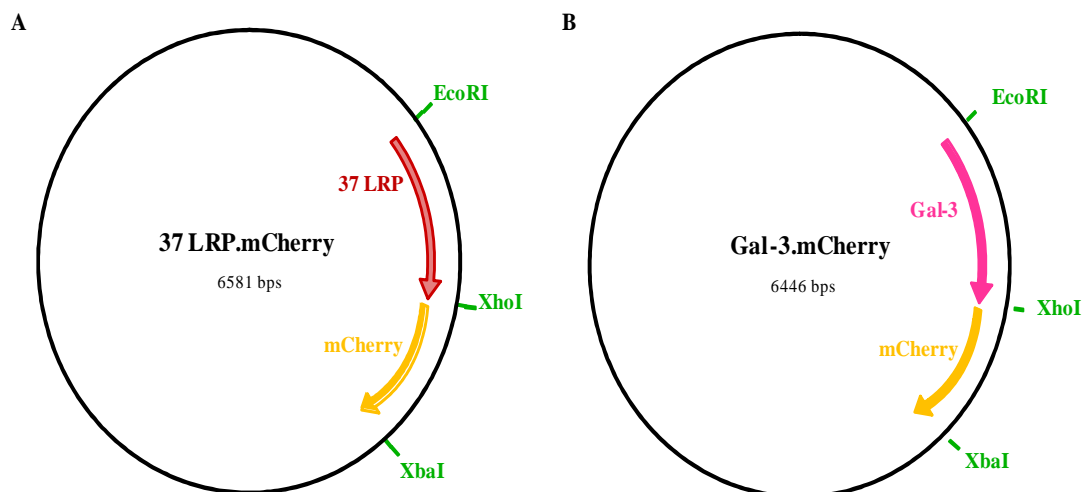
Figure 2.2: **A map of the 37 LRP and Gal-3.mCherryv constructed by cloning of mCherry into pcDNA3.1zeo containing 37 LRP and Gal-3.** The plasmids contain ampicillin resistance gene.

2.5.11. PCR site-directed mutagenesis.

The generated pcDNA3.1 zeo mammalian expression vector carrying the wild type 37 LRP and Gal-3 cDNA that is C-terminally fused to vYFP, vYNL and vYCL were used as templates and mutants were generated by site directed mutagenesis. The PCR mutagenesis reaction contained in a total volume of 50µl: 10µl of 5x reaction (PfuUltra), 5-50ng of dsDNA template, 1µg/µl final concentration of each of the oligonucleotide primers (Table 2.5) both containing the desired mutation which are complementary to opposite strands of the dsDNA, 20mM final concentration of dNTPs mix (Roche) and dH2O. After that 1µl of PfuUltra high-fidelity DNA polymerase (2.5U/ µl) was added to each reaction mix the primers are extended during temperature cycling (Table 2.6), and allow the generation of a mutated plasmid containing staggered nick. Then the PCR product was treated with Dpn I endonuclease to digest the remaining parental DNA template and to select for mutation-containing synthesized DNA. Subsequently, transformation was carried out into E. coli JM109 competent cells that were plated on an LB/ampicillin plate for the selection after recovering the cells for an hour at 37°C. Then samples were sent for sequencing. All generated constructs are described in Table 2.7 and primers used in all cloning procedures are described in Table 2.4 and 2.5.

Primers	Sequence (5- 3)[a]
LRP.FP.M.C148A	cctacctaccattgcgctggctaacacagattctcctctg
LRP.RP.M.C148A	cagaggagaatctgtgttagccagcgcaatggtaggtagg
LRP.FP.M.C163A	tggacattgccatcccagccaacaacaagggagctc
LRP.RP.M.C163A	gagctcccttgttgttggctgggatggcaatgtcca
Gal-3.FP.M.C173A	gagaacaacaggagagtcattgttgccaatacaaagctggataataactg
Gal-3.RP.M.C173A	cagttattatccagctttgtattggcaacaatgactctcctgttgttctc

Table 2.5: Primers used for site-directed mutagenesis of laminin receptor and Galectin-3.

Segment	Cycles	Temperature	Time
1	1	95°C	30 seconds
2	16	95°C	30 seconds
		55°C	1 minute
		68°C	4.5 minute

Table 2.6: Cycling Parameters for the QuikChange II-E Site-Directed

Mutagenesis Method.

Name of construct	Description	Vector	Restriction sites
37 LRP.vYFP	Laminin receptor wild type fused to venus yellow fluorescent protein (vYFP)	pcDNA3.1zeo	EcoRI /XhoI
37 LRP.vYNL	Laminin receptor wild type fused to N-terminal of venus yellow fluorescent protein (vYNL)	pcDNA3.1zeo	EcoRI /XhoI
37 LRP.vYCL	Laminin receptor wild type fused to C-terminal of venus yellow fluorescent protein (vYCL)	pcDNA3.1zeo	EcoRI /XhoI
Gal-3.vYFP	Galectin-3 wild type fused to venus yellow fluorescent protein (vYFP)	pcDNA3.1zeo	EcoRI /XhoI
Gal-3.vYNL	Galectin-3 wild type fused to N-terminal of venus yellow fluorescent protein (vYNL)	pcDNA3.1zeo	EcoRI /XhoI
Gal-3.vYCL	Galectin-3 wild type fused to C-terminal of venus yellow fluorescent protein (vYCL)	pcDNA3.1zeo	EcoRI /XhoI
37 LRP.C148AvYFP	Laminin receptor fused to venus yellow fluorescent protein (vYFP) containing cysteine mutated to alanine at position 148	pcDNA3.1zeo	EcoRI /XhoI
37 LRP.C163AvYFP	Laminin receptor fused to venus yellow fluorescent protein (vYFP) containing cysteine mutated to alanine at position 163	pcDNA3.1zeo	EcoRI /XhoI
37 LRP.C148/163AvYFP	Laminin receptor fused to venus yellow fluorescent protein (vYFP) containing cysteines mutated to alanines at positions 148/163	pcDNA3.1zeo	EcoRI /XhoI
37 LRP.C148AvYCL	Laminin receptor fused to C-terminal of venus yellow fluorescent	pcDNA3.1zeo	EcoRI /XhoI

	protein (vYCL) containing cysteine mutated to alanine at position 148		
37 LRP.C148AvYNL	Laminin receptor fused to N-terminal of venus yellow fluorescent protein (vYNL) containing cysteine mutated to alanine at position 148	pcDNA3.1zeo	EcoRI /XhoI
37 LRP.C163AvYNL	Laminin receptor fused to N-terminal of venus yellow fluorescent protein (vYNL) containing cysteine mutated to alanine at position 163	pcDNA3.1zeo	EcoRI /XhoI
37 LRP.C148AvYFP	Laminin receptor fused to venus yellow fluorescent protein (vYFP) containing cysteine mutated to alanine at position 148	pcDNA3.1zeo	EcoRI /XhoI
37 LRP.C163AvYFP	Laminin receptor fused to venus yellow fluorescent protein (vYFP) containing cysteine mutated to alanine at position 163	pcDNA3.1zeo	EcoRI /XhoI
Gal-3.C173AvYFP	Galectin-3 fused to venus yellow fluorescent protein (vYFP) containing cysteine mutated to alanine at positions 173	pcDNA3.1zeo	EcoRI /XhoI
Gal-3.C173AvYCL	Galectin-3 fused to C-terminal of venus yellow fluorescent protein (vYCL) containing cysteine mutated to alanine at position 173	pcDNA3.1zeo	EcoRI /XhoI
Gal-3.C173AvYNL	Galectin-3 fused to N-terminal of venus yellow fluorescent protein (vYNL) containing cysteine mutated to alanine at position 173	pcDNA3.1zeo	EcoRI /XhoI
37 LRP.C163AvYNL	Laminin receptor fused to N-terminal of venus yellow fluorescent protein (vYNL)	pcDNA3.1zeo	EcoRI /XhoI

	containing cysteine mutated to alanine at position 163		
37 LRP.mCherry	Laminin receptor fused to N-terminal of mCherry	pcDNA3.1zeo	EcoRI /XhoI
Gal-3.mCherry	Galectin-3 fused to N-terminal of mCherry	pcDNA3.1zeo	EcoRI /XhoI

Table 2.7: Names and descriptions of constructs used in this project.

2.5.12. Restriction endonuclease digestion

Restriction digestion reactions were routinely carried out in a 20 µl final volume. Unless otherwise stated, 1 µg of DNA (for using in sub-cloning), was digested as a double digest with appropriate enzymes and compatible buffers. Restriction endonuclease enzymes and buffers were purchased from New England Biolabs or Roche and used according to the directions of the manufacturer.

2.5.13. Ligation Reaction

Appropriate amounts of vector and insert DNA were combined in a 1:3 ratios in a sterile microcentrifuge tube and the reaction was assembled in 10µl final volume. A typical ligation reaction contained; 100 ng insert, 50-100 ng plasmid DNA, 1 µl T4 DNA ligase (New England Biolabs), 1 µl 10 × ligation buffer (New England Biolabs), and where required dH_2O was added to make a final volume of 10 µl. The ligation reaction was incubated at 16°C for 1h and then overnight at 4°C. An aliquot of 1.5 µl was used to transform E. coli JM109 competent cells.

2.5.14. Transformation

Briefly, an aliquot of 50 µl of frozen competent E. coli cells JM109 (Promega), was thawed on ice 5 min prior to transformation. 100 ng of plasmid DNA was added to cells and mixed gently by stirring with a pipette tip. The cells were incubated on ice for 20 min followed by heat shock at 42°C in water bath for 50 s

without shaking. Immediately after heat treatment, the cells were transferred on to ice for 2 min. 400 μl of S.O.C medium (Invitrogen)was added to the cells and the cell suspension was incubated at 37°C for 1.5 hr with shaking at 250 rpm. The transformation reaction was plated out as 100μl, 150 μl, and 200 μl, on LB agar containing appropriate antibiotic and incubated overnight at 37°C.

2.5.15. DNA sequencing

DNA constructs were sequenced in both directions using T7 and BGH primers at the School of Biomedical Sciences (University of Nottingham) on an ABI 377 automated DNA sequencer.

2.6. Cell line and cell culture condition

Primary human brain microvascular endothelial cells (HBMECs, ScienCell Research Laboratories) were cultured in human fibronectin coated flasks (Biocoat, BD-Falcon) at 37°C, 5% CO_2 in endothelial cell medium (ECM, Science Cell Research Laboratories) supplemented with endothelial cell glial supplement (ECGS, Science Cell Research Laboratories), 1% (v/v) antibiotic-antimycotic solution (Gibco) and 10% (v/v) fetal bovine serum (FBS, Science Cell Research Laboratories). Astrocytes were cultured at 37°C, 5% CO2 in Astrocyte Medium (AM, Science Cell Research Laboratories) supplemented with astrocyte glial supplement (AGS, Science Cell Research Laboratories), 1% (v/v) antibiotic-antimycotic solution (Gibco) and 10% (v/v) fetal bovine serum (FBS, Science Cell Research Laboratories). Neuro2a , mouse neuroblastoma cell line (N2a, ATCC via LGC Standards) were cultured at 37°C, 5% CO2 in Eagle's Minimum Essential Medium (EMEM, ATCC) supplemented with1% (v/v) antibiotic-antimycotic solution (Gibco) and 10% (v/v) fetal bovine serum (FBS,

Science Cell Research Laboratories). COS7 cells were grown in Dulbecco's modified Eagle's medium (DMEM, Invitrogen) supplemented with 1% (v/v) antibiotic-antimycotic solution (Gibco) and 10% (v/v) fetal bovine serum, at 37°C and 5% CO_2. Cell culture media was changed every two days and cells were split using trypsin-EDTA (Gibco) when they became 90% confluent. Cells were grown the day before transfection in 6-well or 12 well or 24-well plates in order to reach a confluency of 50-70 % on the day of transfection. For immunofluorescence assays, cells were grown on 12 mm diameter glass coverslips with appropriate coating and media.

2.7. Transfection and harvesting cells

Cells were grown the day before transfection in 6-well or 12 well or 24-well plates in order to reach a confluency of 50-70 % on the day of transfection. Cells were transiently transfected with Trans IT-2020 transfection reagent (Mirus) according to the manufacturers' instructions. DNA was complexed with TransIT-2020 in serum-free, antibiotic free media at a ratio of 2μg DNA: 1μl TransIT-2020 at room temperature for 25 min. 250μl of DNA: TransIT-2020 complex was added to each well of the 6 well plate or 100μl DNA: TransIT-2020 complex was added to each well of the 12 well plates. After 4 hr of incubation, the media was changed and the transfected cells were cultured at 37°C in a 5% CO_2 atmosphere for 24 hours. After 24 hours, cells grown on coverslips were fixed with 4% PFA and subjected to immunofluorescence staining and confocal microscopy as described in section 2.5 and 2.6, respectively. Transfected cells in 6 well plates were washed with ice-cold 1X phosphate buffered saline (PBS) and harvested by scraping in 2x SDS sample buffer or subjected to subcellular fractionation. For

subcellular fractionation, cells were harvested and washed twice with ice-cold PBS and separated into cytosolic, membrane, soluble and chromatin bound nuclear, and cytoskeleton fractions (Subcellular Protein Fractionation Kit, Thermo Scientific), according to the manufacturer's protocol.

2.8. Sodium dodecyl sulfate polyacrylamide gel electrophoresis

The recombinant proteins were electrophretically separated by 7.5% SDS-PAGE (Appendix B) using Mini- Protean III equipment (BIO-RAD) at a constant 30mA per gel with a 200V voltage limit for approximately 40-45 min. Protein samples were resuspended in $1 \times$ or $5 \times$ SDS sample buffer (Appendix B) and heated at 100°C for 5 min. An aliquot of 10µl of sample was loaded into each well of the gel and 10µl of pre-stained broad range protein markers (New England Biolabs) were loaded into an adjacent lane. Proteins separated by SDS-PAGE were visualized by staining with SimplyBlue SafeStain (Invitrogen) or PageBlueTM Protein Stain Solution (Fermentas) according to the manufacturer's instructions.

2.9. Immunoblot analysis

For Immunoblot analysis, the proteins separated by 10% SDS-PAGE were transferred onto a nitrocellulose membrane (Biorad) in semi-dry blotting buffer (Appendix B) using a Trans-Blot SD semidry transfer cell (BIO-RAD) at a constant currant of 14 mA for approximately 30 min. The membranes were blocked with PBS containing 1% bovine serum albumin (BSA, sigma) for 1 hour at RT. The membranes were then probed with primary antibodies (in PBS-1% BSA) for 1 hr at room temperature or overnight with shaking at 4°C. The following day, the membranes were washed three times 15 min each with Tris Buffered Saline-Tween (TBS-T), and incubated into secondary antibody (anti-

mouse IgG conjugated to alkaline-phosphtase or anti-rabbit conjugated to alkaline phosphtase or anti-rat IgG conjugated to alkaline-phosphtase) (Sigma) at the concentration of 1:30,000 for 1 h at RT. After 1 h the membranes were washed six times with TBS-T for 10 min each time. The membrane was then developed using the BCIP (5-bromo-4- chloro-3-indolylphosphate) ‑ Nitro Blue Tetrazolium liquid substrate (PerkinElmerTM). Primary antibodies included anti-GFP rabbit polyclonal antibody (sc-8334, Santa Cruz) (1:200), anti-mCherry rabbit polyclonal antibody (632496, Clontech), anti-penta-His Tag antibody (Sigma); anti-InH37 LRPP (In house laminin receptor precursor) rabbit polyclonal antibody (1:1000); rat monoclonal anti-Galectin-3 Mac-2 (clone M3/38, 125402, BioLegend) (1:1000) and anti-galectin-3 mouse monoclonal antibody (MAB4033, Millipore) (1:1000).

2.10. Immunofluorescence

Cells transfected with required constructs were fixed on cover slips with 4% paraformaldehyde (PFA) in PBS for 10 minutes at room temperature before being washed twice with PBS and incubated in 4% BSA in PBS (blocking solution) for one hour at room temperature. Then cover slips were incubated with primary antibody(s): primary antibody(s): anti-GFP rabbit polyclonal antibody (sc-8334, Santa Cruz) (1:100); anti-6737 LRP Mlu5 and Ab711(Abcam) (1:100); anti-InH37 LRPP rabbit polyclonal antibody (1:100); rat monoclonal anti-mouse galectin-3 Mac-2 (clone M3/38, 125402, BioLegend) (1:200); goat polyclonal anti-human galectin-3 (AF1154, R and D systems) (1:100) and mouse monoclonal anti-human galectin-3 antibody (MAB4033, Millipore) (1:100) in PBS/4% BSA for 1hr. Coverslips were washed 20 times in PBS-T, 40 times in PBS and

incubated with secondary antibody(s): anti-mouse Alexa Fluor 647 antibody (1:2000); anti-mouse Alexa Fluor 680 antibody (1:100); anti-rabbit Alexa Fluor 680 antibody (1:100); anti-rabbit Alexa Fluor 488 antibody (1:400); anti-mouse Alexa Fluor 488 (1:400); anti-goat Alexa Fluor 488 (1:400); anti-rat Alexa Fluor 647 (1:400); (all from Molecular Probes), in PBS/4% BSA for 1hr and washed 20 times in PBS-T, 40 times in PBS and 20 times in dH$_2$O. Coverslips were mounted using Fluoromount (Sigma) mounting media and images obtained by confocal microscope (Zeisis LSM700).

2.11. Confocal microscopy

Images were captured using a Zeiss LSM700 confocal microscope (Carl Zeiss, Ltd., Welwyn, UK) using Plan-Apochromat 63x/1.4 Oil DIC M27. Alexa 488 and vYFP, mCherry, Alexa 680 and 647 and Hoechst were detected using the following lasers respectively 488 nm or 561 nm or 639 nm or 405 nm nmlasers were used. The image size was 1024×1024 with 8 averages taken per frame and a pinhole size of 1 Airy Unit. All control images were captured with the same laser power, gains and zoom settings. Identical linear adjustments to contrast and brightness were made to representative images in the figures for presentation purposes. Images were captured using the Zen 2009 software package and processed by Image J and CS4 photoshop.

2.12. Flow cytometry

Flow cytometric analysis of cell surface receptors was performed by incubation of HBMECs with mouse monoclonal anti-67 LR antibody MLuC5 (8 or 4µg/µl; Abcam) or mouse monoclonal anti-Galectin-3 (20µg/ml; Millipore, Chemicon) /10^6 cells for 1hr at 4˚C. Then cells were washed three times with PBA buffer

(0.5% BSA and 0.5% sodium azide) and exposed to (1:50 dilution) of Alexafluor 467goat anti-mouse IgM or 488 goat anti-mouse IgG (all from Molecular Probes) for 1hr at 4°C. After washing with PBA buffer, cells were resuspended in 250µl of 0.5% paraformaldehyde and subjected to flow cytometry (Coulter Altra Flow Cytometer). In some experiments the cells were incubated with different bacterial proteins (rPorA, rPilQ and Loop4 all at 20µg/ml) for 2hr at room temperature before incubation with primary antibody. For BiFC analysis, COS7 cells were grown in 6-well plates and 24 hours after transfection, cells were gently detached using cell dissociation solution (Sigma), washed with PBA buffer (0.5% BSA and 0.5% sodium azide) and resuspended in 0.5% paraformaldehyde in PBS and subjected to flow cytometry (Coulter Altra Flow Cytometer). Data acquisition and analysis were performed with weasel 2.5 software. In each case, 50,000 cells were counted in triplicate and used to calculate the average BiFC signal intensity $\pm$ SE. Full-length YFP fluorescence signal was used as the interassay reference for maximal fluorescence in each experiment, against which the BiFC signal intensities were compared.

2.13. Adhesion and invasion assay

2.13.1. Preparation of meningococci

N. meningitidis strains, MC58-WT were streaked onto chocolate agar plates and incubated as described in section 2.11. The following day, meningococci were cultured into 10ml BHI Brain Heart Infusion (Appendix B) and incubated at 37°C with shaking (200 rpm) until the OD600 reach 0.5.

2.13.2. Preparation of cells

N2a cells were cultured in EMEM supplemented with 1% antibiotic-antimycotic solution (Gibco) and 10% fetal bovine serum were transiently transfected with galectin-3 and grown to confluence in 24-well tissue culture plates (Costar) at 37°C, 5% CO_2. Prior to all experiments, mono-layers were transferred to EMEM supplemented with 2% FCS to remove the antibiotics.

2.13.3. Association assay

Association assays were performed essentially as previously described (Oldfield et al., 2007). Briefly, N2a monolayers were infected with 1 $x10^7$ cfu of meningococci (multiplicity of infection of 300) (confirmed retrospectively by plating out aliquots of serially diluted inoculums) and left to associate for 2 h in 5% CO_2 at 37°C. To assess total cell association, monolayers were washed four times with 1 ml 1 × PBS per well. The monolayers were then disrupted and homogenized in 1 ml 0.1% saponin in PBS. Meningococci were enumerated by serial dilution of the homogenized suspensions and subsequent determination of colony-forming units by plating 10 µl spots from appropriate dilutions of the lysates on agar.

2.13.4. Invasion assay

N2a monolayers were infected as described in section 2.13.3, but were left to associate for 4 h in 5% CO_2 at 37°C. The media was then removed and 1 ml EMEM containing gentamicin (100µg/ml) were added per well to kill the extra-cellular bacteria for 30 mins. Prior to further steps, aliquots of the gentamicin-containing supernatants were plated out to confirm killing of extra-cellular bacteria. Furthermore, the susceptibility of all meningococcal strains to

gentamicin at 100 µg/ ml was confirmed prior to testing. To assess cell invasion, monolayers were washed three times with 1 ml 1 × PBS per well. The monolayers were then disrupted and homogenized in 1 ml 0.1% saponin in PBS. Meningococci were enumerated by serial dilution of the homogenized suspensions and subsequent determination of colony-forming units by plating 50 µl aliquots from appropriate dilutions of the lysates on agar.

2.14. Animal study

2.14.1. Ethics statement

Mice experiments described in the present study were conducted at the animal facility of Wenner-Grens Institute, Stockholm University. Animal care and experiments were conducted adhering to the institution's guidelines for animal husbandry. All protocols were approved by the Swedish Ethical Committee on Animal Experiments (Approval ID: N316/10).

2.14.2. Mouse strains

The hCD46Ge transgenic mouse line (CD46$^{+/+}$) was created using B6C3F1 hybrids. It harbors the complete human CD46 gene and expresses CD46 in a human-like pattern (Mrkic et al., 1998). Previous studies have shown that this mouse model can develop meningococcal disease (Johansson et al., 2003; Johansson et al., 2005).

2.14.3. Mouse infection studies

Serogroup B N. meningitidis MC58 and the mutant strains were grown for 18 hours at 37 °C in a 5% CO_2 atmosphere on GC agar (Difco) supplemented with Kelloggs (Kellogg et al., 1968). Bacteria were suspended in GC liquid and each

mouse was challenged intraperitoneally (i.p.) with 1.2×10^9 CFU in 100μL GC liquid. Experiments were performed with 6–8 week old mice (n=10 mice per group). In control group, mice were challenged i.p. with 100μL GC liquid. The health status of all mice was closely monitored for 7 days. At indicated time points, whole blood samples were collected from the tail vein for measurement of cytokines, chemokines and bacteremial levels. (Brain were collected at the end of the experiment and stored in 4% formaldehyde).

2.14.4. Immunofluorescence

Paraffin embedded tissue sections of mice brains were subjected to immunofluorescence staining by an antigen retrieval method. The sections were deparaffinized in xylene and rehydrated through graded ethanols. For antigen retrieval, the slides were autoclaved for 5 mins in 10 mmol/L sodium citrate buffer (pH 6.0) and cooled for 10 minutes at room temperature. Sections washed one time with PBS-T and three times with PBS for 5 minutes each time and blocked for 1 hour in 4% BSA in PBS/0.3% Triton X-100 at room temperature. Sections were incubated overnight with the two antibody combinations of anti-InHLRPP rabbit polyclonal antibody (1:100) and rat monoclonal anti-mouse Galectin-3 Mac-2 (clone M3/38, 125402, BioLegend) (1:10) in 4% BSA in PBS/0.3% Triton X-100 at 4 °C. After washing, the slides were incubated with secondary antibody(s): anti-rat Alexa Fluor 647 antibody (1:100) and anti-rabbit Alexa Fluor 488 antibody (1:200); in 4% BSA in PBS/0.3% Triton X-100 for 1hr at room temperature. Following extensive washing, sections were covered with Fluoromount (Sigma) mounting media and images obtained by confocal microscope (Zeisis LSM700). Controls for unspecific binding by secondary

antibodies were included in each staining. Brain tissue sections obtained from eight mice were analyzed and images from two mice are presented. Fluorescence intensity quantified by ImageJ software.

2.15. Real time quantitative PCR (qPCR)

2.15.1.   Induction of HBMECs

The propagation of HBMECs was described in section 2.1.7. The HBMEC monolayer was grown to confluence in T25 tissue culture flasks and induced with the recombinant meningococcal proteins (rPorA, rPilQ and Loop4 of PorA) at a concentration of 20μg/ml or PBS (as a negative control). Then, cultures were re-incubated for 24 hr at 37°C with 5% CO_2 after which monolayer were washed with cold PBS and total RNA was extracted as described in section 2.2.2. The cells were examined by microscopy before and after induction to exclude any infection.

2.15.2.   Extraction of total RNA and cDNA synthesis

Total RNA was extracted using an RNeasy Plus Micro kit (QIAGEN) in conjunction with the QIA shredder system (QIAGEN) according to the manufacturer's instructions. The quality of RNA samples was verified by measuring the optical density (OD, 260/280) absorption ratio of 1.8 (range 1.8-2). To ensure the removal of any residual DNA contamination, the RNA samples were incubated with RNAase-free Turbo-DNAse I (Ambion) at 37°C for 20min, and then DNAase I was heat-inactivated at 65°C for 10min. The total RNA was cleaned up and concentrated using RNeasy MinElute Cleanup kit (QIAGEN) according to the manufacturer's instructions and the OD measured again. Further confirmation of DNA removal from RNA samples was examined by PCR

amplification of the 37 LRP gene using 37 LRPP-F1 and 37 LRPP-R2 primers (Table 2.7) with 1μg of RNA as template and 37 LRP PCR product as positive controls. cDNA was obtained using QuantiTect Reverse Transcription Kit (QIAGEN) according to the manufacturer's instructions.

2.15.3.   Primer optimization, standard curves and qPCR

Quantitative PCR was performed using AB7500 Real time PCR system (Applied Biosystem) and Power SYBR green master mix (Roche) according to the manufacturer's instructions. Primers specific to 37 LRP and B-actin (Table 2.8) were designed and used for amplification of 98bp and 55bp fragments, respectively. Primers were optimized using different concentrations (0.5-9μM) of forward and reverse primers with 10 ng/μl of HBMEC cDNA utilized as template and 2x buffer of Power SYBR Green Master Mix for both 37 LRP and β-actin PCR reaction. To test PCR efficiency, a standard curve was generated with serial fivefold dilution of a known amount (100 ng/μl) of HBMEC cDNA using 3μM of forward and 9μM of reverse primers. A standard curve was plotted for 37 LRP and B-actin using template dilution versus CT and ΔCT values. The qPCR reaction mixture (25μl total volume) consisted of: 2μl of cDNA (1ng/ μl); 12.5μl of Power SYBR green master mix; 3μM of forward and 9μM of reverse primers and H2O. Reactions started with a 2min hold at 50°C, then 10min at 95°C followed by 40 cycles of denaturation at 95°C for 150sec followed by annealing/extending at 60°C for 1min. Quantification was relative to untreated HBMECs and was determined by the ΔΔCT method as described previously (Livak & Schmittgen, 2001).

Gene	Forward oligonucleotide sequence (5'- 3')	Reverse oligonucleotide sequence (5'- 3')
Laminin receptor	GGAAAAGTGATGGCATCTATATCA	ATCAGCAGGGTTTTCAATGG
B-actin	GCGCGGCTACAGCTTCA	CTTAATGTCACGCACGATTTCC

Table 2.8: Forward and reverse primers sequences used in qPCR experiments

2.15.4. Data analysis

The ΔΔCt method for real-time relative quantitative PCR with power SYBR Green detection was used to estimate the 67 kDa 37 LRP gene expression in HBMECs. Analysis of real-time PCR amplification data was performed using SDS software (Applied Biosystems). Standard curves for target and endogenous gene were plotted showing CT value versus log of initial concentration of cDNA. The slope of the standard curve was calculated to describe the efficiency of PCR (if the PCR amplification is exponential, resulting in a doubling of product in every cycle, the slope will be −3.3 as 3.3 cycles are required to generate a 10-fold increase in product). The expression of the target gene (6737 LRP) in the experimental samples (induced HBMECs with rPorA, Loop4 of PorA and rPilQ) relative to a control calibrator (HBMECs treated with PBS) and B-actin as endogenous gene, was analyzed based on the relative quantification approach as recommended in AB 7500 User Bulletin (Applied Biosystems).

3. Chapter 3: Investigation *of N. meningitidis* binding to Galectin-3

3.1. Introduction:

Adhesion of N. meningitidis to host cell surfaces is mediated by its Type IV pili (T4p) (Scheuerpflug et al., 1999) and the cellular receptor for T4p was proposed to be CD46 (Kallstrom et al., 1997). A further study reported CD46-independent adhesion (Kirchner et al., 2005), which necessitates further characterization of the initial attachment. After initial adhesion of host cell, the poly-saccharide capsule and T4p expression is downregulated (Deghmane et al., 2002) allowing more intimate adhesion, which is further maintained by outer membrane opacity proteins, including Opa and Opc (Moore et al., 2005; Virji et al., 1993a; Virji et al., 1994). Opa and Opc can interact directly with heparan sulphate proteoglycans HSPGs (Prince et al., 2001; Virji et al., 1999). In addition, interaction of Opc with serum proteins vitronectin mediates bacterial binding to endothelial integrins αVβ3 and α5β1 (Unkmeir et al., 2002; Virji et al., 1994). Opc may also directly bind to extracellular matrix (ECM) proteins, such as vitronectin and fibronectin (Prince et al., 2001). Moreover, Opa protein binds carcinoebryonic antigen-related cell adhesion molecules (CEACAMs) (Virji et al., 1999).

Recently, it has been found that bacteria causing meningititis including Neisseria meningitidis target the 67 kDa laminin receptor (67 LR) on the surface of human and rodent brain microvascular endothelial cells (Orihuela et al., 2009). The 37-kDa/67-kDa laminin receptor acts as cell surface receptor for many other neurotropic pathogens including bacterial cytotoxin necrotizing factor-1 (CNF-1) of E. coli K1(Kim et al., 2005), prions (Ludewigs et al., 2007) and various viruses (Akache et al., 2006; Bondarenko et al., 2003; Sakoonwatanyoo et al., 2006; Wang et al., 1992). Dimerization status of the 67 LR has not yet been elucidated. Previous reports suggest homo or heterodimerization of the 67 LR precursor form

37 kDa LRP (37 LRP) with galectin-3 (Gal-3) (Buto et al., 1998; Castronovo, 1993; Landowski et al., 1995). Interestingly, Gal-3 is a ß-galactosidase binding proteins, which belongs to S-type lectin (termed galectin) family (Barondes et al., 1994a), and plays an important role in host–pathogen interactions and inflammation (Vasta, 2009). Galectins were initially called S-type lectins (i.e., thiol-dependent), because some members appear to require reducing conditions to exhibit their biological function (Leffler et al., 2004). However, this name is no longer considered appropriate as many other galectins maintain their biological function in the absence of reducing agent (Leffler et al., 2004). Galectin-3 is also known to interact with ß-galactoside containing glycans on the surface of many invading pathogens and host cell (reviewed in Vasta 2009).

The glycans covering the surface of many pathogens are added to proteins by a process called glycosylation; the most common post translational modification of proteins. There are two types of glycosylation in bacterial pathogens: N-glycosylation and O-glycosylation. In N- linked glycosylation which is best exemplified by a system in Campylobacter jejuni, the glycan is covalently attached to the amino groups of asparagines residues in the sequence of type Asn-Xaa-Ser/Thr, where Xaa is any amino acid except for proline (Kowarik et al., 2006). The O-linked glycans are associated covalently with the hydroxyl groups of serines or threonines. The Type IV pilin (PilE) of pathogenic Neisseria was one of the first examples of an O-glycosylated glycoprotein (Power et al., 2000). Depending on the host strain, two types of O-linked trisaccharides have been identified in N. meningitidis pili, these include: Gal-β1, 4-Gal-α1,3-DATDH (DATDH represents 2, 4-diacetamido-2, 4, 6-trideoxyhexose) (Stimson et al., 1995), or Gal-β1, 4-Gal-α1, 3-GATDH (GATDH represents 2-glyceramido-4-

acetamido-2, 4, 6-trideoxyhexose) (Chamot-Rooke et al., 2007) (Table 3.1). Another truncated O-linked disaccharide, Gal-α1, 3GlcNAc, is also present in N. meningitidis strain 8013 (Marceau et al., 1998) (Table 3.1).
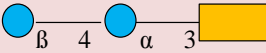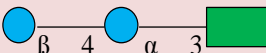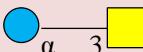
Protein target	OTase	OTase transfer abilities	Amino acids modified	Sugars transferred	Ref.
Pilin (PilE)	PglL	Promiscuous; multiple O-linked repeats	Serine 63	Gal-β1, 4-Gal-α1, 3-DATDH	(Stimson et al., 1995)
				Gal-β1, 4-Gal-α1, 3-GATDH	(Chamot-Rooke et al., 2007)
				Gal-α1, 3GlcNAc	(Marceau et al., 1998)

Table 3.1: Structure of meningococcal O-linked glycosylated pilin. Adapted from (Nothaft & Szymanski, 2010) *Key to Symbols:

◯ Gal ☐ GlcNAc ▯ DATDH ▮ GATDH

Pilin glycosylation genes (pgl) encode the enzymes required for synthesis and transfers of glycans to meninigococcal PilE have recently been identified (Chamot-Rooke et al., 2007; Power et al., 2000; Power et al., 2003). These glycans synthesized by the sequential action of pglD, pglC and PglB (for DATDH) or PglB2 (for GATDH) are summarized in Figure 3.1. The O-linked glycan is transferred onto Ser63 of PilE by pilin glycosylation ligase, PglL (O-OTases) (Power et al., 2006) (Figure 3.1). Mutations of pglL produce non glycosylated pilin, which is not recognized by antibodies specific for N. meningitidis C311 trisaccharide (Power et al., 2006). Interestingly, a recent report

has found that the meningococcal outer membrane protein AniA is O-glycosylated (Ku et al., 2009).
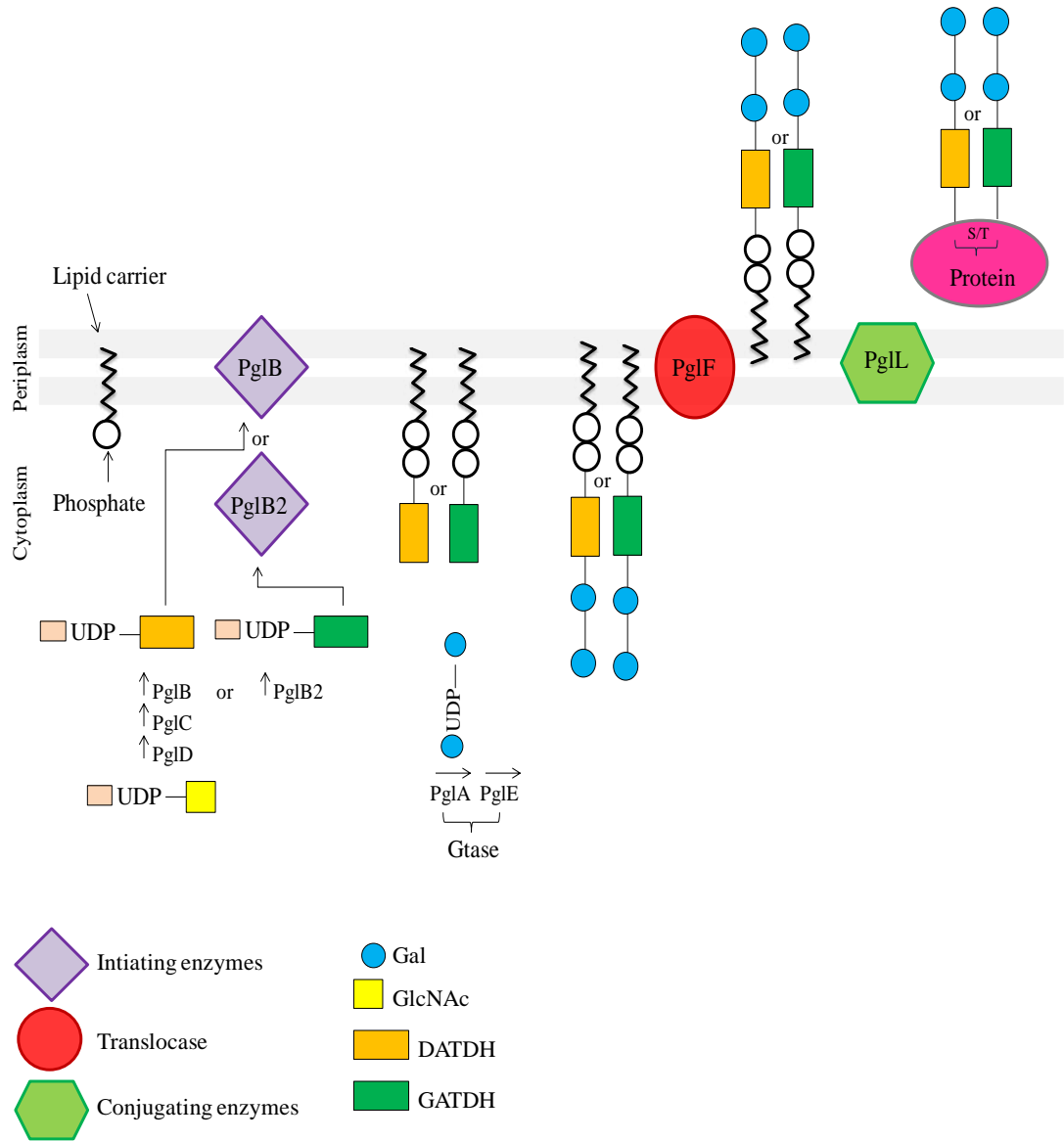
Figure 3.1: overview of Neisseria O-linked pathways for protein glycosylation. Block transfer of oligosaccharides from the lipid anchor to the protein target, as occurs in Neisseria meningitidis. First, an initiating enzyme (PglB or PglB2) links a sugar residue (DATDH or GATDH) onto the lipid carrier at the plasma membrane. Further glycan (galactose) residues are then added by a set of glycosyltransferases (Gtase). After assembly, the lipid-linked saccharide is moved across the membrane by translocase (PglF). Finally, a conjugating enzyme (PglL), transfers the

glycan to Ser63 of the pilin subunit PilE or to Ser/Thr residues in other periplasmic and membrane proteins. (Hug & Feldman, 2011; Nothaft & Szymanski, 2010).

A variety of bacteria, including S. pneumonia (Sato et al., 2002), H. Pylori (Fowler et al., 2006), N. gonorrhea (John et al., 2002) , P. aeruginosa (Gupta et al., 1997), Escherichia coli O86 (Stowell et al., 2010) and Klebsiella pneumonia (Mey et al., 1996) have been found to bind Gal-3. This binding is suggested to be mediated by bacterial lipopolysaccharide (LPS) either engaging the Gal-3 C-terminal CRD (carbohydrate recognition domain, lectin-domain) or the N-terminal (non-lectin domain) or both. Other microbial ligands have also been shown to bind Gal-3, these include: Candida albicans oligomannosides (Kohatsu et al., 2006), T. gondii glycosylphosphatidylinositols (Debierre-Grockiego et al., 2010), Leishmania major lipophosphoglycan (Pelletier & Sato, 2002), Trypanosoma cruzi 45- (mucin), 32-, and 30-kDa surface proteins (Moody et al., 2000), Mycobacteria phosphatidylinositol mannosides and mycolic acid (Barboni et al., 2005; Beatty et al., 2002) and P. mirabilis fimbriae (Altman et al., 2001).

Importantly, Gal-3 contributes to the innate immune response against many pathogens. In this context, it exerts a fungicidal effect on Candida albicans (Kohatsu et al., 2006) and a bacteriostatic effect on S. pneumonia (Farnworth et al., 2008). Other studies suggest that pathogen-Gal-3 interaction mediates the adhesion of the pathogen and thus enhances the infection process (described in detail in Chapter 1) (Cerliani et al., 2011). For example, transient expression of Gal-3 increased H. pylori adhesion to host cell (Fowler et al., 2006). Moreover,

Gal-3 also mediates P. mirabilis adhesion to Madin-Darby canine kidney (MDCK) cells (Altman et al., 2001).

Much attention has been paid recently to the role of Gal-3 in the CNS (Bellac et al., 2007; Coimbra et al., 2006; Mok et al., 2007; Reichert & Rotshenker, 1999). During pneumococcal meningitis (PM), Galectin-3 is up regulated in the cortex and hippocampus (Bellac et al., 2007; Coimbra et al., 2006). Distribution of Galectin-3 in different regions of infant rat brain and predominant expression in inflammatory cells highlight the role of neuroinflammation in the pathophysiology of PM (Coimbra et al., 2006). In addition, in an experimental prion disease model, induced Gal-3 expression has been shown in activated microglia (Mok et al., 2007). Importantly, based on the known structure of meningococcal LOS, the terminal oligosaccharide glycans are predicted to be recognized by Gal-3 (Vasta, 2009) which has been confirmed recently by (Paola Quattroni, 2010). Although binding of Galectin-3 with meningococcal LOS is shown to be interrupted by lactose, some residual binding to meniningococci has been found in the presence of lactose (Paola Quattroni, 2010). Such remaining binding suggests involvement of additional meningococcal ligands other than LOS that mediate the rest of Galectin-3 binding with N. meningitidis.

The aims of this chapter were to examine the binding of lactose bound Gal-3 to N. meningitidis, and identify non-LOS meningococcal ligands that bind Gal-3.

3.2. Results:

3.2.1. N. meningitidis binds rGal-3

It has been predicted and recently shown that the Galectin-3 binds the lactosamine residue of meningococcal LOS (Quattroni et al., 2012; Vasta, 2009). In order to identify non-LOS meningococcal ligands that binds Gal-3, lactose bound Gal-3 was used and its binding with N. menigitidis was examined using ELISA. Purified recombinant galectin-3 full molecule (rGal-3) or it's carbohydrate recognition domain (rCRD) was immobilized on an ELISA plate, and then probed with DIG-labelled wild type meningococci. It is notable that the rGal-3 and rCRD used in this study were both lactose bound. Helicobacter pylori (strain 26695), which is known to bind Gal3 was used as positive control (Fowler et al., 2006). As shown in Figure 3.2A, N. meningitidis (MC58) bound Gal-3 to a greater extent than H. pylori. In addition, the CRD part of Gal-3 was able to bind N. meningitidis strain MC58 but significantly less than the whole Gal3 molecule (Figure 3.2B, P = 0.0001). This result showed meningococcal binding with lactose bound Gal-3 full molecule and its CRD.

A
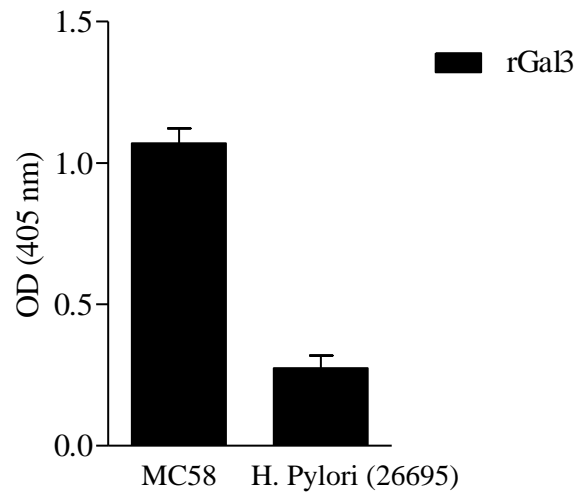
B
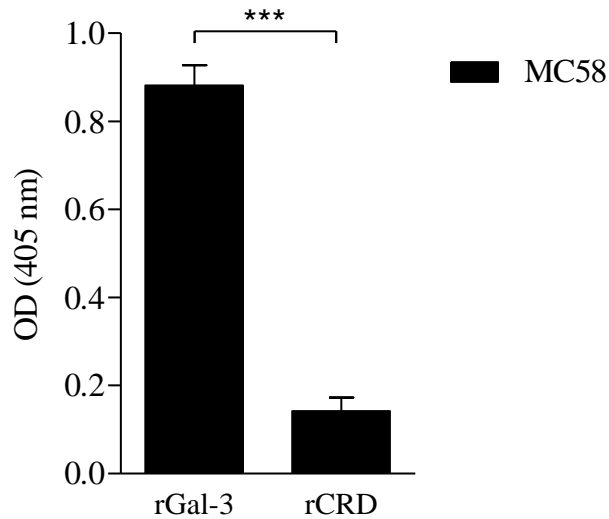
Figure 3.2: Binding of N. meningitidis to rGal-3 and its C-terminal. ELISA plates were coated with rGal-3 full molecule and rCRD. Dig-labelled N. meningitidis (MC58) and H. pylori (as negative control) were used to probe the plates and binding was measured by detecting the digoxigenin using anti-digoxigenin. BSA-coated wells were included as a negative control, and the mean value obtained from the bacteria-BSA coated wells was subtracted from rGal-3 and rCRD coated wells. The data represent the mean at wavelength of 405 nm ± SEM (error bars) of a sample tested in triplicate. Experiments were repeated three times, with consistent results. (Student's t-test; ***P < 0.001).

3.2.2. Meningococcal Galectin-3 binding is not inhibited by carbohydrates

Competition assay using different competing glycans (Table 3.2) was done to examine if the binding of rGal-3 to MC58 will be affected by these glycans or not. As shown in Figure 3.3A, the binding of MC58 to rGal-3 was not inhibited by preincubation of MC58 with different concentrations of lactose, confirming that the lactose-binding sites of Gal-3 were occupied by lactose-liganding. Other glycans were also tested for their ability to interrupt meningococcal Galectin-3 interaction. Similarly, the binding of rGal-3 to MC58 was not reduced in the presence of H type II, lewis x and y and galactose (Figure 3.3B).
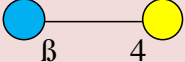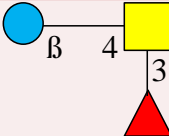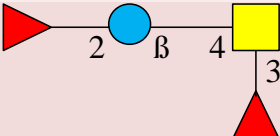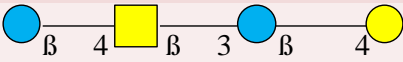
Name of sugar	Structure*	Sequence
Galactose	●	Gal
Fucose	▲	Fuc
Lactose	●—○ ß 4	Galß-4Glc
Lewis x	●—■ ß 4 ┃3 ▲	Galß-4GlcNAc 3 | Fucα1
Lewis y	▶—●—■ 2 ß 4 ┃3 ▲	Fucα1-2Galß-4GlcNAc 3 | Fucα1
H II	●—■—●—○ ß 4 ß 3 ß 4	Galß-4GlcNAcß-3Galß-4Glc

Table 3.2: Carbohydrates used in rGal-3 competition assay. *Key to Symbols:

▲ Fuc ● Gal ○ Glc ■ GlcNAc

A
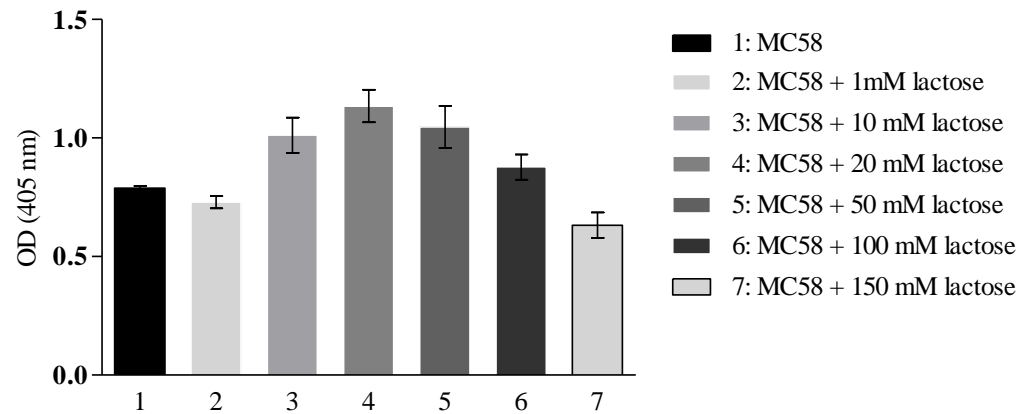
B
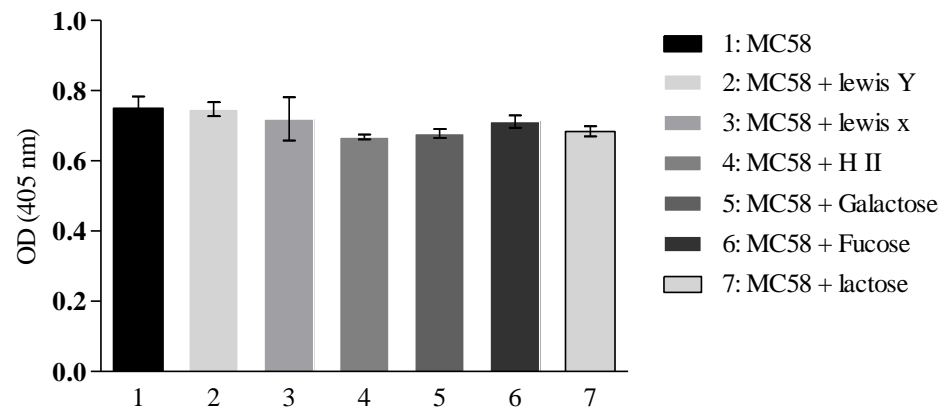
Figure 3.3: Meningococcal binding to rGal-3 in the presence ofcarbohydrate.

Binding of digoxigenin-labelled N. meningitidis strain MC58 to immobilized rGal-3 was not inhibited by pre incubation with different concentrations of lactose (A) or different sugars at concentration 30 µg/ml (B). BSA-coated wells were included as a negative control, and the mean value obtained from the bacteria-BSA coated wells was subtracted from rGal-3 coated wells. Binding of the MC58 in the absence of sugars served as positive control. The data represent the mean of optical density at a wavelength of 405 nm ± SEM (error bars) of a sample tested in triplicate. Experiments were repeated three times, with consistent results.

3.2.3.   Binding of meningococcal clinical isolates to rGal-3

To investigate whether other N. meningitidis strains (different serogroups and MLST types) could bind rGal-3, 25 N. meningitidis clinical isolates were analyzed for rGal-3 binding in comparison with the serogroup B MC58 strain. The results clearly indicate that all meningococcal strains bind Gal3, albeit to variable degrees, irrespective of their invasiveness, phenotypic characteristics or geographical distribution (Figure 3.4).
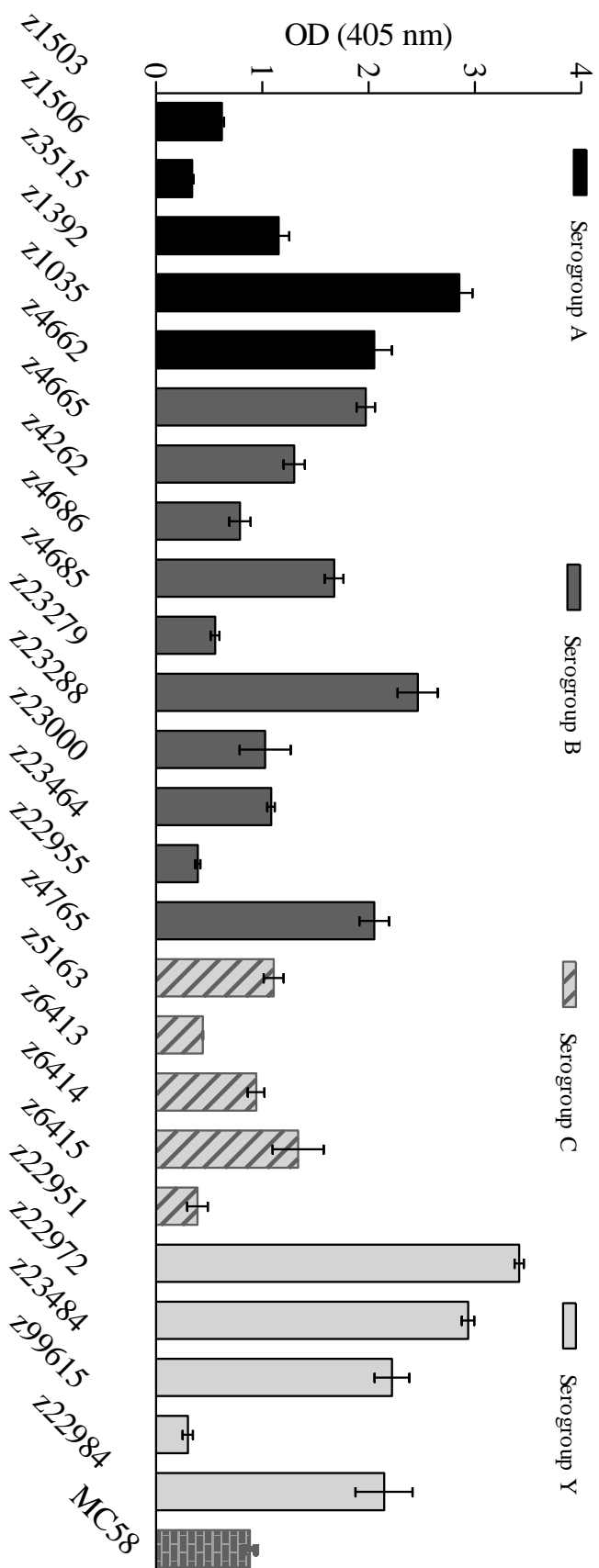
Figure 3.4: N. meningitidis clinical isolates bind rGal-3. N. meningitidis strain MC58, and 25 clinical isolates were digoxigenin labeled and allowed to interact with rGal-3 in an ELISA plate. Twenty five strains isolated were capable of galectin-3. The data represent the mean (OD) at wavelength of 405 nm ± SEM (error bars) of a sample tested in triplicate. Experiments were repeated three times, with consistent results.

3.2.4. Meningococcal Galectin-3 binding is mediated by pilus component

3.2.4.1. Retagging

To identify the non-LOS meningococcal surface ligands that mediate interaction with lactose-liganded Gal3, we employed the re-tagging (a contact-dependent cross-linking) approach in conjunction with SDS-PAGE, immunoblotting and MALDI-TOF, as previously described (Marceau et al., 1998). The principle of this technique is based on the use of a receptor-bound multifunctional crosslinker consisting of a biotin-group and a photo-reactive group, the ultraviolet irradiation covalently binds to the target adhesin, and afterwards, in a reducing condition the biotin tag will be transferred to the target protein and transfer of the biotin tag to the bound adhesin (Mahdavi et al., 2002). The re-tagging identified meningococcal PilQ and PilE as adhesins for rGal-3 as demonstrated in Table 3.3.

Gene number and name	Mass in kilodalton (kDa)	Score	Descrption of protein matched
PilQ NMB1812	82.4	2463.12	Type IV pilus biogenesis and competence protein N. menigitidis sergroup B
PilE NMB0018	18.1	2029.04	Type IV pilus pilin protein N. menigitidis sergroup B

Table 3.3: Mass spectrometry analysis of reactive bands identified from meningococcal MC58 exposed to cross linked rGal-3 (using MASCOT dataset).

3.2.4.2. ELISA

In order to further confirm the retagging results, meningococcal mutants lacking PilE and PilQ were examined in ELISA experiments for their abilities to bind Gal-3. As shown in Figure 3.5, both ΔpilQ and ΔpilE mutants showed significantly reduced Gal3 binding when compared with the wild type parent strain (P = 0.0114 and P = 0. 0.0165, respectively). Mutation of PorA (another integral outer membrane protein which binds LR) had no effect on Gal3 binding (negative control). Attempts were made to generate double knock outs of PilE and PilQ in order to examine its binding with rGal-3. Different approaches including; natural transformation, electroportaion (Duenas S et al., 1998) and chemical transformation (Bogdan et al., 2002) were carried out to obtain the clone. However, all these attempts were unsuccessful because transformation of meningococci depends on bacterial piliation, and both pilQ and PilE single mutants are non-piliated.
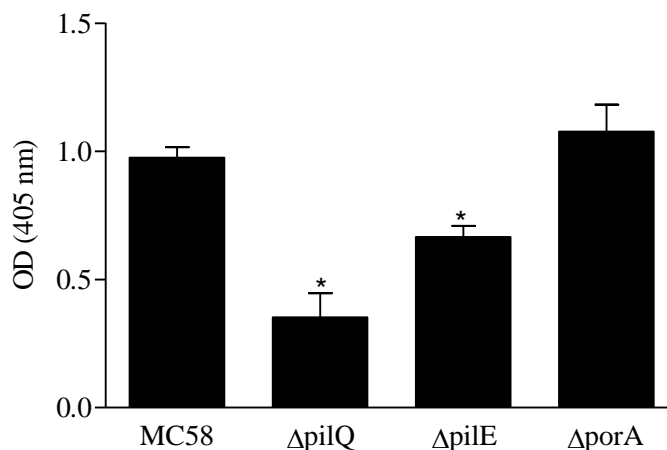
Figure 3.5: Meningococcal ligands mediate Galectin-3 binding. Binding of digoxigenin-labelled MC58 and corresponding mutants; ΔpilQ, ΔpilE, and ΔporA

(used as negative control) to rGal-3 coated ELISA plate. BSA-coated wells were included as a negative control, and the mean value obtained from the bacteria-BSA coated wells was subtracted from rGal-3 coated wells. The data represent the mean (OD) at wavelength of 405 nm ± SEM (error bars) of a sample tested in triplicate. Asterisks indicate the significant decrease of ΔpilQ and ΔpilE mutants binding to rGal-3 compared with MC58 wild type strain. Experiments were repeated three times, with consistent results. (Student's t-test; *P < 0.05).

3.2.5.   rGal-3 interacts with meningococcal LR ligands

Previous reports suggest hetero-dimerization of 67 LR with Gal-3 (Nelson et al., 2008). Moreover, 67 LR initiates contact of meningococci with the BBB (Orihuela et al., 2009). So, the possible interaction between rGal-3 and purified rLR and also the corresponding meningococcal LR- ligands, PorA and PilQ, was examined. SDS-PAGE and Western blot analysis was performed to confirm the expression. As shown in (Lane 5, Figure 3.6; 7 and 8 A and B) rPilQ (82 kDa), rPorA (42 kDa) and rLR (37 kDa) were expressed after IPTG induction and gave the expected size around 82, 42 and 37 kDa, respectively. Furthermore, the expressed proteins were purified under denaturing conditions, using immobilized metal affinity chromatographyand the purity was verified by SDS-PAGE and Western blot analysis (Lane 7, Figure 3.6; 7 and 8 A and B). In contrast, the expected bands were not observed in the negative control samples, E. coli JM109 and E. coli BL21(DE3) containing the blank plasmids PQE70 and pET28a (Lanes 3 and 6, Figure 3.8; 5 and 6 A and B). These results confirm the specificity and purity of the expressed proteins.
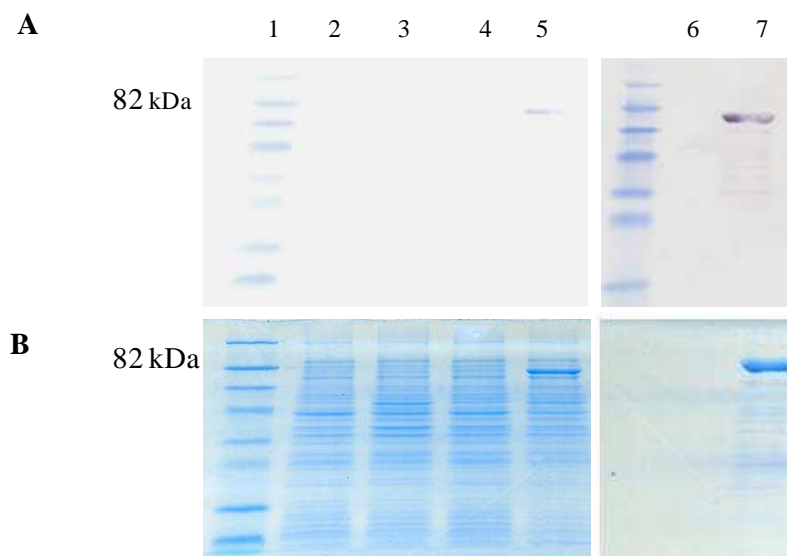
Figure 3.6: Analysis of expressed and purified 6× His-tagged rPilQ protein using metal affinity chromatography. (A) Western blot analysis; (B) SDS-PAGE analysis (Lane 1, prestained protein marker; Lane 2, Non induced E. coli PQE70 as negative control; lane3, IPTG induced E. coli JM109 PQE70 as negative control; Lane4, Non induced E. coli JM109 pPilQPNJ072 ; Lane5, IPTG induced E. coli JM109 pPilQPNJ072; Lane 6, Purified extract from E. coli JM109 PQE70 as negative control; Lane 7, Purified recombinant PilQ (rPilQ).
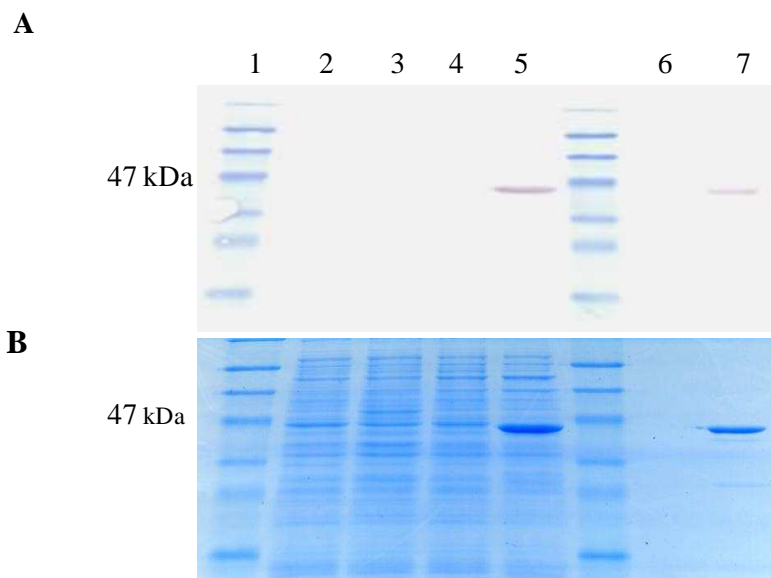
Figure 3.7: Analysis of expressed and purified 6× His-tagged rPorA protein using metal affinity chromatography. (A) Western blot analysis; (B) SDS-PAGE analysis (Lane 1, prestained protein marker; Lane 2, Non induced E. coli JM109 PQE70 as negative control; lane3, IPTG induced E. coli JM109 PQE70 as negative control; Lane4, Non induced E. coli JM109 pPorAQE30; Lane5, IPTG induced E. coli JM109 pPorAQE30; Lane 6, Purified E. coli JM109 PQE70 as negative control; Lane 7, Purified recombinant PorA (rPorA).
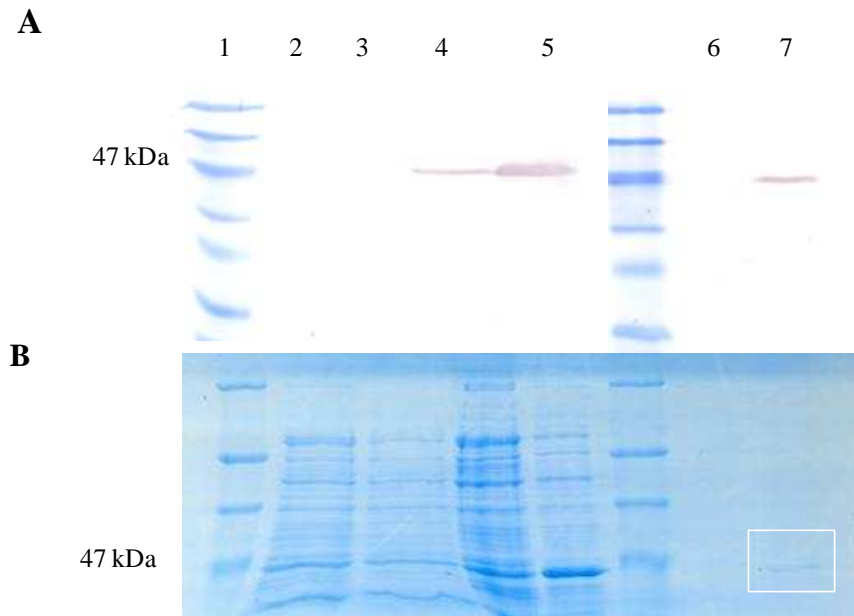
Figure 3.8: Analysis of expressed and purified 6× His-tagged rLR protein using metal affinity chromatography. (A) Western blot analysis; (B) SDS-PAGE analysis (Lane 1, prestained protein marker; Lane 2, E. coli BL21(DE3) pET28a as negative control; lane3, IPTG induced E. coli BL21(DE3) pet28a as negative control; Lane4, Non induced E. coli BL21(DE3) pET28LR; Lane5, IPTG induced E. coli BL21(DE3) pET28LR; Lane 6, Purified extract from E. coli BL21(DE3) pET28a as negative control; Lane 7, Purified recombinant LR (rLR).

The ELISA plate were coated with rGal-3, blocked and later challenged with each purified protein (rPorA and rPilQ) or loop 4 synthetic peptide. This loop has been shown to be essential for rPorA-rLR binding (Abouseada, 2009). After rigorous washing, antibodies against each protein were added to detect the interaction between the bacterial proteins and rGal-3. Immobilized galectin-3 was able to interact with each of the three proteins and loop 4 synthetic peptide, and the binding was significant (***P < 0.001 and **P < 0.01) in comparison to the negative control (BSA) used for each protein (Figure 3.9A). Stronger binding was noted for rPilQ (Figure 3.8A) with immobilized galectin-3, confirming previous

results where the binding decreased in the PilQ deletion mutant but not with the PorA deletion mutant (Figure 3.8A).

When the adsorbed rGal-3 and soluble phase proteins were reversed, such that rGal-3 was allowed to interact with rPilQ, rPorA, rLR and loop 4 synthetic peptide immobilized onto ELISA plates. The binding of adsorbed proteins with soluble Gal-3 was detected by antibodies against Gal-3. Similarly to solid phase rGal3, also Gal-3 in soluble phase soluble one bound rPilQ, rPorA, rLR and synthetic loop 4 peptide significantly (***P < 0.001 and **P < 0.01; Figure 3.9B).
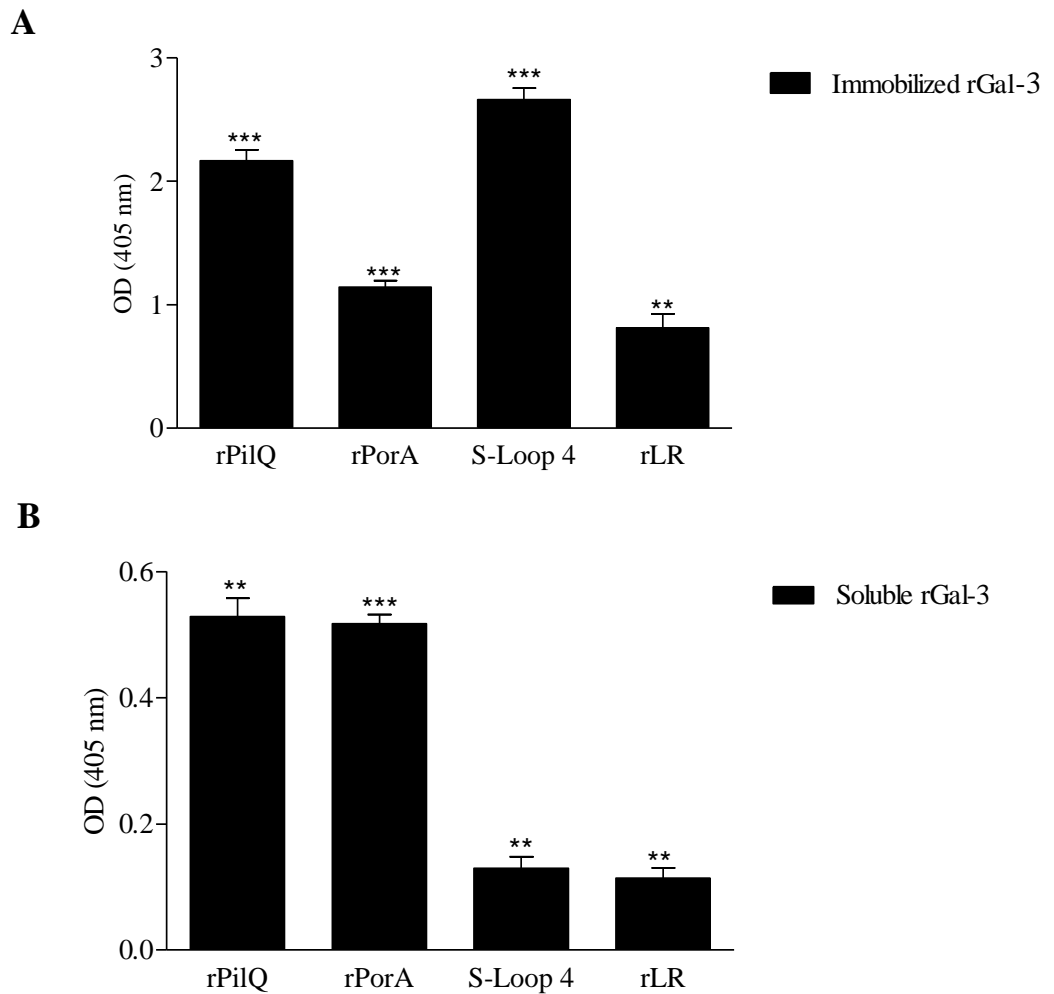
Figure 3.9: Binding of meningococcal proteins to immobilied and soluble rGal-3. Specific binding of recombinant purified proteins (LR, PorA and PilQ) and synthetic peptide (Loop 4 of PorA) to immobilized rGal-3 (A) or soluble rGal-3 to immobilized purified proteins (rLR, rPorA and rPilQ) and synthetic peptide loop 4 (B) coated ELISA plates. BSA-coated wells were considered as a negative control, and the mean value obtained from each purified protein - BSA (A) or rGal-3-BSA (B) coated wells was subtracted from rGal-3 coated wells (A) or purified proteins coated wells (B). The data represent the mean (OD) at a wavelength of 405 nm ± SEM (error bars) of a sample tested in triplicate. Asterisks indicate the significant binding of purified proteins

to rGalectin compared with BSA. Experiments were repeated three times, with consistent results. (Student's t- test; ***P < 0.001, **P < 0.01).

3.2.6.   O-glycans play roles in Gal3 binding

To investigate the impact of PilE glycosylation on the meningococcal binding to rGal-3, different pilin glycosylation mutants ΔpglC, ΔpglL and ΔpglC/L were generated and their binding with rGal-3 was compared with the MC58 wild type strain using ELISA. Mutation of pglC, pglL and pglC/L dramatically decreased rGal-3 binding by the organisms (p < 0.0001; Figure 3.10). Furthermore, using a deletion mutant lacking the gene encoding the glycosyl transferase (lgtF), which is required for chain elongation from the core lipid A-$(KDO)_2$-Hep_2, a very low but nevertheless significant Gal3-binding in comparable level with pilin glycosylation mutants was observed (Figure 3.10).
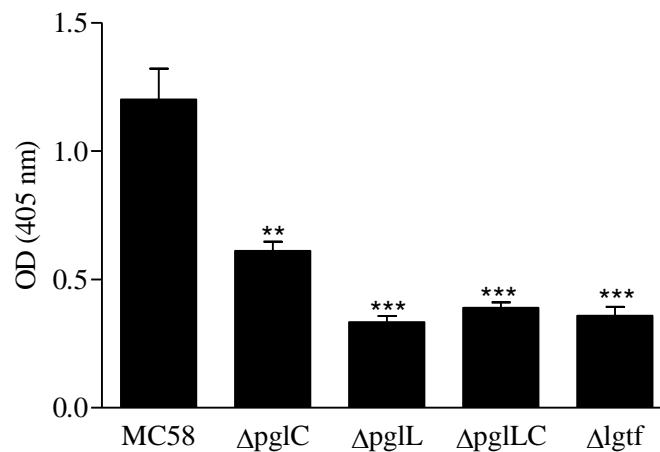
Figure 3.10: Meningococcal PilE O-glycans participate in rGal-3 binding. Binding of digoxigenin-labelled N. meningitidis (MC58), ΔpglC, ΔpglL, ΔpglC/L and Δlgtf to rGal-3 coated ELISA plate. BSA-coated wells were included as a negative control, and the mean value obtained from the bacteria-BSA coated wells was subtracted

from rGal-3 coated wells. The data represent the mean (OD) at a wavelength of 405 nm $\pm$ SEM (error bars) of a sample tested in triplicate. Asterisks indicate the significant decrease of ΔpglC, ΔpglL, ΔpglC/L and Δlgtf binding to rGal-3 compared with MC58 wild type strain. Experiments were repeated three times, with consistent results. (Student's t test; ***P < 0.001, **P < 0.01).

3.3. Discussions:

The gram-negative bacterium N. meningitidis continues to cause septicemia and meningitis across the world. It has the ability to cross the tight junction of the BBB and gain access to the CSF, where it can cause meningitis. Recently, much attention has focused on understanding the mechanism of interaction between the pathogen and BBB, which has led to the identification of several host receptors and pathogen adhesins (Orihuela et al., 2009; Unkmeir et al., 2002; Virji et al., 1994). The 37 LRP/67 LR is one of these receptors identified recently, which is targeted by meningococcal PorA and PilQ, pneumococcal CbpA and OmpP2 of H. influenza (Orihuela et al., 2009).

Prevention of the 37 LRP/67 LR interaction with meningitis causing pathogens, by administration of polypeptides mimicking the binding proteins expressed on the surface of these pathogens, has been used as an approach for the development of a vaccine (St. Jude Children's Research Hospital, 2008; University of Nottingham, 2009). Importantly, it has been suggested that the 37 LRP/67 LR underlies the CNS tropism of the three most common bacteria causing meningitis: N. meningitidis, S. pneumonia and H. influenza (Orihuela et al., 2009). Such significance of the 37 LRP/67 LR in term of meningococcal CNS tropism and as therapeutic target for treatment or prevention of meningococcal disease, require further characterization of the 67 LR dimer form in the BBB. Several studies suggest heterodimerization of 37 LRP with Gal-3 to form mature 67 LR (Buto et al., 1998; Castronovo et al., 1992). Galectin-3 is a ß-galactoside binding lectin that acts as receptor for many pathogens (Vasta, 2009). Although, both 37 LRP/67 LR and Gal-3 exist in different cells and organs and participate in different disease, their role in the CNS has only emerged recently (Bellac et al., 2007; De

Giusti et al., 2011; Gauczynski et al., 2001; Mok et al., 2007; Orihuela et al., 2009).

In the literature, the interaction of Gal-3 with meningococcal LOS is predicted based on the presence of a carbohydrate moiety, N-acetyl lactoseamine (Gal-GlcNAc), a known ligand for Gal-3 within the N. meningitidis LOS (Vasta, 2009). Such prediction has been verified recently by Quattroni and co-workers (2012), who showed that the presence of lactose, a known ligand for Gal-3, partially inhibited meningococcal binding with Gal-3. This reveals involvement of other bacterial ligands in addition to the LOS in Gal-3 binding. Therefore, lactose bound Galectin-3 has been used in the current study in an attempt to identify non-LOS meningococcal ligands. The series of results provided in this chapter show that lactose liganded Gal-3 binds N. meningitidis and that the N-terminal domain of Gal-3 appears to mediate the majority of this interaction (Figure 3.2). Nevertheless, the CRD domain of Gal-3 also binds meningococci, but to a less extent when compared to the N-terminal domain (Figure 3.2). Importantly, Gal-3 binding was not limited to the reference strain used, but extended to 25 other meningococcal clinical isolates (Figure 3.3). This indicated that the binding of Gal-3 is conserved among meningococcal clinical isolates.

The retagging approach was used in the current study to identify non-LOS meningococcal ligands that bind lactose bound Gal-3. This approach identified the outer membrane protein (PilQ) and the major pilin subunit (PilE) as the two potential N. meningitidis adhesins for lactose liganded Gal-3 (Table 3.3). Mutations of meningococcal PilE and PilQ genes significantly reduced Gal3 binding when compared with wild type parent strain (Figure 3.5), confirming the

retagging approach results. Interestingly, PilQ is a known adhesin for 37 LRP/67 LR (Orihuela et al., 2009), which is an antigenically conserved outer membrane secretin (Hansen & Wilde, 1984) that is fundamental for type IV pilus expression at the cell surface (Tonjum et al., 1998). It has a doughnut-like appearance with an apparent cavity (Frye et al., 2006) and forms a large (960 kDa) homododecamer complex, which is capable of generating bactericidal antibodies (Corbett MJ, 1988). Immunization with the PilQ complex has been shown to elicit bactericidal and opsonic antibodies in mice as well as protect mice against bacteremic meningococcal disease (D. Halliwell, 2004). Although it is an abundant outer membrane protein, mice immunized with OMVs containing upregulated PilQ produced higher levels of anti-PilQ antibodies (Jan T. Poolman, 2006). Recombinant PilQ significantly bound soluble and immobilized human rGal-3, supporting the demonstrated decrease in PilQ null mutant binding to rGal-3 (Figure 3.9). Previous work showed that the rPilQ used were able to bind rLR in ELISA and inhibited the meningococcal interaction with the rLR (Abouseada, 2009). Additionally, fluorescent beads bearing rPilQ bound LR in mice, as seen through cranial window (Orihuela et al., 2009). There is no evidence yet for PilQ glycosylation, suggesting possible protein-protein interaction with Gal-3. This suggestion is in agreement with a previous study showing that Mannose binding lectin (MBL), another type of lectin, binds nonglycosylated outer membrane proteins, Opa and PorB, of N. meningitidis in a carbohydrate independent manner (Estabrook et al., 2004).

Surprisingly, recombinant purified PorA and its loop 4 peptide, which appears to be important for the 37 LRP/67 LR-PorA interaction (Abouseada, 2009), also bound rGal-3 (Figure 3.9). However, in the context of intact MC58 bacteria,

neither retagging nor ELISA identify PorA as an adhesin for Gal-3, revealing that PorA might be sterically hindered by other surface structures, which may be affecting its recognition by rGal-3. One of the limitations of the above ELISA data is that the bacterial proteins (rPilQ, rPorA and rLR) and peptide (loop 4 of PorA) were used in ELISA at equal-weight (5µg/ ml) but not at equi-molar concentrations. This might contribute to the observed increase in binding of loop 4 peptide with Gal-3 compared with other bacterial proteins (Figure 3.9A). In future investigations it will be necessary to use equimolar concentrations of these bacterial proteins and peptide to test their binding with Gal-3.

Taking into consideration that the PorA mutant is still expressing meningococcal Gal-3 ligands (PilQ and PilE), this may compensate PorA deletion and explain the non-diminishing binding of ΔPorA with rGal-3. However, N. meningitidis PilQ null mutants are non piliated and form pilus fibers trapped in the periplasm and not exported to the bacteria surface (Carbonnelle et al., 2006; Tonjum et al., 1998). Additionally, another study has showed that deletion of PilQ in N. gonorrhea led to expression of extra cellular rare pilus filament (Drake & Koomey, 1995). In general, all Neisseria sp. PilQ mutants lack the property of autoagglutination and are non competent for DNA transformation which dependent on functional pilus expression (Drake & Koomey, 1995; Tonjum et al., 1998). These indicate that the T4p produced by PilQ mutant is not properly functional. Therefore, the observed reduction of ΔpilQ binding to rGal-3 appears to have resulted from deletion of PilQ and non functional PilE collectively (Figure 3.5). It is possible therefore that N. meningitidis PilE facilitates initial adhesion with Gal-3, then when the T4p expression is downregulated to enable intimate contact, the Pilus retracts and thus the PilQ firmly binds Gal-3. A

secondary intimate contact could be mediated through PorA, more specifically its surface exposed loop 4.

Another meningococcal Gal-3 ligand is PilE, the major pilin subunit protein of the type IV pilus (T4p). T4p play important roles in the initial adhesion to human cells and survival of meningococci in the human host during both colonization and disease (Pelicic, 2008; Pujol et al., 1997; Virji et al., 1991). PilE is expressed as prepilin and cleaved by a prepililn peptidase, PilD, to form the pilus fibre, which extrudes through PilQ. PilE is known to undergo several post-translational modifications including O-glycosylation (Banerjee & Ghosh, 2003). The meningococcal O-glycan is synthesized by the sequential action of the pilin glycosylation (pgl) enzymes, including pglC, and final sugar molecule is transferred onto PilE by the action of the ligase pglL (Power et al., 2006). Interestingly, the current study showed that the mutation of pglL or pglC or both of them, dramatically decreased Gal3 binding by the organisms (Figure 3.10). It is interesting that pglL or pglC enzymes are not involved in meningococcal LOS biosynthesis and their mutation has no effect on the LOS structure or function (Kahler et al., 2001; Power et al., 2000; Power et al., 2006). These strongly suggest that at least part of the Gal3-meningococcus binding is mediated by PilE's O-glycan modification, which does not appear to compete with the LOS glycans.

Such interaction of N. meningitidis pilin O-glycan with Gal-3 may have important role in meningococcal pathogenesis. Since in P. aureginosa, pilin glycosylation is suggested to be a strong virulence factor. In this study, mutation of the pilO gene analogue of the N. meningitidis pglL gene, decreased bacterial twitching

motility, increased specificity to pilus specific bacteriophage and significantly decrease survival in the lung environment (Smedley et al., 2005). In a previous study, N. meningitidis strain 8013 pilin glycan showed no deffect on bacterial piliation and/or adhesion (Marceau et al., 1998). However, a recent study demonstrated that pilin glycosylation is engaged in invasion of N. gonorrhoeae into host cells (Jennings et al., 2011).

It would be useful to use complementation approaches to genetically confirm that meningococcal-Gal-3 binding is mediated by PilQ and PilE. However, it should be noted that PilQ protein is required for the natural transformation of N. meningitidis as mentioned earlier (Drake & Koomey, 1995; Tonjum et al., 1998). Thus, it is not possible using this technique to complement the pilQ mutant. In the other hand, several attempts were made to generate PilE complemented mutants using natural transformation, electroportaion (Duenas S et al., 1998) and chemical transformation (Bogdan et al., 2002), however, all these attempts were unsuccessful.

To the best of our knowledge, this is the first in vitro study demonstrating the contribution of N. meningitidis pilus components (PilE and PilQ) in Gal-3 binding. This finding is unique because most studies in the field of Gal-3-baterial binding have mainly focused on LPS as potential ligands. Interestingly, one study has shown that non agglutination fimbriae (NAF) of P. mirabilis binds Gal-3 in the outer membrane fraction of Madin-Darby canine kidney (MDCK) by overlay analysis (Altman et al., 2001). In this study, a monoclonal antibody against Gal-3 N-terminal (Mac-2) inhibited the interaction between P. mirabilis and MDCK

cells. Furthermore, there was no detectable binding between P. mirabilis LPS and Gal-3 (Altman et al., 2001).

In summary, the data represented in this chapter shows that Gal-3 targets N. meningitidis via its N-terminal (non-lectin domain). This binding was preserved among different meningococcal clinical isolates. Additionally, Gal-3 targets the major pilin subunit, PilE and pilus secretin PilQ of meningococci. Interestingly, knocking out pglL and pglC genes decline Gal-3 binding, which reveal the participation of PilE O-glycan in the Gal-3 interaction with meningococci. Moreover, soluble recombinant proteins (LR, PilQ and PorA) and loop 4 synthetic peptide of PorA bind immobilized Gal-3 and vice versa.

4. Chapter 4: Surface distribution of Laminin Receptor and Galectin-3.

4.1. Introduction:

N. meningitidis must cross the BBB to cause meningitis. The BBB itself provides a stable environment for neural function by controlling the passage of molecules across the brain, and protects the brain from any microorganisms and toxins that are circulating in the blood (Kim, 2008). It is composed of brain microvascular endothelial cells, astrocytes and pericytes (Kim, 2008). Brain microvascular endothelial cells (BMEC) form the front line defense against invading pathogens. Subsequently, most of the research into meningococcal meningitis has focused on the interaction between meninigococci and brain endothelial cell lines. They differ from peripheral endothelial cells as they are continuous and characterized by tight intracellular junctions, high transendothelial electrical resistance and reduced level of endocytotic vesicles (Rubin & Staddon, 1999). Astrocytes are the most abundant cells in the CNS, which provide physical and nutritional support for neuron. In addition, an in vitro study has shown that the biogenesis of brain endothelium tight junctions is controlled by a factor produced from astrocytic end-feet ensheathing brain capillaries (Arthur et al., 1987). Importantly, astrocytes are activated by CNS microbial pathogens, including Neisseria meningitidis and inflammatory cytokines, hence, playing significant role in CNS inflammation (Chauhan et al., 2008).

The availability of in vitro models (HBMECS, astrocytes and microglia) enables a better understanding of meningococcal pathogenesis. Therefore, to understand the role of Gal-3 as a potential meningococcal host receptor, and to investigate its possible dimerization with 37 LRP to form the 67 LR heterodimer, the surface distribution and expression pattern of 67 LR, 37 LRP and Gal-3 in HBMECs and astrocytes will be investigated in this chapter.

Galectin-3 is a unique β-galactoside binding lectin, which consists of three different domains: an N-terminal domain (ND), a repeated collagen-like sequence rich in proline, glycine, tyrosine and glutamine residues, and a CRD domain (Figure 4.1) (Barondes et al., 1994b). Galectin-3 exists in the cytoplasm and can be translocated to the nucleus, exported to the cell surface and excreted by a non-classical, ER/Golgi-independent secretory pathway outside of cells (Dagher et al., 1995; Hughes, 1999; Sato & Hughes, 1994).

C-terminal CRD domain

PGAYPG(x)1-4

N-terminal domain
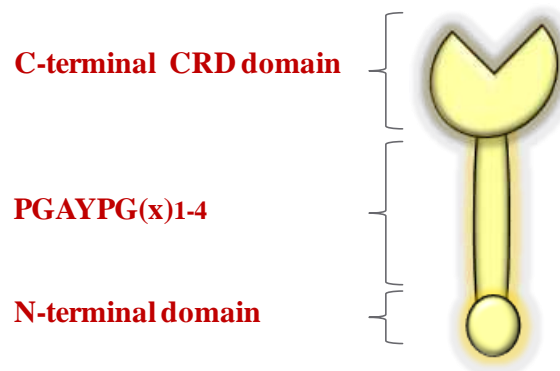
Figure 4.1. Schematic representation of the Galectin-3 structure. The Gal-3 is composed of: the carbohydrate recognition domain (CRD) of about 130 amino acid residues, the proline-, glycine-, and tyrosine-rich repeating domain of about 100 amino acid residues and the N-terminal domain of about 30 amino acid residues. The figure was adopted from (Barondes et al., 1994b).

Many of the Gal-3 biological activities depend on its cellular localization. For instance, cytoplasmic Gal-3 inhibits cell apoptosis through binding with apoptosis repressor Bcl-2 (Yang et al., 1996). In addition, and in the cytoplasm, Galectin-3 interacts with activated GTP-bound K-Ras, and this interaction has shown to be involved in Gal-3-mediated transformation (Elad-Sfadia et al., 2004). In the

nucleus, Galectin-3 acts as pre-mRNA splicing factor, and is involved in the regulation of gene transcription (Dagher et al., 1995; Lin et al., 2002). Although the nuclear and cytoplasmic localization of Gal-3 is well established, several factors have been reported to affect its localization. These factors include: the source of the cell under study, cell type, culture conditions, and proliferation status of the cell (Dumic et al., 2006). On the other hand, extracellular Gal-3 is involved in cell-cell and cell-matrix interactions, immune reaction and angiogenesis, by binding to the glycan moiety of cell surface glycoconjugates, via the CRD (Dumic et al., 2006). In addition, cell surface Gal-3 mediates homotypic cell adhesion by bridging through branched, soluble complementary glycoconjugates (Inohara et al., 1996). Moreover, it has been shown recently that surface Gal-3 confers resistance to death-receptor mediated apoptosis by immobilizing them in glycan nano-clusters (Mazurek et al., 2012).

In addition to cellular localization, post-translational modification of Gal-3 is involved in the regulation of its biological function. Galectin-3 undergoes two distinct post-translational modifications: its cleavage and phosphorylation. There are two serines at positions 6 and 12 of the Gal-3 N-terminal domain that have been reported to be phosphorylated by casein kinase 1 (Huflejt et al., 1993). The serine phosphorylation reduces Gal-3 binding to its glycoprotein ligands, such as laminin, which is proposed to be involved in the regulation of the multivalent binding activity of Gal-3 (Mazurek et al., 2000). It also plays a role in the translocation of Gal-3 between the nucleus and the cytoplasm (Cowles et al., 1990). In addition, it appears to be required for the anti-apoptotic activity of Gal-3 (Yoshii et al., 2002). This was evident by the ability of wild type Gal-3, but not serine substituted Gal-3, to protect human breast carcinoma cells from cisplatin-

induced apoptosis (Yoshii et al., 2002). Additionally, phosphorylation of Gal-3 at tyrosine residue was reported to be important for the repair of hepatocytes injured by administration of CCl4 (Yamazaki et al., 2001). The other post-translational modification of Gal-3 is its susceptibility to cleavage by certain matrix metalloproteinases, MMP-2 and MMP-9 at the Ala62–Tyr63 peptide bond (Ochieng et al., 1998). The cleavage of Gal-3 is involved in progression of cancer, angiogenesis and apoptosis resistance in mouse models (Nangia-Makker et al., 2007).

The 67 LR is a non-integrin cell surface receptor, which plays an important role in normal physiological and pathological state. Isolation of 67 LR from cells shows a size at 67 kDa on the denaturing polyacrylamide gel, however, its gene encodes a protein of only 33 kDa, which migrates with an apparent molecular mass of 37 kDa on SDS-PAGE (Nelson et al., 2008). This 37 kDa gene product of 67 LR is well established to be a precursor form, named 37 LRP (37 kDa laminin receptor precursor) (Menard et al., 1997; Nelson et al., 2008). Interestingly, the 37 LRP has been found to be associated with the 40S ribosome, and also interacts with histones in the nucleus, in addition to its function as a precursor for the cell surface laminin binding receptor 67 LR (Ardini et al., 1998; Kinoshita et al., 1998).

Several hypotheses have been suggested, including posttranslational modification or formations of homo- or hetero-dimers, to explain mature 67 LR and 37 LRP molecular mass discrepancies (Landowski et al., 1995; Simona Butò, 1998). Landowski and Butò have shown that 37 LRP is post translationally modified by acylation (Fatty acylation is the covalent attachment of long chain fatty acids to

proteins) to form the surface mature form of 67 LR (Landowski et al., 1995; Simona Butò, 1998). Protein acylation is one of the major post-translational modifications, which is involved in protein trafficking, protein-protein interaction, lipid raft association, membrane targeting and protein signalling (Towler, Gordon et al. 1988; Resh 1999). The most common types of eukaryotic protein acylation are N-myristoylation, and S-palmitoylation. The N-myristoylation is the stable addition of 14-carbon saturated fatty acids to a glycine in the N-terminal end of the amino acid chain, via an amide bond (Resh, 1999; Towler et al., 1988). The N-myriosylated protein has a consensus recognition sequence (Met-Gly-X-X-X-Ser/Thr) in which methionine is removed co-translationally by methionine aminopeptidase, and then myristic acid is linked to the glycine via an amide bond (Resh, 1999; Towler et al., 1988).

S-palmitoylation or more specifically S-acylation refers to the covalent attachment of palmitate or other long chain fatty acids to the thiol of cysteine residues via an ester link. Due to the labile nature of the thioester linkage, the S-acylation is reversible (Resh, 1999; Towler et al., 1988). Another type of fatty acylation is called N-palmitoylation, and was first described in the secreted Sonic Hedgehog protein (Pepinsky et al., 1998). In N-palmitoylation, the palmitate is added irreversibly to a cysteine residue at the N terminus of a protein via an amide link. Another report has shown that N-palmitoylation occurs also at the N-terminal glycine of $G_{S\alpha}$ (Mumby et al., 1994).

It has been reported that the 67 LR is acylated by three fatty acids: palmitate, oleate and stearate (Landowski et al., 1995). In another study, formation of 67 LR was found to be inhibited by a fatty acid synthase inhibitor, such as cerulenin (Simona Butò, 1998). Furthermore, treatment with hydroxylamine led to cleavage

of 67 LR, suggesting ester-bound fatty acids, mainly palmitate, bound to cysteine (Buto et al., 1998). On the other hand, there was no effect on the size of protein after O-glycanase, neuraminidase or Endo-F glycosidase treatments (Landowski et al., 1995). Taken together, this indicated the involvement of S-acylation specifically palmitoylation in the 67 LR maturation process, however, glycosylation did not play a role in this process. The palmitoylation occurs most commonly on cysteine residues, and interestingly, the 67 LR has two-cysteine residues at position 148 and 163 in the C-terminal, which may be the amino acids subjected to palmitoylation.

Both Gal-3 and 67 LR are multifunctional proteins that are ubiquitously expressed in a variety of tissues and cell types including endothelial cells (Orihuela et al., 2009; Thijssen et al., 2008). To understand the dimerization status of 67 LR as a homo or heterodimer with Gla-3, the distribution and expression pattern of these receptors will be investigated in this Chapter.

Fluorescent tagging of cellular protein is a useful method to visualize cellular distribution of many proteins including Gal-3 and 67 LR/37 LRP. The green fluorescent protein (GFP) was first isolated from the jellyfish, Aequorea victoria and found to be an ideal fluorescent tag for direct visualization of protein in living cells (Prasher et al., 1992). This protein consists of 240 amino acids, and folds into an 11 ß-sheet barrel that accommodates an internal distorted helix. The chromophore is generated by auto-catalytic cyclisation and subsequent oxidation of three amino acids (Ser65, Tyr66, and Gly67) that are located in the central portion of the internal helix (Figure 4.2) (Rose et al., 2010). Residues at position

66 and 67 are strictly conserved in all known GFP like proteins, while serine 65 may vary. Different GFP variants that cover a broad spectrum of fluorescence excitation and emission wavelengths have been identified recently (Nagai et al., 2002). These variants result from alteration of the three amino acids constituting the chromophore, as well as the surrounding residues. Because the maturation of the GFP chromophore takes a long time, and it is highly sensitive to experimental conditions such as PH and salt contents, the Venus YFP has been developed (Nagai et al., 2002) (Figure 4.2). This variant of YFP is characterized by fast maturation, bright fluorescence and insensitivity to environmental changes and will be used in the current study (Nagai et al., 2002).
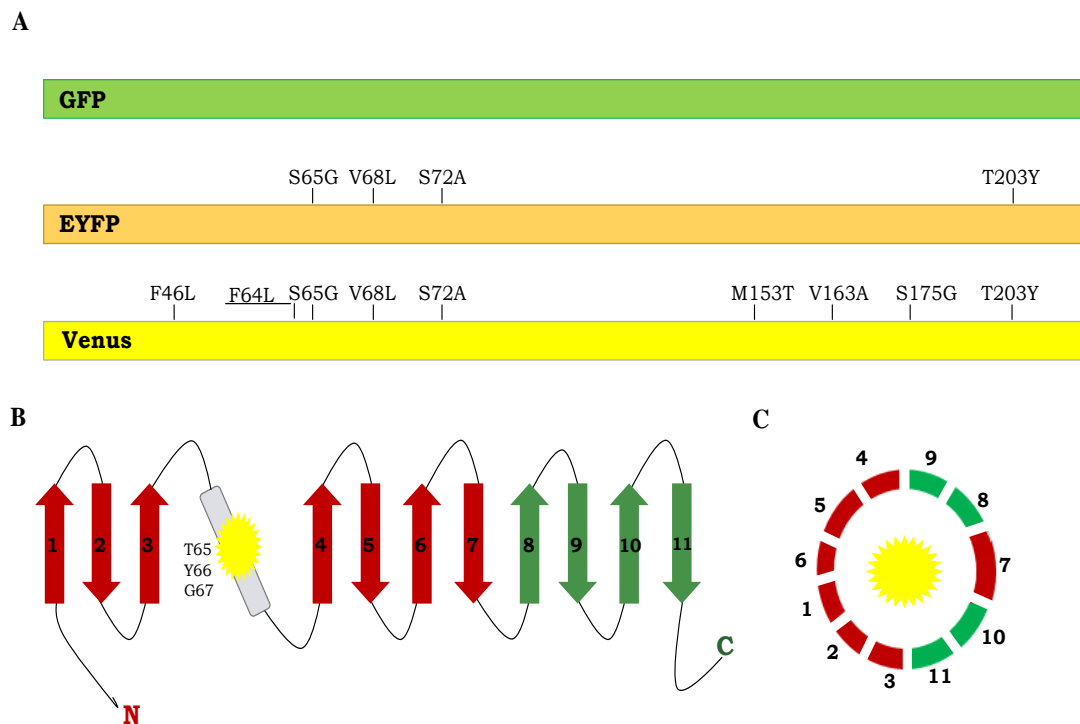
Figure 4.2: Structure of Green Fluorescent Protein (GFP). (A) A schematic view of the green fluorescent protein (GFP) and two of its variants (EYFP and Venus YFP). The indicated residues are substitutions from GFP. Adapted and modified from

(Shyu et al., 2006). (B) A schematic diagram showing the structure of Aequorea fluorescent protein, which is composed of 11 β strands. The amino acids, which develop into the chromophore, are located in a helix, connecting strand 3 with 4 (Rose et al., 2010). (C) A schematic diagram showing formation of β barrel structure upon refolding of the non fluorescent fragments generating the chromophore, as indicated by yellow star in the centre. Adapted and modified from (Rose et al., 2010).

Previously, 37 LRP tagged to different fluorescent proteins have been used to study its subcellular distribution with prion protein (PrP) in baby hamster kidney (BHK) cells (Nikles et al., 2008). In addition, Galectin-3 labelled with GFP and other GFP variants was utilized in previous studies to understand the subcellular distribution of Gal-3 with different cellular proteins (Nakahara et al., 2006).

The key aim of this chapter was to study surface distribution of Gal-3, 67 LR and 37 LRP. The expression and surface distributions of endogenous receptors were studied by; western blot, flow cytometry and immunofluorescence staining. The Receptors were then cloned into different fluorescent proteins to facilitate characterization of receptor distribution and subsequent understanding of receptor dimerization in Chapter 5. Moreover, investigation of the effect of cysteine substitutions into alanine at position 148 and 163 of 37 LRP, on the cellular distribution of fluorescently labelled receptors, was carried out.

4.2. Results:

4.2.1. Surface distribution of endogenous 67 LR, 37 LRP and Gal-3

To understand the expression and surface distribution of Gal-3 as a potential host receptor for meningococci, and of 67 LR/37 LRP, for its possible heterodimerization with Gal-3, several approaches including Western blotting, flow cytometry and immunofluorescence were carried out.

4.2.1.1. Immunoblotting

Total cell extracts of primary HBMECs, the major component cells of the BBB, were analyzed by immunoblotting to assess receptor expression using anti-67 LR, anti-37 LRP, and anti-Gal-3 antibodies. As shown in Figure 4.2A, a polyclonal antibody Ab711, directed against amino acids residue 263-283 of the laminin receptor (Castronovo et al., 1991b), detected both 37 LRP and 67 LR, at a predicted molecular mass of 37 kDa and 67 kDa, respectively. Whereas InHLRP antibody, which was directed against recombinant LR, recognised only a 37 kDa band (Figure 4.3B, lane 1). Both Ab711 and InHLRP antibodies detect recombinant LR in western blot (Figure 4.3A and B, lane 3), revealing antibody specificity. Furthermore, Gal-3 was detected with an apparent molecular mass of approximately 30 kDa, using a monoclonal antibody against human Gal-3 (mab4033) (Figure 4.3C, lane 1). This antibody is directed against the N-terminal of Gal-3, and reacted with recombinant Gal-3 (Figure 4.3C, lane 3). Another polyclonal antibody against Gal-3 recognized the same band (data not shown). The results have shown that primary HBMECs express 67 LR, 37 LRP and Gal-3.
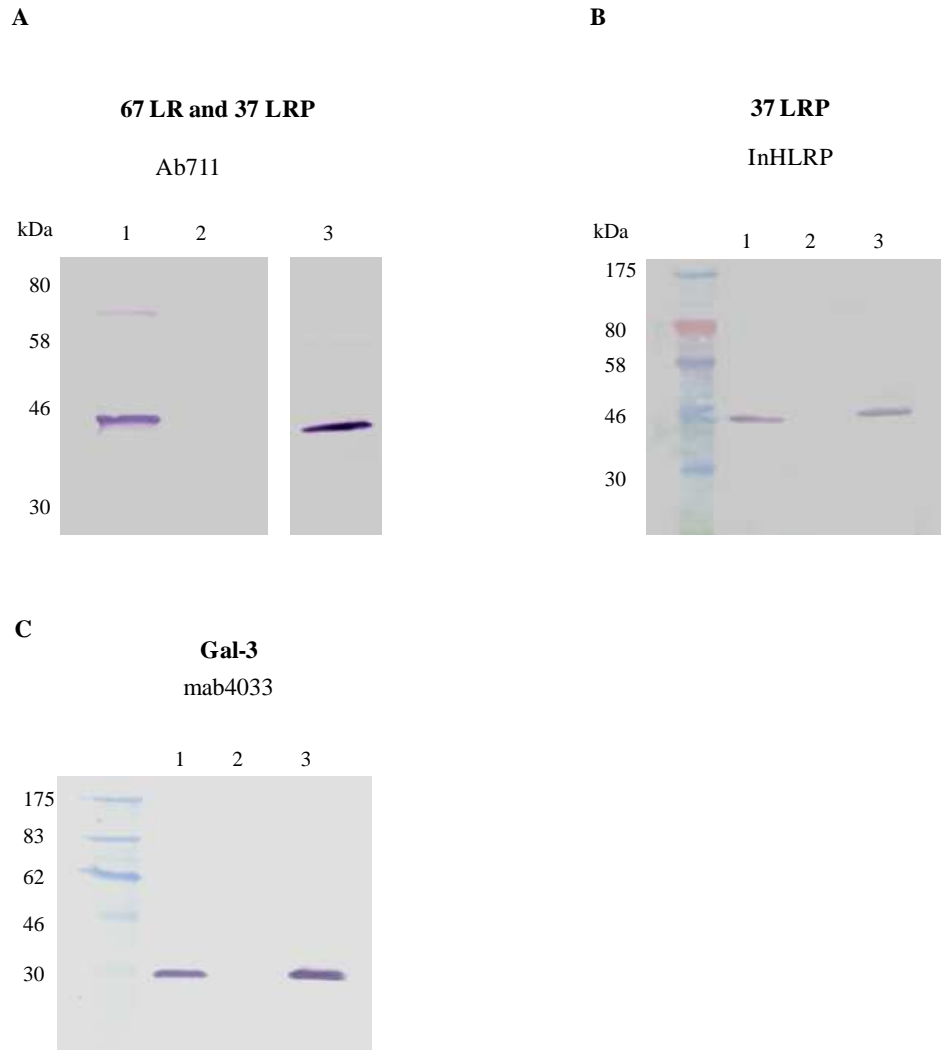
Figure 4.3: Immunoblotting analysis of 67 LR, 37 LRP and Gal-3 expression in HBMECs. Samples were separated on a 10% SDS-PAGE and blots were incubated with anti-67 LR (Ab711; 1:1000) (A), anti-37 LRP (InHLRP; 1:1000) (B), and anti-Gal-3 (mab4033; 1:10000) (C), then detected with anti-rabbit and anti-mouse alkaline phosphatase (1:10,000 dilution) for 67 LR and its precursor form and Gal-3, respectively. Lane 1, Total HBMECs cell extracts; Lane 2, Bovine serum albumin as negative control; and Lane 3, Purified rLR (A and B) and rGal-3 (C) as positive control.

4.2.1.2. Surface expression by flow cytometry

Next, surface expression of Gal-3 in HBMECs was examined and compared with 67 LR and its precursor using flow cytometry analysis. As shown in Figure 4.4, histograms analysis of FACS data showed the right shift of HBMECs and approximately 70%, 80% and 64% of the cells expressing 67 LR, 37 LRP and Gal-3 on their surface, respectively. The results indicated that Gal-3 was localized on the surface of HBMECs in comparable levels with 37 LRP and 67 LR.
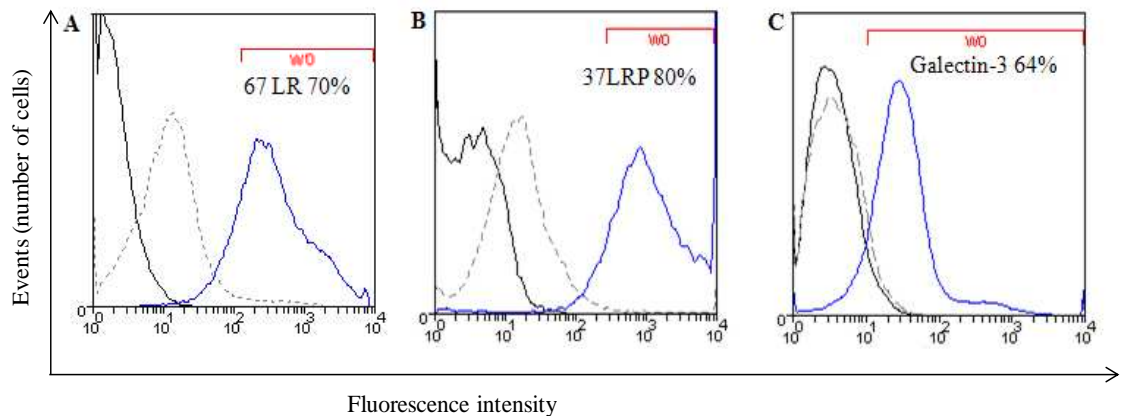
Figure 4.4: Flow cytometric analysis of cell surface localization of 67 LR, 37 LRP and Gal-3 in HBMECs. HBMECs were analyzed for (A) 67 LR, (B) 37 LRP and (C) Gal-3 surface levels. HBMECs incubated for 1 h at 4°C with 1:10 dilutions of anti-67 LR (Mlu5) (A), 37 LRP (InHLRP) (B) and Gal-3 (mab4033) (C) antibodies. Followed by detection with a 1:50 dilution of Goat anti-mouse IgM Alexa Fluor 647 (A), Goat anti-rabbit IgG Alexa Fluor 488 (B) and Goat anti-mouse IgG Alexa Fluor 488 (C) for 1h at 4°C, and the cells were analysed by flow cytometry. Histogram overlays of HBMECs alone (black curves), HBMECs incubated with secondary antibodies alone as the negative control (dot curves), and HBMECs incubated with primary and secondary antibodies (blue curve), were generated showing intensity of fluorescence on the x-axis and number of cells (events) on the y-axis. Fifty thousand cells were counted per

experiment, and W0 is the marker region, which indicates the fluorescence from positive staining. Percentages indicate the proportion of events within region W0, subtracted from secondary antibodies as a background in percentage.

4.2.1.3.   Immunofluorescence

To get more insight in the surface distribution pattern of the Gal-3 and different isoforms of 67 LR, immunofluorescence staining was performed on fixed non permeabilized HBMECs. Apical membranes staining of 67 LR using Mlu5 and Ab711 antibodies showed distinct punctuated staining in HBMECs as shown in Figure 4.5. On the other hand, 37 LRP showed more diffuse membrane staining (Figure 4.5). Galectin-3 exhibited diffuse and punctate membrane staining using the mab4033 antibody (Figure 4.5). Use of other polyclonal and monoclonal (Mac-2) anti-Gal-3 antibodies resulted in a similar staining pattern (data not shown). To compare the pattern of the surface-expressed receptors in other constituents of the BBB, immunofluorescence staining was also performed on a human astrocyte cell line. As demonstrated in Figure 4.5, patterns of the Gal-3, 67 LR and 37 LRP expressions in astrocytes were similar to those observed in HBMECs. In addition, positive diffuse staining for the 37 LRP and Gal-3 were exhibited in COS7 cells, which was the cell line used later for transfection of constructed receptors. Control experiments were performed with secondary antibodies alone, to rule out the possibility of a nonspecific fluorescence signal.

A

HBMECs

HBMECs

67 LR
MluC5

67 LR
Ab711

HBMECs

HBMECs

Gal-3
mab4033

37 LRP
InHLRP

B

Astrocyte

Astrocyte

67 LR
MluC5
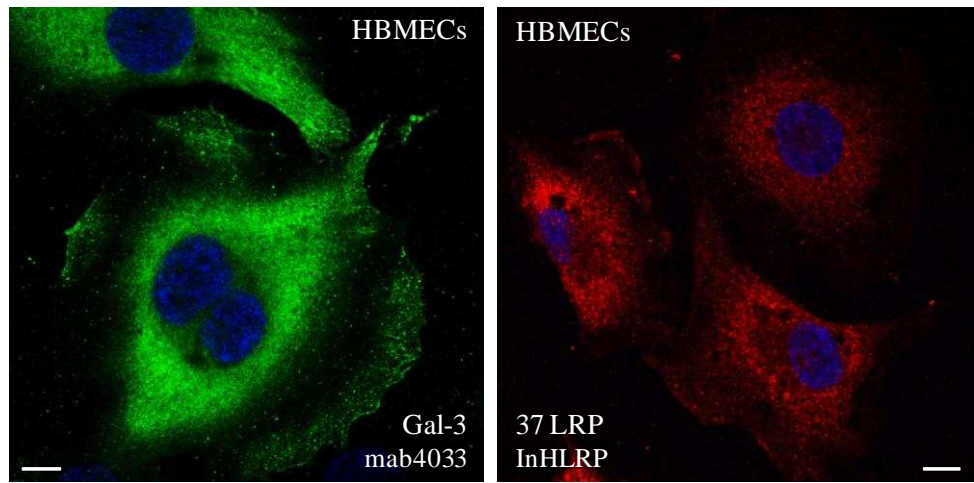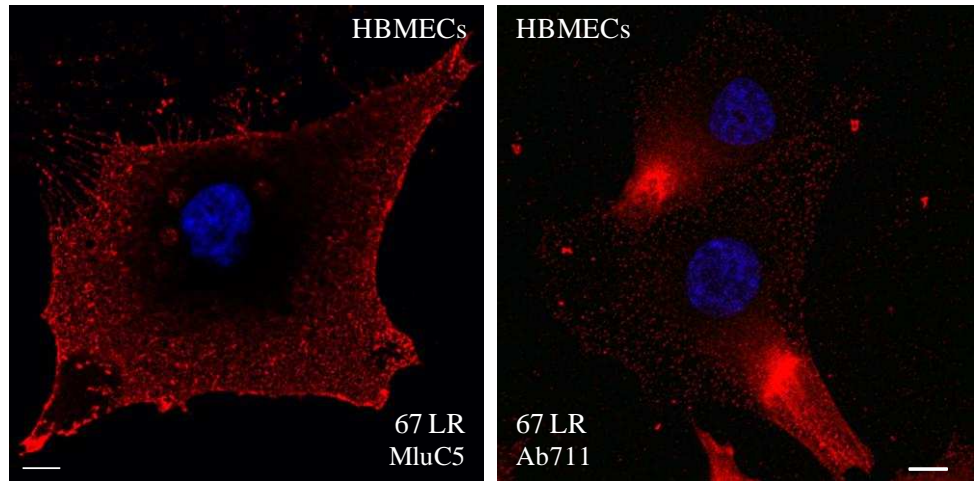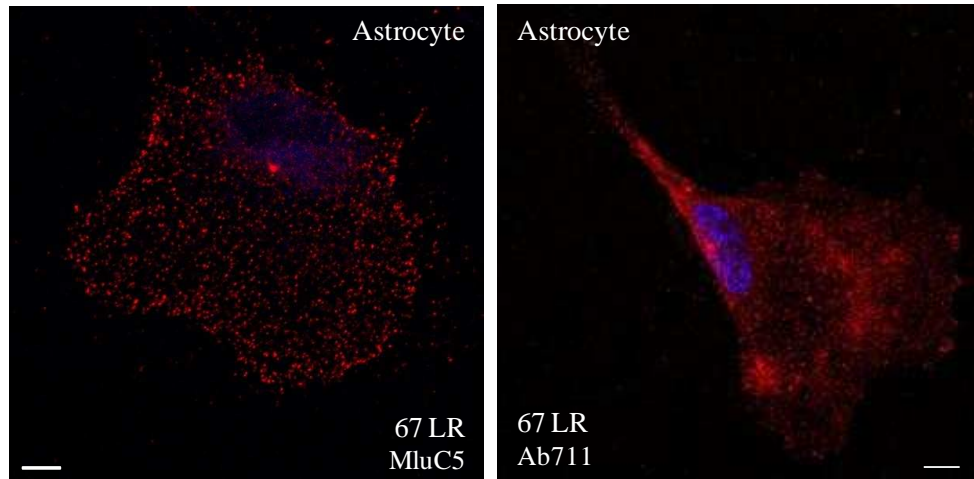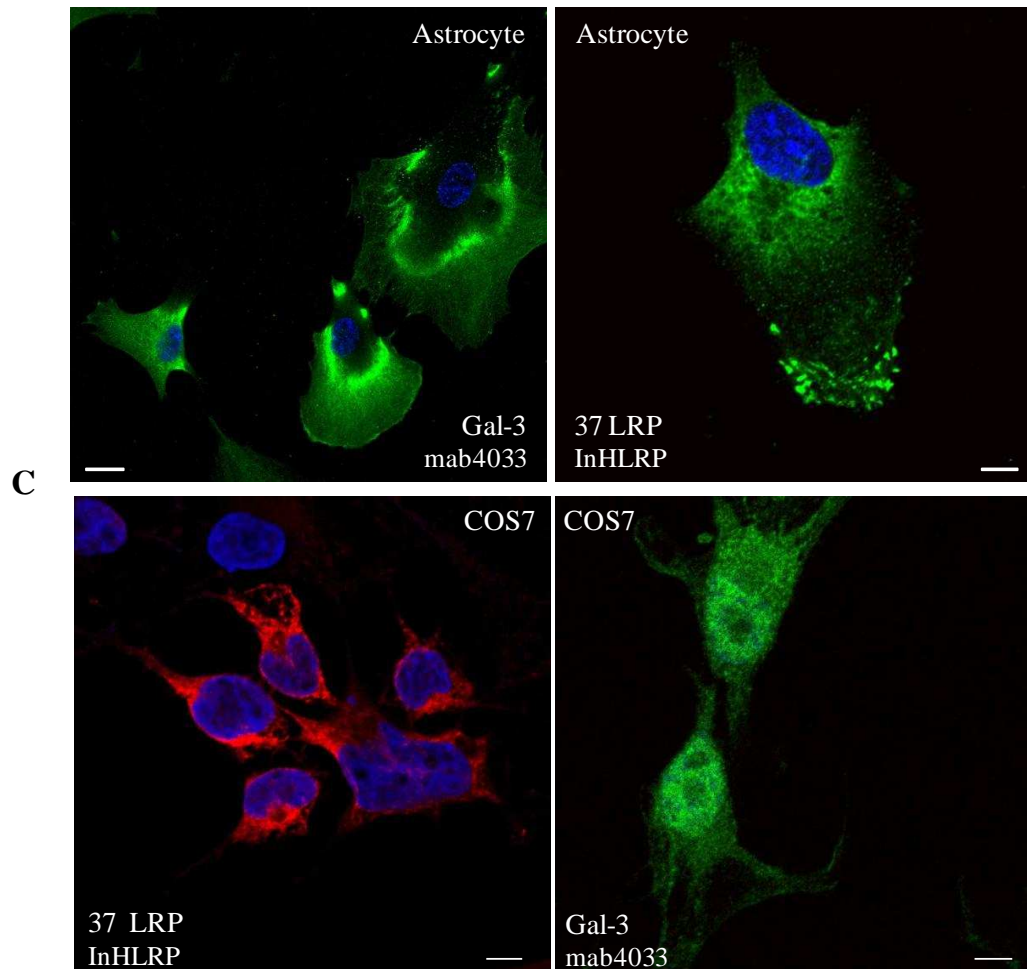
67 LR
Ab711

Figure 4.5: Immunofluorescence staining of 67 LR, 37 LRP and Gal-3 in HBMECs, astrocytes and COS7 cells. Representative confocal microscopic images of immunofluorescence labelled HBMECs, astrocytes and COS7 cells, to determine the surface localization of 67 LR, 37 LRP and Gal-3. The cells grown on coverslips were fixed with 4% paraformaldehyde and stained with; two anti-67 LR (MluC5 and Ab711), anti-37 LRP (InHLRP) and anti-Gal-3 (mab4033), and secondary antibody(s); Alexa Fluor 647, 680 and 488 antibody. Nuclei are stained with Hoechst 33258. Coverslips were mounted using Fluoromount (Sigma) mounting media and images obtained by confocal microscope (Zeisis LSM700). Scale bars represent 0.06µm.

4.2.2. Construction of 37 LRP and Gal-3 tagged to vYFP constructs in mammalian expression vectors

In order to study surface distribution of 37 LRP and Gal-3 in living cells, the C terminus of 37 LRP and Gal-3 were fused to the full length Venus yellow fluorescence protein (vYFP). Furthermore, and for subsequent studying of receptors homo or heterodimers using the biomolecular fluorescence complementation (BiFC) method (described in detail in Chapter 5), the 37 LRP and Gal-3 were C terminally tagged with non-Fluorescent BiFC fragments (i.e., C-terminus of Venus,vYCL or N-terminus of Venus, vYNL). The cDNAs of 37 LRP and Gal-3 were amplified using forward primers designed to add a EcoRI restriction site and a Kozak sequence, prior to the start codon of 37 LRP and Gal-3, and reverse primers remove the stop codon and introduce a XhoI restriction site to the 37 LRP and Gal-3, as described earlier in 2.6.1. A 888 bp and a 725 bp fragment, encoding cDNA sequences of 37 LRP and Gal-3, respectively were successfully amplified by PCR (Figure 4.6A and B). A single band with the expected sizes of 0.8 and 0.7 kb was observed for the 37 LRP and Gal-3, respectively, by agarose gel electrophoresis.
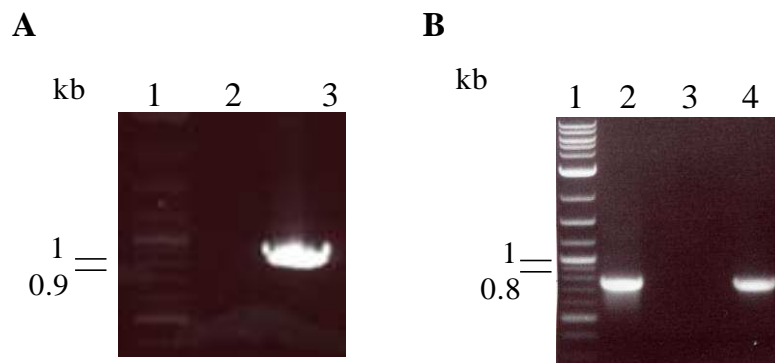
Figure 4.6: Gel electrophoresis showing amplification of 37 LRP and Gal-3 fragments. PCR amplification using pET28LR and cDNA sequences of human Gal-3 as templates for 37 LRP and Gal-3 gave an expected band at 888 bp and 725bp,

respectively. Lanes 1A and B, DNA markers; lanes 2A and 3B, negative control primer only without any template; lanes 3A and 4B, PCR product of 37 LRP and Gal-3 respectively; and Lane 2B, PCR product of Gal-3 using human brain cDNA as a positive control.

The 37 LRP and Gal-3 fragments were purified from the gel and subjected to poly-A tailing, then ligated into the pGEM-T easy vector. Ligation products were transformed into E. coli JM109 and transformants were cultured into LB agar containing ampicillin, IPTG and X-gal. White colonies were selected, which indicate successful ligation, and screened by colony PCR (Figure 4.7 A and B). Several clones were identified to contain the 37 LRP and Gal-3 inserts by observing correct sizes of DNA fragments, corresponding to 37 LRP and Gal-3 alongside a band amplified with the same primers using 37 LRP and Gal-3 PCR purified product as a positive control (Figure 4.7 A and B).

A

B
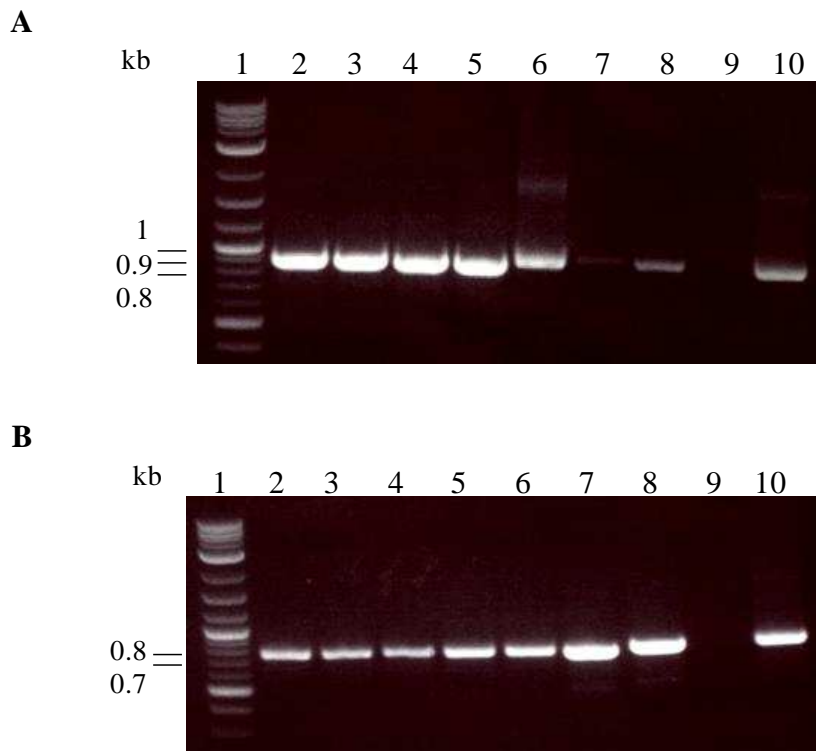
Figure 4.7: Colony PCR for pGEM-T 37 LRP and Gal-3 transformants. PCR screening for selected white colonies containing pGEM-T 37 LRP (A) and Gal-3 (B) transformants. Lanes 1A and B, DNA markers; lanes 2, 3, 4, 5, 6 and 7A and B are different selected white colonies containing 37 LRP and Gal-3 fragments, respectively; Lanes 10A and B, are positive controls containing 37 LRP and Gal-3 PCR purified product as a templates, respectively; and Lanes 9A and B, are negative controls containing primers only without any template.

The 37 LRP and Gal-3 inserts were digested from pGEM-T vector using EcoRI and XhoI restriction enzymes which digested the vector into two fragments (Figure 4.8 A and B). The resulted digestion products at 3kb, 888 bp and 725 bp 37 LRP and Gal-3, respectively, which confirmed the successful digestion of the pGEM-T vector.
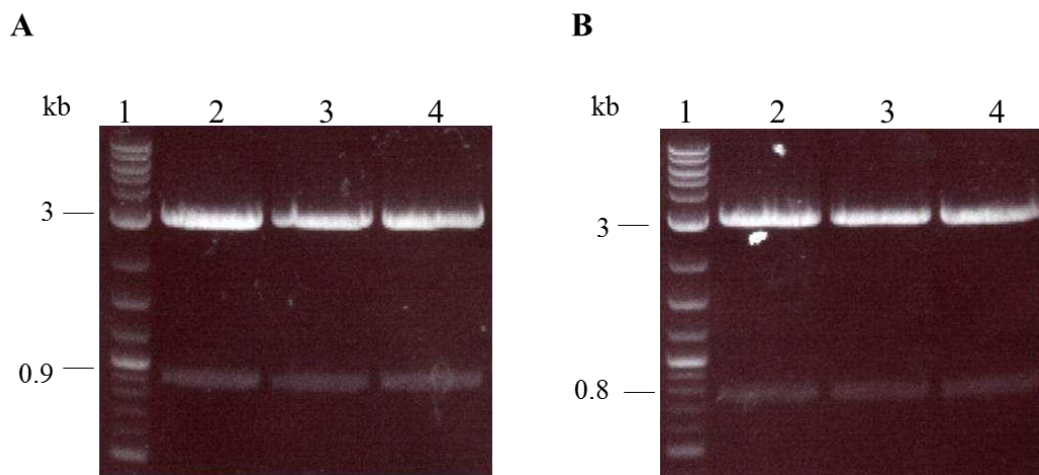
Figure 4.8: Verification of pGEM-T of 37 LRP and Gal-3 constructs. Plasmids were prepared from expected transformants and were confirmed by EcoRI and XhoI digestion. Lanes 1A and B, DNA markers; lanes 2, 3 and 4A and B, Plasmids after EcoR I and XhoI digestion showing linear size at 888bp and 725bp for the 37 LRP and Gal-3, respectively.

The vector pcDNA3.1zeo containing either full length or the C or N terminal regions of venus YFP were pre digested with the EcoRI and XhoI enzymes to be prepared for subsequent ligation (Figure 4.9).
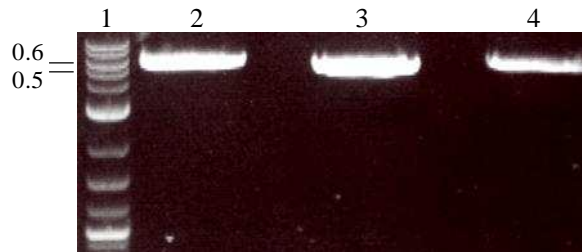
Figure 4.9: Restriction and digestion confirmation of pcDNA3.1zeo YFP, YCL and YNL constructs. pcDNA3.1zeo vector containing vYFP, vYCL and vYNL were subjected for EcoRI and XhoI digestion. Lanes 2, 3 and 4, Plasmids after EcoRI and XhoI digestion showing linear size at 5.7kb, 5.5kb and 5.3kb for pcDNA3.1zeo vector containing vYFP, vYCL and vYNL, respectively.

Subsequently, the digested and gel extracted Gal-3 and 37 LRP inserts were ligated into the N-terminus of: [1] pcDNA3.1zeo vector, containing the full length Venus yellow fluorescence protein (vYFP) to generate 37 LRP.vYFP and Gal-3.vYFP; [2] pcDNA3.1zeo vector containing the N-terminal of Venus yellow fluorescence protein (vYNL) to generate 37 LRP.vYNL and Gal-3.vYNL; and [3] pcDNA3.1zeo vector containing the C-terminal of Venus yellow fluorescence protein (vYCL) to generate 37 LRP.vYCL and Gal-3.vYCL. The ligated products were transformed into E. coli JM109 and selected colonies were screened by colony PCR (Figure 4.10 A and B). The DNA sequencing of generated constructs confirmed successful cloning. For ease of reference, all given names of generated constructs are described in Table 2.7.
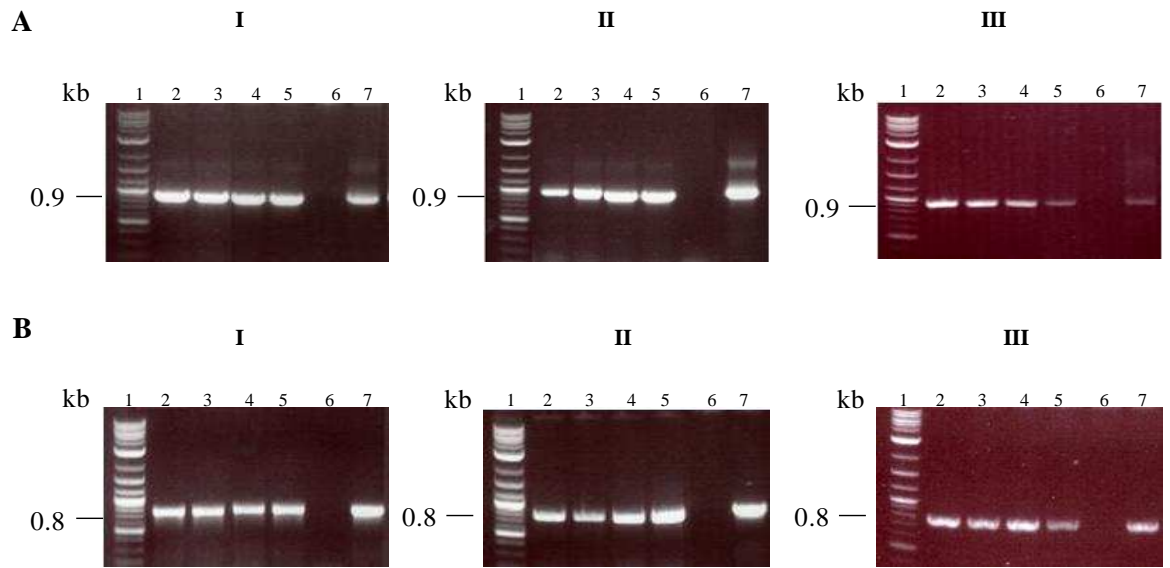
Figure 4.10: Colony PCR for pcDNA3.1 YFP, YCL and YNL 37 LRP and Gal-3 trasformants. PCR screening for selected colonies containing 37 LRP (A) and Gal-3 (B) fused to vYFP (I), vYNL (II) and vYCL (III) transformants. Lanes 1I, II and III, DNA markers; lanes 2, 3, 4 and 5 are different selected white colonies containing 37 LRP (A) and Gal-3 (B) fragments, respectively cloned into vYFP (I), vYNL (II) and vYCL (III); Lanes 7A and B, are positive controls containing 37 LRP and Gal-3 PCR purified product as a templates, respectively; and Lanes 6A and B, are negative controls containing primers only, without any template.

4.2.3. Construction of 37 LRP and Gal-3 in mammalian expression vectors containing mCherry

To visualize both receptors after transfection in eukaryotic cells, the 37 LRP and Gal-3 were cloned into another fluorescent protein (mCherry), in addition to vYFP to enable their coexpression. The cDNA of mCherry was amplified using primers designed to add XhoI and XbaI restriction sites and to remove the start codon, as described earlier in 2.6.1. A 711bp fragments encoding cDNA a sequence of the mCherry was successfully amplified by PCR (Figure 4.11). A single band with the expected size of 0.7kb was observed for the mCherry fluorophore, by agarose gel electrophoresis.
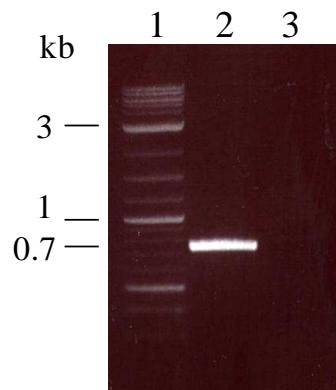
Figure 4.11: Amplification of mCherry fragment. PCR amplification using cDNA sequences of mCherry as templates gave an expected band at 711 bp. Lane 1, DNA marker; lane 2, PCR product of mCherry; and lane 3, negative control primers only without any template.

The 37 LRP.vYFP and Gal-3.vYFP vectors were digested with the XhoI and XbaI enzymes to remove the vYFP fragment. As shown in Figure 4.12, the vYFP fragments were successfully digested from both vectors at 0.7 bp.
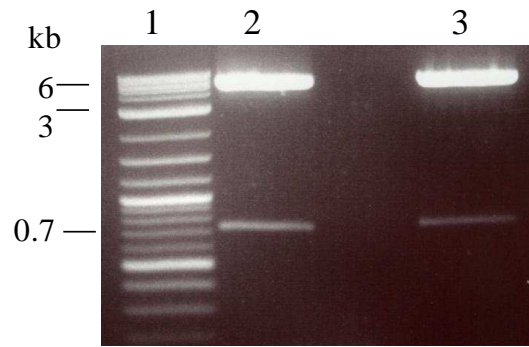
Figure 4.12: Restriction and digestion of 37 LRP.vYFP and Gal-3.vYFP constructs. 37 LRP.vYFP and Gal-3.vYFP were subjected for XhoI and XbaI digestion. Lane 1, DNA marker; Lane 2 and 3, Plasmids after XhoI and XbaI digestion showing linear sizes at 0.7 kb for vYFP, and 6.4 kb and 6.3kb for pcDNA3.1zeo vector containing 37 LRP and Gal-3, respectively.

Following this process, digested plasmids containing the 37 LRP and Gal-3 fused to pcDNA3.1zeo were extracted from the gel and ligated into the pre digested mCherry PCR product. Ligation products were transformed into E.coli JM109 and selected colonies were screened by colony PCR (Figure 4.13A and B). The DNA sequencing confirmed successful cloning and the constructs called 37 LRP and Gal-3.mCherry.
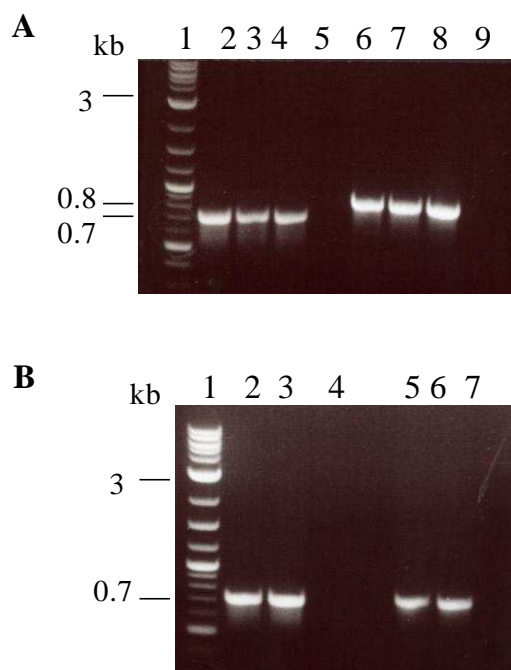
Figure 4.13: Colony PCR for 37 LRP and Gal-3-mCherry transformants.

PCR screening for selected colonies containing 37 LRP.mCherry (A) and Gal-3.mCherry (B) transformants. Lanes 1A and B, DNA markers; lanes 2, 3 and 4A, and 6, 7 and 8A, are different selected containing 37 LRP fragments using primers that amplify mCherry and 37 LRP, respectively; Lanes 2 and 3B, and 5 and 6A, are different selected containing Gal-3 fragments using primers that amplify mCherry and Gal-3, respectively. Lanes 5A and 4B, are negative controls containing mCherry primers only without any template. Lanes 9A and 7B, are negative controls containing receptor primers only without any template.

4.2.4. Expression of fluorescently labelled 37 LRP and Gal-3

The expression of vYFP-labelled 37 LRP and Gal-3 was investigated by confocal microscopy of transiently transfected primary HBMECs. Firstly, HBMECs were grown on fibronectin-coated glass cover slips in 12-well plates. Then, cells were transfected with different amounts of the 37 LRP and Gal-3.vYFP plasmids (1-4.5µg) using different amounts of the Trans IT-2020 transfection reagent (0.5-2.5µl). The Trans IT-2020 transfection reagent was used in this work due to its serum compatibility and high efficiency of transfection. Subsequently, the expression of vYFP labelled receptors was visualized by confocal microscopy as described earlier in Chapter 2. The optimal amount of plasmid DNA was 2µg per 1µl of transfection reagent in 12 well plates (data not shown), as higher amount of plasmids and transfection reagent were cytotoxic and changed the cell morphology. Preliminarily, all the optimization experiments were performed 48h post-transfection until the amounts of plasmid and transfection reagent were optimised. Afterwards, the expression of fluorescently labelled receptors in transiently transfected HBMECs were compared between 24 and 48h, after transfection by western blot analysis using an anti-GFP antibody. As shown in Figure 4.14, a reactive band was detected at 67 kDa in the cell lysates of cells transfected with 37 LRP fused to vYFP at 24 and 48h post-transfection, which was absent from the lysate of non-transfected cells (Figure 4.14). Surprisingly, a band with apparent molecular weight of 67 kDa, larger than predicted molecular weight (57 kDa), was also observed in Gal-3.vYFP transfected cells lysates at 24 and 48h post-transfection. Both receptors showed high expression level at 24h post-transfection (Figure 4.14). This demonstrated that 37 LRP and Gal-3 fused to vYFP, were successfully expressed in HBMECs and reached highest levels of

expression 24h post-transfection. Therefore, all future transfection experiments were conducted at 24h post-transfection.
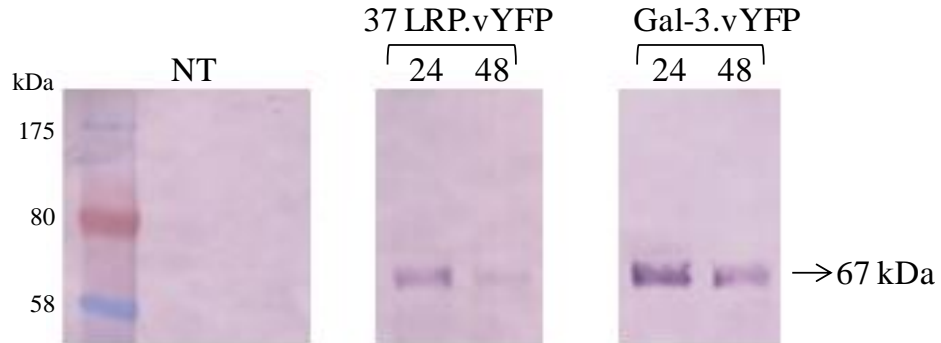
Figure 4.14: Expression of fluorescently labelled 37 LRP and Gal-3 in HBMECs at different time points. Whole cell lysates from 37 LRP.vYFP or Gal-3.vYFP transiently transfected or non-transfected (NT) primary HBMECs were harvested under reducing conditions (10% DTT in sample loading buffer) 24h and 48h post-transfection and immunoblotted with anti-GFP antibody at (1:100) dilution, followed by (1:30000) dilution of anti-rabbit conjugated to alkaline phosphatase, and subsequently detected by the NBT/BCIP substrate as described in Chapter 2. Western blot analysis confirmed higher expression of both constructs at 24h.

The expression of generated constructs was further characterized by transfection in COS7 cells (a mammalian cell line), using antibodies to GFP, 37 LRP (InHLRP) and Gal-3 (mab4033). COS7 cells were used because of their high transfection efficiencies and expression levels. Immunoblotting using anti-GFP antibody showed that 37 LRP.vYFP expressed at 67 kDa in a similar fashion to HBMECs (Figure 4.15A). In addition, the N and C terminal domains of venus YFP fused to 37 LRP were expressed at expected molecular weights of 61 kDa and 52 kDa, respectively (Figure 4.15A). However, Gal-3.vYFP was detected at

57 kDa (predicted molecular weight) (Figure 4.15B) which is smaller than molecular weight demonstrated in HBMECs. Both Gal-3 tagged to the N and C terminal of vYFP were expressed at 50 kDa and 40 kDa, respectively (Figure 4.15B). Further immunoblotting using InHLRP antibody, detected 37 LRP at 67 kDa, 61 kDa and 52 kDa, which corresponds to the molecular weight of 37 LRP fused to vYFP, vYNL and vYCL, respectively (Figure 4.15C). In addition, endogenously expressed 37 LRP was detected in both non-transfected and transfected COS7 cells (Figure 4.15C). Similarly, Gal-3 monoclonal antibody (mab4033) recognised endogenous Gal-3 and Gal-3 fused to the full and fragments of vYFP at the predicted molecular weights, as shown in Figure 4.15D.
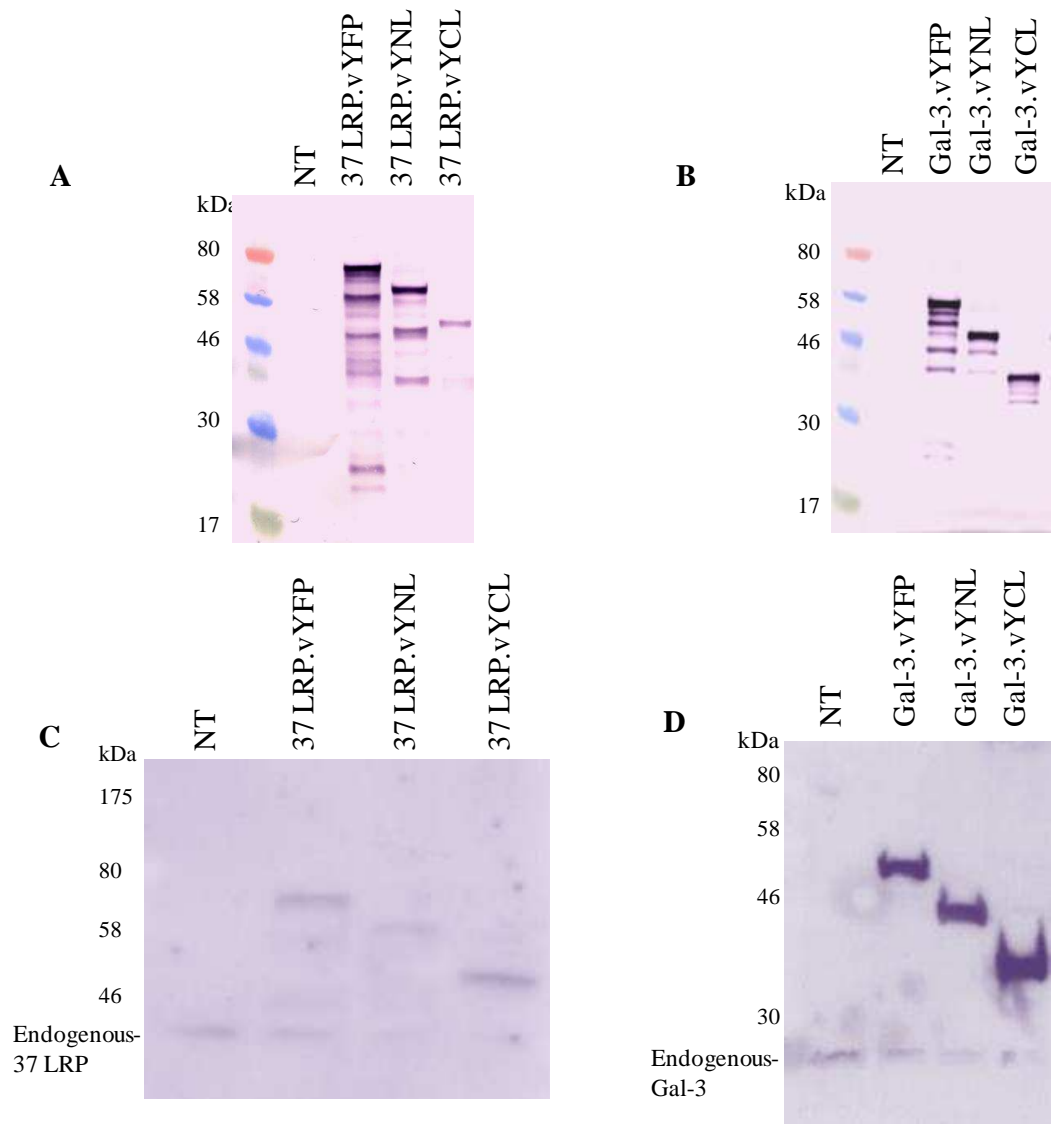
Figure 4.15: Expression of vYFP, vYNL and vYCL tagged 37 LRP and Gal-3 in COS7 cells. (A, B, C and D) Whole cell lysates of COS7 cells transiently transfected with the indicated constructs, and analyzed 24h post transfection, under reducing conditions (10% DTT in sample loading buffer), and subjected to SDS-PAGE. The cell lysates were then immunoblotted using antibodies against GFP (1:100) dilution (A and B), 37 LRP (InHLRP) (1:1000) dilution (C) and Gla-3 (mab4033) (1:1000) dilution (D), followed by (1:30000) dilution of anti-rabbit or anti-mouse conjugated to alkaline phosphatase, and subsequently detected by NBT/BCIP substrate as described in Chapter 2. Lysates of non-transfected (NT) cells were used as negative controls. Western blot analysis confirmed the expression of the transfected constructs.

4.2.5. Sub-cellular localization of fluorescently labelled 37 LRP and Gal-3

To visualize the subcellular localization of the vYFP-fused 37 LRP and Gal-3, HBMECs, COS7 and N2a cells were transiently transfected and analyzed by confocal microscopy. The N2a, mouse neuroblastoma cell line, does not express endogenous Gal-3 (Gauczynski et al., 2001) as confirmed by immunoblotting of N2a cells lysate using anti-mouse Gal-3(Mac-2) antibody (Figure 4.16). Thus, the N2a cells were used for further experiments, described in Chapter 6, to study the role of Gal-3 in adhesion and invasion of N. meningitidis.
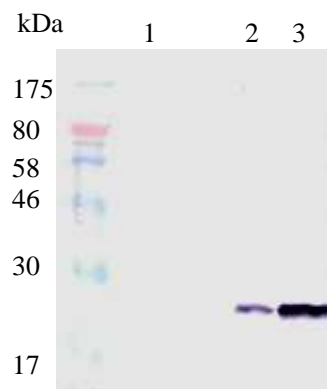
Figure 4.16: Endogenous expression of Gal-3 in different cell lines. Whole cell lysates of N2a (1), HBMECs (2) and CaCo II (3) were subjected to immunoblotting with the anti-Gal-3 (Mac2) antibody at 1: 1000 dilution, followed by 1:30000 dilution of anti-rat IgG conjugated to alkaline phosphtase, and subsequently detected by the NBT/BCIP substrate, as described in Chapter 2.

The fluorescently labelled 37 LRP and Gal-3, revealed a punctate pattern of expression on the apical membrane and cytoplasm, but not in the nuclei of HBMECs (Figure 4.17A). In contrary, the vYFP tagged receptors showed more diffuse distribution in the membrane, cytoplasm and nuclei in the COS7 and N2a

cells (Figure 4.17A). Furthermore, and to verify surface expression of venus labelled 37 LRP and Gal-3, immunofluorescence staining was performed on fixed non-permeabilizied N2a cells using an anti-GFP antibody. As shown in Figure 4.17B, the 37 LRP and Gal-3.vYFP were expressed on the cell surface of non-permeabilizied N2a cells.

For further confirmation of the observed distribution of these receptors, COS7 cells were transfected with 37 LRP.vYFP and Gal-3.vYFP constructs and subcellular fractionation carried out, the expression was then examined by western blot analysis using the anti-GFP antibody. Both receptors were present in the cytoplasmic, membrane, cytoskeleton, soluble and chromatin bound nuclear fraction (Figure 4.17C and D). The results of the western blot analysis in subcellular localization support the demonstrated distribution of YFP-tagged receptors in confocal images.

A

HBMECs 37 LRP. vYFP

HBMECs Gal-3. vYFP

COS7 37 LRP. vYFP

COS7 Gal-3. vYFP

N2a 37 LRP. vYFP

N2a Gal-3. vYFP

B

venusYFP

Anti-GFP(vYFP)

Merge

37 LRP.vYFP

N2a

Gal-3.vYFP

N2a
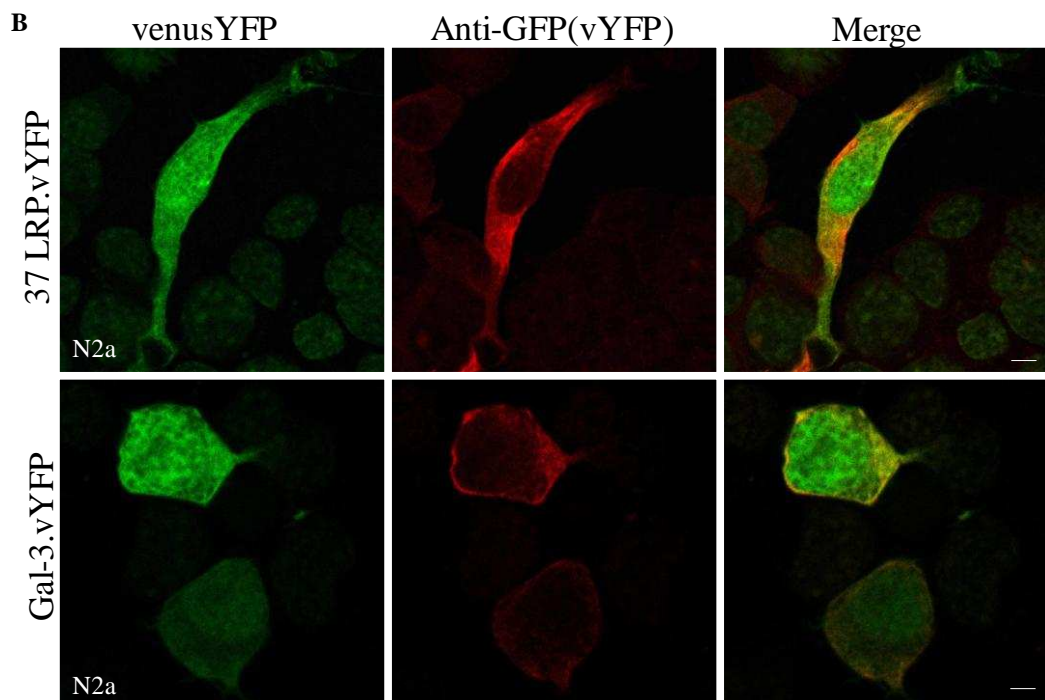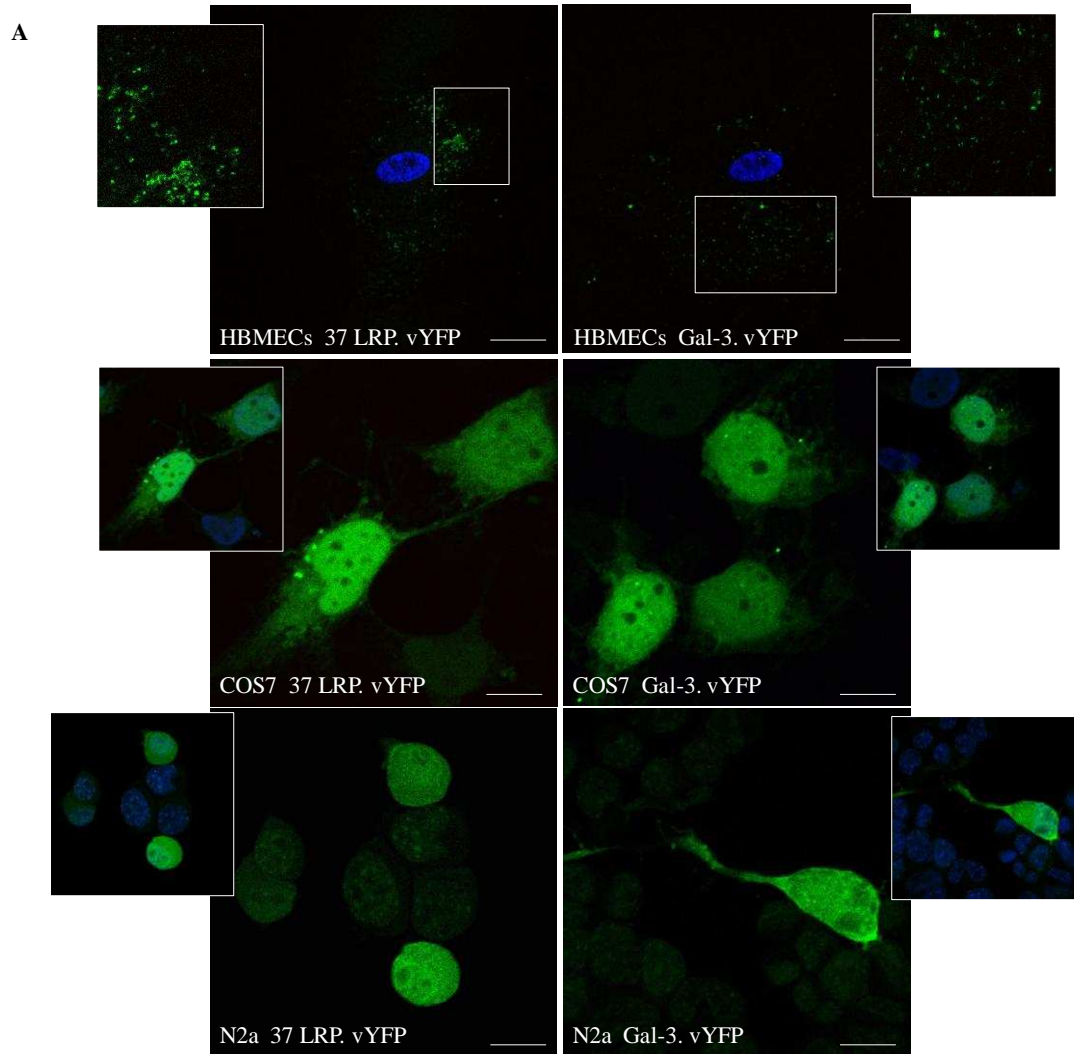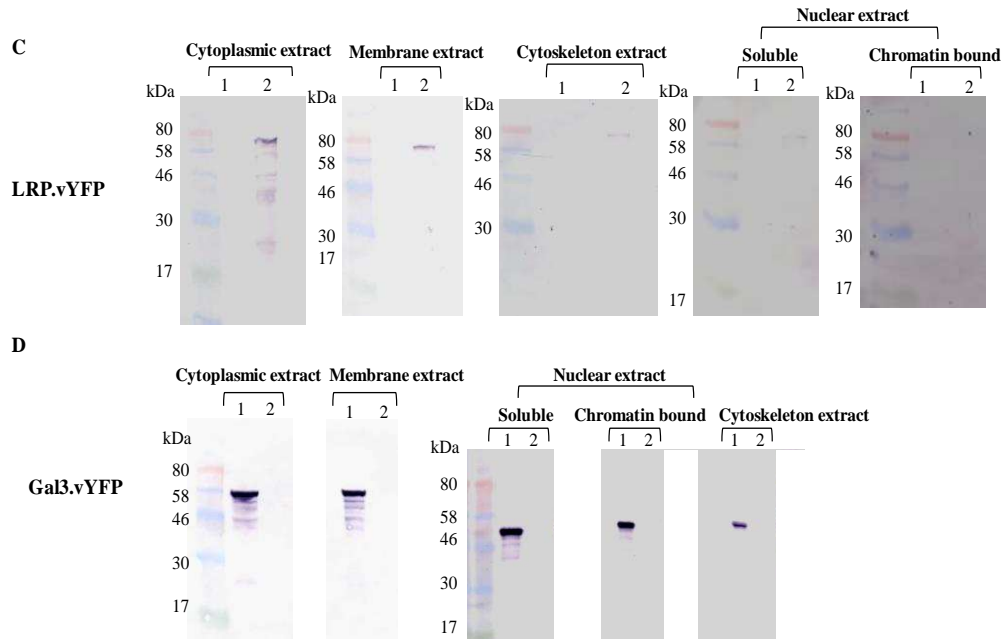
Figure 4.17: Subcellular localization of vYFP conjugated 37 LRP and Gal-3.

Representative confocal microscopic images of (A) HBMECs, COS7 and N2a cells transiently transfected with 37 LRP.vYFP or Gal-3.vYFP and 24 h post transfection. The cells were fixed with 4% paraformaldehyde and nuclei are stained with Hoechst 33258. Scale bars represent 0.15µm, 0.05 and 0.09 µm for HBMECs, COS7 and N2a, respectively. (B) Immunofluorescence of fixed non-permeabilized N2a cells, which were transfected with the indicated constructs, as mentioned above. The cells were then stained with anti-GFP antibody (1: 100), followed by Alexafluor 680 (1:100). Merged images indicate co-localization of vYFP tagged receptors on the cell surface of non-permeabilized N2a cells. Scale bars 0.05 µm. (C and D) Western blots of COS7, were transiently transfected with vYFP tagged 37 LRP and Gal-3, confirming their expression in different cellular fractions. Lanes 1C and 2D: untransfected COS7 total cell lysates of the cytoplasm, membrane, cytoskeleton, nuclear soluble and chromatin-bound proteins in each fraction. Lanes 2C and 1D: Detection of 37 LRP and Gal-3 expression in different subcellular fractions, extracted from tranfected COS7 with 37 LRP vYFP & Gal-3 vYFP, respectively, using anti-GFP as described in Chapter 2.

4.2.6.   Investigation of the role of Cys148 and 163 in 37 LRP acylation.

Acylation (most likely palmitoylation) of 37 LRP is required for the formation of 67 LR and its targeting to the cell surface (Buto et al., 1998; Landowski et al., 1995). However, the site of palmitoylation is not yet determined. Palmitoylation occurs most commonly on cysteine residues, but also on threonine, serine, and lysine. Accordingly, the amino acid sequence of human 37 LRP contains 14 serine, 23 threonine and 2 cysteine residues, which might be subjected to palmitoylation. In the current study, we decided to focus on the two-cysteine residues at positions 148 and 163 for further investigation of the 37 LRP palmitoylation.

4.2.6.1.   Construction of vYFP-37 LRP and Gal-3 cysteine mutants in mammalian expression vectors

To investigate if one or both of the C-terminal cysteine residues account for the palmitoylation of 37 LRP and the subsequent homo or heterodimerization of 67 LR, constructs were created in which the cysteines, towards the carboxyl terminus of 37 LRP, were substituted with alanines and fused to full length C or N termini of vYFP. The 37 LRP.C148A, 37 LRP.C163A and 37 LRP.C148/163A fused to vYFP, vYNL and vYCL were successfully generated by site directed mutagenesis of the 37 LRP, tagged to vYFP, vYNL and vYCL. The mutagenesis protocols followed were based on the Stratagene's QuickChange site-directed mutagenesis method. A pair of primers, both containing the desired mutations, were designed to be complementary to the template DNA (Table 2.5). Following PCR mutagenesis, the original non-mutated parental DNA was removed from PCR by Dpn I digestion and then transformed into E. coli JM109, and plated on selective

LB/ampicillin plates. Plasmids were extracted from the resulting colonies and sent for DNA sequencing. As shown in Figure 4.18, the sequencing results confirmed the amino acids substitutions.
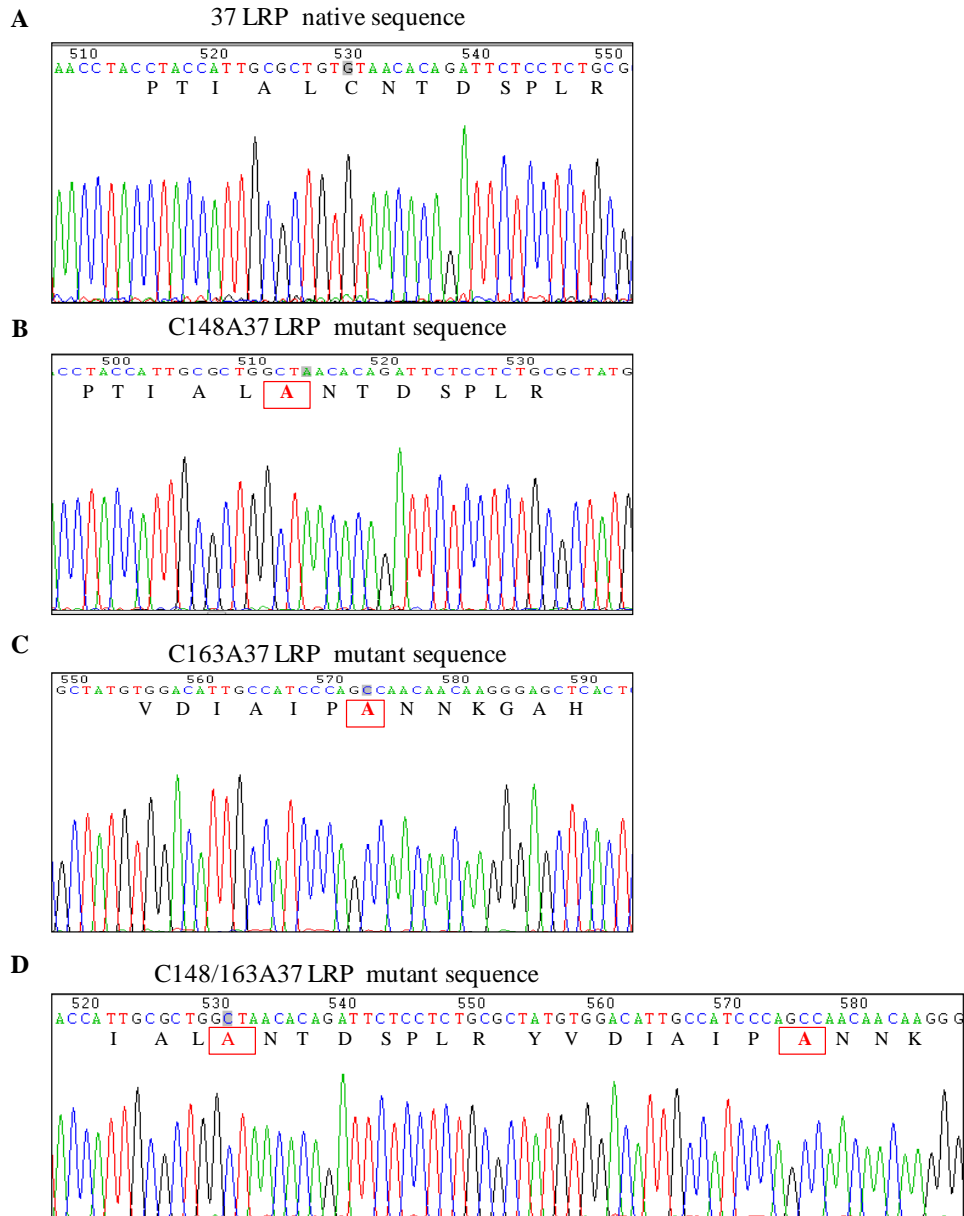
Figure 4.18: Sequence chromatograms showing substitution of the 37 LRP cysteines following site directed mutagenesis. Site directed mutagenesis was performed on the 37 LRP.vYFP templates. Automated DNA sequencing confirmed the mutation of 37 LRP.C148 (B), 37 LRP.C163 (C) and 37 LRP.C148/163 (D) to alanine. Sequencing data were viewed in Chromas lite version 4.02.

4.2.6.2. Expression of fluorescently labelled 37 LRP cysteine mutants

In order to characterize the expression of generated cysteine-substituted constructs, 37 LRP.vYFP wild type and cysteine-substituted constructs were transfected into COS7, and expression was examined 24h post transfection by western blot and flow cytometry. As shown in Figure 4.19A, all 37 LRP cysteine-substituted constructs (C148, C163 and C148/163A) were expressed and their expressions were comparable to 37 LRP wild type, at approximately 67 kDa. Then, flow cytometry was used to quantify the expression of each mutant. The flow cytometry analysis revealed similar expression of wild type and mutant receptors (Figure 4.19B).
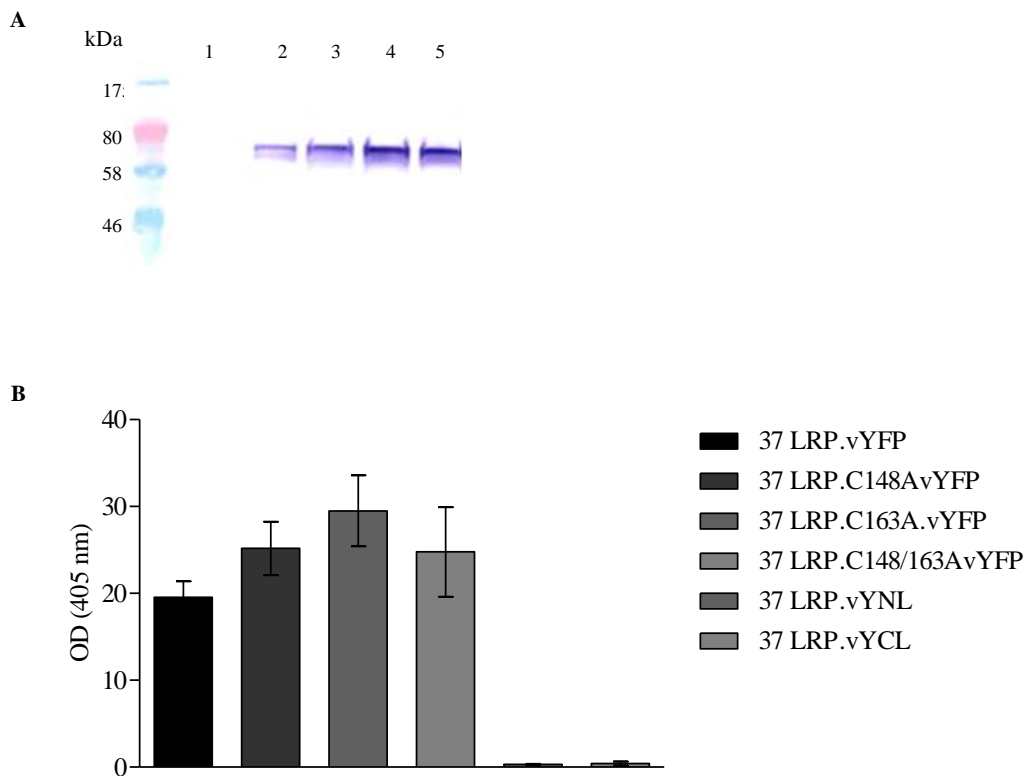
Figure 4.19: Expression of fluorescently labelled 37 LRP cysteine substituted mutants in COS7. (A) Whole cell lysates of COS7 cells transiently transfected with vYFP tagged 37 LRP, 37 LRPC184A, 37 LRPC163A and 37 LRPC163/184A (lane 2,3,4 and 5, respectively) were subjected to immunoblotting using anti-GFP antibody as

described in Chapter 2. Western blot analysis confirmed the expression of receptors cysteine mutants at comparable level to the wild type. (B) COS7 cells were transfected with constructs as indicated above and Venus fluorescence was analyzed by flow cytometry. Results are expressed as percentage of the specific fluorescence signal to the value of 37 LRP.vYFP. Bars represent the mean ± SEM of three independent experiments.

4.2.6.3. Subcellular localization of vYFP-tagged cysteine-substituted 37 LRP

To examine the effect of cysteine substitution on subcellular expression patterns of these receptors, 37 LRP.vYFP wild type and cysteine substituted constructs were transfected into HBMECs and their subcellular localization was examined by confocal fluorescence microscopy. As shown in Figure 4.20A, 37 LRP cysteine mutants were expressed in HBMECs and their pattern was comparable to wild type receptors. All cysteine-substituted mutants showed the punctate cell surface distribution on the apical surface of HBMECs.

For further investigation of the 37 LRP cysteines substitution on subcellular distribution of these receptors, wild type and cysteine substituted constructs were transfected into COS7 and subcellular fractionation analysis was carried out. Similar to wild type 37 LRP, all the Cys mutants were still predominantly present in the cytoplasmic, membrane, cytoskeleton, soluble and chromatin bound nuclear fraction, suggesting that the replacement of any of the two Cys is not affecting normal receptor distribution (Figure 4.20B).
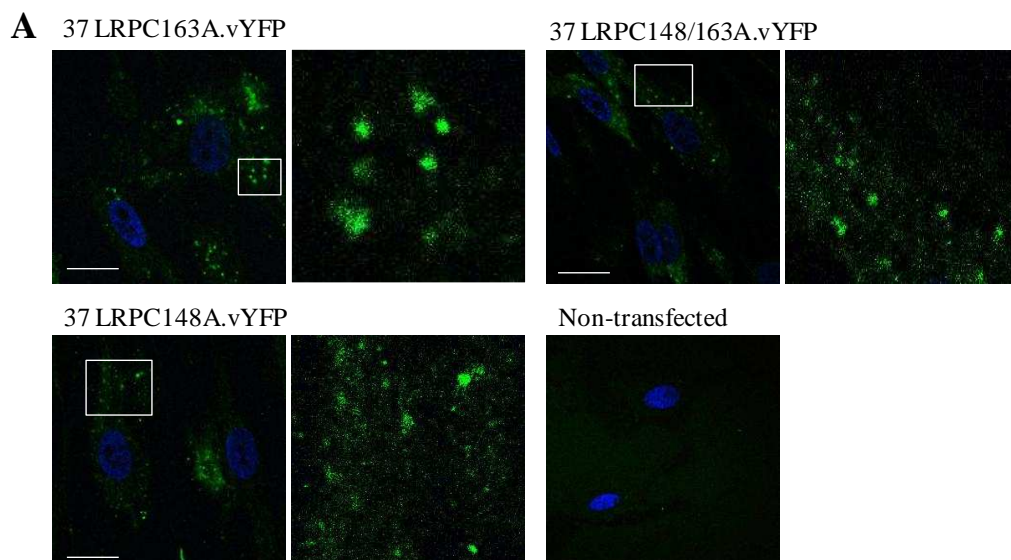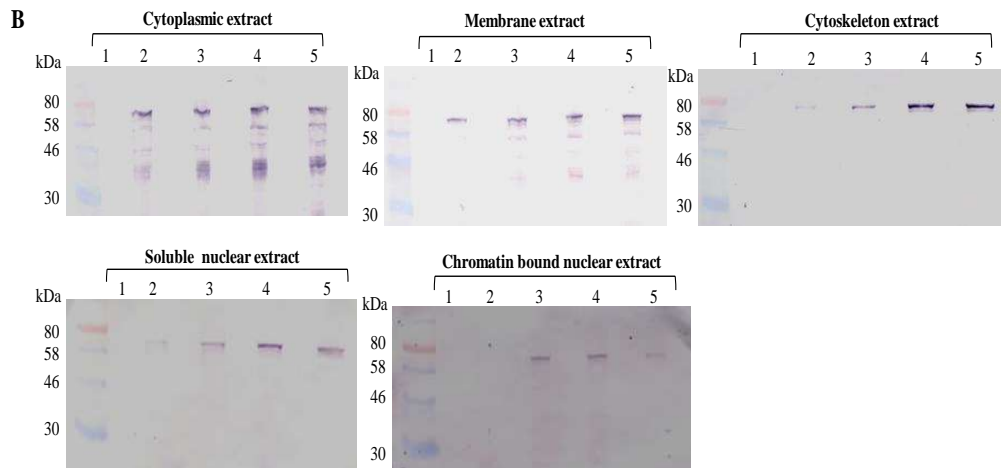
Figure 4.20: Subcellular localization of vYFP labelled 37 LRP and 37 LRP cysteine mutants. (A) Representative confocal microscopic images of HBMECs transiently transfected with indicated constructs as described in Chapter 2 and 24 hrs post transfection. The cells were fixed with 4% paraformaldehyde and nuclei were stained with Hoechst 33258. Scale bar 0.1μm. (B) Western blot of COS7 transiently transfected with vYFP tagged 37 LRP and 37 LRP cysteine mutants, confirming their expression in different cellular fractions. Lanes 1B: untransfected COS7 total cell lysates of cytoplasmic, membrane, cytoskeleton, nuclear soluble and chromatin-bound in each fraction as described in Chapter 2. Lanes 2, 3, 4 and 5B:COS7 transfected with vYFP tagged LR wild type, LR C148A, LRC163A & LRC148/163A, respectively, and detected with anti-GFP as described in Chapter 2.

4.3. Discussion:

The data presented in chapter 3, clearly showed that Gal-3 binds N. meningitidis (Figure 3.2), and two meningococcal Gal-3 ligands were identified including; PilQ and PilE (Figure 3.9). Interestingly, PilQ is known as an adhesin for 67 LR/37 LRP (Orihuela et al., 2009). Particularly, the 67 LR originates from homo or heterodimerization of its precursor (37 LRP) with Gal-3 (Buto et al., 1998; Landowski et al., 1995). Such binding of meningococcal PilQ to both receptors raised the question of a possible role for the 67 LR heterodimer with Gal-3 in meninigococcal meningitis. To address this question the current chapter studied the cell surface distribution and expression pattern of the Gal-3, 67 LR and 37 LRP.

Expression of Galectin-3, 67 LR and its precursor in HBMECs were confirmed by Western blotting. One band was observed for Gal-3 in the lysate of HBMECs as previously described in other endothelial cells (Anna I. Markowska 2010). On the other hand, Ab711 antibody detected two bands at molecular weights corresponding to mature and precursor forms of 67 LR. These bands were shown previously in Western blotting of rat brain endothelial cells (rBCEC), immunoblotted with Ab711 antibody (Orihuela et al., 2009). Furthermore, immunoblotting of HBMECs using an antibody generated against purified recombinant LR (InHLRP) recognized only a band corresponding to the precursor form 37 LRP (Figure 4.3B). This was also demonstrated in a previous study, where only the precursor form of the receptor was detected on western blots with antibody called W3, which raised against full length 37 LRP (Gauczynski et al., 2001). Although, 67 LR and 37 LRP share common epitopes (Buto et al., 1998;

Landowski et al., 1995), their antibodies appear to have different recognition spectra. As some of these antibodies react exclusively with 67 LR or 37 LRP or both of them, as observed in a previous study (Baloui et al., 2004). This suggests that these antibodies recognize an epitope exposed differently depending on whether the receptor is in a precursor or mature state. Additionally, the corresponding epitopes may be exquisitely sensitive to the presence of SDS and heat denaturation, discussed in (Baloui et al., 2004; Menard et al., 1997).

Flow cytometric analysis revealed surface expression of Gal-3 in HBMECs using an antibody against the Gal-3 N-terminus (Figure 4.4). This result corroborated the surface localisations of Gal-3 in different endothelial cells (Fukushi et al., 2004; Markowska et al., 2011; Saint-Lu et al., 2012). This localization strongly supports the potential role of Gal-3 as a receptor for N. meningitidis in the BBB. Because Buto et al (1998) had previously suggested dimerization between Gal-3 and 37 LRP to form 67 LR, their cell surface localization was also investigated by flow cytometry. Both 67 LR and its precursor were located on the surface of HBMECs at a comparable level to Gal-3, as revealed by flow cytometry (Figure 4.4). For detection of 67 LR, the monoclonal antibody, termed Mluc5, was used instead of Ab711 because it recognizes only 67 LR not 37 LRP (Martignone et al., 1992), while in case of its precursor, InHLRP antibody was utilized. In line with our results, previous studies have shown that 67 LR (Ardini et al., 1998; Fujimura et al., 2005) and 37 LRP (Gauczynski et al., 2001; Zuber et al., 2008) were expressed on the cell surface of different cells using flow cytometry analysis. In all these studies, 37 LRP was detected by using antibodies that recognize only 37 LRP in western blot, however, the fact that these antibodies might detect 67 LR in flow cytometry cannot be excluded.

Immunofluorescence staining showed a diffuse and punctate pattern of staining of Galectin-3 on the surface of HBMECs (Figure 4.5A). The punctate staining represents a dot-like staining pattern that has been described previously for Gal-3 in other endothelial cells, human umbilical vein endothelial cells (HUVECs) (Thijssen et al., 2008). This discrepancy in the staining pattern may be related to the difference in origins of the endothelial cells used. The current study used endothelial cells isolated from the brain instead of umbilical vein. To our knowledge, to present, there is no other report in the literature demonstrating the staining patterns of Gal-3 in HBMECs exclusively. Because one of the main objectives of this study was to investigate 67 LR dimerization status, the expression pattern of 67 LR and its precursor on the surface of HBMECs was characterized by immunofluorescence staining. Two anti-67 LR antibodies (Mluc5 and Ab711) were used to stain 67 LR in HBMECs in order to avoid epitope-restricted profiles, which might affect 67 LR antigen behaviour. The 67 LR showed a punctate staining pattern over the surface of HBMECs using Mluc5 antibody (Figure 4.5A). This pattern was similar to previously shown for HBMECs stained with Mluc5 antibody (Kim et al., 2005). In addition, strong punctuate and some diffuse staining at the cell periphery was observed with Ab711 antibody staining for HBMECs. The MLuC5 antibody is known to identify only the mature receptor 67 LR, but not the 37 LRP, while Ab711 antibody recognizes the precursor and mature form of 67 LR. With this in mind, it appears that the diffuse pattern obtained by Ab711 antibody reflects 37 LRP staining. While the unique punctate staining pattern displayed by Mluc5 and Ab711 antibodies represent 67 LR, additionally, a more diffuse pattern of staining was obtained with InHLRP antibody (Figure 4.5A). This antibody is assumed to

detect the precursor form of the receptor, based on its recognition of 37 LRP only in western blot. As a result, these data revealed that 67 LR and its precursor were localized at the cell surface of HBMECs in a punctate and diffuse pattern, respectively. Taking into consideration that conversion of 37 LRP to 67 LR is as yet unclear and will be studied in detail in Chapter 5. It should be noted that further work has been done by our group (Dr. Lee Wheldon) showed clearly that there were obvious differences in Gal-3, 67 LR and its precursor staining between fixed non-permeabilized and permeabilized cells. The Mluc-5 antibody showed positive nuclear staining of 67 LR in permeabilized cells. While both 37 LRP and Gal-3 displayed more evenly distributed staining in the cytoplasm of permeabilized cells when compared with unevenly distributed staining patterns in non- permeabilized cells staining.

For comparison purposes, receptor expression pattern was further characterized in primary astrocytes by immunofluorescence staining. The presence of the Gal-3 and 37 LRP, and its mature form 67 LR, at the plasma membrane of non-apermeabilizied astrocytes was demonstrated in our study (Figure 4.5B). Importantly, astrocytes displayed comparable staining patterns of Gal-3, 67 LR and 37 LRP with HBMECs, suggesting a similar repertoire of receptor expression. This finding might be an interesting observation with regard to meningococcal meningitis, since meningococci elicited significant elevations in astrocyte numbers (Astrogliosis) during infection (Chauhan et al., 2008). Hence, these receptors might contribute to the potential role of astrocytes in initiation or progression of the immune response after pathogen invasion (Chauhan et al., 2008).

For further characterization of receptor subcellular localization and subsequent study of their dimerization in chapter 5, 37 LRP and Gal-3 were cloned into the full length and N or C terminus of vYFP, respectively. Venus was used owing to its fast and efficient maturation and its strong fluorescence intensity as demonstrated in previous studies (Robida & Kerppola, 2009; Shyu et al., 2006). The expressions of cloned receptors were detected by western blot and confocal microscopy. The 37 LRP fused to vYFP expressed at the expected molecular weight in HBMECs and COS7 cells (Figure 4.14). These results are in agreement with a previous study where 37 LRP tagged C-terminally into EGFP, ECFP and DsRed were expressed at similar molecular weight of 37 LRP.vYFP (Nikles et al., 2008). In COS7 cells, the Gal-3.vYFP plasmid expressed protein of the expected molecular weight in Western blotting of either GFP and/or Gal-3 (Figure 4.15), which corroborates previously published data (Nakahara et al., 2006). However, in HBMECS the Gal-3 fused to vYFP, expressed at approximately 67 kDa, which was a slightly higher than expected molecular weight (60 kDa). This heterogeneity could be attributed to different post-translational modifications of the protein in the primary HBMECs. Confocal microscopic analysis of HBMECs transiently transfected with 37 LRP and Gal-3 tagged to vYFP showed punctate pattern of expression (Figure 4.17A). Of interest, the observed punctate distribution of 37 LRP-vYFP in the surface of HBMECs resembled punctate staining of endogenous 67 LR. While the punctate expression of Gal-3-vYFP reflects the punctate staining reported for endogenous Gal-3 by our study (Figure 4.5A) and previous studies (Delacour et al., 2007; Thijssen et al., 2008). In addition to punctate staining, some diffuse staining was also observed for endogenous Gal-3 in the current study (Figure 4.5A). This differential pattern

may be due to the difference in methods used between direct visualization of vYFP expression and indirect immunofluorescence staining. Another possibility is that Gal-3 antibody may cross-react with other members of the galectin family, which share sequence homology with Gal-3, leading to observed diffuse staining.

In COS7 cells, which were used in the current study as the transfection host, the vYFP labelled 37 LRP and Gal-3 were diffusely distributed in the whole cells as shown by confocal microscopy (Figure 4.17A). This pattern supports diffuse distribution of endogenous 37 LRP and Gal-3 in the surface of COS7 cells (Figure 4.5C). In addition, subcellular fractionation analysis independently confirmed the confocal microscopy data, and demonstrated expression of Fluorescent tagged receptor in the membrane, cytoplasm and nuclear fractions of COS7 cells (Figure 4.17B). These results are in agreement with a previous study, which showed that 37 LRP fused to EGFP was expressed in the nuclei, cytoplasm and cell surface of transiently transfected BHK cells (Nikles et al., 2008). The same distribution pattern was also observed previously with Gal-3 fused with GFP in COS7 cells (Nakahara et al., 2006). Taking into consideration that the present study has focused on the receptors located at the cell surface, which confirmed by detection of vYFP labelled 37 LRP and Gal-3 in cell membrane fractions of transfected COS7 cells.

One of the main objectives of this study was to investigate the role of Gal-3 in meningococcal adhesion and invasion, which will be described in Chapter 6. To achieve this aim, N2a cells, which lack the expression of endogenous Gal-3 were employed. These cells were extensively used in previous studies to investigate the role of 67 LR/37 LRP in prion disease (Gauczynski et al., 2001; Gauczynski et

al., 2006). Diffuse expression of vYFP-receptors was demonstrated in N2a cells and their surface localization was confirmed by immunofluorescence staining (Figure 1.17B). Such pattern reflects immunofluorescence staining of endogenous and overexpressed 37 LRP in N2a cells as shown by a previous study (Gauczynski et al., 2001). Importantly, the observed surface localization of Gal-3.vYFP in N2a cells verifies their suitability as model to study role of Gal-3 in adhesion and invasion of N. meningitidis.

It is known that 67 LR is formed by homo or hetero-dimerization of the acylated 37 LRP (mainly palmitoylated), which is required for cell surface delivery of 67 LR. Therefore, cysteines at position 148 and 163 of 37 LRP.vYFP were substituted to alanines, to investigate if this substitution will affect targeting of 67 LR to the cell surface. In HBMECs, mutant constructs showed the same punctate distribution pattern of native receptors (Figure 4.20A). Based on western blot and flow cytometry analysis there was no significant difference in molecular weight and cellular expression between native receptor and mutants in COS7. Cellular fractionation coupled with Western blotting illustrated that the localization of cysteine mutants was indistinguishable from wild type 37 LRP (Figure 4.20B). These results collectively revealed that the substitution of the selected cysteine does not affect receptor expression, cell surface targeting and localization. It might be interesting to detect 67 LR surface expression in cells transfected with native and cysteine mutants using the Mluc5 antibody in flow cytometry. Therefore, future studies on these cysteine-substituted constructs are recommended.

Based on the experimental data presented herein, expression and surface localization of the endogenous Gal-3, 67 LR and its precursor form 37 LRP in primary HBMECs were verified by western blotting, flow cytometry and immunofluorescence staining. A similar pattern of receptor expression was observed in astrocytes. Furthermore, expression of vYFP labelled receptors revealed a punctate staining pattern in HBMEC, and a diffuse pattern in COS7 and N2a cells. Additionally, their surface expression were confirmed, indicating that tagging of 37 LRP and Gal-3 with vYFP did not affect their surface localization. Finally, substitution of the two-cysteine residues to alanines within the C-terminal of 37 LRP, which is thought to be involved in acylation, showed no noticeable differences in membrane localization between native and mutants receptors, suggesting involvement of other amino acid residues in 67 LR acylation.

5.1. Introduction:

Previous studies have suggested that 67 LR is a heterodimer derived from dimerization of 37 LRP and Galectin-3 (Gal-3) (Castronovo et al., 1992; Simona Butò, 1998). Both Gal-3 and 67 LR are non-integrin laminin binding proteins. Gal-3 binds to β-galactosides and the poly-N-acetyl-lactosamine residues of laminin, while 67 LR binds laminin into two binding sites: the YIGSR, a short sequence of the β1 chain, and peptide G (Nelson et al., 2008). Moreover, Gal-3 is found in the cytoplasm and nucleus as 37 LRP, and on the cell surface as 67 LR, and excreted extracellularly by unknown mechanisms (Barondes et al., 1994b; Nelson et al., 2008).

Among evidences that support heterodimerization of 67 LR with Gal-3 is the fact that 67 LR can be eluted from a laminin affinity column by lactose, galactose and N-acetyllactoseamine (Castronovo et al., 1992). Additionally, Laminin recognition by 67 LR is lactose dependent since treatment of laminin with endo-β-galactosidase enzyme, which disrupts linear type 2 poly-N-acetyl lactoseamine, abolishes its binding with 67 LR and Gal-3 (Castronovo et al., 1992). As a result, recognition of laminin by 67 LR and Gal-3 is depending on the N-acetyllactoseamine moiety (Castronovo et al., 1992). Immunoblotting of human carcinoma cell extract, which proved to express 67 LR and 37 LRP, using a polyclonal antibody directed against Gal-3, recognized a band at 67 kDa, which is the same size of mature 67 LR, but not at 37 kDa (Simona Butò, 1998). Furthermore, antibodies generated against other lectins, such as HLBP14 (human laminin binding protein 14), also detect lactose eluted 67 LR and Gal-3 laminin binding proteins in Western blotting (Castronovo et al., 1992). In conclusion, all these findings indicate that 37 LRP might form heterodimers with other acylated

proteins carrying the Gal-3 epitope, and produce the mature receptor form 67 LR (Figure 5.1).

On the contrary to heterodimerization theory, amino-acid compositions of 67LR were found to be identical to 37 LRP, suggesting a homodimer (Landowski et al., 1995). Another study showed that both 67 LR and 37 LRP co-exist on the surface of N2a cells, a cell which does not express Gal-3 (Gauczynski et al., 2001). That revealed Gal-3 or any other lectin is not obligate for surface expression of 67 LR. Therefore, so far the issue of 67 LR dimerization is not yet determined. A general scheme for the mechanisms of cell surface distribution of different forms of LR and Gal-3 is illustrated in Fig. 5.1.
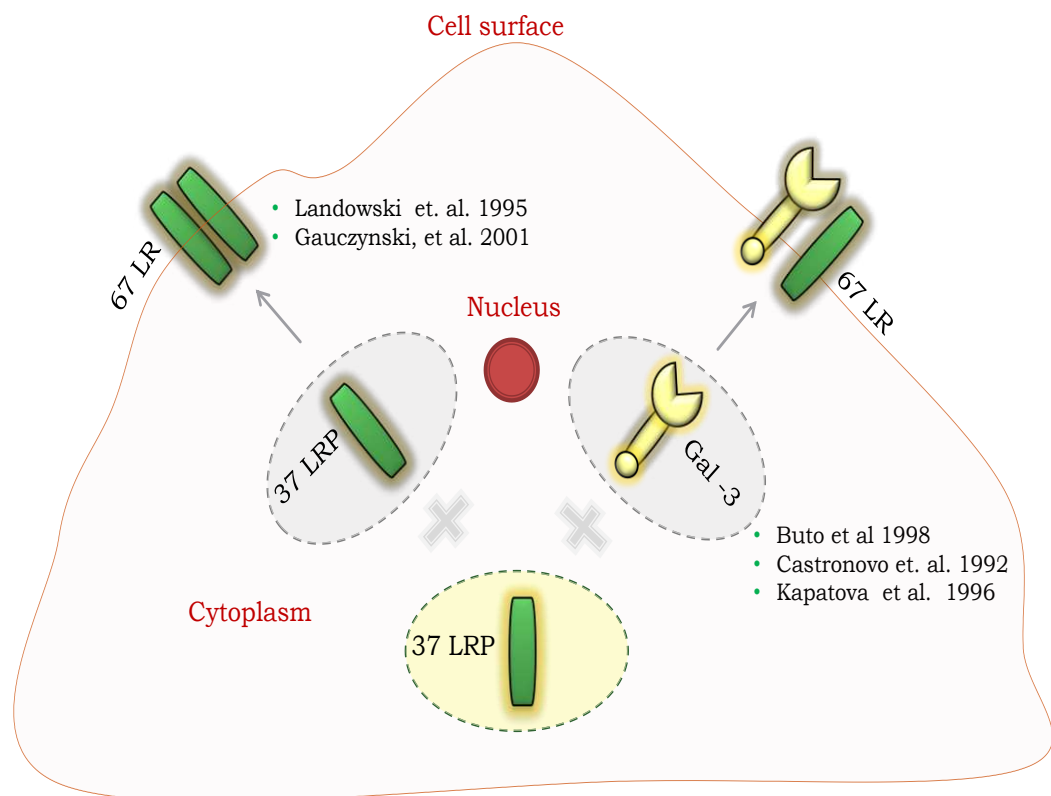
Figure 5.1: Speculations of the 67 LR dimerization status. The 67 LR would be obtained by the association between the 37LRP and Gal-3 or 37 LRP and 37 LRP

forming 67 LR hetero or homodimers, respectively. Reproduced from (Menard et al., 1997).

In addition, Gal-3 exists as a monomer in solution (Morris et al., 2004). In the absence of Gal-3 glycan ligands, it can form homodimer and self associates via its CRD (Yang et al., 1998) (Figure 5.2) and a cysteine at position 186 was shown to be required for such homodimerization in murine Gal-3 (Woo et al., 1991). Whereas, in the presence of glycan ligands, Gal-3 can multimerize upto a pentamer, through its N-terminus (Barondes et al., 1994b) (Figure 5.2). Binding of Gal-3 to specific ligands mediate its cellular action.
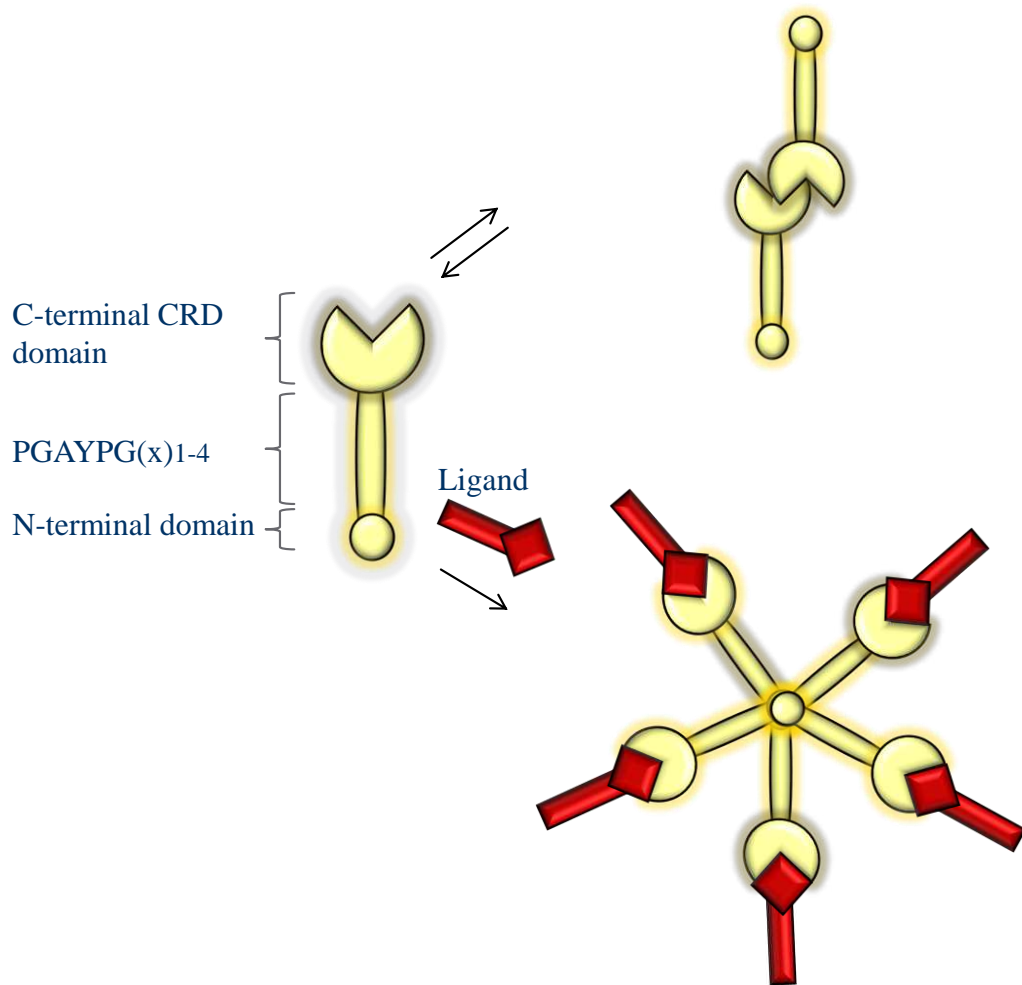
Figure 5.2. Schematic representations of the monomeric structure of Gal-3 and Gal-3 dimerization, through its CRD, in the absence of binding ligands and polymerization, and through its N-terminal domain in the presence of carbohydrate binding ligands. The figure was adopted from (Newlaczyl & Yu, 2011)**.**

Advanced non-invasive fluorescent-based approaches have been used recently to study protein-protein interactions, such as receptor dimerization, in living cells. These approaches include bimolecular fluorescence complementation (BiFC) (Kerppola, 2008; Shyu et al., 2006) and fluorescence resonance energy transfer (FRET) (Miyawaki et al., 1997). BiFC was utilized in the current study to

investigate 67 LR dimerization status in mammalian cells. The principle of BiFC is based on the generation of a fluorescent signal from two separate non-fluorescent fragments, which are brought together by the association of two potential interacting proteins fused to the fragments (Hu et al., 2002; Kerppola, 2008) (Figure 5.2A). An in vitro study has shown that the development of BiFC is a two steps process (Hu et al., 2002). In the first step, the N and C terminal domains of the fluorescent protein fragments refold into the ß-barrel structure when brought into close proximity. This step can be disturbed by untagged competitors only initially after the association begins, revealing rapid (half time 1 min) and irreversible properties of the association step (Figure 5.2A). The second step is chromophore maturation, which involves slow autocatalytic oxidation reaction, to generate fluorescent a BiFC complex with a half-life of approximately 50 min (Hu et al., 2002). This step is the rate limiting step for detection of BiFC.

Until now, more than 200 protein-protein interaction have been visualized successfully by the BiFC approach (Kerppola, 2006). This owes to the capability of this method to visualize and determine subcellular distribution of interacting proteins in living cells without invasive immunostaining (Kerppola, 2006; Kerppola, 2008). Additionally, the complementation of fluorescent fragments in the BiFC method, result in the production of new fluorescence, which is simple to detect and analyse (Kerppola, 2006; Kerppola, 2008). However, BiFC has some limitations: the irreversible complementation of the fluorescent fragments, the intrinsic ability of the fluorescents fragments to associate under certain condition, and the time required for fluorophore maturation (Hu et al., 2002; Kerppola, 2008). These limitations should be taken into consideration when designing any BiFC experiment.

Two distinctive positions in GFP variants have been used to split intact proteins. The two positions of fragmentation represent amino acid residues 155 and 173 (Figure 5.2B). In Hu. et al 2002 study, fragment of EYFP were used to develop the BiFC method. However, these fragments require preincubation at 30°C to visualize the BiFC signal. To overcome this limitation, several fragments of GFP variants were used to develop new BiFC fragments. Among these variants, Venus, a known YFP mutant (Figure 5.2B), which is characterized by fast maturation at 37°C and bright fluorescence as described in Chapter 4 (Nagai et al., 2002). Interestingly, fragments of Venus, truncated at either residue 155 or 173, were shown to enhance the efficiency of BiFC complementation, and allow experiments in mammalian cells to be performed under physiological conditions (Shyu et al., 2006). Other fragments of different fluorescent proteins, such as CFP, GFP and mCherry have been identified and used in BiFC (Rose et al., 2010).
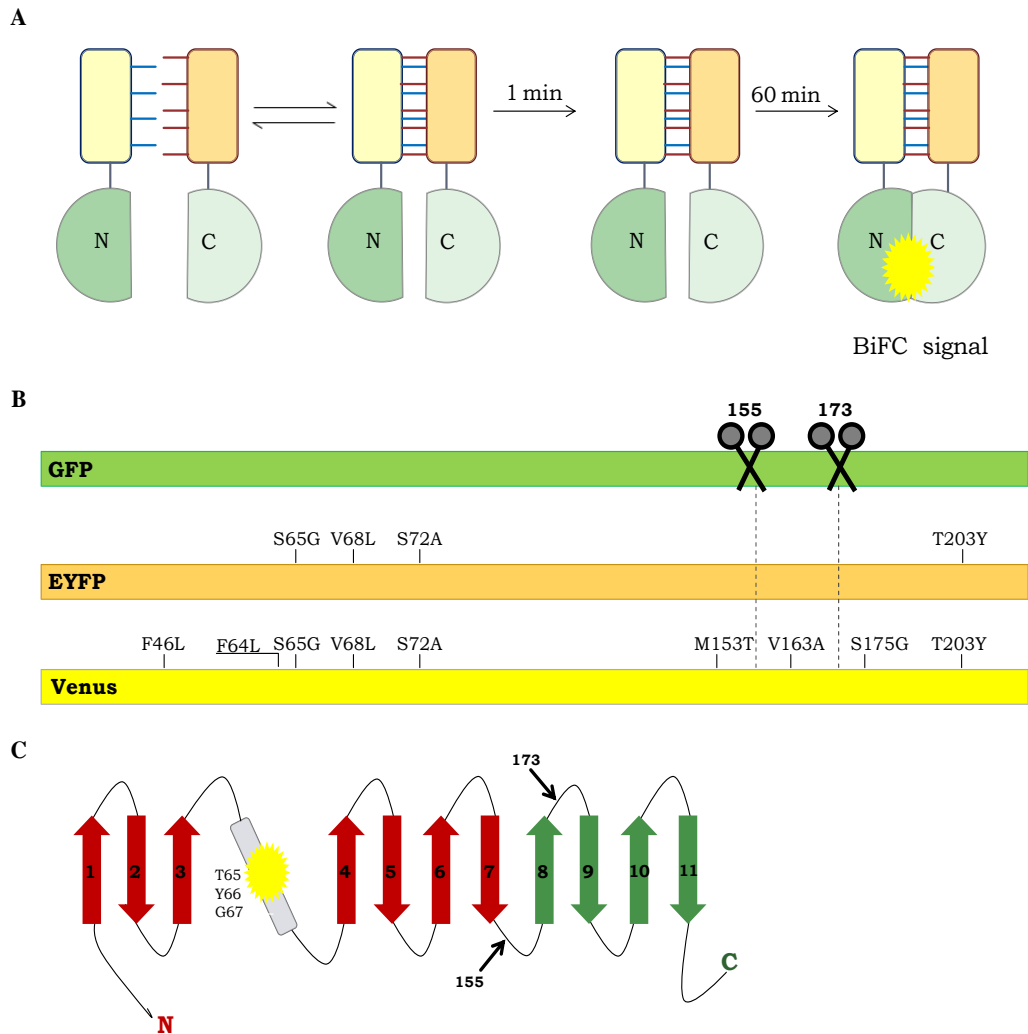
Figure 5.2: Principle of bimolecular fluorescence complementation. (A) Schematic diagram showing the interaction between two potential interacting proteins fused to N-terminal and C-terminal fluorescent protein fragments (N and C, respectively). The potential interacting proteins can associate and dissociate reversibly until the fluorescent protein fragments refold to form a fluorescent protein. This is followed by subsequent maturation of the chromophore, over a longer time period, to generate the fluorescent BiFC complex. Adapted and modified from (Hu et al., 2002; Rose et al., 2010). (B) A schematic view of the green fluorescent protein (GFP) and two of its variants (EYFP and Venus YFP). The positions of splitting in fluorescent proteins are indicated with scissors symbols. Adapted and modified from (Shyu et al., 2006). (C) A schematic diagram showing the structure of Aequorea fluorescent protein, which is

composed of 11 β strands. The arrows reveal the most common position of truncation to produce the non-fluorescent half fragments. Adapted and modified from (Rose et al., 2010).

The aim of this chapter was to investigate homo- and hetero-dimerization among the 37 LRP and Gal-3 to form mature 67 LR in mammalian cells using immunofluorescence, coexpression of receptors tagged with the mCherry or vYFP, ELISA and BiFC confocal microscopy and flow cytometry. This chapter also aimed to explore whether substitution of the Gal-3 cysteine residue, which is required for Gal-3 homodimer formation, affects Gal-3 dimerization with 37 LRP, using BiFC. Moreover, other cysteine residues in 37 LRP, which were thought to be involved in acylation, were substituted into alanine and further examined for their ability to form BiFC signal comparable to native receptors.

5.2. Results:

5.2.1. Colocalization of laminin receptor and Galectin-3

5.2.1.1. Immunofluorescence

Homo and heterodimerization of 67 LR was suggested by previous studies (Buto et al., 1998; Castronovo et al., 1992; Gauczynski et al., 2001; Landowski et al., 1995). Therefore, double immunofluorescence staining of non-permeabilized cells was used to examine the colocalization of 67 LR, 37 LRP and Gal-3. As shown in Figure 5.3A, a merged image of the common punctate staining of 67 LR using Mlu5 antibody (red) and the diffuse staining of 37 LRP using InHLRP antibody (green) revealed co-localization of 67 LR with 37 LRP in HBMECs and astrocytes. Interestingly, the merged images of the red fluorescent signal corresponding to either 67 LR or 37 LRP and green fluorescent signal (Gal-3) showed a strong co-localization (yellow) of Gal-3 with 67 LR in HBMECs and astrocytes (Figure 5.3B) or 37 LRP (Figure 5.3C) in HBMECs, astrocytes and COS7 cells.

A

HBMECs

37LRP (InHLRP)

67 LR (MluC5)

67 LR (MluC5) & 37LRP (InHLRP)

Astrocyte

37LRP (InHLRP)

67 LR (MluC5)

67 LR (MluC5) & 37LRP (InHLRP)

B

HBMECs

67 LR (Ab711)

Gal-3 (mab4033)

Gal3 (mab4033)
& 67 LR (Mluc5)

Astrocyte

Gal-3 (mab4033)

67 LR (Ab711)

67 LR (Ab711) & Gal-3 (Mab4033)

C

HBMECs

Gal3 (mab4033)

37 LRP (InHLRP)

Gal3 (mab4033) & 37 LRP (InHLRP)

Astrocyte

37 LRP (InHLRP)

Gal-3 (mab4033)

37 LRP (InHLRP) & Gal-3 (mab4033)
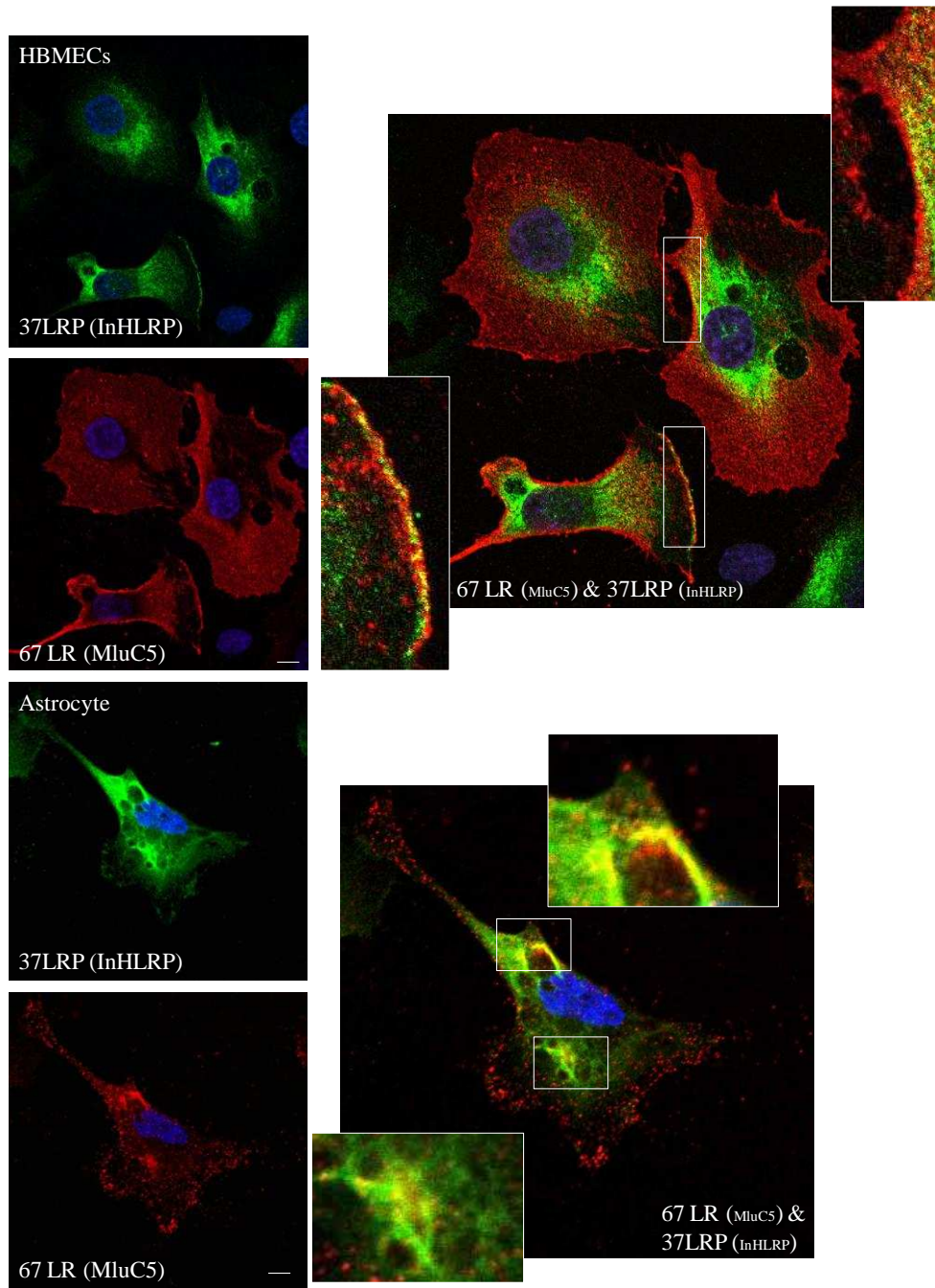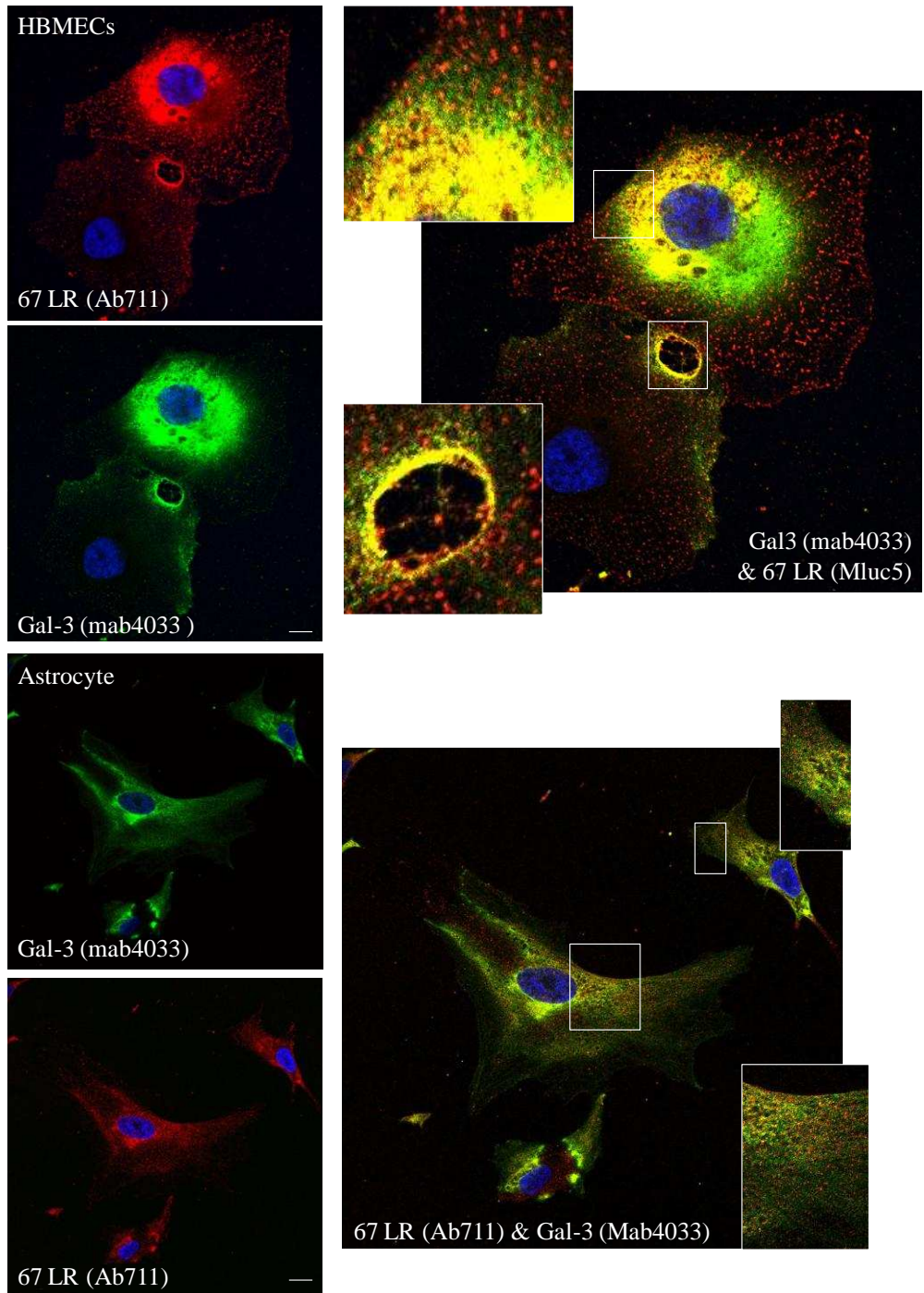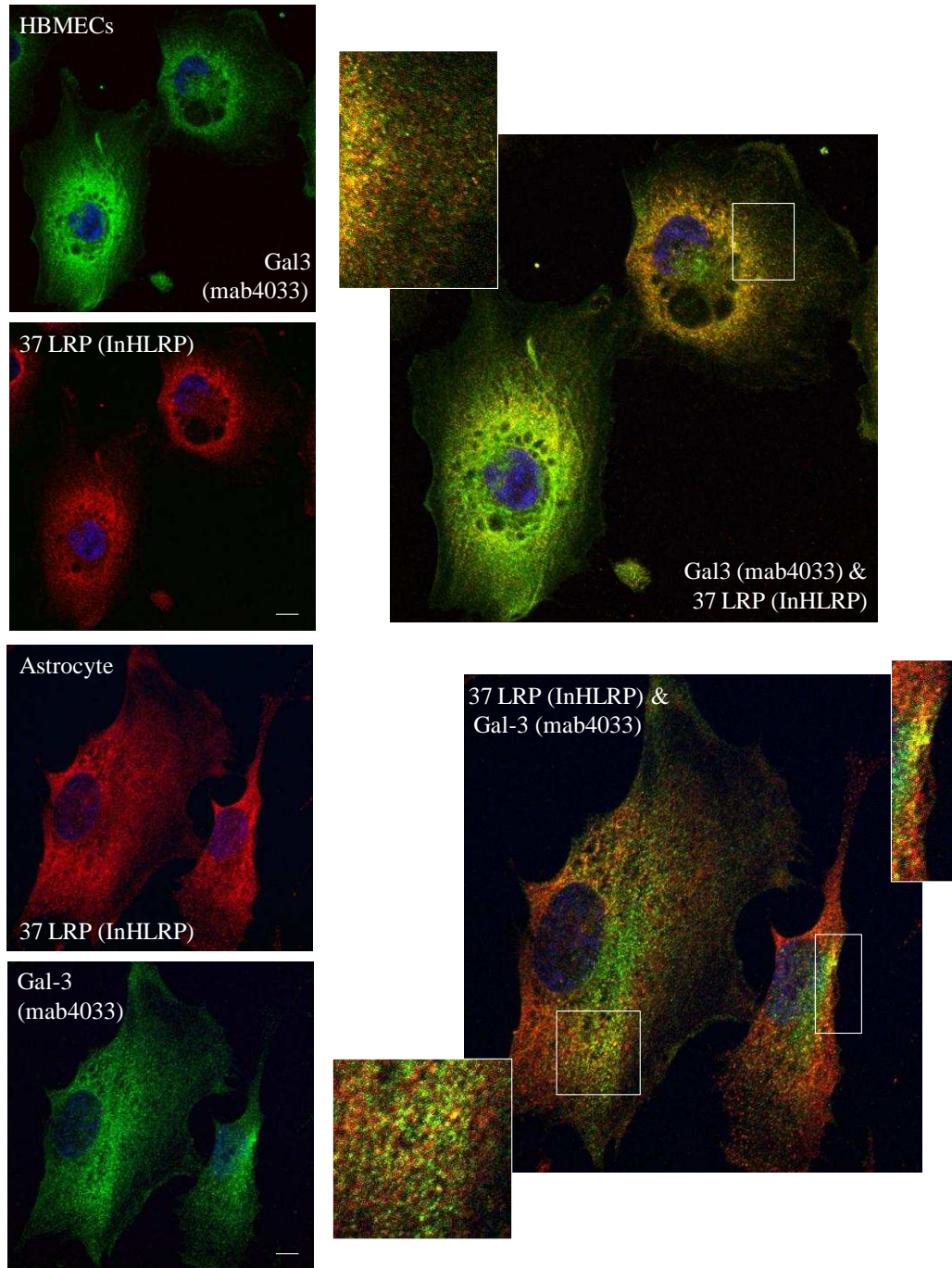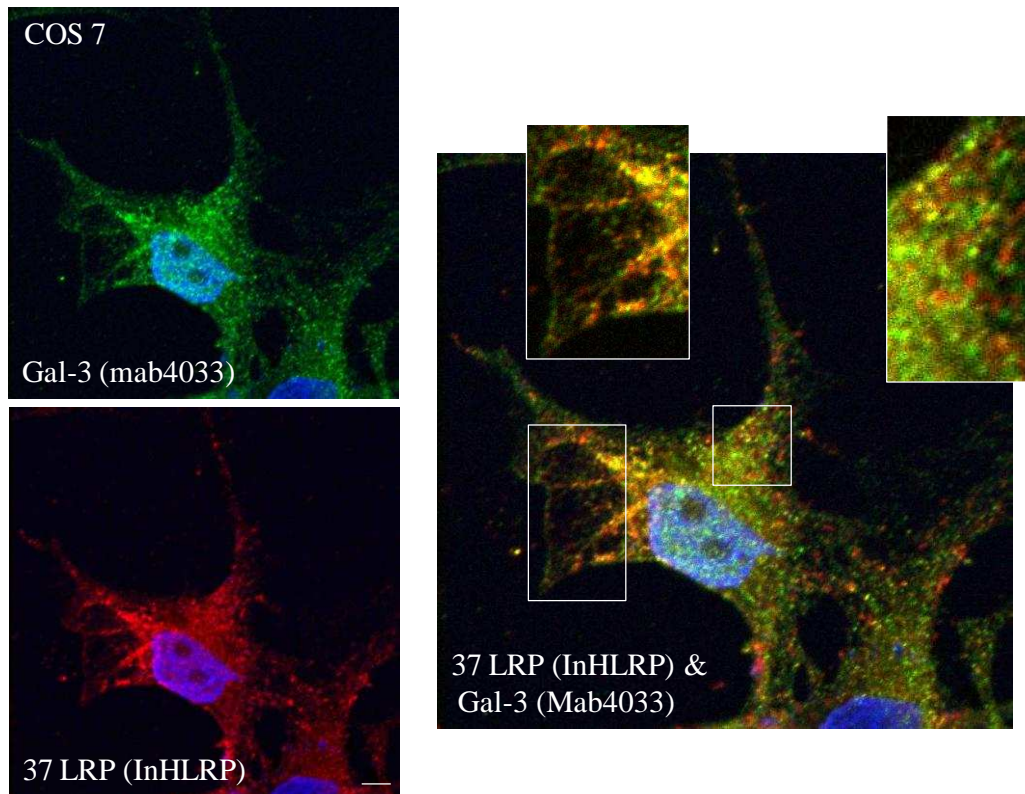
Figure 5.3: Double immunofluorescence staining shows colocalization of 67 LR with 37 LRP and 67 LR/37 LRP with Galectin-3 in HBMECs, astrocyte and COS7. Representative confocal microscopic images of immunofluorescence double labelled HBMECs, or astrocytes, or COS7 cells, to determine receptor surface co-localization. The cells grown on coverslips were fixed with 4% paraformaldehyde and co-stained with anti-67 LR (MluC5) and anti-37 LRP (InHLRP) (A), anti-67 LR (Ab711) and anti-Gal-3 (mab4033) (B), or anti-37 LRP (InHLRP) and anti-Gal-3 (mab4033) (C) and secondary antibody(s); Alexa Fluor 647 ,680 and 488 antibodies. Areas of overlap appear yellow in the merged images, illustrating co-localization of 67 LR with 37 LRP (A), 67 LR and with Gal-3 (B), and 37 LRP with Gal-3 (C). Nuclei are stained with Hoechst 33258, and appear blue. Scale bars represent 0.09µm (HBMECs), 0.2µm (Astrocytes) and 0.05µm (COS7 cells).

5.2.1.2. Coexpression of fluorescently tagged receptors

Double immunofluorescence staining suggests colocalization of 67 LR with its precursor (37 LRP) and Gal-3. To further characterize their colocalization, receptors were fused C-terminally to mCherry (monomeric red fluorescent protein, RFP), as described in Chapter 4, to enable their coexpression with vYFP tagged receptors. The expression of generated constructs was examined by Western blot analysis using an anti-mCherry antibody. Western blotting of COS7 cells, transiently transfected with 37 LRP or Gal-3 fused to mCherry, yielded bands of 67 and 60 kDa, representing the sum of the molecular weights of the receptor and fused fluorescent protein (Figure 5.4). Cotransfection of 37 LRP.vYFP and 37 LRP.mCherry or Gal-3.mCherry resulted in a colocalization in the nuclear, cytoplasmic compartments and on the cell surface (Figure 5.5A and B). As a positive control, Gal-3.mCherry and Gal-3.vYFP were coexpressed, since earlier studies have shown Gal-3 dimerization (Nieminen et al., 2007; Woo et al., 1991). In addition, distribution of Gal-3.vYFP and Gal-3.mCherry almost completely overlapped (Figure 5.5C).
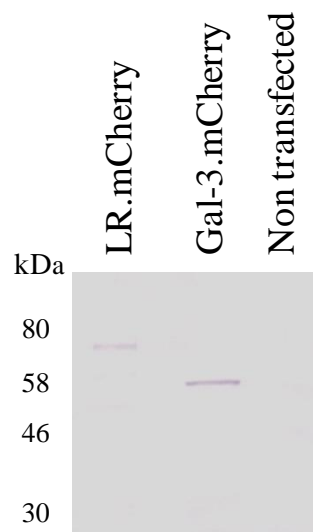
Figure 5.4: Immunoblot analysis indicates expression of 37 LRP and Galectin-3 fused to mCherry. Whole cell lysates of COS7 cells, transiently transfected with the indicated constructs, as described in Chapter 2, and subjected to SDS-PAGE. The cell lysates were then immunoblotted using anti-mCherry rabbit polyclonal antibody at a 1:1000 dilution followed by a 1:30000 dilution of anti-rabbit conjugated to alkaline phosphtase, and subsequently detected by the NBT/BCIP substrate as described in Chapter 2. Western blot analysis confirmed the expression of the transfected constructs.
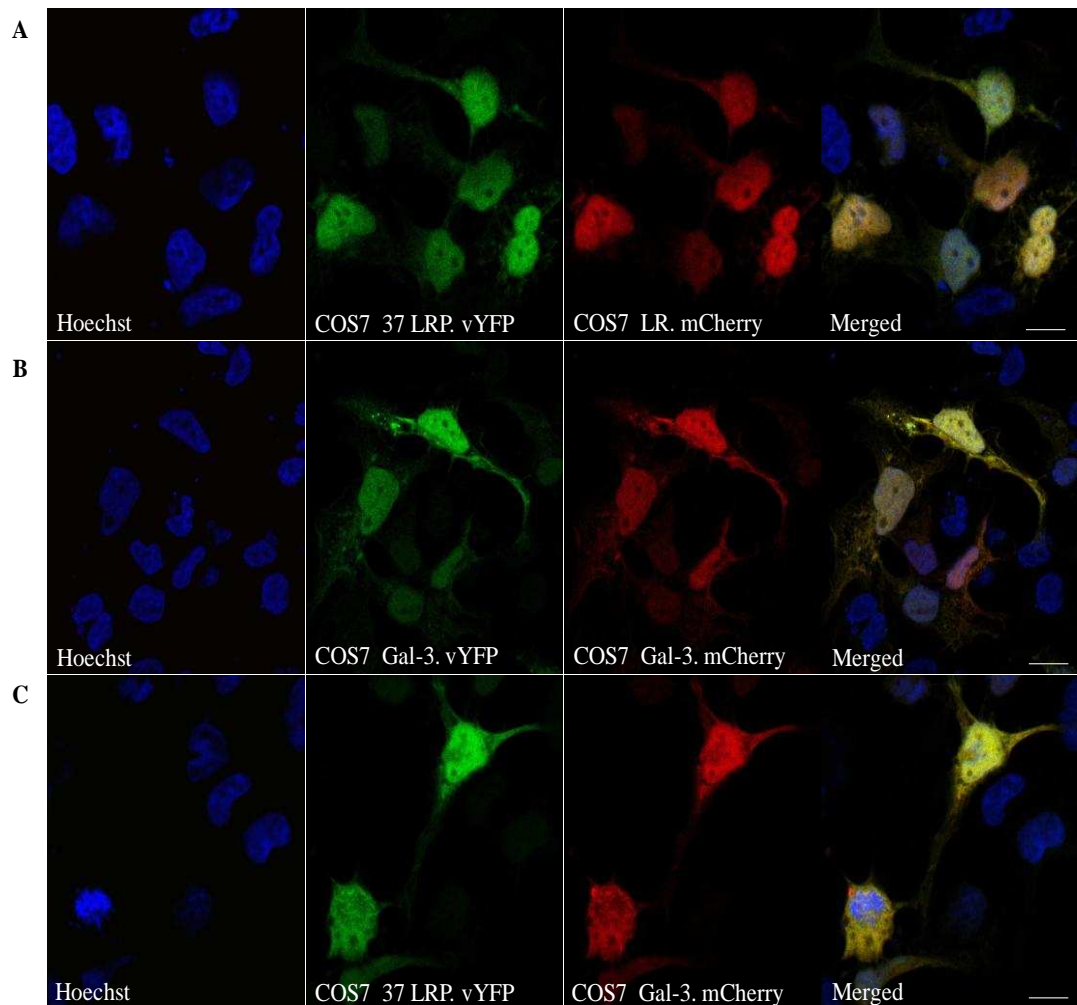
Figure 5.5: Colocalization of the 37 LRP.vYFP with mCherry coupled 37 LRP and Galectin-3. Representative confocal microscopic images of COS7 cells

transiently cotransfected with 37 LRP.vYFP and 37 LRP.mCherry (A) or 37 LRP.vYFP and Gal-3.mCherry (C) or Gal-3.vYFP and Gal-3.mCherry (B), and 24h post transfection the cells were fixed with 4% paraformaldehyde and nuclei stained with Hoechst, as described in Chapter 2. Scale bars represent 0.15µm.

5.2.1.3. ELISA

Immunofluorescence and cotransfection data indicated that 37 LRP colocalize with Gal-3 (Figures 5.3 and 5), which supports previous ELISA results (Figures 3.8). In order to determine which part of Gal-3 interacts with 37 LRP, either Gal-3 full molecule or its CRD, was immobilized on an ELISA plate and 37 LRP binding activity was assessed. As shown in Figure 5.6, recombinant LR bound to the CRD significantly ($p= 0.0004$) when compared with the negative control (BSA), with a level comparable to that determined for the rLR interaction with the Gal-3 full molecule. This result suggests that the CRD of Gal-3 mediates the majority of the Gal-3 interaction with 37 LRP.
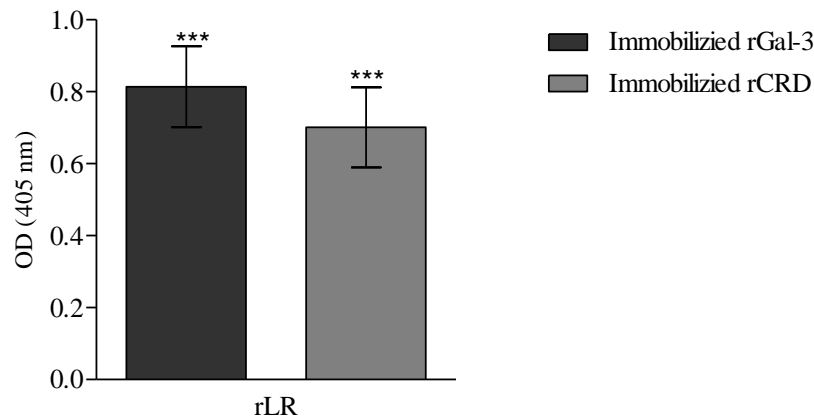
Figure 5.6: Interaction of rLR and rGal-3. Specific binding of recombinant purified LR with immobilized rGal-3 full molecule and rCRD coated ELISA plates. BSA-coated wells were considered as a negative control, and the mean value obtained from rLR-BSA coated wells was subtracted from rGal-3 and rCRD coated wells. The data represent the mean (OD) at wavelength of 405 nm ± SEM (error bars) of a sample tested in triplicate. Experiments were repeated three times, with consistent results. Asterisks indicate the significant binding of purified proteins to rLR compared with BSA. (Student's t- test; ***$P < 0.001$).

5.2.1.4.   BiFC (Biomolecular fluorescence complementation)

The bimolecular fluorescence complementation (BiFC) approach was used to characterize the possible homo- and heterodimerization of 37 LRP and Gal-3. To this end, the C terminus of the 37 LRP and Gal-3 was fused to the N-terminal or C-terminal fragment of the Venus YFP, a derivative of YFP (Nagai et al., 2002) as described in Chapter 4, and then transfected into HBMECs, N2a and COS7 cells. The overall strategy of BiFC was outlined in Figure 5.7. Interestingly, Venus fluorescence was detected, indicating successful complementation of YFP (cYFP) and formation of BiFC complex by confocal microscopy. This result demonstrated the formation of both 67 LR homodimer (Figure 5.8A and B) and 37 LRP and Gal-3 heterodimers (Figure 5.8A and B) in HBMECs and N2a. BiFC complexes showed a punctate distribution on the apical surface of HBMECs (Figure 5.8A) and smooth uniform distribution in N2a cells (Figure 5.8B). As a previous study showed Gal-3 dimerization (Woo et al., 1991), Venus fragments (YNL or YCL) fused to the C-terminal region of Gal-3 were cotransfected into HBMECs and N2a cells for further characterization of observed BiFC complexes, above. As represented in Figure 4B, Gal-3 was able to form homodimers and produce a comparable signal to that produced from 67 LR homo and heterodimers in N2a (Figure 5.8B). However, in HBMECs no BiFC signal was detected (Figure 5.8A).

The subcellular distribution of YFP-complemented receptors was not apparently different from that observed with receptors labelled with full length vYFP (Figure 4.17A). When cells were transfected with single constructs containing receptors fused to either C or N fragments of YFP, no fluorescence was observed, as the YFP fragments by their own are not fluorescent (Figure 5.8A and B).

To confirm construct surface expression, N2a cells, transiently transfected or co-transfected with Venus fragments tagged into receptors, were immunostained with antibodies specific for GFP-tag, confirming their expression (Figure 5.8B). Each Venus fragment fused to a receptor was expressed successfully and no comparable fluorescence signal to complemented fragments was detected in the Venus channel, as expected (Figure 5.8B). Furthermore, the receptor dimerization was additionally analyzed by flow cytometry. As primary HBMECs are relatively difficult to transfect, thus, COS7 cells, transiently transfected or cotransfected with receptors fused to Venus full length and its fragments, and 24h post transfection, were subjected to flow cytometry. As expected, the BiFC signal was detected for the interaction of 37 LRP.vYNL/37 LRP.vYCL, 37 LRP.vYNL/Gal-3.vYCL and vice versa, whereas only a very low background fluorescence was observed for sole 37 LRP.vYNL and 37 LRP.vYCL, Gal-3.vYCL and Gal-3.vYNL (Figure 5.8B). Taken together, the results revealed the formation of 37 LRP and Gal-3 as a homo- and/or hetero- dimer receptor in the HBMECs, N2a and COS7 cells.
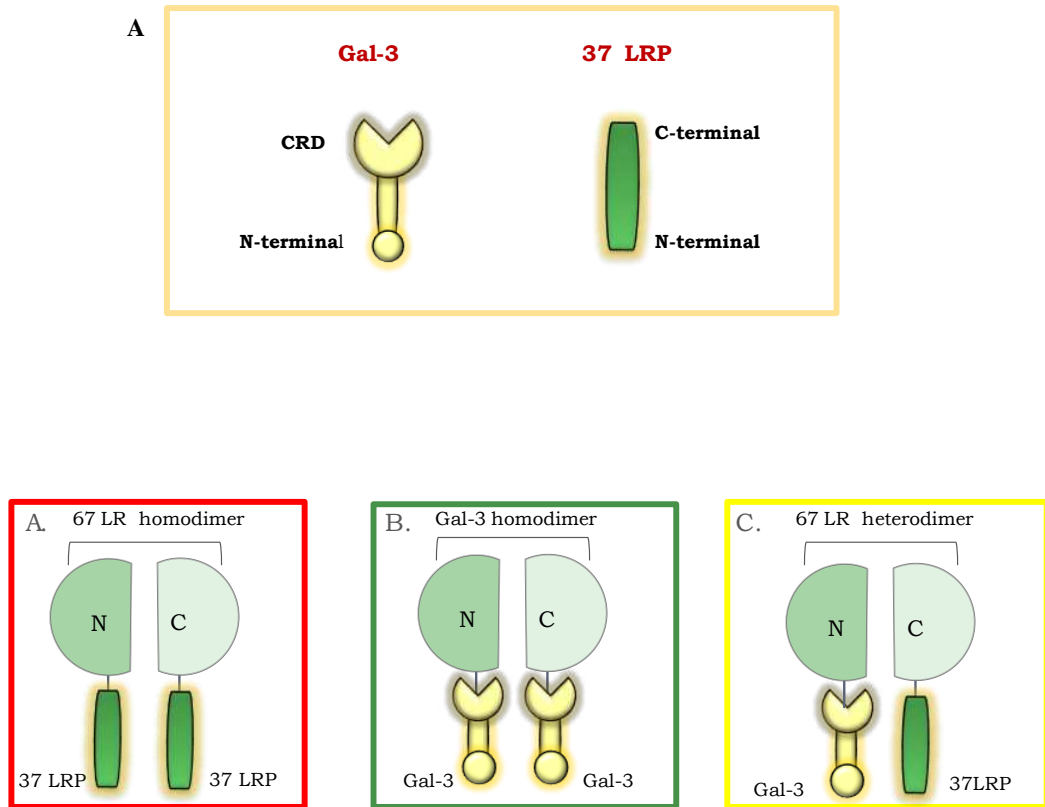
Figure 5.7: Biomolecular fluorescence complementation (BiFC) strategy used in this project. (A) Typical Gal-3 and 37 LRP structure. The C terminals of 37 LRP and Gal-3 were fused to the N-terminus of vYFP (N) and the C-terminus of vYFP (C) and receptors interaction will lead to BiFC complementation and vYFP generation. Two models were tested for possible interactions between 37 LRP and 37 LRP (A.), 37 LRP and Gal-3(C.), whereas model (B.) Gal-3 and Gal-3 was used as a positive control for the BiFC method.

A

Venus YFP(BiFC)

HBMECs Gal-3. vYCL

HBMECs 37 LRP. vYCL

HBMECs Gal-3. vYNL& vYCL

HBMECs 37 LRP. vYCL & Gal-3. vYNL

HBMECs 37 LRP. vYNL& vYCL

HBMECs Gal-3. vYNL

HBMECs 37 LRP. vYNL

B

Venus YFP(BiFC)

Anti-GFP (vYFP)

Merge

N2a 37 LRP. vYCL

N2a 37 LRP. vYNL

N2a Gal-3. vYCL

N2a Gal-3. vYNL

N2a 37 LRP. vYNL & Gal-3. vYCL

N2a Gal-3. vYNL & vYCL

N2a 37 LRP. vYNL& vYCL

C

37 LRP homdimerization

Legend:
- 37 LRP.vYFP
- 37 LRP.vYNL & 37 LRP.vYCL
- 37 LRP.vYNL
- 37 LRP.vYCL

37 LRP & Gal-3 heterodimerization

Legend:
- 37 LRP.vYFP
- Gal-3.vYFP
- 37 LRP.vYNL & Gal-3.vYCL
- 37 LRP.vYCL & Gal-3.vYNL
- 37 LRP.vYNL
- 37 LRP.vYCL
- Gal-3.vYNL
- Gal-3.vYCL

Gal-3 homodimerization

Legend:
- Gal-3.vYFP
- Gal-3.vYCL & Gal-3.vYNL
- Gal-3.vYNL
- Gal-3.vYCL

Figure 5.8: Detection of 37 LRP and Galectin-3 dimerization using BiFC and flow cytometry. Representative confocal microscopic images of the primary HBMECs (A) or N2a (B) transiently co-transfected with indicated construct and 24 hrs post transfection the cells were fixed with 4% paraformaldehyde and nuclei stained with Hoechst (A) or anti-GFP antibody (1: 100) followed by Alexafluor 680 (1:100) (B). Fluorescence was detected in cells co-expressing 37 LRP.vYNL and 37 LRP.vYCL, or Gal-3.vYCL and Gal-3.vYNL, revealing successful complementation of Venus fragments (A and B). No fluorescence was detected in cells transfected with either half of Venus fused to 37 LRP or Gal-3 (A and B). Immunostaining of N2a cells that were transfected with the same previous constructs using anti-GFP, confirms the cell surface expression of receptors tagged into Venus fragments (B). Scale bars represent 0.15 µm and 0.09 µm for HBMECs and N2a, respectively. (C) Flow cytometry revealed 37 LRP & Gal-3 dimerization. COS7 cells were transfected with constructs as indicated above and Venus fluorescence was analyzed by flow cytometry as described in Chapter 2. Results are expressed as percentage of the specific fluorescence signal to the value of 37 LRP.vYFP and Gal-3.vYFP. Bars represent the mean ± SE of three independent experiments.

5.2.2. Colocalization of 37 LRP and Galectin-3 dimers with InHLRP antibody

Previous immunostaining of Venus full length and its fragments, fused to Gal-3 and 37 LRP, using the anti-GFP antibody, confirm the expression and surface localization of transfected constructs in N2a cells (Figure 5.8B). Both 67 LR and 37 LRP are expressed endogenously on the surface of N2a cells, confirming a previous study (Gauczynski et al., 2001). To examine whether BiFC complexes formed by 37 LRP and Gal-3 were co-localized with endogenous 37 LRP, the distribution of BiFC complexes was compared with anti-37 LRP immunofluorescence. Firstly, the immunofluorescence of endogenous 37 LRP, in non-transfected fixed non-permeabilizied N2a cells, was carried out using both the InHLRP antibody. The 37 LRP showed diffuse membrane staining on the surface of N2a cells (Figure 5.9).
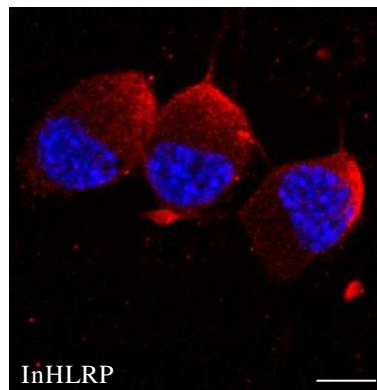
Figure 5.9: Immunofluorescence staining of 37 LRP in N2a cells. Representative confocal microscopic images of immunofluorescence labelled N2a cells to detect localization of 37 LRP. The cells grown on coverslips were fixed with 4% paraformaldehyde and stained with anti-37 LRP (InHLRP), and secondary antibody: AlexaFluor 680. Nuclei were stained with Hoechst 33258. Scale bar represents 0.05µm.

Then, N2a cells were transiently transfected with 37 LRP fused to vYFP or cotransfected with receptors fused to Venus fragments and stained with the InHLRP antibody. 37 LRP homo- and hetero- dimers with Gal-3 were colocalized with diffuse staining of 37 LRP (Figure 5.10).
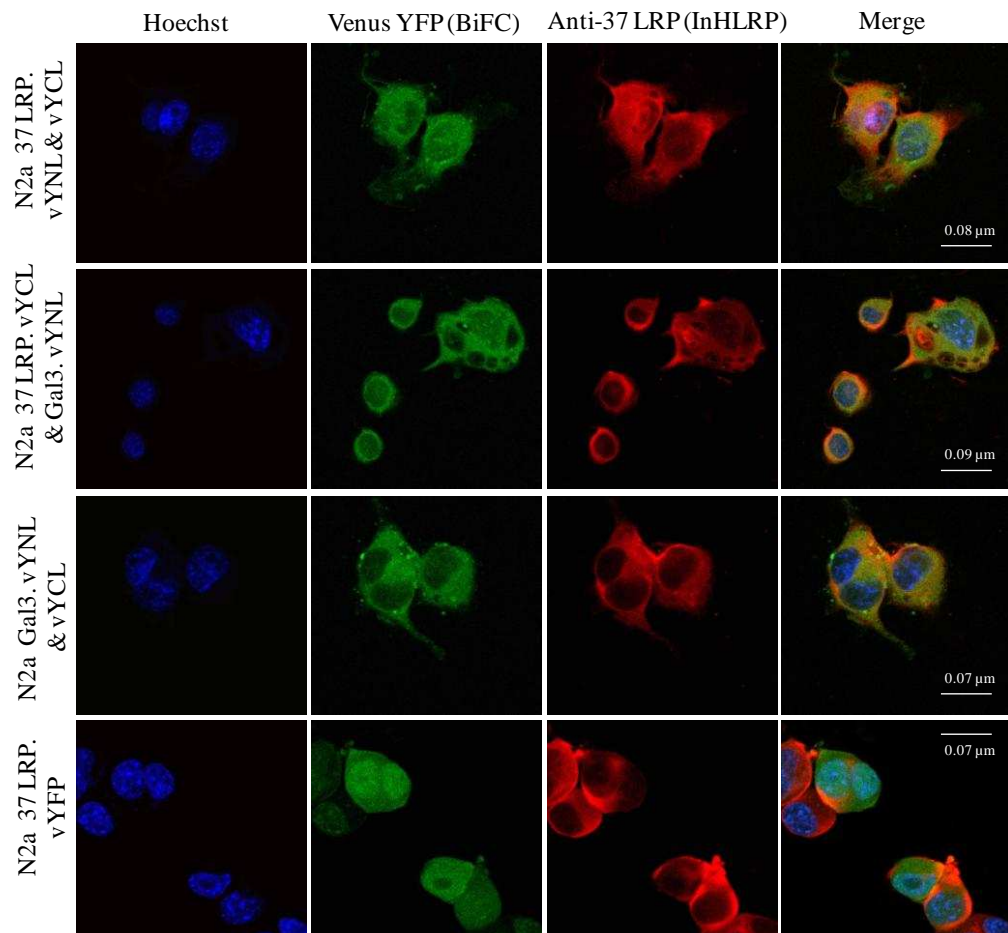
Figure 5.10: Distribution of 37 LRP and Gal-3 BiFC complexes and anti-37 LRP immunofluorescence. Representative confocal microscopic images of N2a transiently co-transfected with indicated constructs, as described in Chapter 2, and 24 h post transfection. The cells were fixed with 4% paraformaldehyde and stained with anti-37 LRP (InHLRP) followed by Alexa Fluor 680 and nuclei stained with Hoechst. Transfection of 37 LRP.vYFP served as the control.

5.2.3.   Investigation of Galectin-3 and 37 LRP dimerization

As our data revealed that 37 LRP and Gal-3 forms homo and heterodimers in cells, we were interested in how these receptors formed dimers. Galectin-3 has one cysteine residue in the C-terminus (Figure 5.11), which was shown to be required for dimerization of murine Gal-3 (Woo et al., 1991). Therefore, the homologous cysteine in human Gal-3 at position 173 was further investigated in this study, for its role in Gal-3 homo and heterodimerization with 37 LRP.

```
Carbohydrate Binding Domain

Dog     153  FGIPAGPLTVPYDLPLPGGVKPRMLITILGTVRPSANR
Rat     119  FGAPTGPLTVPYDMPLPGGVMPRMLITIIGTVKPNANS
Mouse   121  YGVPAGPLTVPYDLPLPGGVMPRMLITIMGTVKPNANR
Human   107  YGAPAGPLIVPYNLPLPGGVVPRMLITILGTVKPNANR


Dog     LALDFKRGNDVAFHFNPRFNEDNKRVIVCNTKLDNIWGKEERQAAFPFESGKPFK
Rat     ITLNFKKGNDIAFHFNPRFNENNRRVIVCNTKQDNNWGREERQSAFPFESGKPFK
Mouse   IVLDFRRGNDVAFHFNPRFNENNRRVIVCNTKQDNNWGKEERQSAFPFESGKPFK
Human   IALDFQRGNDVAFHFNPRFNENNRRVIVCNTKLDNNWGREERQSVFPFESGKPFK


Dog     IQVLVESDHFKVAVNDAHLLQYNHRMKNLPEISKLGISGDIDLTSASYAMI  296
Rat     IQVLVEADHFKVAVNDVHLLQYNHRMKNLREISQLGIIGDITLTSASHAMI  262
Mouse   IQVLVEADHFKVAVNDAHLLQYNHRMKNLREISQLGIIGDITLTSANHAMI  264
Human   IQVLVEPDHFKVAVNDAHLLQYNHRVKKLNEISKLGISGDIDLTSASYTMI  250
```

Figure 5.11: The conservation of cysteine residues in the CRD of Galectin-3 among different species. Reproduced from (Herrmann et al., 1993).

5.2.3.1.   Construction of Galectin-3 cysteine mutants in mammalian expression vectors

To examine if the cysteine of human Gal-3 is also required for Gal-3 homodimerization, and furthermore, heterodimerization with 37 LRP, mutants were created in which the cysteine toward the carboxyl terminus of Gal-3 was substituted with alanine and fused to the full length, N or C-terminal ends of vYFP. The Gal-3.C173A tagged to vYFP, vYNL and vYCL were successfully

generated by site directed mutagenesis as described in Chapter 2 and 4 (Figure 5.12).
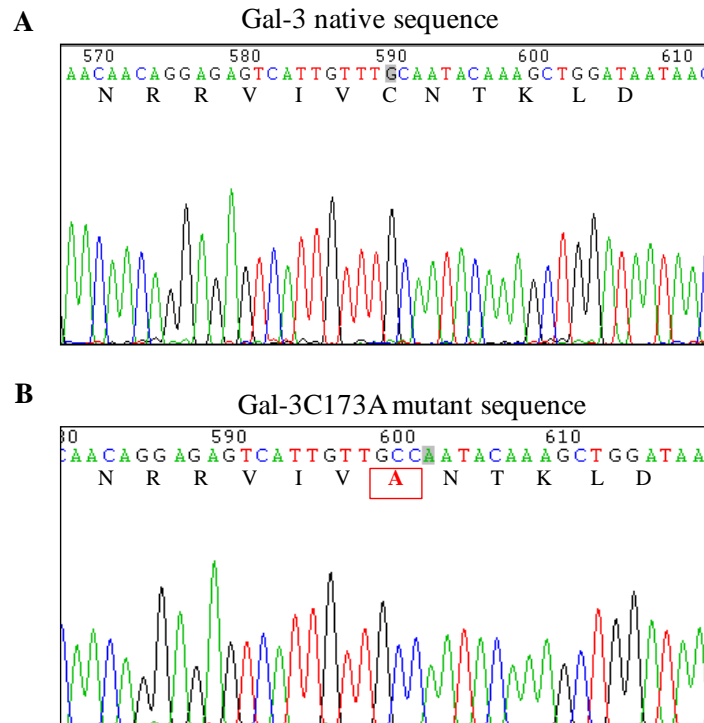
Figure 5.12: Sequence chromatograms showing substitution of the Galectin-3 cysteine residue following site directed mutagenesis. Site directed mutagenesis was performed on the Gal-3 fused to vYFP, vYNL and vYCL templates. Automated DNA sequencing confirmed the mutation of Gal-3.C173 to alanine (B). Sequencing data were viewed in Chromas lite version 4.02.

5.2.3.2. Expression of fluorescently labelled Galectin-3 cysteine mutants

To examine the expression of generated constructs Western blot analysis of cell lysates from transfected COS7 cells were performed using anti-GFP antibody. As shown in Figure 5.13, a band of approximately 60 kDa was detected in Western blots of cells transfected with plasmids encoding Gal-3.C173AvYFP plasmid

(Figure 5.13A, lane 3). The Gal-3 cysteine substituted construct expressed at the same molecular weight of native Gal-3.vYFP construct (Figure 5.13A, lane 2) and no significant difference between their expression level was observed, as indicated by flow cytometry analysis (Figure 5.13B). In addition, the BiFC fragments fused to Gal-3 cysteine substituted were expressed at the expected molecular weights (Figure 5.13A, lanes 4 and 5).
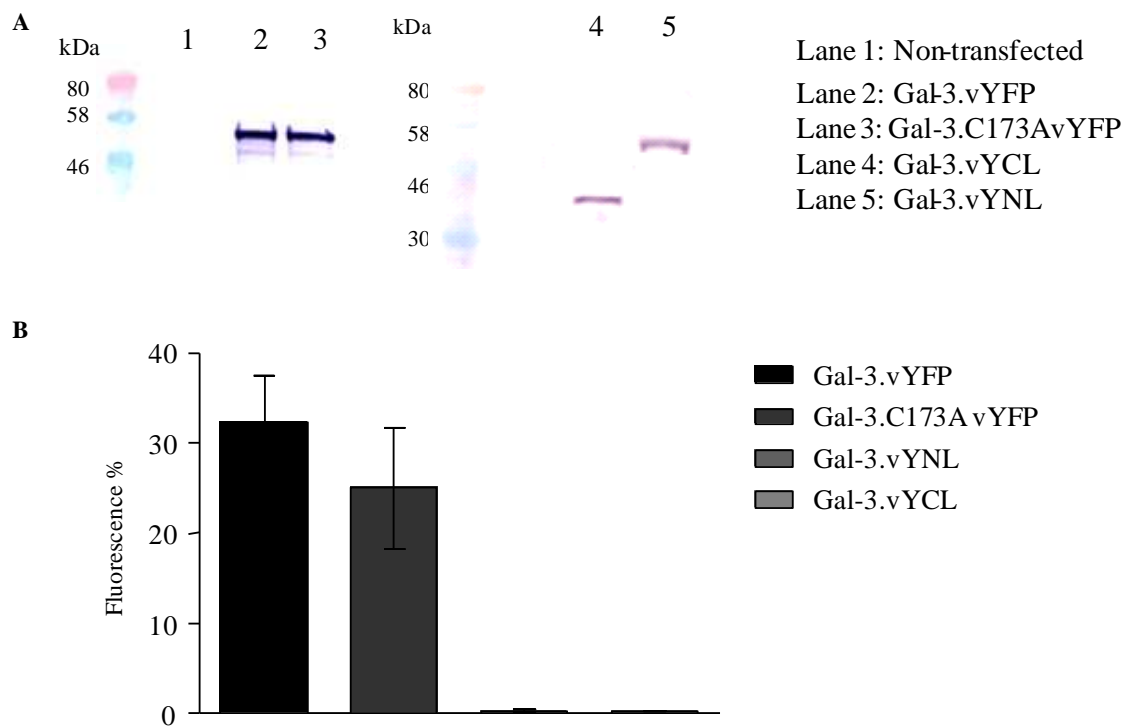
Figure 5.13: Expression of fluorescently labelled Galectin-3 cysteine substituted mutants in COS7 cells. (A) Whole cell lysates of COS7 cells transiently transfected with indicated constructs as described in Chapter 2, and immunoblotted with anti-GFP antibody, confirming expression of Gal-3 cysteine substituted constructs at the expected molecular weight. (B) COS7 cells were transfected with constructs as indicated above and Venus fluorescence was analyzed by flow cytometry as described Chapter 2. The flow cytometry data revealed no significant difference between Gal-3 native and cysteine mutant in the levels of expression.

5.2.3.3. Subcellular localization of vYFP-tagged cysteine-substituted Galectin-3

To examine the effect of cysteine substitution on subcellular expression patterns of the Gal-3 wild type and cysteine substituted constructs were transfected into HBMECs and subcellular localization was examined 24h post transfection by confocal fluorescence microscopy. As shown in Figure 5.14A, the Gal-3 cysteine mutant was expressed in a punctate staining pattern, comparable to the staining pattern of wild type receptors in HBMECs. In addition, subcellular fractionation of the Gal-3 Cys mutant gave the same distribution pattern of the Gal-3 wild type in COS7 cells (Figure 5.14B). However, the Gal-3 Cys mutant cytoskeleton extract showed an extra band, which was lacking in the wild type (Figure 5.14B, cytoskeleton fraction lane: 3).

A Gal-3.vYFP

Gal-3C173A.vYFP

B

Cytoplasmic fraction   Membrane fraction

Nuclear fraction

Soluble   Chromatin bound   Cytoskeleton fraction
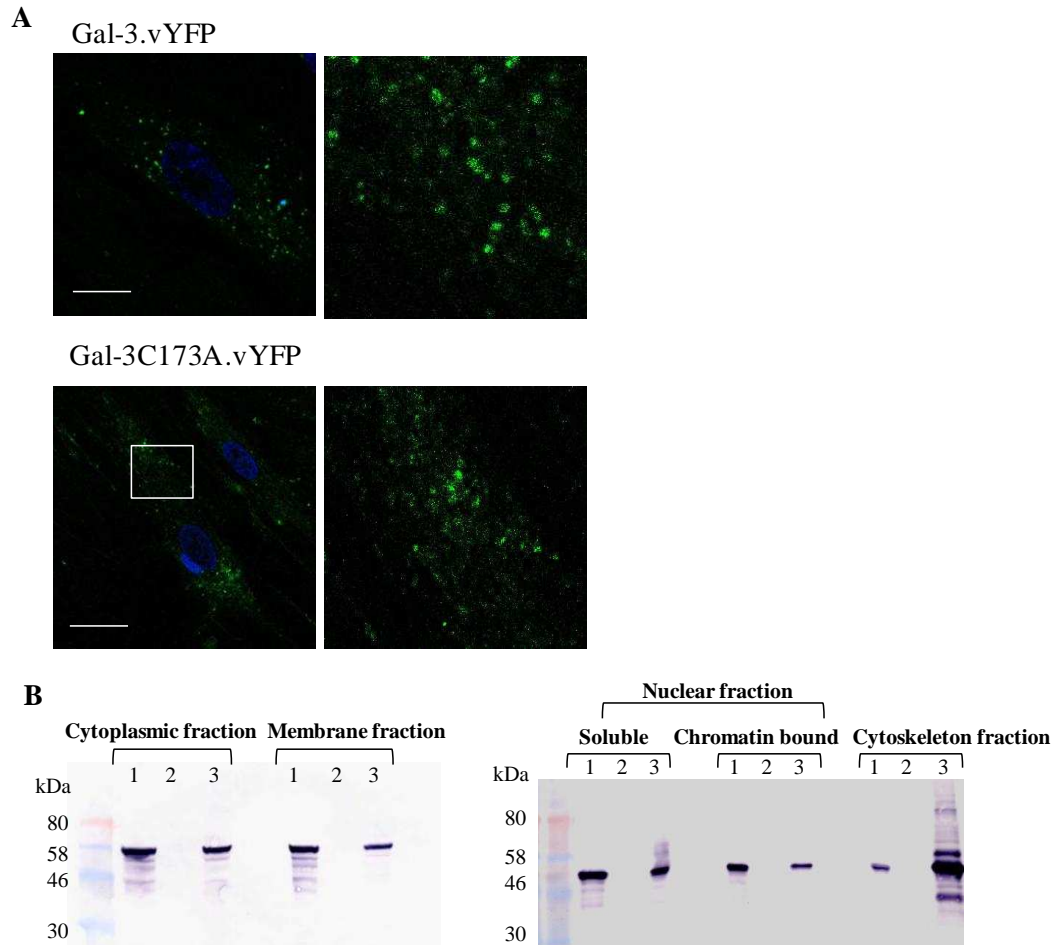
Figure 5.14: Subcellular localization of vYFP labelled Galectin-3 cysteine mutants. (A) Representative confocal microscopic images of HBMECs transiently transfected with indicated constructs as described in Chapter 2, showing similar punctate expression of Gal-3 and its cysteine substituted mutant. Scale bar represents 0.1µm. (B) Western blot of COS7 transiently transfected with vYFP tagged Gal-3 and Gal-3 cysteine mutant, confirming their expression in different cellular fractions. Lane 2B: untransfected COS7 cell total cell lysate of cytoplasmic, membrane, nuclear soluble, chromatin-bound and cytoskeleton in each fraction as described in Chapter 2. Lanes 1 and 3: COS7 cells transfected with vYFP tagged Gal-3 wild type and Gal-3C173A, respectively, and detected with anti-GFP, as described in Chapter 2.

5.2.3.4. The impact of cysteine 173 substitution on 37 LRP and Galectin-3 heterodimerization

Next, the effect of Gal-3 Cys 173 mutation on the homo- and hetero-dimerization of Gal-3 and 37 LRP was investigated by flow cytometry. This substitution led to significant reduction in Gal-3 homodimerization as revealed by reduced BiFC signal in COS7 cells cotransfected with the Gal3.C173A vYNL and Gal3.C173A vYCL mutant, when compared with wild type homodimer (p=0.029, Figure 5.15B). Concomitantly, the heterodimer form consisting of the wild-type 37 LRP and Gal-3 mutant receptor, showed a significant reduction in signal (p=0.025, Figure 5.15A). Using different heterodimer combinations of 37 LRP and Gal-3 mutant also demonstrated a significant reduction in signal (p=0.006, Figure 5.15A).

A

37 LRP.vYNL	+	-	+	-	+	-	-	-	-	-
Gal3.vYCL	+	-	-	-	-	-	-	+	-	-
Gal3.C173A.vYCL	-	-	+	-	-	-	-	-	-	+
37 LRP.vYCL	-	+	-	+	-	+	-	-	-	-
Gal3.vYNL	-	+	-	-	-	-	+	-	-	-
Gal3.C173A.vYNL	-	-	-	+	-	-	-	-	+	-

B

Gal3.vYNL	+	-	-	-	-	-	-
Gal3.vYCL	+	+	-	+	-	-	-
Gal3.C173A.vYCL	-	-	+	-	-	+	-
Gal3.C173A.vYNL	-	+	+	-	+	-	+
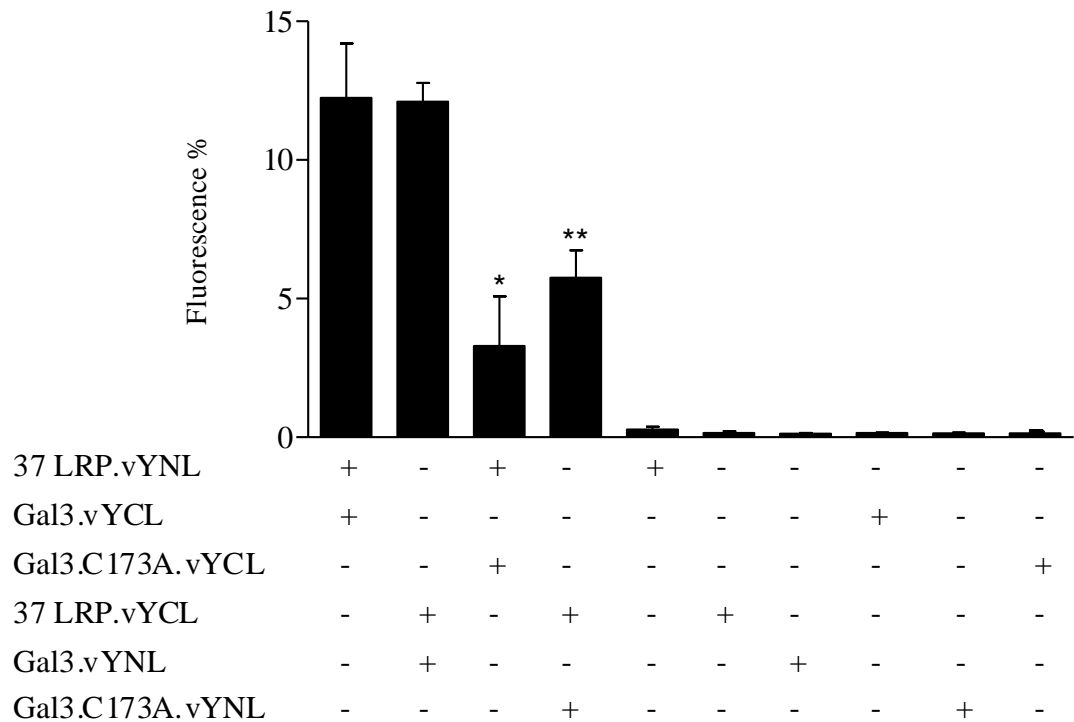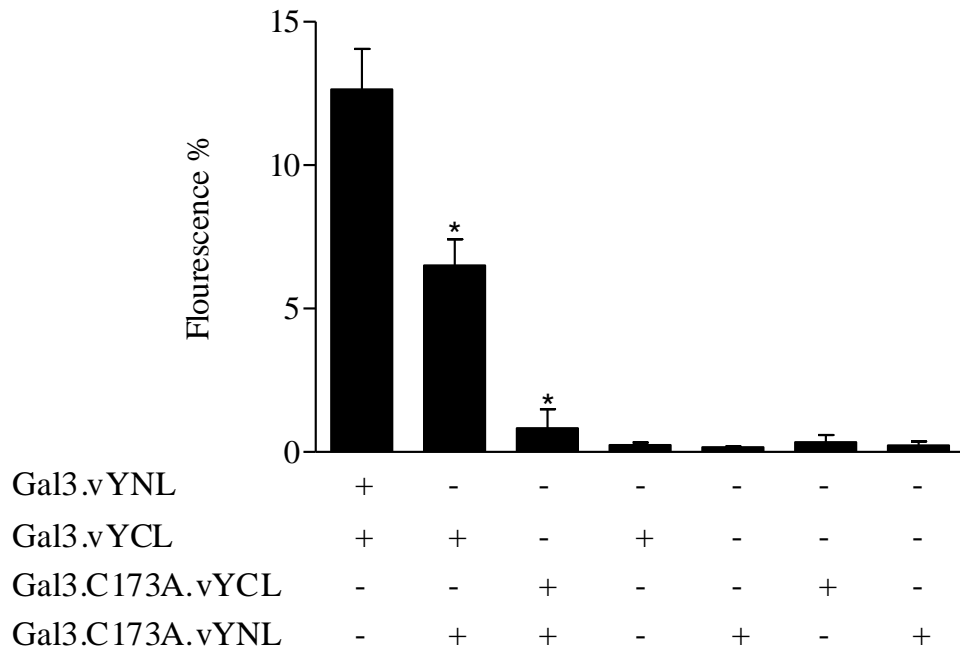
Figure 5.15: Galectin-3 cysteine-173 affects homo- and hetero-dimerization.

Flow cytometry analysis of COS7 cells transfected with indicated constructs and 24h post transfection. The Venus fluorescence was analyzed by flow cytometry. Substitution of Gal-3 cysteine 173 to alanine significantly reduced its homo- (B) and hetro-dimerization with 37 LRP (A). Results are expressed as percentage of the specific fluorescence signal to the value of 37 LRP.vYFP and Gal-3.vYFP, as described in Chapter 2. Bars represent the mean ± SE of three independent experiments. (Student's t- test; **P < 0.01, *P < 0.05).

5.2.4.   Substitution of 37 LRP cysteines 148 and 163 does not abolish 37 LRP and Gal-3 dimerization

Furthermore, 67 LR has been demonstrated previously to be acylated (Buto et al., 1998). As described earlier in the previous chapter, two cysteine residues (C148, C163) in the C- terminus of 37 LRP, were substituted to alanine to investigate if these cysteines accounted for total acylation (palmitoylation) of 67 LR. According to cellular fractionation results, there were no effects on 37 LRP cellular localization. To further investigate if the substitutions (C148A, C163A) may effect 37 LRP homodimerization, mutants were created, in which the cysteines toward the carboxyl terminus of 37 LRP were substituted with alanines and fused into Venus fragments. To examine the expression of generated constructs, Western blot analysis of cell lysates from transfected COS7 cells were performed using the anti-GFP antibody. As shown in Figure 5.16, LRC148A and C163A fused to the Venus fragments were expressed at the expected molecular weight.
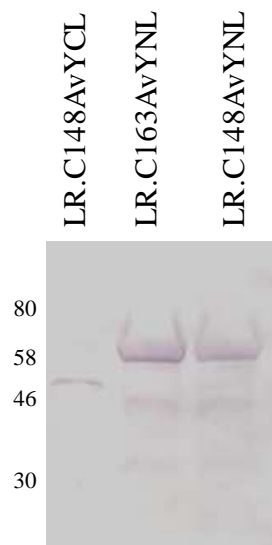
Figure 5.16: Immunoblot analysis for expression of cysteine substituted 37 LRP fused to Venus fragments. Whole cell lysates of COS7 cells transiently

transfected with the indicated constructs and immunoblotted with anti-GFP antibody as described in Chapter 2, confirming their expression at the expected molecular weight.

Subsequently, the homo and heterodimerization of 37 LRP and Gal-3, was analyzed by flow cytometry. Mutation of C148A and C163A does not affect 37 LRP homo- or hetero-dimer formation, as confirmed by flow cytometry (Figure 5.17).
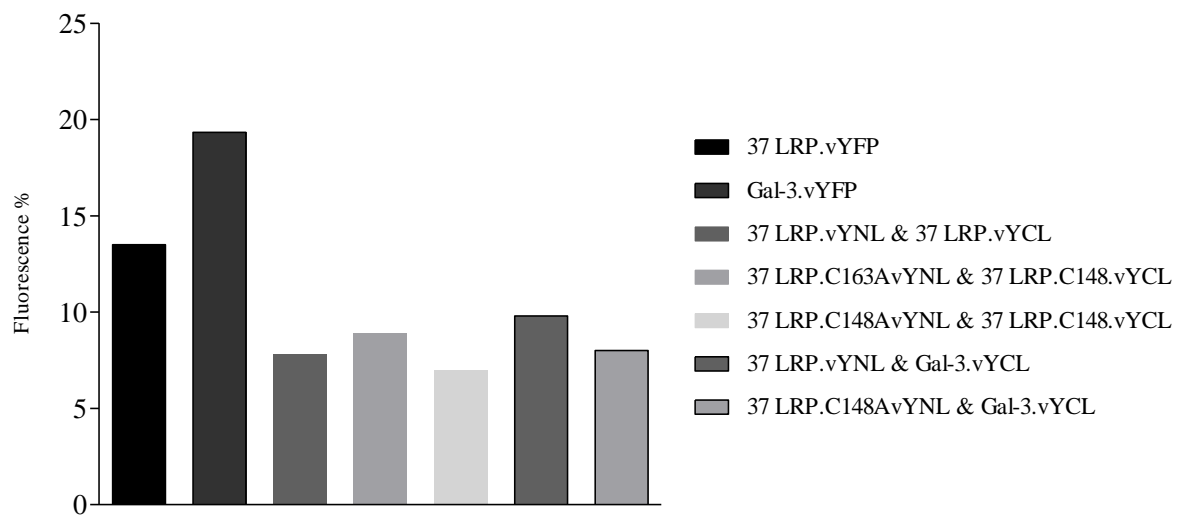
Figure 5.17: Substitution of cysteines 148 and 163 of 37 LRP do not affect 37 LRP homo- or hetero- dimerization. Flow cytometric analysis of COS7 cells transfected with the indicated constructs and the Venus fluorescence was analyzed by flow cytometry as described in Chapter 2. Substitution of 37 LRP cysteines 148 and 163 into alanine does not significantly affect its homo or hetrodimerization with Gal-3.

5.3. Discussion:

Previous studies have predicted the existence of 67 LR as a homo- (Gauczynski et al., 2001; Landowski et al., 1995) or hetero- dimer with Gal-3 (Buto et al., 1998; Castronovo et al., 1992) on the cell surface. The emerging roles of 67 LR and Gal-3 in CNS infections, including bacterial meningitis (Bellac et al., 2007; Orihuela et al., 2009) necessitate further understanding of their configuration in the BBB. Therefore, this chapter was designed to focus on the investigation of the 67 LR dimerization status, employing several approaches.

In terms of infection, the surface localization of 67 LR, whether as homo- or hetero- dimer is a prerequisite for initiation of N. meningitidis adhesion to the BBB (Orihuela et al., 2009). The data of the previous chapter confirmed that 67 LR, 37 LRP and Gal-3 are located on the surface of HBMECs and astrocytes, as BBB components, and other mammalian cells (COS7 and N2a). In light of these data, we first sought to further characterize the surface distribution of the 67 LR homodimer and/or heterodimers, using dual immunofluorescence staining. In the present work, the dual immunofluorescence staining revealed co-localization of endogenously expressed 67 LR with its precursor, and both of these proteins with Gal-3 on the surface of HBMECs, astrocytes and COS7 cells. Because the Mluc5 antibody specifically recognizes the 67 LR, but not the precursor form, it was used instead of the Ab711 antibody to detect the co-localization of 67 LR with 37 LRP. While InHLRP antibody recognized only the 37 LRP form by Western blot analysis as shown previously in Figure 4.3. Thus, the observed staining pattern of 67 LR with 37 LRP on the apical surface of HBMECs and astrocytes indicates distinct populations of 67 LR and 37 LRP (Figure 5.3A). Whilst 37LRP still exhibited a more diffuse staining pattern, often polarised and with an apparent

inverse correlation to the degree of 67 LR staining, 67 LR staining was punctate. There was some colocalization of the two receptor populations on the cell surface (Figure 5.3A, yellow colour). In this context, it should be noted that the present colocalization images of 67 LR and its precursor are visual-based and therefore highly prone to bias. Therefore, quantitative analysis of colocalization of 67 LR with 37 LRP within cell body and specific sub-cellular structure, named laminin rrich structures (LRS), was conducted in our laboratory (Oral communication with Dr. Lee Wheldon). This data revealed minimal colocalization of 37 LRP and 67 LR in areas of the cell devoid of LRS (14 ± 1.6%), comparing with a significantly increased colocalization at LRS (48.5 ± 2.2%) (Dr. Lee Wheldon, unpublished data). Importantly, the proportion of 37 LRP-associated 67 LR or 67 LR-associated 37 LRP was not significantly different on the cell body (14 ± 1.6% compared to 12 ± 2.1%, respectively) (Dr. Lee Wheldon, unpublished data). Notably, whilst many cells exhibited both 37 LRP and 67 LR surface staining, cells that were particularly enriched for one receptor displayed reduced levels of the other (Dr. Lee Wheldon, unpublished data). This apparent inverse correlation was subsequently confirmed by direct comparison of mean fluorescence intensity measurements of both 37 LRP and 67 LR on the same cell (Dr. Lee Wheldon, unpublished data). This suggests existence of 67 LR as 37 LRP homodimer, which corroborates findings of a previous study, where the amino acid composition of 67 LR was found to be identical to 37 LRP (Landowski et al., 1995). Another study suggests that the homodimerization of 67 LR, based on the detection of 67 LR and 37 LRP at the plasma membrane fractions of N2a cells, by Western blot analysis (Gauczynski et al., 2001) using a monoclonal antibody, which recognizes both 37 LRP and 67 LR. However, N2a cells lack expression of

endogenous Gal-3 (Gauczynski et al., 2001). Interestingly, the current study found that Gal-3 was colocalized predominantly with 37 LRP on the apical surface of HBMECs, astrocytes and COS7 cells, which endogenously express Gal-3 (Figure 5.3C). Similar results were obtained with second rat monoclonal (Mac-2) and goat polyclonal (AF1154) antibodies to Gal-3 (data not shown). In addition to 37 LRP, clear colocalization was observed between Gal-3 and Ab711 polyclonal antibody against 67 LR (Figure 5.3B). Measuring the co-localization coefficient of 37 LRP and Gal-3 showed that approximately half of the surface-localized 37 LRP associated with Gal-3 on the cell (50 ± 5.9%) or at LRS (62.6 ± 6.9%) (Dr. Lee Wheldon, unpublished data). Such colocalization between Gal-3 and 67 LR was further charcterizied using Mluc-5 antibdy, which is known to detect only 67 LR (Oral communication with Dr. Lee Wheldon). Both monoclonal (mab4033) and polyclonal (AF1154) Gal-3 antibodies demonstrated an almost perfect (>90%) co-localization with 67 LR stained with Mluc-5 antibody. In contrast, minimal colocalization was demonstrated between monoclonal (Mac-2) Gal-3 antibody and 67 LR stained with Mluc-5 antibody on the cell (9.4 ± 2.1%) or at LRS (6.1 ± 1.3%) (Dr. Lee Wheldon, unpublished data). A previous study has shown that the antibody against Gal-3 can detect 67 LR on immunoblots of detergent cell extracts (Buto et al., 1998). In addition, 67 LR can be eluted from a laminin affinity column using lactose and N-acetyllactoseamine, a known ligand for Gal-3 (Castronovo et al., 1992). All these studies support our finding of observed colocalization of Gal-3 with 67 LR and its precursor.

Further investigation for the association of 37 LRP-37 LRP and 37 LRP-Gal-3 to form 67 LR homo- or hetero-dimer respectively, was performed using receptors

labelled with a different spectral fluorescent protein. This approach allows visualization of the interaction between fluorescently tagged 37 LRP and Gal-3 in different cellular compartments, providing a number of findings that cannot be detected by immunofluorescence staining. This approach was used before to characterize the subcellular localization of 37 LRP and a prion protein (Nikles et al., 2008). The vYFP and mCherry are well-characterized spectral variants of GFP and RFP, respectively, and have been used for dual imaging of two different receptors. The subcellular localization of each receptor, fused to vYFP and other fluorescent proteins, was observed in Chapter 4 (Figure 4.16) and previous reports (Nakahara et al., 2006; Nikles et al., 2008), respectively. This study showed that the 37 LRP.vYFP colocalized with 37 LRP.mCherry and Gal-3.mCherry when both receptors were coexpressed in a cell (Figure 5.5A and B), suggesting that 37 LRP formed homo- and hetero-dimers with Gal-3, and reflecting dual immunofluorescence staining of endogenous receptors (Figure 5.2C). Such pattern of almost complete overlapping of coexpressed receptors in COS7 cells were expected, since both 37 LRP and Gal-3 are located in the nucleus, cytoplasm and the cell surface. In addition, whether or not, the obtained colocalization signal only represent homo- or hetero- dimer forms of 67 LR, cannot be concluded from this experiment. This is because 37 LRP and Gal-3 are multifunctional proteins that interact with many cellular proteins (Dumic et al., 2006; Nelson et al., 2008). However, the main limitation of this approach was the ability to produce adequate transfection efficiency, which would lead to expression of the protein at varying ratios. Thus, subpopulation of cells, expressing one of two constructs were found. To overcome the limitations of dual immunofluorescence staining and fusion of

receptors to fluorescent proteins, a specific method to detect receptor dimerization called BiFC was used.

In our study, the BiFC approach was used as an applicable method for direct visualization of receptor dimerization and their subcellular localization in many types of cells, under physiological conditions (Hu et al., 2002; Kerppola, 2006). Interestingly, and for the first time, we have shown by BiFC that 67 LR exists in homo- and hetero- dimer forms with Gal-3 in different mammalian cells, indicating cell type independent interactions. In HBMECs, the pattern of BiFC expression was unique, as fluorescence resulting from complementation of 67 LR homo- and hetero- dimers, was punctate throughout the apical surface and excluded from the nuclei (Figure 5.8A). In contrast to HBMECs, BiFC complexes exhibited more diffuse distribution throughout the cells in N2a cells (Figure 5.8B). This pattern of distribution mirrored that of 37 LRP and Gal-3 fused to full-length vYFP, as shown in Chapter 4 (Figure 4.17). Taking into consideration that the BiFC signal observed may represent receptors that interact with each other directly, as homo or heterodimers, and/or they are present in the same complex. A previous study has shown that both 67 LR and 37 LRP are distributed on the surface of N2a cells (Gauczynski et al., 2001). The surface localization of 67 LR homo- and hetero-dimers fused to BiFC fragments in N2a cells in our study, was confirmed by immunostaining of the GFP tag (Figure 5.8B). It was clearly shown that the surface expression pattern of BiFC complexes were comparable to wild type receptors fused to vYFP (Figure 4.17B). This indicates that fusion of Venus fragments does not disturb receptor cell surface localization. Moreover, co-staining with the 37 LRP antibody revealed partial colocalization of the 67 LR dimers with receptor precursor (Figure 5.10).

Utilizing flow cytometry, as a more quantitative method to detect BiFC signal, showed successful complementation of receptor BiFC fragments, confirming the confocal microscopy results. In both flow cytometry and confocal microscopy, the fluorescence intensity of the BiFC signal is lower than the fluorescence resulting from 37 LRP and Gal-3 fused to vYFP (Figure 4.17) in N2a and COS7 cells. This was expected since the BiFC signal, resulting from receptor complementation, is not comparable to the signal result from receptors fused to full length fluorescent protein.

The ability of Gal-3 to homodimerize (Woo et al., 1991) and oligmerize (Nieminen et al., 2007) make it a suitable positive control for the BiFC experiment. In agreement with these studies, Gal-3 homodimers were successfully obtained by the BiFC method in COS7 and N2a cells, but unexpectedly, not in HBMECs (Figure 5.8 A, B and C). The failure of Gal-3 to homodimerize in HBMECs is not easily explained.

The fluorescent protein fragments have the tendency to associate under certain condition. Usually to validate specificity of BiFC signal, association between unrelated protein and one of the genuine interacting proteins are investigated. However, multifunctionality and numerous interactions of 37 LRP and Gal-3 with different cellular proteins and receptors render choosing of other proteins, as a negative control, unfavourable. Based on a previous study, cysteine residue at position 186 of murine Gal-3 was found to be responsible for Gal-3 homodimer formation (Woo et al., 1991). Therefore, in this study, a single cysteine residue (Cys173) at the CRD of human Gal-3 was substituted into alanine and fused to Venus fragments to validate BiFC signal using flow cytometry. In agreement with

another report (Woo et al., 1991) using the BiFC method, this substitution abolished Gal-3 homodimerization (Figure 5.15B), validating our BiFC approach. Interestingly, such substitutions also significantly affect Gal-3 heterodimerization with 37 LRP (Figure 5.15A). Mutation of the sole cysteine (C173A), within the CRD of human Gal-3, did not interfere with the subcellular distribution of Gal-3 as shown by subcellular fractionation analysis (Figure 5.14). Of interest, this cysteine is highly conserved among species (Woo et al., 1991). Woo et al and co-workers (1991), suggested that the covalent disulfide bond mediates Gal-3 dimerization. However, in the current study, Gal-3 is still able to dimerize with 37 LRP cysteine substituted constructs, which rules out the possibility that 67 LR heterodimers were formed by disulfide bonds between Gal-3 Cys173 and 37 LRP Cys148 or Cys163. This is consistent with other studies that have shown that the 67 LR is not sensitive to reducing agents (Fujimura et al., 2012; Landowski et al., 1995).

Another study has suggested that the C-terminal region of 37 LRP is involved in the formation of 67 LR, due to its high conservation among vertebrates (Menard 1997). Also, the mutation of Gal-3 cysteine 173, which is located in the CRD of Gal-3, significantly reduced its heterodimerization with 37 LRP. In addition, in vitro binding assays revealed that rLR bound Gal-3 full molecule and its CRD significantly, and with almost similar affinity (Figure 5.6). Collectively, these findings led to assumption that the heterodimerization appears to be mediated by the C-terminals of both 37 LRP and Gal-3. Although Gal-3 CRD is involved in the 67 LR heterodimer formation, there is no evidence for 67 LR glycosylation (Castronovo et al., 1991a; Landowski et al., 1995), suggesting a protein-protein interaction between 37 LRP and Gal-3. This assumption is supported by the fact

that Gal-3 CRD is known to interact with several intracellular non glycosylated proteins in a carbohydrate-independent manner (Bawumia et al., 2003; Shimura et al., 2004; Shimura et al., 2005). It is therefore likely that the 37 LRP associates with Gal-3 in the cytoplasm, and is then targeted to the cell surface by acylation, as suggested by previous studies (Buto et al., 1998).

Among reported intracellular interacting partners for Gal-3 is active K-Ras (Elad-Sfadia et al., 2004). The K-ras is an important member of the Ras family, which play an important role in the control of signaling cascades that regulate cell proliferation, differentiation, survival, and death. Interactions of Gal-3 with active K-ras was found to be farnesyl-dependent since immunoprecipitation of Gal-3 was decreased significantly in the lysate of unfarnesylated K-Ras (C185S) (Elad-Sfadia et al., 2004). Farensylation is a type of lipid modification, where 15-carbon farnesyl isoprenoid is added to the thiol group of the cysteine residue, by the enzyme protein farnesyltransferase (FTase). A further report has identified a hydrophobic pocket in Gal-3 CRD that is predicted to accommodate the farnesyl group of K-Ras (Ashery et al., 2006). Importantly, this pocket is crucial to mediate K-Ras.GTP nanocluster formation and signal output (Shalom-Feuerstein et al., 2008). Thus, it is possible that 37 LRP becomes acylated in the cytoplasm and interacts with Gal-3 via its CRD hydrophobic pocket, in a manner similar to the interaction of Gal-3 with active K-Ras. Interestingly, the Gal-3 cysteine 173 was one of the amino acids that have been identified within the hydrophobic pocket that adapt farensyl binding. Such existence of this cysteine within this pocket may participate in the heterodimerization of Gal-3 with 37 LRP, since the disulfide bond theory was not applicable.

In summary, the data presented in this chapter provide new insights into an understanding of 67 LR dimerization status. Double immunofluorescence staining and coexpression of the fluorescent fusion receptors confirm colocalization of endogenously and transiently transfected receptors. Importantly, and using the BiFC method, presence of 67 LR as homo or heterodimers is demonstrated by confocal microscopy and flow cytometry. Of interest, the cysteine residue 173 of Gal-3 is involved in the formation of Gal-3 and 37 LRP heterodimers.

6. Chapter 6: Laminin Receptor and Galectin-3 expression

6.1. Introduction:

Because of the potential role that Gal-3 recently played in CNS infection, including meniningitis, and in light of our data that Gal-3 dimerized with 37 LRP to form 67 LR, this chapter focuses on studying the role of Gal-3 in meningococcal adhesion and invasion, and furthermore investigates Gal-3 and 37 LRP expression in response to meningococci and meningococcal 67 LR/37 LRP ligands.

After attachment of meningococci to brain endothelial cells, which is mediated by meningococcal T4p and several other adhesins, including PorA and PilQ (described in detail in Chapter 3), two mechanisms that have been suggested to be used by N. meningitidis to cross brain endothelial cells: transcellular transport (Nassif et al., 2002) and paracellular entry via opened tight junction (Coureuil et al., 2009). Recently, an in vitro study has shown that N. meningitidis can be internalized within vacuoles in human brain microvascular endothelial cells (Nikulin et al., 2006). Also, N. meningitidis has been found to recruit polarity complex and disrupt the intercellular junctions of brain endothelial cells, enabling meningococcal passage via a paracellular route (Coureuil et al., 2009). This resulted from the activation of the β2-adrenergic receptor/β-arrestin signalling pathway by the T4p (described in detail in Chapter 1).

N. meningitidis is an obligate human pathogen, and this characteristic hinders development of animal models. However, this has been circumvented by development of transgenic mice. Among these transgenic mice one expresses human CD46, a proposed receptor for meningococcal T4p (Johansson et al., 2003). These mice were shown to be susceptible to meningococcal disease after

intranasal challenge, revealing enhanced interaction between T4p and the murine nasopharynx (Johansson et al., 2003). Thus, these models provide an efficient tool for studying bacterial pathogenesis and evaluating vaccine efficacy. In the present study, mice expressing CD46 will be used to investigate role of Gal-3 and 67 LR/37 LRP in meningococcal disease.

Galectin-3 expression has been reported by previous studies to be upregulated in human meningothelial cells challenged with meningococcal secreted proteins (MSP) (Robinson et al., 2004), in experimental pneumococcal meningitis (Bellac et al., 2007; Coimbra et al., 2006) and other CNS infections (De Giusti et al., 2011; Mok et al., 2007). In addition, several other pathogens also induce Gal-3 expression, including: Helicobacter pylori, human immunodeficiency virus (HIV), and Trypanosoma cruzi (Fowler et al., 2006; Schroder et al., 1995; Vray et al., 2004). On the other hand, expression of 67 LR has been found to be increased in pneumococcal meningitis (Orihuela et al., 2009). Moreover, upregulation of 67 LR expressions in response to CNF1-expressing E. coli K1 was shown recently in HBMECs (Kim et al., 2005). In this context, expression of both 67 LR and Gal-3 is induced by host cell exposure to inflammatory cytokine, such as TNFα and INF-γ (Jeon et al., 2010; Orihuela et al., 2009). Based on these reports, it is possible that the recently identified meningococcal laminin receptor ligands will affect the expression of 67 LR and its associated surface molecules, including Gal-3, to promote bacterial internalization.

The identified meningococcal LR adhesins were outer membrane proteins PorA and PilQ (Orihuela et al., 2009). PorA is a 47 kDa meningococcal outer membrane protein (OMP), and forms trimeric cation-selective pores that allow the

traffic of water-soluble nutrients of up to 600 Da in size. Based on topology models, the protein is predicted to traverse the outer membrane via 16 β-sheets that create eight extracellular loops (van den Elsen et al., 1999). Two of these loops (loops 1 and 4) are strongly immunogenic and able to provoke bactericidal antibodies (van den Elsen et al., 1999). Preliminary data showed that loop 4 of rPorA is essential for LR binding (N. Abouseada, personal communication). The other meningococcal LR ligand, PilQ, is an antigenically conserved 82 kDa OMP that is fundamental for type IV pilus expression. It has a doughnut-like appearance with an apparent cavity (Frye et al., 2006) and forms a large (960 kDa) homododecamer complex which is capable of generating bactericidal antibodies.

Therefore, the focuses of this chapter were to assess the role of Gal-3 in meningococcal adhesion and invasion, to investigate whether the meningococci will affect 67 LR/37 LRP and Gal-3 expression in infected mice, and to examine if meningococcal LR ligands will induce 67 LR and Gal-3 expression in HBMECs.

6.2. Results:

6.2.1.   Enhanced invasion of MC58 in Galectin-3 expressed N2a cells

N2a (mice neuroblastoma) cells, a cell line that does not express endogenous Gal-3 as demonstrated previously by immunoblotting (Figure 4.16), were used to examine the role of Gal-3 in meningococcal adhesion and invasion. To achieve this, first, cells were transfected with human Gal-3 containing plasmid vector and its expression and surface localization was verified by immunoblotting and immunofluorescence staining. The expression of vYFP-tagged Gal-3 in transfected cells was confirmed by immunoblotting, as shown in Figure 6.1A. In addition, as demonstrated in Figure 6.1B, strong positive staining was observed with anti-Gal-3 (Mac-2) antibody in the cell surface of transfected cells only. Further, immunofluorescence analysis of Gal-3.vYFP transfected non-permeabilized N2a cells employing 37 LRP antibody showed that Gal-3 and 37 LRP colocalize on the surface of these cells (Figure 6.1B).

Then, cell association assay was performed to compare the adhesive and invasive capacity of MC58 to Gal-3 transfected and non-transfected N2a cells. Interestingly, the number of internalized (Figure 6.1C) but not associated bacteria (data not shown) significantly increased ($p = 0.005$) in Gal-3 transfected cells when compared with untransfected cells. To exclude the possibility that the enhanced invasion was due to transfection, control empty vector was transfected into N2a cells. As shown in Figure 6.1C, there is no significant difference between meningococcal invasion in the empty vector-transfected and non-transfected cells, excluding the possibility that enhanced invasion was due to transfection.
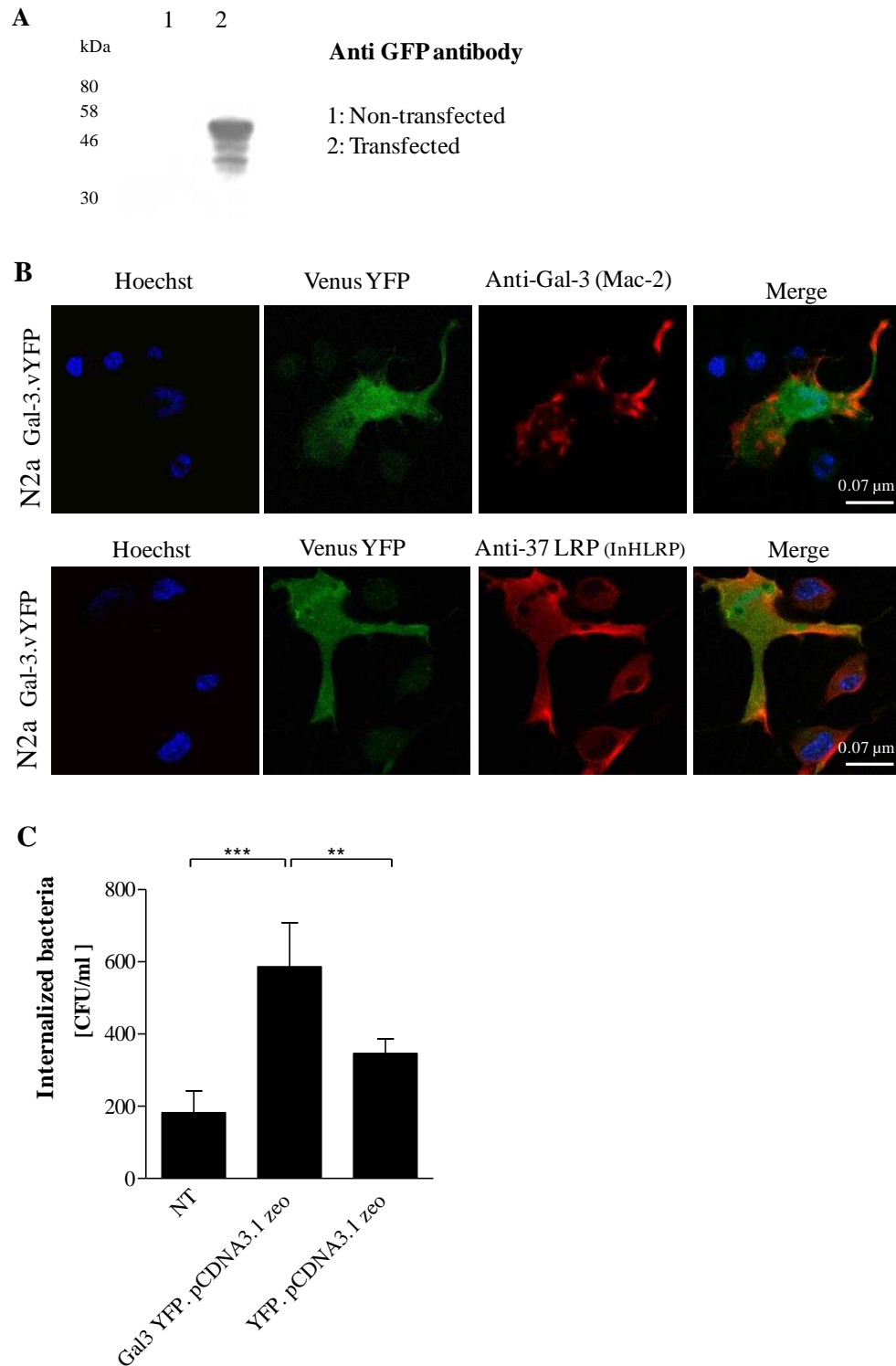
Figure 6.1: Galectin-3 expression enhances MC58 invasion of N2a cells. N2a

cells were transiently transfected with plasmid containing Gal-3.vYFP, and one day after

transfection the expression of recombinant protein was determined by Western blotting

(A) from total cell lysates using anti-GFP antibody as described in Chapter 2. Surface

localization of Gal-vYFP in transfected cells was confirmed by immunofluorescence staining of non-permeabilized cells using anti-Gal-3 (Mac-2) antibody (B) and its co-localization with endogenous 37 LRP using anti-37 LRP (InHLRP) antibody as described in Chapter 2. Scale bars are shown. (C) MC58 invasion to N2a cells expressing Gal-3 was performed. The transfected and non-transfected N2a cells were infected with MC58 for 2h at an MOI (multiplicity of infection) of 300 and incubated at 37ºC. For invasion assay, the cells were cultured for an additional 30min with 100 µg/ml gentamycin to kill any extracellular bacteria. Gal-3 transient expression enhanced the invasion of MC58 into N2a cells as compared with those of transfected with empty vector and non-transfected cells. Each value is the mean ± SEM of nine samples compiled from three independent experiments. Asterisks indicate the significant increase of MC58 invasion into Gal-3 transfected cell when compared with empty vector transfected and non-transfected cells (NT), respectively. (Student's t- test; **p < 0.01,*** p < 0.001.)

6.2.2. Study of the expression of Gal-3 and 37 LRP in CD46 brain tissues of mice infected with MC58

Previous studies showed increased expression of Gal-3 and 67 LR in pneumococcal meningitis (PM) and other infections. To determine the expression of 37 LRP and Gal-3, and further confirm their colocalization in CD46 brain tissues of MC58 infected mice, double immunofluorescence staining for 37 LRP and Gal-3 was performed. As shown in Figure 6.2A, both 37 LRP (green) and Gal-3 (red) are expressed and colocalized (yellow) in the brains of both MC58 infected and non-infected mice. As displayed in Figure 6.2B and C, Gal-3 and 37 LRP expression showed significantly greater fluorescence intensity in infected mice when compared with the non-infected group (p = 0.0001). These results were consistent with results from the visualization under the fluorescence microscope in Figure 6.2A.

A

MC58 infected | Non infected

37 LRP

Gal-3

Merge

Phase contrast

B

37 LRP

Flourescence intensity

***

Infected | Non-infected

C

Galectin-3

Flourescence intensity

***

Infected | Non-Infected
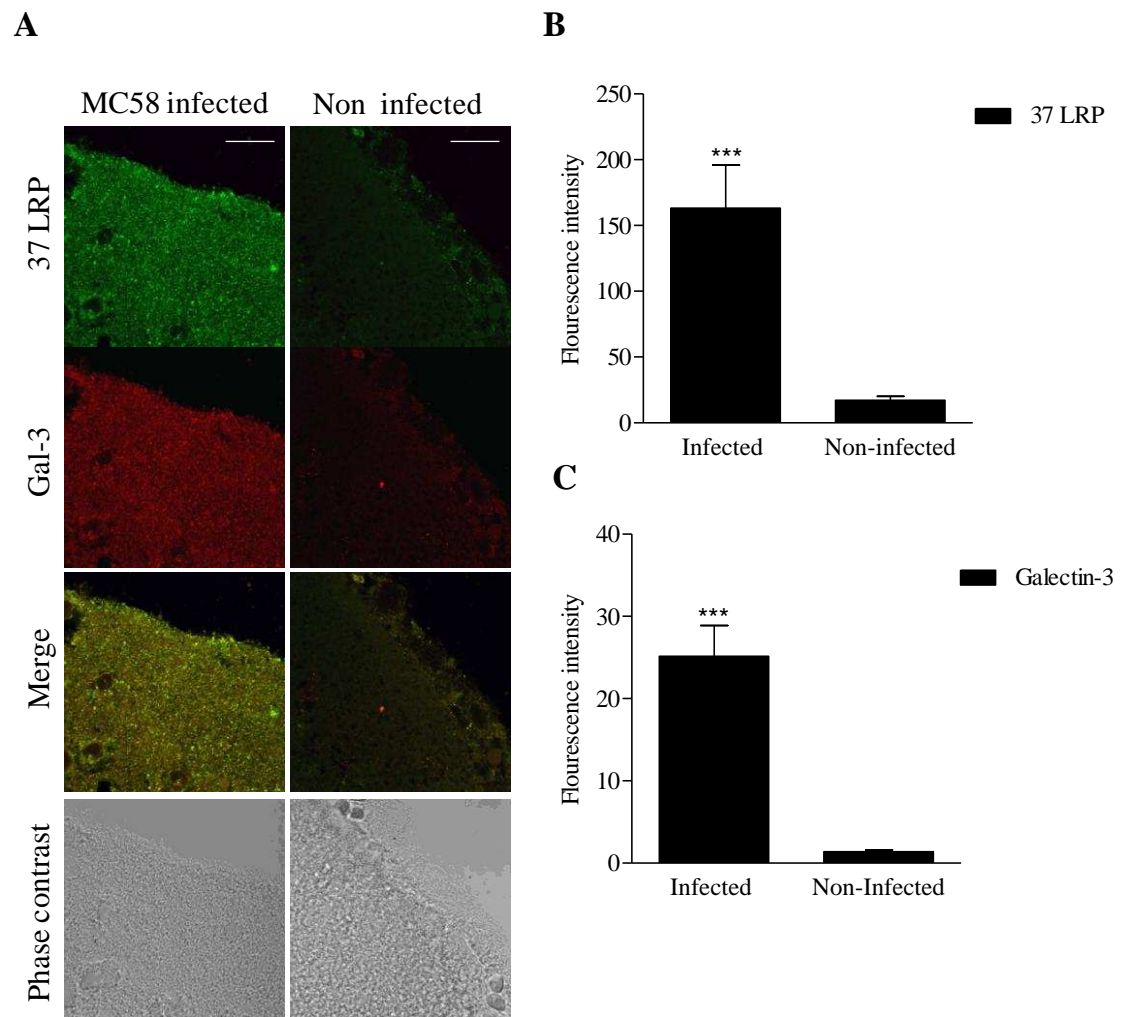
Figure 6.2: Up-regulation of 37 LRP and Galectin-3 expression in the brain of MC58 infected mice. (A) Sections of brain tissues were stained for 37 LRP (green) and Gal-3 (red) in MC58 infected and non-infected mice. Merge images indicate co-localization (yellow) of the 37 LRP and Gal-3 in the brain. Scale bars 0.06µm. (B and C) immunofluorescence intensity for Gal-3 (B) and 37 LRP (C) were measured in the brains of four randomly chosen MC58 infected and another four uninfected mice. Fluorescence intensity was greatest for 37 LRP and Gal-3 in infected mice when compared with non-infected (Student's t test; ***p < 0.001). Data are presented as mean ± SEM of eighty-four values taken randomly from each of four mice (twenty-one values / mouse) of each group. Quantification of fluorescence intensity by ImageJ software.

6.2.3. Meningococcal 37 LRP/67 LR ligands recruit 67 LR and Gal-3 to surface of HBMECs

To examine the effect of meningococcal 37 LRP/67 LR adhesins on the surface level of 67 LR and Gal-3, HBMECs were treated with different 37 LRP/67 LR-binding bacterial proteins or PBS as negative control for 2h and the surface level of 67 LR and Gal-3 were measured by flow cytometry. As represented in Figure 6.3A and B, the surface level of both 67 LR and Gal-3 was increased in cells treated with rPilQ, Loop 4 of PorA and, more prominently, rPorA protein, when compared with PBS treated cells.
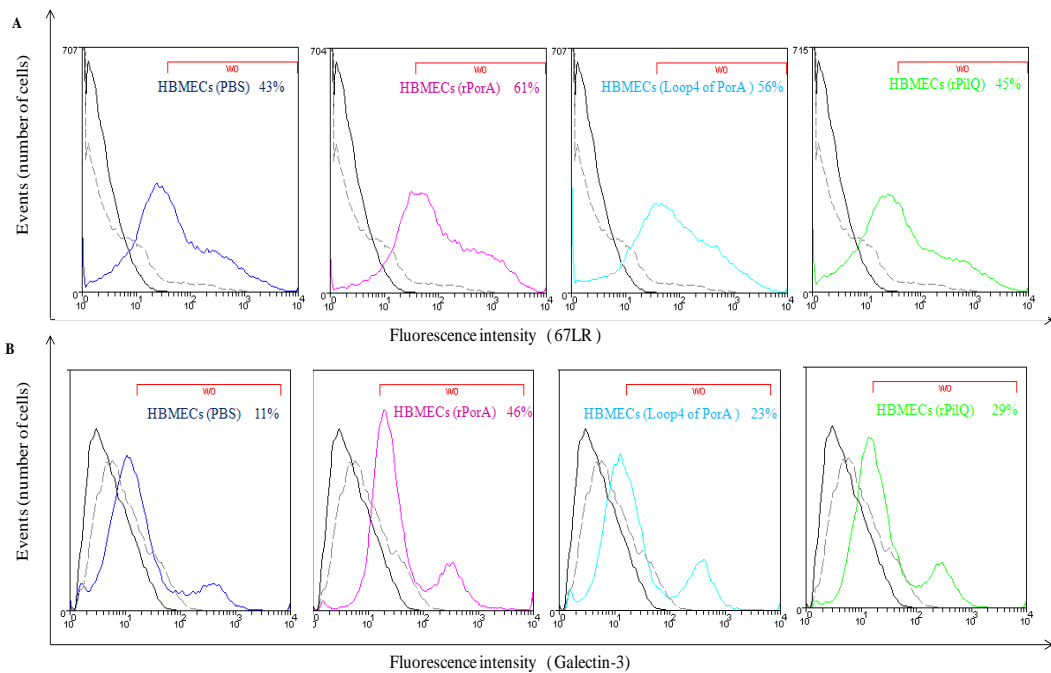
Figure 6.3: Detection of 67 LR and Galectin-3 surface level in response to meningococcal LR ligands using flow cytometry. HBMECs were analyzed for (A) 67 LR and (B) Gal-3 surface levels after incubation with 20μg/ml of different bacterial proteins rPorA (pink curve), loop4 of PorA (turquoise curve) and rPilQ (green curve) or PBS (blue curve). The 67 LR and Gal-3 surface levels were detected using the anti-67 LR (Mlu5) and anti-Gal-3 (mab4033) antibodies, followed by appropriate secondary

antibodies as described in Chapter 2. Histogram overlays of HBMECs alone (black curves), HBMECs incubated with secondary antibodies alone as negative control (dot curves), and HBMECs incubated with primary and secondary antibodies pre-treated with PBS (blue curve) or different bacterial proteins, including rPorA (pink curve), loop4 of PorA (torques curve) and rPilQ (green curve), were generated as described in Chapter 2, revealing induction of 67 LR (A) and Gal-3 (B) in HBMECs treated with different bacterial proteins. Experiments were repeated three times, with consistent results.

6.2.4. Detection of 37 LRP transcription in response to bacterial ligands

To investigate the effect of meningococcal LR ligands on the transcriptional level of 37 LRP/67 LR in HBMECs, qPCR was carried out.

6.2.4.1. Purity of the RNA samples

Total RNA was extracted from monolayer of HBMECs induced for 24h with different bacterial proteins (rPorA, rPilQ and loop 4 of PorA) or PBS as a negative control. Quality of extracted RNA was examined by measuring the $OD_{260/280}$ ratio, and all samples fell within a ratio of 1.8 to 2. The purity of extracted RNA was further confirmed by PCR. LR specific primers which amplify 888 bp from genomic sequence were used in PCR using 1µg of RNA from all samples. No detectable PCR product was obtained, which confirmed the purity of RNA (Figure 6.4, lanes 1-4). A positive control (Figure 6.4, lanes 5 and 6) produced the expected band at 888bp, and no band was obtained in the negative control (Figure 6.4, lane 7) which ensures primer specificity and successful PCR reaction.
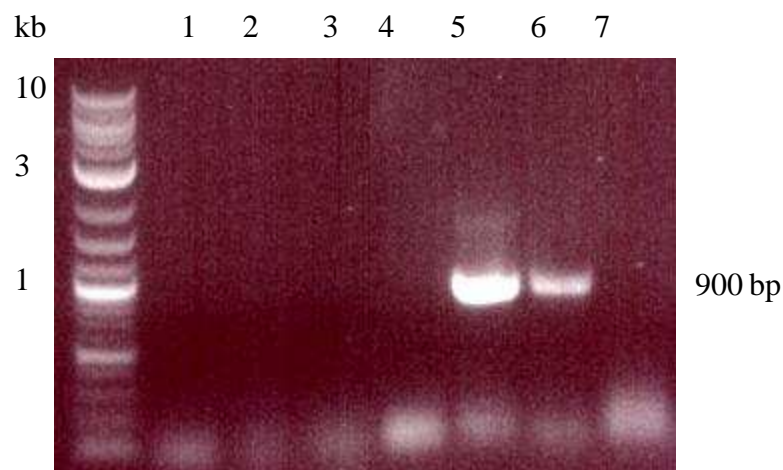
Figure 6.4: Assessment of extracted RNA purity by PCR. RNA of HBMECs treated with PBS (lane 1), (20µg/ml) of rPorA (lane 2), Loop 4 of PorA (lane 3) and

rPilQ (lane 4). PCR product of 37 LRP and human cDNA (lanes 5 and 6) respectively as positive controls. Negative control primer only without any template (lane 7).

6.2.4.2.   cDNA

cDNA to be used in qPCR analysis was prepared by RT-PCR of RNA extracted from untreated and treated HBMECs. As shown in Figure 6.5, all cDNA samples produce 37 LRP/67 LR at the expected size (888 bp).
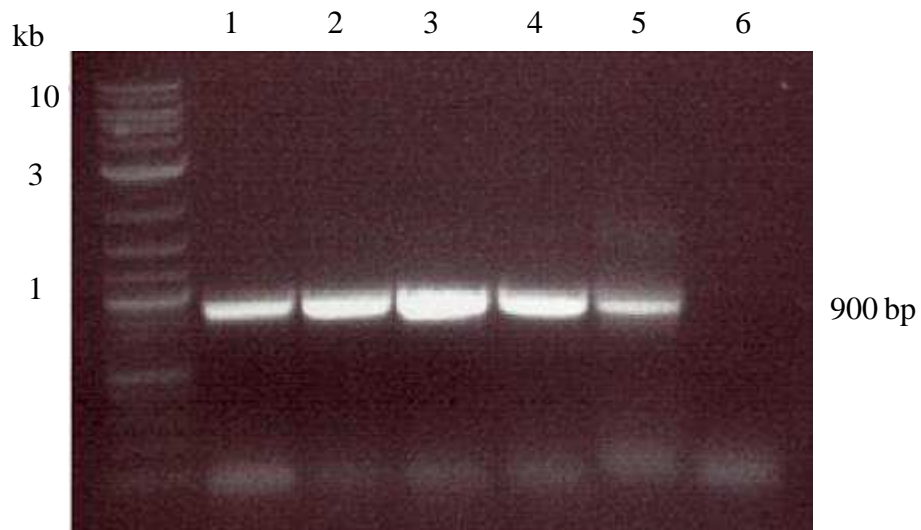
Figure 6.5: RT-PCR for extracted RNA. cDNA synthesised from RNA of HBMECs treated with PBS (lane 1), (20µg/ml) of rPorA (lane 2), Loop 4 of PorA (lane 3) and rPilQ (lane 4). PCR product of 37 LRP (lane 5). Negative control primer only without any template (lane 7).

6.2.4.3. Optimization of qPCR 37 LRP and β-actin primer concentrations

To use the prepared cDNA in qPCR, specific primers should be designed to amplify only short fragments ranging from 50 to 120 bp for 37 LRP and β-actin. Primers were designed to amplify 98bp and 55bp of 37 LRP and β-actin, respectively. The primer concentrations were optimized using different ratios of the primers in a series of experiments. Figures 6.6A and B showed the amplification plot (cycle threshold, CT versus fluorescence, Rn) of 37 LRP (gene of interest) and β-actin (endogenous gene) respectively for all primer ratios used. The CT is defined as the amplification cycle number in which the curve crosses a specified threshold. The Rn is the normalized fluorescence signals which are generated in the reaction. The mixture of 3μM forward and 9μM reverse primer produce an amplification plot with both the lowest cycle threshold (CT) value and highest fluorescence (Rn). As a result, all experiments were done using 3μM of forward and 9μM of reverse primer for both 37 LRP and β-actin.

A   Laminin receptor

3µM LR forward primer
9µM LR reverse primer

B   β-actin

3µM LR forward primer
9µM LR reverse primer
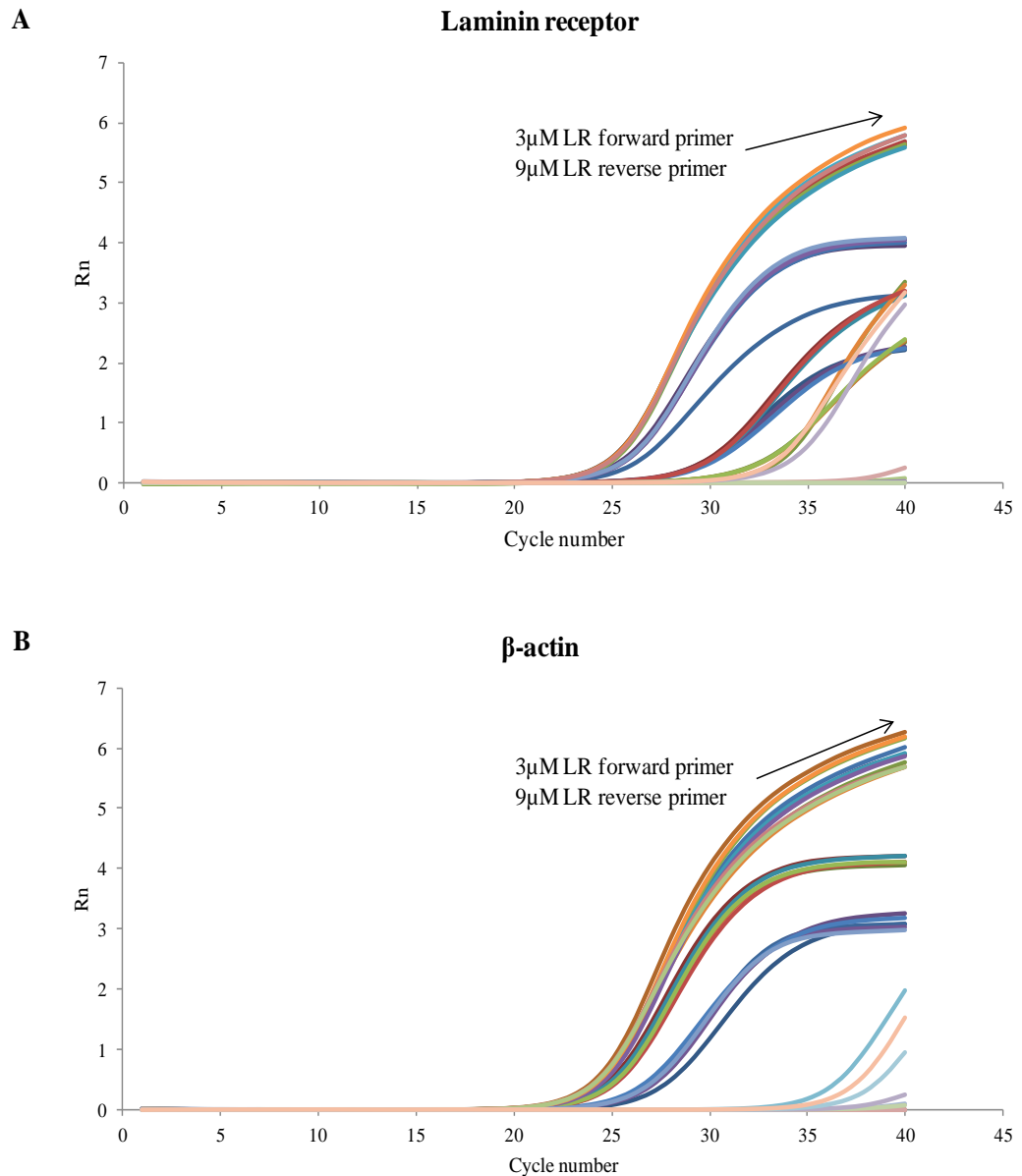
Figure 6.6: Optimization of 37 LRP and β-actin primers concentration.
Primer concentration dependent amplification plots of 37 LRP (A) and β-actin (B).
Forward and reverse primers were examined at different concentrations (0.5-9 µM) using
fixed 10 ng/µl of HBMECs cDNA for 37 LRP and β-actin. The amplification blot
indicated that the 3µM of forward and 9µM of reverse primer were the optimal primer
concentrations for 37 LRP (A) and β-actin (B).

6.2.4.4. Standard curves of 37 LRP and β-actin

To calculate relative transcriptional levels of the genes of interest using the delta delta CT(ΔΔCT) method (Livak & Schmittgen, 2001), the reaction efficiency of PCR was calculated. HBMEC cDNA was used as a template to perform standard curves for 37 LRP and β-actin in order to examine the PCR efficiency and linearity of template amplification. As shown in Figure 6.7, the slope of standard curves was -3.229 and -3.258 for 37 LRP and B-actin respectively, revealing 100% efficient PCR amplification; the efficiency was calculated according to the following equation: E= (10 — 1/slope — 1) x 100. Figure 6.7 demonstrated a linear correlation between the cDNA and CT values. Moreover, the correlation coefficients were 0.994 and 0.999 for 37 LRP and B-actin respectively, confirming the accuracy of the amplification efficiency.
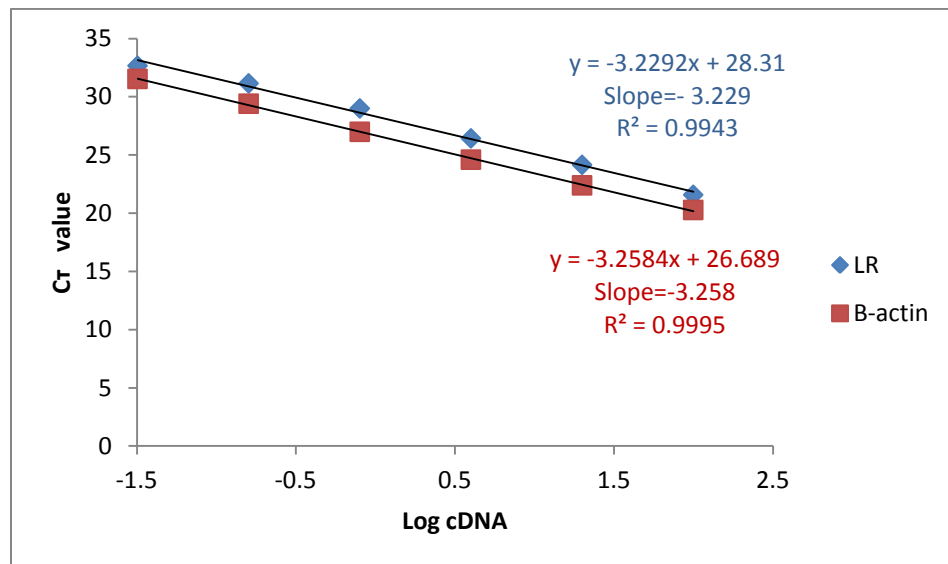
Figure 6.7: Standard curves for 37 LRP and β-actin to evaluate efficiency of qPCR. Standard curves were established for 37 LRP (blue diamond) and B-actin (red square) using log cDNA against CT values. Each point represents the mean of triplicate values for each 37 LRP and β-actin.

6.2.4.5.   Validation of $2^{-\Delta\Delta CT}$ method

There are different methods for analysis of relative quantification of gene expression, such as the delta delta cycle threshold (ΔΔCT) method (Livak & Schmittgen, 2001). This method can be used when the amplification efficiencies of the target and reference are approximately equal. Assessment of the amplification efficiency can be measured by studying ΔCT (CT (Target)–CT (Endogenous)) changes with different dilutions of cDNA. Identical efficiencies of the target (37 LRP) and reference gene (β-actin) are indicated by slope values close to zero. As a result, the ΔCT (CT 37 LRP–CT B-actin) was calculated and plotted versus log cDNA as represented in Figure 6.8. The slope of the line is 0.029, thus the ΔΔCT method can be used to analyze the data.
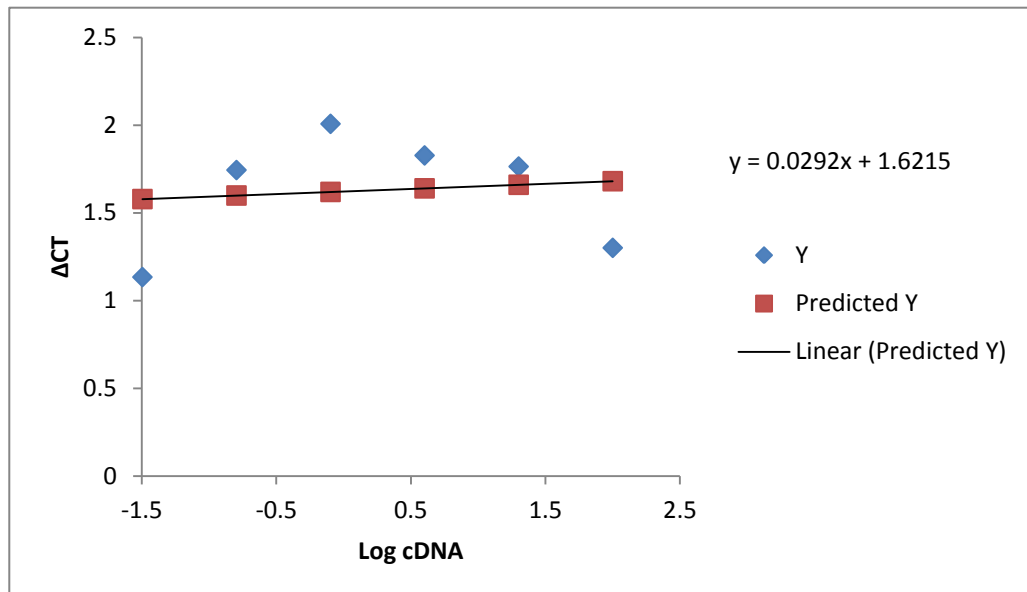
Figure 6.8: Validation of $2^{-\Delta\Delta CT}$ method. The ΔCT (CT 37 LRP–CT B-actin) was calculated and plotted versus log cDNA of HBMECs. The data fit using linear regression analysis (no=3).

6.2.4.6. Relative 37 LRP gene expression in HBMECs treated with LR binding bacterial protein

Quantitative PCR (qPCR) was utilized to examine the effect of meningococcal LR ligands on the transcription level of 37 LRP. To achieve that, monolayers of HBMECs were incubated for 24h with different bacterial proteins (rPorA, rPilQ and loop 4 of PorA) or PBS as a negative control. Then, total RNA was extracted from treated HBMECs and RNA was reverse-transcribed and qPCR used. The ratios of gene expression levels were calculated using the ΔΔCT method (Livak & Schmittgen, 2001). The data were normalised against β-actin. As shown in Figure 6.9, Loop4 of PorA and rPilQ induces 37 LRP expression significantly more than PBS ($p<0.0001$). Recombinant PorA increases 37 LRP expression but to a lesser extent than loop 4 synthetic peptide and rPilQ. Although there was a trend for an increase in 37 LRP expression with treatment with rPorA, the difference was not statistically significant ($p = 0.1507$).
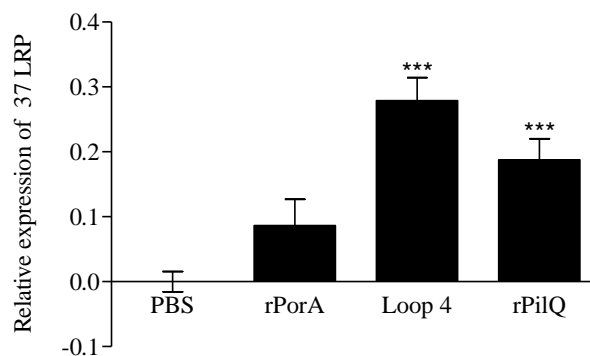
Figure 6.9: Changes in 37 LRP gene expression in the induced HBMECs. HBMECs monolayer was treated with 20µg/ml of rPorA, Loop 4 of PorA and rPilQ or PBS for 24h. Total RNA was extracted and subjected to relative quantification (RQ) using the ΔΔCT method. The qPCR was used to check 37 LRP expression and a log of RQ was plotted using β-actin as an endogenous control and PBS sample as a calibrator.

Each value is the mean ± SEM of nine samples compiled from three independent experiments. (Student's t-test; ***$p < 0.001$).

6.3. Discussion:

The heterodimerization of 37 LRP with Gal-3 to form 67 LR (Chapter 5) and in vitro binding of N. meningitidis to Gal-3 (Chapter 3) were encouraging to study the potential role of Gal-3 in meningococcal adhesion and invasion in this chapter. Interestingly, transient expression of Gal-3 significantly increased MC58 invasion into N2a cells (Figure 6.1C). This is in accordance with a previous study which showed that transfection of Gal-3 enhances H. pylori adhesion to Cos-1 cells, which naturally express low levels of Gal-3, when compared with non-transfected cells (Fowler et al., 2006). A recent study has reported the recruitment of Gal-3 into vacuole disrupted by an invasive pathogen (Paz et al., 2010). Other Galectins, such as Gal-1, increase HIV infectivity by enhancing viral adhesion (Mercier et al., 2008; St-Pierre et al., 2011). Also Gal-1 promotes adhesion of Trichomonas vaginalis to cervical epithelium (Okumura et al., 2008). Thus, the increase in meningococcal invasion mediated by Gal-3 suggests that Gal-3 might enhance meningococcal infection. How Gal-3 contributes in N. meninigitidis invasion and the underlying mechanism is not yet clear. It will be interesting to investigate such a mechanism in future studies.

Since Gal-3 heterodimerizes with 37 LRP to form 67 LR (described in Chapter 5), involving Gal-3 cysteine 173, there might be a cooperative mechanism between these receptors' heterodimers in meningococcal infection. In an attempt to investigate if the obtained increase in meningococcal entry to N2a cells was related to 67 LR heterodimer in addition to Gal-3 itself, Gal-3 C173A mutant, which does not dimerize with 37 LRP, was transfected into N2a cells, and the capability of meningococci to adhere to and invade N2a cells was measured. The meningococcal adhesion and invasion into N2a cells was comparable between

Gal-3 wild type and cysteine substituted construct (data not shown). These results signify the role of Gal-3 in meningococcal invasion, even if its cysteine has been substituted. Taking into consideration that N2a cells lack the endogenous expression of Gal-3, therefore, the behaviour of these receptors' dimers in other cells expressing both receptors, such as HBMECs, could show specific functions.

An interesting finding of the current study was the upregulation of Gal-3 and 37 LRP expression in response to N. meningitidis in the brain of CD46 expressing mice (Figure 6.2A and B). In agreement with this result, previous studies have demonstrated increased expression of Gal-3 in in human meningothelial cells exposed to secreted proteins from meningococci (Robinson et al., 2004). In another study reported by Bellac et al. (2007), expression of Gal-3 was found to be increased in the cortex and hippocampus of pneumococcal meningitis-infected rat, which corroborates our finding (Figure 6.2). In addition to bacterial meningitis, other CNS infections, such as prion (Mok et al., 2007) and Junín virus (JUNV) encephalitis (De Giusti et al., 2011) was associated with upregulation in Gal-3 expression. In the context of bacterial meningitis, all illustrated studies have related the increased Gal-3 expression and its role in neuroinflammation and also anti-apoptotic activity. However, results of several other studies have suggested that Gal-3-pathogen interactions might mediate pathogen adhesion and thus promote infection (Cerliani et al., 2011). For example, adhesion of H. pylori to the gastric epithelial cells increases expression and secretion of Gal-3, which has been suggested to enhance infection (Fowler et al., 2006). Another relevant study has reported that the increased expression of Gal-3 has promoted adhesion of T. cruzi to host cells (Kleshchenko et al., 2004). With this in mind, the possibility that the upregulation of Gal-3 expression might enhance meningococcal infection

by mediating more bacterial entry is strongly recommended, specifically when considering our finding that Gal-3 promoted meningococcal invasion into N2a cells (Figure 6.1).

The demonstrated increased expression of 37 LRP in meningococcal infected mice (Figure 6.2) corroborates Orihuela, Mahdavi et al. (2009) study which showed that the expression of 67 LR is upregulated in mice challenged with pneumococci by immunohistochemical staining of 67 LR in lung and brain of infected mice. Furthermore, CNF1 expressing E. coli K1, but not Δcnf1 mutant, increased the total amount of 67 LR as evidenced by Western blot analysis and immunofluorescence staining of 67 LR in HBMECs (Kim et al., 2005). In Orihuela and Mahdavi et al. (2009) study, the upregulation of 67 LR expression on the surface of host cells was found to be required for bacterial adherence. This was further supported by previous reports' findings, which demonstrated that high density of CEACAM expression is required for cellular invasion of N. meningitidis in an Opa-CEACAM dependent manner, even in capsulated organisms (Griffiths et al., 2007; Rowe et al., 2007). Thus, increased expression of 37 LRP in the brain of N. meningitidis infected mice might induce meningococcal adhesion.

Flow cytometery analysis showed that the recruitment of 67 LR and Gal-3 to the cell surface of HBMECs was increased in response to meningococcal 37 LRP/67 LR ligands, including rPilQ, rPorA and Loop 4 of PorA, when compared with PBS (Figures 6.3A and B). The purpose of this experiment was detailed investigation for the effect of each meningococcal 37 LRP/67 LR adhesin on the surface level of 67 LR and its dimer Gal-3 in vitro. The observed increase in 67

LR surface level was reported by previous studies which showed that the incubation of human melanoma cells with laminin induces 67 LR and its precursor expression on the cell surface (Romanov et al., 1994; Romanov et al., 1995). Romanov et al. (1995) study has further reported that the laminin induction of 67 LR and 37 LRP expression was blocked by cycloheximide (protein synthesis inhibitor), revealing that the induction was depenent on protein synthesis (Romanov et al., 1995). Of interest, meningococcal 37 LRP/67 LR ligands also increased the recruitment of Gal-3 to the surface of HBMECs (Figure 6.3B). Since PilQ was one of the identified meningococcal-Gal-3 adhesins, therefore, induction of Gal-3 surface level in response to its ligand was anticipated. Upregulation of Gal-3 expression in response to several pathogens was reported previously (Bellac et al., 2007; De Giusti et al., 2011; Fowler et al., 2006; Mok et al., 2007). It should be noted that most of theses studies do not differentiate between surface and intracellular Gal-3. However, a recent study showed that the S. mansoni soluble egg antigens (SEA) induced surface expression of Gal-3 on CD$^+$ T cells (Zaccone et al., 2009). This antigen was demonstrated previously to bind Gal-3 via its N-acetyl-lactosamine residues (van den Berg et al., 2004). Not only pathogen ligands but also several host cellular ligands were found to induce Gal-3 surface expression. In this context, Greco et al.*'s* (2004) study has reported that an increased expression of Gal-3 on the surface of cells from adenoma patients was accompanied by an increase of its ligand (90k) in blood plasma of those patients (Greco et al., 2004). This increase in Gal-3 surface expression and its ligand (90k) plasma level was suggested to be used as a marker for differentiation between non-malignant and malignant colon cancers. On the other hand, surprisingly, Gal-3 surface level was increased also

upon treatment of HBMECs with other meningococcal LR adhesins, rPorA and its loop 4 peptide. Since PorA was not identified in the current study as Gal-3 adhesin (discussed in Chapter 3), it is possible that the observed increase in Gal-3 surface level in response to LR bacterial ligands (rPorA and its loop 4 peptide) might be because of the association of Gal-3 with 37 LRP to form 67 LR. Importantly, rPorA induced the most robust increase in surface 67 LR and Gal-3 levels. Meningococcal major porin PorA has immunogenic and adjuvant properties as reported by previous studies. One of these studies has found that recombinant PorA (rPorA) induced dendtritc cell (DC) maturation, which was reflected by reduced receptor-mediated endocytosis (Al-Bader T, 2004). It also increased production of the chemokine IL-8, RANTES, macrophage inflammatory protein-1 alpha and beta (MIP-α and β) and augmented expression of CD40, CD54, CD80, CD86 and the major histocompatibility complex class II molecules, indicating T cell activation (Al-Bader T, 2004). However, in terms of meningococcal adhesion only recently PorA was identified as bacterial ligand for 67 LR, as mentioned earlier. As a result, the observed increased of 67 LR and Gal-3 surface levels in response to meningococcal adhesins could increase the strength of bacterial adhesion and leads to increased cellular invasion by meningococci, as increased CECAM receptor density helps to overcome the inhibitory effects of bacterial capsule and increased bacterial entry into the cells (Bradley et al., 2005; Griffiths et al., 2007; Rowe et al., 2007; Virji et al., 1992). Whether the observed recruitment of receptors to the cell surface in response to bacterial proteins resulted from increased receptor transport or de novo synthesis cannot be concluded from the current study. It would be interesting in a future

study to examine the influence of protein synthesis inhibitor on the recruitment of 67 LR and Gal-3 to cell surface after stimulation with meningococcal ligands.

Furthermore, in the present study, qPCR was used to examine whether the bacterial proteins will affect gene expression of 37 LRP in HBMECs. The qPCR results revealed that the gene expression of 37 LRP in HBMECs is increased in response to loop4 peptide of PorA, rPilQ and, to a lesser extent, rPorA (Figure 6.9). Loop 4 synthetic peptide was employed in the qPCR to avoid possible LPS contamination which might associate with purification of recombinant outer membrane proteins (rPorA and rPilQ). This peptide contains a terminal cysteine residue at each end to form a bridge between the peptide ends to simulate the loop structure. The significant increase of 37 LRP expression as a result of loop 4 was an interesting finding as loop 4 appears to be essential for rPorA-LR binding (Abouseada, 2009). In addition, loop 4 of PorA has been shown to elicit bactericidal antibodies which provide protection against infection (Saukkonen et al., 1989). The significant potentiation of 37 LRP expression by loop 4 peptide more than whole rPorA might be because rPorA is purified under denaturing conditions, so protein conformation including surface exposure of loop 4 will be changed and differs from the native trimer form of the protein, while loop 4 peptide contains a terminal cysteine residue at each end to form a bridge between the peptide ends to stimulate loop structure. This could explain reduced influence of rPorA when compared with its loop 4 peptide in term of 37 LRP expression. Another 37 LRP/67 LR meningococcal adhesin rPilQ (82 kDa) significantly increased 37 LRP expression more than rPorA, but not loop 4. Another relevant study has shown that the TNF-α increases 67 LR expression in a rat brain capillary endothelial cell (rBCEC6) at protein level (Orihuela et al., 2009). This

was evident by immunoblotting of rBCEC6 lysates using Ab711 antibody which detects the mature (67 LR) and precursor (37 LRP) forms of the receptor and showed gradual increase in the expression level of 67 LR and its precursor in response to TNF-α (Orihuela et al., 2009). Therefore, it will be useful to study 37 LRP/67 LR expression at the protein level by Western blotting in a future study. In the context of bacterial meningitis, meningococcal porin and secretin (PilQ) are considered the second bacterial ligands after E. coli K1 CNF (Kim et al., 2005) that induce 67 LR gene expression on HBMECs. Interestingly, both PorA and PilQ are outer membrane proteins and strong vaccine candidates (D. Halliwell, 2004; Jan T. Poolman, 2006; Vermont et al., 2003). It is noteworthy that both rPorA and rPilQ were also shown previously to induce transient increases in calcium release in HBMECs using confocal microscopy (Abouseada, 2009). In addition, meningococci are known to release outer membrane vesicles (OMVs) or blebs in vivo during infection, which play an important role in immune evasion and inflammation (Devoe & Gilchrist, 1973). Blebs are formed by circular pieces of the outer membrane carrying a number of different OMPs and LOSs. This feature was used to develop a vaccine against meningococci serogroup B where outer membrane proteins presented in LOS depleted OMVs (Fredriksen et al., 1991). More interestingly, 37 LRP/67 LR meningococcal adhesins are constituents of OMVs or blebs (Post et al., 2005) which might act as additional microbial signal that induce 67 LR expression in vivo, taking into consideration that these OMVs have been shown to correlate with severity of the meningococcal disease (Brandtzaeg et al., 1992b).

It is noteworthy that the 67 LR exists as a homo- and heterodimer with Gal-3, so it is possible that the upregulation of 37 LRP/ 67 LR expression in response to

meningococcal LR ligands might be not mediated solely by receptor homodimers, but also heterodimers form with Gal-3. Attempts were made to study the expression of Gal-3 in response to meningococcal LR ligands, but the available time did not allow further optimization for qPCR.

In conclusion, the results presented in this chapter revealed that expression of Gal-3 enhanced meningococcal invasion into N2a cells. Both 37 LRP and Gal-3 expression were upregulated in response to N. meningitidis infection in the meninges of CD46 expressing mice. Furthermore, incubation of HBMECs with purified proteins of meningococcal LR ligands increased the recruitment of 67 LR and Gal-3 to cell surface and increased gene expression of 37 LRP at the mRNA level.

7. Chapter 7: General discussion

7.1. General Discussion

N. meningitidis remains the leading cause of meningitis and septicaemia worldwide (Harrison et al., 2009). The incidence of meningococcal disease ranges from 0.5 to 1000 cases per 100, 000 of the population each year, in the sporadic outbreaks observed across Europe and during epidemics in the meningitis belt in sub-Saharan Africa, respectively (Hill et al., 2010; Stephens et al., 2007). Of the estimated 1.2 million cases of invasive meningococcal disease, 135,000 deaths are thought to occur annually worldwide, even with antibiotic treatment (WHO, 2001); furthermore, patients who survive meningococcal disease suffer from long-term neurological complications, such as epilepsy, neurological damage and deafness (Dawson et al., 1999; Grimwood et al., 2000). Meningococcal vaccines were thus introduced, in an attempt to control and prevent the disease. The introduction of conjugated vaccines against meningococcal serogroup C to routine immunization in different countries has led to a dramatic decline in the incidence of the disease and the asymptomatic carriage caused by serogroup C (Gasparini & Panatto, 2011). In many countries, quadrivalent vaccines have been used for years in the prevention of meningococcal disease caused by serogroups A, C, Y and W-135 (Tan et al., 2010); however, as yet, there are no vaccines that are broadly effective against serogroup B meningococci, which is the predominant cause of meningococcal disease in developed countries (Harrison et al., 2009). This is due to similarities between the serogroup B polysaccharide capsule and the human neurological antigen. As a result, the immunogenicity of the meningococcal serogroup B capsule is poor in humans and its use in the development of vaccines has thus been avoided, in order to prevent the development of potential

autoimmune disease. Despite the availability of a preventative vaccine against some serogroups and the sensitivity of the organisms to several antibiotics, N. meningitidis remains a major threat to human health. Alternative approaches in the prevention of meningococcal disease are thus required and this necessitates a greater understanding of the host-pathogen interaction, which may also enable new vaccine and therapeutic strategies.

N. meningitidis is a highly-invasive Gram-negative bacterium that is capable of causing outbreaks of meningitis, septicaemia and septicaemic shock, which can kill within hours of the appearance of symptoms. In order to approach the meninges from the nasopharynx, the meningococci must cross two cellular barriers: firstly, the epithelial cell barrier in the nasopharynx and, secondly, the endothelial barrier in the brain. In this context, Neisseria meningitidis uses numerous adhesins and secreted virulence factors to interact with the various host cell receptors that mediate bacterial adhesion and invasion of human cells (Orihuela et al., 2009; Unkmeir et al., 2002; Virji et al., 1994). These adhesins act in a sequential manner and in concert, resulting in high avidity interactions, which are often a prelude to cellular invasion and tissue penetration (Virji, 2009). Some of these adhesins have been identified to target multiple host receptors (Virji, 2009).

In terms of the host receptors, 37 LRP/67 LR has recently been identified by a researchers in our group as being targeted by meningococcal PorA and PilQ, pneumococcal CbpA and OmpP2 of H. influenza (Orihuela et al., 2009). These pathogens are the most common cause of bacterial meningitis and it has been suggested that their interactions with 37 LRP/67 LR underlie their CNS tropism

(Orihuela et al., 2009). Interestingly, of the three strains of meningitis bacteria, N. meningitidis is the only one with two 37 LRP/67 LR-binding surface adhesins: this may reflect the importance of, and the affinity required for, this binding. Of interest is the fact that the identified meningococcal ligands for 37 LRP/67 LR have been utilised as a strategy in the development of vaccines (St. Jude Children's Research Hospital, 2008; University of Nottingham, 2009). This strategy is based on the interruption of the interaction of these pathogens with 37 LRP/67 LR, through the administration of polypeptides mimicking the binding proteins expressed on the surface of these pathogens (St. Jude Children's Research Hospital, 2008; University of Nottingham, 2009). Another bacteria that causes meningitis, Escherichia coli K1, also targets the same receptor via its cytotoxic necrotising factor 1 (CNF1) (Chung et al., 2003): the interaction of CNF1 with 37 LRP/67 LR induces the E. coli K1 invasion of endothelial cells in the human brain (Kim et al., 2005). Recently, pharmacological agents (etoposide) were shown to prevent the invasion of HBMECs by E. coli K1 and this significantly decreased the development of meningitis in experimental mice (Zhu et al., 2010). Interestingly, a reduction in the expression of 37 LRP/67 LR is the mechanism that underlies the preventive effect of etoposide on E. coli K1 invasion (Zhu et al., 2010).

The 37 LRP/67 LR is a non-integrin laminin receptor, which is expressed in different cells, including brain endothelial cells, and acts as a receptor for a versatile range of neurotropic pathogens (Menard et al., 1997; Nelson et al., 2008). A number of previous studies have suggested that the homodimerization of the receptor precursor (37 LRP) or the heterodimerization of this precursor with an interesting partner Galectin-3 (Gal-3) forms the mature 67 LR (Buto et al.,

1998; Castronovo, 1993; Landowski et al., 1995); however, the dimerization status of 37 LRP/67 LR is not yet clear. The significance of 37 LRP/67 LR as a therapeutic target in bacterial meningitis, including meningococcal disease, and its potential contribution to meningococcal CNS tropism necessitates further characterisation of the dimerization status of the receptor, which was one of the major aims addressed by the current study.

The potential dimerization of 37 LRP/67 LR with Galectin-3 is of particular interest: this is because Galectin-3 is a multi-talented lectin that interacts with several pathogens and is involved in their pathogenesis through its functions in innate immunity or as pathogen receptor. In addition, the role of Galectin-3 in CNS infections, such as prion disease, encephalomyelitis and pneumococcal meningitis (PM), has emerged recently (Bellac et al., 2007; Coimbra et al., 2006; Mok et al., 2007; Reichert & Rotshenker, 1999). Recently, Galectin-3 has been shown to bind N. meningitidis and this interaction has been shown to require an intact LOS (Quattroni et al., 2012). Although Quattroni et al (2012) study has shown that the presence of lactose leads to the inhibition of Gal-3 binding, some remaining binding was also observed; thus, the fact that other meningococcal ligand(s) also imply in bacterial binding with Gal-3 cannot be excluded. The aim of this study was to determine the non-LOS meningococcal surface molecules that mediate bacterial binding with Gal-3, using a lactose liganded form of Gal-3.

In the current study, the binding of the lactose liganded Gal-3 with N. meningitidis was demonstrated and the majority of this binding was largely attributed to the N-terminal domain of Galectin-3. Some binding was also exhibited by the CRD of Gal-3, but was markedly less than the N-terminal

domain. Notably, several meningococcal clinical isolates were able to bind Gal-3 in differential binding densities, regardless of their serogroups and geographical distribution. Quattroni et al. (2012) undertook an immunohistochemical analysis of tissue from patients with meningococcal infection and this revealed the colocalisation of meningococci with Gal-3. The observed in-vivo colocalisation suggests the binding of Gal-3 with N. meningitidis which was further confirmed by in-vitro binding assay, using flow cytometry and fixed-label meningococci (Quattroni et al., 2012). A comparison of the full molecule of the Gal-3 and its CRD demonstrated that the Gal-3 full molecule is required for meningococcal binding (Quattroni et al., 2012). Despite the use of lactose liganded Gal-3 in the current study, the findings of our research are in accordance with the findings of Quattroni & Li et al (2012) study. However, the observed binding of Gal-3 CRD to meningococci in the current study was more apparent in our study than in Quattroni et al study.

Quattroni et al. (2012) demonstrated that the binding of meningococci with Gal3 can be inhibited by very high doses of lactose (100mM). In addition, deletion mutants lacking various LOS-related glycosyltransferase genes (IgtA, IgtB, Isi1, icsB and galE) significantly reduce meningococcal ability to bind Gal3 (Quattroni et al., 2012). Thus, Quattroni et al (2012) concluded that the binding of meningococci with Galectin-3 is dependent on intact LOS. In the current study, the non inhibitable binding of meningococci with Gal-3 in the presence of increasing concentrations of lactose, up to 150mM, was observed: this was due to the fact that the Gal-3 used in the current study is lactose liganded. Such a result does not neglect the involvement of meningococcal LOS in Gal-3 binding, as the lactose-liganding did not necessarily block all LOS-carbohydrate binding sites on

Gal3. Because meningococcal LOS has extended lactose (e.g. LacNAc), which have five times a higher affinity for Gal3 than lactose (Agrwal et al., 1993; Sato & Hughes, 1992; Seetharaman et al., 1998). In addition, conformational changes in Gal3 after the initial interaction can potentially increase affinity, possibly via the involvement of the N-terminal domain of Gal3 and its CDR (Agrwal et al., 1993). This was verified by the very low but nevertheless significant Gal3 binding exhibited in this study by the lgtf mutant, which produces a truncated LOS molecule lacking chain containing LacNAc moiety.

Galectin-3 is widely distributed in various cellular compartments (nuclei, cytoplasm, cell surface and extracellular) and thus bacteria can take advantage of this molecule through the engagement of different bacterial ligands at various stages of infection. For example, bacterial surface adhesins may use cell surface Gal-3 to adhere or invade and other secreted bacterial proteins may utilise intracellular Gal-3 (for example, in their nuclear shuttling) and extracellular Gal-3, in order to activate the innate immune system. Thus, despite the reported involvement of LOS in the interaction of Gal-3 with meninigococci, the contribution of other non-LOS meningococcal ligands cannot be ruled out.

In the current study, a retagging approach was used, in order to identify non-LOS meningococcal-Gal-3 ligands. Two bacterial ligands were identified: the secretin PilQ and its associated pilin molecule PilE. The contribution of these adhesins to the recognition of the meningococci by Gal-3 was confirmed via observed significant reduction in the binding of corresponding mutants to Gal-3.

PilQ is a conserved secretin that is fundamental for pilus extrusion and is naturally expressed at very high levels (Martin et al., 1993). It is interesting to note that PilQ

is already identified as an adhesin for 37 LRP/67 LR (Orihuela et al., 2009). In previous studies, it has been suggested that PilQ could be a potential vaccine candidate (D. Halliwell, 2004; Jan T. Poolman, 2006); indeed, a recent study demonstrated that the sera from mice, when immunised with a purified rPilQ fragment (406-770), was strongly bactericidal against N. meningitidis serogroups A and B (Haghi et al., 2012). PilQ is not glycosylated; thus, its binding with Gal-3 appears to be mediated through a protein-protein interaction. This binding pattern is consistent with the carbohydrate independent binding of another lectin (namely, mannose binding lectin (MBL)) with non-glycosylated meningococcal outer membrane proteins Opa and PorB (Estabrook et al., 2004). The identification of PilQ as an adhesin for Gal-3 represents the second non-LOS bacterial ligand, after P. mirabilis fimbriae (Altman et al., 2001).

PilE is the major subunit that forms the shaft of the pilus fiber (Craig et al., 2006), a hair-like structure that is extruded to the external surface via the PilQ (Martin et al., 1993). The fiber rapidly extends for several micrometres from the bacterial surface, in order to initiate contact with the host cells, before retracting (twitching motility). The pilus has long been considered a primary adhesion factor (Pelicic, 2008; Pujol et al., 1997; Virji et al., 1991) and plays a major role in maintaining adherence to endothelial cells under high-flow conditions (Mikaty et al., 2009). This and the twitching motility are thought to help the organism crawl until it comes into intimate contact with the host cells, where other bacterial surface adhesins and their corresponding receptors interact. Furthermore, anti-(PilE) pilin antibodies have been detected in patients infected with N. meningitidis confirming the immunogenicity of PilE (Poolman et al., 1983). However, the high level of antigenic variability detected between PilE proteins hinders the development of a

pilus-based vaccine (Svanborg Eden et al., 1983). Interestingly, a recent study found that the major pilin genes are highly conserved within N. meningitidis disease isolates, representing ST-8 and ST-11 clonal complexes (Cehovin et al., 2010), suggesting the reconsideration of pilus as a vaccine candidate.

The adhesin properties of pilus are believed to be mediated by the PilC protein at its tip and the numerous post-translational modifications, including O-glycosylation, at its shaft (PilE subunits) (Banerjee & Ghosh, 2003). Identified types of O-linked glycans in N. meningitidis include Gal-β1, 4-Gal-α1, 3-DATDH (DATDH represents 2, 4-diacetamido-2, 4, 6-trideoxyhexose) (Stimson et al., 1995), Gal-β1, 4-Gal-α1, 3-GATDH (GATDH represents 2-glyceramido-4-acetamido-2, 4, 6-trideoxyhexose) (Chamot-Rooke et al., 2007). Gal-α1 3GlcNAc is also present in the N. meningitidis strain 8013SB (Marceau et al., 1998). These glycans are synthesised in the cytoplasm by the sequential action of pglD, pglC and PglB (for DATDH) or PglB2 (for GATDH), then flipped into the periplasmic space by pglF flippase and block transferred onto Ser63 of PilE by the pilin glycosylation ligase PglL (Power et al., 2006). In the current study, the mutagenesis of pglL, pglC and pglLC radically reduced the binding of meningococci to Gal3, indicating that the glycosylation of PilE has a clear role in this binding.

The involvement of PilE O-glycan in the interaction of Gal-3 with meningococci may justify the observed binding of the CRD. A question that must be raised is why, in Quattroni et als' (2012) study, was the binding of CRD with meningococci markedly less than in our study? This may have been due to the fact that we used a lactose-bound form of the CRD, which might have changed

the conformation of the molecule and increased its binding affinity. This explanation is supported by a previous NMR study on liganded Gal-3, which showed that the carbohydrate binding site was found to be more open in the bound state (Umemoto et al., 2003). Given the fact that the CRD of Gal-3 has an extended carbohydrate site, which enables it to accommodate complex glycan binding (Seetharaman et al., 1998), it is possible that the extended spectrum of the CRD also enables the accommodation of the binding of PilE O-glycans. However, it should be noted that, in addition to the CRD of Gal-3, the N-terminal domain is also implicated in the various interactions of Gal-3 with glycans. A mutagenesis analysis of Gal-3 supported the contribution of Tyr102 and some adjacent residues in carbohydrate binding (Barboni et al., 2000). In addition, the multimerisation of the N-terminal, in terms of the interaction of the CRD and the glycoconjugate, led to the formation of Gal-3 pentamers, facilitating increasingly diverse interactions with several glycoconjugated ligands (referred to as positive co-operativity). This was best exemplified in the demonstrated inhibition of H. pylori 26695 LPS binding to gastric epithelial cells (by antibodies) against the N-terminal part of Gal-3 (Fowler et al., 2006). Thus, it could be that both the CRD and the N-terminal domain of Gal-3 participate in the interaction of Gal-3 with glycosylated pilin.

Current observations of Gal-3 binding to the glycosylated meningococcal molecule (PilE) in addition to LOS (Quattroni et al., 2012) will assist future studies (as the majority of studies regarding the bacterial interactions of Gal-3-have focused particularly (and, in some instances, solely) on LPS). In this context, a member of other host lectins, such as the C-type lectin receptor (MGL), was shown to bind distinct LOS glycoforms and the N-linked glycoproteins of

Campylobacter jejuni (van Sorge et al., 2009). This corroborates our findings, suggesting the potential ability of host lectins (including Galectin-3) to recognize multiple glycosylated ligands within the same pathogen. It should be noted that the pgl genes encode an N-linked protein glycosylation system share features with lipopolysaccharide (LPS) O-antigen biosynthesis (Alaimo et al., 2006; van Sorge et al., 2009). While in meningococci, the Pgl enzymes are not involved in meningococcal LOS biosynthesis and their mutation has no effect on the structure or function of the LOS (Power et al., 2000; Power et al., 2006). It is noteworthy that neisserial pglL (O-Otase) contains a Wzy_C motif, which is conserved in all O-OTases, but it is also found in WaaL ligases, which catalyze the transfer of the O antigen to the lipid A core of bacterial LPS. However, the meningococci bacteria produces LOS rather than LPS, as it lacks O-antigen repeat and therefore excludes the involvement of pglL in the biosynthesis of LOS (Preston et al., 1996). This provides more specificity to the observed reduction in the binding of Gal-3 with pglL, pglC and pglLC mutants, to be attributed only to O-glycans decorating PilE. Interestingly, a careful examination of the mutants used in Quattroni et als' (2012) study revealed that one of LOS mutants demonstrated a marked reduction in Gal-3 binding (the galE mutant, which expressed galactose-deficient LOS (Robertson et al., 1993) and galactose deficient PilE glycan) (Stimson et al., 1995). This further confirms the contribution of glycosylated PilE, in terms of the binding of Gal-3 with meningococci.

The glycosylation of pilin is suggested to be one of the bacterial virulence factors that may aid the development of the P. aureginosa infection (Smedley et al., 2005). As a mutation of the pilO gene analogue of the N. meningitidis pglL gene, this leads to a reduction in bacterial twitching motility and decreases the survival

of the bacteria in the environment of the lungs (Smedley et al., 2005). It has also been observed that strains of P. aeruginosa producing glycosylated pilin were commonly found amongst clinical isolates, particularly those isolated from sputum, revealing the involvement of pilin glycans in the pathogenesis of P. aeruginosa (Smedley et al., 2005). In terms of Niesseria meningitidis, it has been suggested that pilin glycosylation influences bacterial cellular adhesion (Stimson et al., 1995; Virji et al., 1993b): such an influence might be mediated in part through meningococcal glycosylated pilin interacting with Galectin-3. It would be interesting if future studies could examine the effect of pglL, pglC and pglLC mutations on bacterial adhesion and the invasion of host cells in-vivo, as pilin glycosylation in the closely-related bacteria N. gonorrhoeae has recently been shown to imply bacterial invasion into host cells (Jennings et al.). A further post-translational modification of meningococcal pilin, phosphoglycerol at serine 93, was recently shown to enable bacterial migration across host cells and dissemination to other hosts (Chamot-Rooke et al., 2011). It thus appears that various post-translational modifications of PilE contribute to meningococcal pathogenesis, in various aspects.

For the first time, the current study provides evidence for the existence of 67 LR as a homo- and hetero dimer with Gal-3. The dimerization of 37 LRP with itself and with Gal3 to form 67 LR homo and heterodimer respectively has long been suggested (Buto et al., 1998; Castronovo, 1993; Landowski et al., 1995). However, the majority of these studies used biochemical approaches, which require detergent cell lysis and thus affect native receptor-receptor interaction. To avoid this disadvantage, the BiFC approach has been used in this study, in order to enable the direct visualisation of receptor interactions non-invasively

(Kerppola, 2008). The expression pattern of the 67 LR homo- and hetro- dimers formed by the complementation of the 37 LRP and Gal-3 fused to BiFC fragments clearly reflects the punctuate staining of endogenous 67 LR and Gal-3 in HBMECs respectively. It should be noted that the endogenous staining of Gal-3 in the HBMECs also showed some diffuse staining. The punctate staining of the endogenous 67 LR in HBMECs was revealed by two antibodies; namely, the Mluc5 and Ab711 antibodies. The Mluc5 antibody is anti-mouse and thus we could not use it, with regards to the dual fluorescence staining and the Gal-3 antibodies (mab4033 and Mac-2) that arose in mice and rats respectively, due to the observed cross-reactivity. Instead, the Ab711 antibody, which is anti-rabbit, was co-stained with anti-Gal-3 (mab4033), revealing the marked extent of colocalization. Also in the current study, the dual immunofluorescence staining of 67 LR and its precursor was performed, using the Mluc5 and InHLRP antibodies respectively. Colocalization between the punctate staining of 67 LR and the diffuse staining of its precursor was noted in the specific cellular compartment only: whether Ab711 and Mluc5 antibodies detect the heterodimer form of 67 LR, in addition to the homodimer, is not clear. Indeed, the BiFC signals of the dimers of both receptors demonstrated a punctate pattern and each form of receptor dimer appeared to have a distinct cellular distribution. In order to clearly distinguish the cellular distribution of the populations of each receptor, it would be useful if the multi-colour BiFC approach was considered in future investigations. In contrast to the punctate pattern, the receptor's homo- and hetero- dimer BiFC complexes were expressed in a diffuse pattern in COS7 and N2a cells, which represented the endogenous staining of 37 LRP and Gal-3. Unlike HBMECs, immunoFluorscence staining using the anti-67 LR antibodies revealed the existence of such a pattern

in the astrocytes, but not in the COS7 and N2a cells. This might be due to the fact that these cells are not maintained in substrate (fibronectin) like HBMECs and the 67 LR expression was down-regulated in a plastic tissue-culture flask.

Recently, a unique interaction between dectin-1(a C-type lectin) and Gal-3 has been shown to function in the proinflammatory response of macrophages to pathogenic fungi (Esteban et al., 2011). Dectin-1 recognises the β-glucan of the fungal cell wall of most fungi, while Gal-3 binds to the β-1,2 oligomannans from the cell wall of certain fungi. In RAW 264.7 macrophages, which express Gal-3 but express little dectin-1, there was no induction of TNF-α after fungal exposure. When the expression of dectin-1 is increased, RAW 264.7 macrophages show a significant TNF-α response, upon exposure to both pathogenic and non pathogenic fungi (Esteban et al., 2011): this indicates that the presence of dectin-1 is required for TNF-α induction. When the levels of Gal-3 are reduced by silencing, the RAW 264.7 macrophage fails to generate the dectin-1-driven TNF-α response after exposure to the pathogenic fungi C. albicans. In contrast, the TNF-α response was not affected, in terms of the RAW 264.7 macrophage being challenged with the non-pathogenic fungi S. cerevisiae after Gal-3 silencing (Esteban et al., 2011). Thus, the Gal-3 acts in concert with dectin-1, in order to modulate the TNF-α response of the macrophage, in terms of the recognition of pathogenic fungi (Esteban et al., 2011). Moreover, the association of Gal-3 with TLR2 displays a similar role and modulates the TLR2-driven inflammatory response (Jouault et al., 2006). In this regard, the current findings, in terms of the heterodimerization between 37 LRP/67 LR and Gal-3, are strongly supported by the binding of PilQ for both. Thus, 37 LRP/67 LR and Gal3 may closely

collaborate in binding to a common target molecule or, conversely, the meningococcus has evolved to exploit both molecules, adding affinity to the cell-cell adhesion, facilitating host cell invasion and/or triggering downstream host-cell signalling. In this context, the engagement of the PilQ-associated pilin molecule, PilE, adds another interesting and more dynamic molecule to the adhesion-receptor complex.

Taking into consideration the notion that 37 LRP/67 LR and Gal3 are broadly distributed in different cellular compartments, their collaborative interaction against the meningococcus or its ligands may not end at interactions with the cell surface (Dumic et al., 2006; Nelson et al., 2008). The two molecules play a joint role in tissue-specific adhesion and in the signalling, internalisation and modulation of host cell responses. 37 LRP/67 LR and Gal3 are both over-expressed in various cancer cells and Gal3 is a regulator of a broad range of cancer cell growths, transformations, apoptosis, angiogenesis, adhesions, invasions and metastases (Nelson et al., 2008; Newlaczyl & Yu, 2011).

In this study, further investigation of Gal-3 and 37 LRP dimer formation revealed that, like the murine Gal3 cys186 (Woo et al., 1991), the only cysteine residue present in human Gal3 (cys173) is critical for both homo- and hetero-dimerization, whereas neither of the two cystienes on 37LR (cys148 and cys163) are required for dimerization. The impact of the mutation of Gal3 (cys173) on the dimerization of Gal-3 with 37LRP/ 67 LR might be of consequence, in terms of the role of this dimer in normal physiological and pathological conditions. Such consequences were not addressed in the current study and it would be interesting

if future studies considered these. In Woo *et als'* (1991) study, the substitution of Gal-3 (cys173) did not affect the binding of the receptor with laminin.

It is well-recognised that 37 LRP/67 LR is subjected to acylation (mainly palmitoylation), which commonly occurs in cysteine residues, in being delivered to the cell surface (Buto et al., 1998; Landowski et al., 1995). In the current study, the mutations of the previously-mentioned cystiene residues of 37LR (cys148 and cys163) do not affect receptor targeting to the cell surface and this was revealed through two findings: the distribution of cysteine-substituted receptors was comparable to the wild-type receptor in the membrane fractions of transfected COS7 cells and the punctate expression of cysteine-substituted receptors was comparable to the wild type receptors in transfected HBMECs. Given the fact that palmitoylation is a reversible process, it is possible that the experimental setting used in the current study does not provide an adequate time frame, in terms of detecting any differences between the cysteine-substituted and wild-type receptors. As mentioned above, further examination of the role of 37LR (cys148 and cys163) in the homo- or hetero- dimerization of 67 LR, using BiFC, revealed that these cysteine residues are not involved in the dimerization of receptors. In agreement with our findings, research conducted by Fujimura et al. (2012) found that the amount of 67 LR was not affected by the presence or absence of the reducing agent. All these results collectively confirm that a Cys residue-mediated disulfide bond is not involved in the formation of the cell-membrane 67LR, although it is possible that these two cysteines are involved in protein stabilisation. With regards to the acylation of 67 LR, it appears that other amino acid residues are involved in the acylation of 37 LRP/ 67 LR. It is interesting to note that Buto et al. (1998) observed an inhibition or decrease in the formation of

67 LR by the fatty acid synthetase inhibitor, cerulenin. Thus, future study is essential, in terms of clarifying the role of acylation in the dimerization of 67 LR, through investigating the effects of cerulenin on the complementation of receptors fused to BiFC fragments.

In Quattroni et al (2012) study has showed that the exogenously added Gal-3 increases meningococcal adhesion to monocyte and THP-1 cells without any effect on bacterial internalisation. They also established that the full-length LOS is required for such an increase in bacterial adhesion, as the adhesion of the LOS mutants to these cells was not affected by the exogenously-added Gal-3 (Quattroni et al., 2012). However, the perincubation of meningococci with Gal-3 did not affect their association with epithelial cells (Quattroni et al., 2012). The focus of Quattroni et al*s' (2012) study was the effects of exogenous Gal-3 on bacterial adhesion, as the secretion of Gal-3 is known to be stimulated in response to bacterial infection. However, a particular interest of the current study was to examine the contribution of the cell surface Gal-3, rather than the secreted form, in terms of meningococcal adhesion and invasion. In order to achieve this, N2a cells were chosen, due to their lack of endogenous Gal-3 expression (Gauczynski et al., 2001). N2a cells were transfected with Gal-3 containing plasmid and the surface localisation of Gal-3 in transfected cells was confirmed immunofluorescence staining. Interestingly, the transient expression of Gal-3 significantly increased the invasion of MC58, but not adhesion to N2a cells: this finding suggests that N. meningitidis may use Gal-3 as a mechanism of host invasion. Such promotion of meningococcal invasion, mediated by Gal-3, strongly suggests that Gal-3 may enhance meningococcal infection. Several studies have suggested that Galectin-3-pathogen interactions may enhance

infection by mediating microbial cellular adhesion. In this context, Galectin-3 may facilitate H. pylori infection, through allowing bacterial adhesion to the gastric epithelium (Cerliani et al., 2011; Fowler et al., 2006). Other galectins, such as Gal-1, increase HIV infectivity by promoting viral adhesion (Mercier et al., 2008; St-Pierre et al., 2011). Gal-1 also enhances the adhesion of trichomonas vaginalis to the cervical epithelium (Okumura et al., 2008). How Gal-3 contributes to N. meninigitidis invasion and the underlying mechanism is not yet clear and it would be both beneficial and interesting to investigate this in future studies.

Meningococci T4P initiates bacterial adhesion to host cells, using an as yet unknown receptor, followed by the activation and recruitment of different host receptors and bacterial adhesins and invasins mediating cell signaling events: this leads to the formation of cortical plaque and subsequent bacterial entry. Although pilus-mediated signalling results in the formation of apparently similar cortical plaque in epithelial and endothelial cells, the signalling pathways are strikingly different in both models (Lecuyer et al., 2012). For example, it has been found that the recruitment of tight junctional proteins in response to N. meningitidis T4p-mediated adhesion is restricted to endothelial cells, but not epithelial cells (Lecuyer et al., 2012). In other instance, unlike brain endothelial cells, meningococcal adhesion to epithelial cells did not recruit or activate the β2-adrenergic receptor/β-arrestin pathway. Considering the discrepancies of T4p-mediated signalling in epithelial and endothelial cells, the observed finding of the Gal-3-mediated enhanced invasion of meningococci into N2a cells may be more significant in relevant cells (endothelial or epithelial cells) and Gal-3 may also contribute to bacterial adhesion. Although Quattroni et al (2012) study did not

report any significant role of exogenously-added Gal-3, in terms of meningococcal adhesion to epithelial cells, the current study demonstrated a distinct punctuate expression of Gal-3 and both dimers of 67 LR on the apical surface of brain endothelial cells. This pattern suggests the localisation of receptors within membrane microdomains referred to as lipid rafts. Lipid rafts are discrete plasma membrane domains that contain high levels of cholesterol, gangliosides, glycosphingolipids, GPI anchored proteins and many acylated & palmitolyated proteins (Simons & Toomre, 2000). Accordingly, lipid rafts and their components act as a concentrating domain for cell signalling molecules (Anderson, 1998). Both Galectin-3 and 67 LR have been shown to be located in lipid rafts in various cell lines (Foster et al., 2003; Fujimura et al., 2005; Hsu et al., 2009; Osterhues et al., 2006). In this context, meningococcal minor pilin PilV has been shown to induce the recruitment of cholesterol, in the formation of cortical plaques. These lipid rafts enable N. meninigitidis to induce the action of polymerisation, in order to form projections at the apical aspect of cells that protect bacteria from shear stress (Mikaty et al., 2009; Trivedi et al., 2011). The depletion of the concentration of cholesterol in the plasma membrane by MßCD (methyl-ß-cyclodextrin), which inhibits the formation of lipid rafts, decreases the recruitment of those cellular components of the cortical plaque under the bacterial microcolonies and renders meningococcal microcolonies sensitive to shear stress (Mikaty et al., 2009). It is thus possible that both Gal-3 and 67 LR (either homo- or hetero- dimers) are located in the lipid raft domain and such localisation may have an impact, in terms of meningococcal infection. An investigation of this possibility would make interesting future research.

One of the most intriguing findings of this study was the upregulation of the Gal-3 and 37 LRP expressions, in response to meningococcal infection in the brains of CD46-expressing mice. Increased expression of Gal-3 was also observed in the spleen tissue of mice challenged with N. meningitidis and in the spleen tissue of patients infected with meningococcal meningitis (Quattroni et al., 2012). In terms of pneumococcal meningitis, the expression of Gal-3 was shown to be upregulated in the brain of infected rats (Bellac et al., 2007). In addition, the expression of 67 LR was increased in the lungs and brains of mice infected with pneumococcal meningitis (Orihuela et al., 2009). In vitro, it has been suggested that the upregulation of 67 LR increases bacterial adhesion (Orihuela et al., 2009). All these findings corroborate the demonstrated increased expression of Gal-3 and 37 LRP in meningococcal- infected mice in the current study. Whether this increase in receptor expression promotes meningococcal infection or not is unclear and cannot be concluded from the current findings. In regards to this, Gal-3 deficient mice have been found to have significantly lower levels of bacteraemia after exposure to N.meningitidis, when compared to wild-type mice, (Quattroni et al., 2012). This indicates that Gal-3 promotes bacteraemic meningococcal disease and various conclusions have been suggested, in order to explain this effect (Quattroni et al., 2012). For example, the observed increased association of Gal-3 to macrophages and monocytes in-vitro could lead to enhanced meningococcal survival by allowing an escape from phagocytosis, promoting bacterial dissemination or affecting the activity of phagocytes (Quattroni et al., 2012). Other studies have highlighted the increased expression of Gal-3 in response to infection and the fact that this is due to its role in neuroinflammation and its anti-apoptotic activity (Bellac et al., 2007). It will be

useful to investigate the level of bacteremia, survival and Gal-3 expression in the brains of Ga-3 deficient mice, after challenging with pilE, pilQ and pglLC meningococcal mutants, and compare the results with those of wild-type mice. Such an experiment will be useful in clarifying the contribution of the binding of Gal-3 with non-LOS meningococcal ligands, in terms of meningococcal pathogenesis.

The current study showed the ability of the purified proteins corresponding to meningococcal 37 LRP/67 LR ligands (rPorA, loop 4 of PorA and rPilQ) in recruiting 67 LR and Gal-3 to the surface of HBMECs. Interestingly, among these proteins, rPorA produced the most prominent effect on the surface level of both receptors. PorA is a known ligand for 37 LRP/67 LR, but not for Gal-3; it thus appears that such recruitment of Gal-3 to cell surfaces, in response to rPorA, is mediated through 37 LRP/67 LR dimers with Gal-3. Although rPorA and its loop 4 bound Gal-3 in ELISA, meningococcal PorA mutant bound Gal-3 in comparable level to wild type bacteria. In addition, the retagging approach did not identify PorA as potential ligands. Despite this, the possibility that Gal-3, in its 67 LR heterodimer form, interacts directly with meningococcal PilE and PilQ and indirectly with PorA (due to the close association between Gal-3 and 37 LRP) cannot be excluded. PilQ also recruits Gal-3 to the cell surface to a greater extent than loop 4 of PorA: this was expected, as PilQ is one of the Gal-3-meningococcal ligands. The use of recombinant PilE and other non-LOS meningococcal Gal-3-ligands was avoided in the current study and this was due to the fact that PilE is subjected to different posttranslational modifications; thus, when expressed in a foreign host (E. coli), it would inevitably lose its natural post-translational modification and the results may not be easily interpretable. In

the case of 67 LR, PorA and its loop 4 recruit 67 LR to the cell surface more than

PilQ. It was of interest that loop 4 of PorA appears to be essential in the binding

of meningococcal PorA with 37 LRP/67 LR (Abouseada, 2009). Whether the

inducible recruitment of bacterial proteins to a cell-surface 67 LR and Gal-3

resulted from recycling or de novo synthesis of the receptor is not yet known.

Kim et al (2005) study has demonstrated that the expression of 67 LR is

upregulated in response to CNF1-expressing E. coli K1 in HBMECs (Kim et al.,

2005). In addition, the expression of 67 LR has been found to increase in the

lungs and brains of mice infected with pneumococcal meningitis (Orihuela et al.,

2009). The current study also demonstrated the upregulation of the expression of

37 LRP in the brains of mice infected with N. meningitidis. In these studies, the

whole bacteria was used and receptor expression was studied through either

immunofluorescence staining or western blot analysis, or both. Thus, the current

study has evaluated the effects of various purified bacterial proteins (rPorA, loop

4 of PorA and rPilQ), rather than whole bacteria, in the gene expression of 37

LRP. In order to achieve this, HBMECs were treated with these proteins for 24

hours and the 37 LRP gene expression was examined by qPCR. The qPCR data

revealed increases in the 37 LRP gene expression in HBMECs treated with loop 4

of PorA, rPilQ and, to a lesser extent, rPorA, when compared with PBS-treated

cells. These results suggest that meningococcal porin (PorA) and secretin (PilQ)

are considered the second bacterial ligands after E. coli K1 CNF (Kim et al.,

2005), which induces the expression of the 37 LRP gene on HBMECs. The

capability of these proteins to induce receptor expression in-vitro may have an

impact on future studies investigating cell-signalling pathways mediated by

meningococcal interaction with 37 LRP/67 LR. Attempts were made to study the

expression of Gal-3 in response to meningococcal ligands, but time restrictions prevented the further optimisation of qPCR. It would be interesting if future studies considered the examination of the protein levels of receptors in cells challenged with these meningococcal proteins.

The prevention of meningococcal interaction with Gal-3 as the host receptor may help in the prevention or treatment of meningococcal meningitis. The determination of the specific epitope that mediates meningococcal PilE and PilQ binding with Gal-3 will facilitate the synthesis of their corresponding peptides, which could be used to prevent receptor-ligand interaction. In addition, the mutation of amino acids residues within the predicted binding sites of PilQ and PilE provide yet another therapeutic strategy. Note that N. meningitidis PilE is subject to antigenic variation, while PilQ is highly conserved.

One of the goals in the treatment of meningococcal disease is the prevention of the damage caused by the host inflammatory response (Somand & Meurer, 2009): the resulting inflammation from bacterial meningitis is responsible for significant negative outcomes, despite antimicrobial treatment (Somand & Meurer, 2009). Various clinical trials have been conducted, in order to investigate the use of anti-inflammatory drugs such as steroids, particularly dexamethasone, in the treatment of bacterial meningitis. Most of the studies supported the use of dexamethasone, at least in adults. Indeed, reduction in hearing loss, neurological sequelae and mortality have been observed in patients treated with dexamethasone, as an adjunct to antibiotics (van de Beek et al., 2007). Other recent studies conducted in Sub-Saharan Africa, however, revealed that the administration of dexamethasone was not efficacious (Molyneux et al., 2002; Scarborough et al., 2007). These

studies were conducted in areas where there was a high prevalence of HIV and thus it is not clear yet if these studies also apply to developed nations (Somand & Meurer, 2009). In adults, it is recommended that dexamethasone is administered before or concurrent with an initial dose of antibiotics and is continued every 6 hours for 4 days (Fitch & van de Beek, 2007; Tunkel et al., 2004). Given the important role of Gal-3 in inflammation during infection, a recent study has found that the intranasal delivery of a plasmid encoding Gal-3 inhibited chronic airway inflammation and remodelling in the murine model of ovalbumin (OVA)-induced asthma (Lopez et al., 2006). It was also demonstrated how the peribronchial inflammatory cells and bronchoalveolar lavage fluid from OVA-challenged mice expressed significantly higher levels of Gal-3 than control mice (Zuberi et al., 2004): these results may indicate differences in the effects of endogenous versus exogenously delivered Gal-3 (Henderson & Sethi, 2009). In term of meningococcal disease, the intranasal administration of Gal-3 may be used as an adjuvant therapy with antibiotic treatment, in order to provide relief from inflammation and improve treatment outcomes.

In conclusion, Gal3 plays an obvious role in the meningococcal-host cell interaction; however, such interaction is complex and requires careful investigation. In response to bacterial invasion, the host cell expresses Gal3, possibly to limit bacterial adhesion (secreted Gal3), suppress self-damaging, exaggerated inflammatory responses or even to induce host-cell apoptosis. Conversely, the organism may induce the over-expression of Gal3, in order to exploit it for the purpose of enhanced adhesion and invasion and to suppress detrimental pro-inflammatory responses and prolong its own survival. Either way, a better understanding of this interaction will help in the design of novel

preventative and/or therapeutic strategies in the battle against invasive meningococcal disease.

7.2. Future direction

Although this study has identified that PilE and PilQ as non-LOS meningococcal Gal-3 ligands, future experiments should be performed to show their relevance in vivo. A potentially useful approach may be to compare Gal-3 expression in CD46 expressing mice infected with ΔPilQ ΔPilE, and ΔPglLC with those infected with wild type meningococci. Survival and level of bacteremia in those infected mice can be also investigated in future study. Future work should also aim to clarify the mechanism(s) of Gal-3 contribution in meningococcal invasion. This could be investigated by Gal-3 silencing in relevant cell line such as HBMECs, followed by subsequent investigation of meningococcal capacity to adhere or invade these cells. Importantly, future studies should also aim to investigate the relevant of the Gal-3 and 37 LRP dimerization in normal physiological and pathological conditions such as, meningococcal meningitis by using silencing strategy.

8. Chapter 8: Bibliography

8.1. References:

Aas, F. E., Lovold, C. & Koomey, M. (2002). An inhibitor of DNA binding and uptake events dictates the proficiency of genetic transformation in Neisseria gonorrhoeae: mechanism of action and links to Type IV pilus expression. Mol Microbiol **46**, 1441-1450.

Abouseada, N. (2009). Role of 37/67-kDa laminin receptor in binding of bacteria causing meningitis, pp. 252. Nottingham: University of Nottingham.

Agrwal, N., Sun, Q., Wang, S. Y. & Wang, J. L. (1993). Carbohydrate-binding protein 35. I. Properties of the recombinant polypeptide and the individuality of the domains. J Biol Chem **268**, 14932-14939.

Ahmad, N., Gabius, H. J., Andre, S., Kaltner, H., Sabesan, S., Roy, R., Liu, B., Macaluso, F. & Brewer, C. F. (2004). Galectin-3 precipitates as a pentamer with synthetic multivalent carbohydrates and forms heterogeneous cross-linked complexes. J Biol Chem **279**, 10841-10847.

Aho, E. L., Dempsey, J. A., Hobbs, M. M., Klapper, D. G. & Cannon, J. G. (1991). Characterization of the opa (class 5) gene family of Neisseria meningitidis. Mol Microbiol **5**, 1429-1437.

Akache, B., Grimm, D., Pandey, K., Yant, S. R., Xu, H. & Kay, M. A. (2006). The 37/67-Kilodalton Laminin Receptor Is a Receptor for Adeno-Associated Virus Serotypes 8, 2, 3, and 9. J Virol **80**, 9831-9836.

Akahani, S., Nangia-Makker, P., Inohara, H., Kim, H. R. & Raz, A. (1997). Galectin-3: a novel antiapoptotic molecule with a functional BH1 (NWGR) domain of Bcl-2 family. Cancer Res **57**, 5272-5276.

Akira, S., Uematsu, S. & Takeuchi, O. (2006). Pathogen recognition and innate immunity. Cell **124**, 783-801.

Al-Bader T, J. K., Humphries HE, Holloway J, Heckels JE, Semper AE, Friedmann PS, Christodoulides M. (2004). Activation of human dendritic cells by the PorA protein of Neisseria meningitidis. Cellular Microbiology **6**, 651-662.

Ala'Aldeen, D. A. A. a. T., D. P. J. (2006). Neisseria meningitidis. In Principles and practice of clinical bacteriology, pp. 199 - 214. Edited by S. H. a. H. Gillespie, P. M. Chichester: John Wiley and Sons.

Alaimo, C., Catrein, I., Morf, L., Marolda, C. L., Callewaert, N., Valvano, M. A., Feldman, M. F. & Aebi, M. (2006). Two distinct but interchangeable mechanisms for flipping of lipid-linked oligosaccharides. EMBO J **25**, 967-976.

Almkvist, J. & Karlsson, A. (2004). Galectins as inflammatory mediators. Glycoconj J **19**, 575-581.

Altman, E., Harrison, B. A., Latta, R. K., Lee, K. K., Kelly, J. F. & Thibault, P. (2001). Galectin-3-mediated adherence of Proteus mirabilis to Madin-Darby canine kidney cells. Biochem Cell Biol **79**, 783-788.

Anderson, R. G. (1998). The caveolae membrane system. Annu Rev Biochem **67**, 199-225.

Ardini, E., Pesole, G., Tagliabue, E., Magnifico, A., Castronovo, V., Sobel, M. E., Colnaghi, M. I. & Menard, S. (1998). The 67-kDa laminin receptor originated from a ribosomal protein that acquired a dual function during evolution. Mol Biol Evol **15**, 1017-1025.

Arthur, F. E., Shivers, R. R. & Bowman, P. D. (1987). Astrocyte-mediated induction of tight junctions in brain capillary endothelium: an efficient in vitro model. Brain Res **433**, 155-159.

Ashery, U., Yizhar, O., Rotblat, B., Elad-Sfadia, G., Barkan, B., Haklai, R. & Kloog, Y. (2006). Spatiotemporal organization of Ras signaling: rasosomes and the galectin switch. Cell Mol Neurobiol **26**, 471-495.

Baloui, H., von Boxberg, Y., Vinh, J., Weiss, S., Rossier, J., Nothias, F. & Stettler, O. (2004). Cellular prion protein/laminin receptor: distribution in adult central nervous system and characterization of an isoform associated with a subtype of cortical neurons. Eur J Neurosci **20**, 2605-2616.

Banerjee, A. & Ghosh, S. K. (2003). The role of pilin glycan in neisserial pathogenesis. Mol Cell Biochem **253**, 179-190.

Barboni, E., Coade, S. & Fiori, A. (2005). The binding of mycolic acids to galectin-3: a novel interaction between a host soluble lectin and trafficking mycobacterial lipids? FEBS Lett **579**, 6749-6755.

Barboni, E. A., Bawumia, S., Henrick, K. & Hughes, R. C. (2000). Molecular modeling and mutagenesis studies of the N-terminal domains of galectin-3: evidence for participation with the C-terminal carbohydrate recognition domain in oligosaccharide binding. Glycobiology **10**, 1201-1208.

Barondes, S. H., Castronovo, V., Cooper, D. N. & other authors (1994a). Galectins: a family of animal beta-galactoside-binding lectins. Cell **76**, 597-598.

Barondes, S. H., Cooper, D. N., Gitt, M. A. & Leffler, H. (1994b). Galectins. Structure and function of a large family of animal lectins. J Biol Chem **269**, 20807-20810.

Bawumia, S., Barboni, E. A., Menon, R. P. & Hughes, R. C. (2003). Specificity of interactions of galectin-3 with Chrp, a cysteine- and histidine-rich cytoplasmic protein. Biochimie **85**, 189-194.

Beatty, W. L., Rhoades, E. R., Hsu, D. K., Liu, F. T. & Russell, D. G. (2002). Association of a macrophage galactoside-binding protein with Mycobacterium-containing phagosomes. Cell Microbiol **4**, 167-176.

Beddek, A. J., Li, M. S., Kroll, J. S., Jordan, T. W. & Martin, D. R. (2009). Evidence for capsule switching between carried and disease-causing Neisseria meningitidis strains. Infect Immun **77**, 2989-2994.

Bellac, C. L., Coimbra, R. S., Simon, F., Imboden, H. & Leib, S. L. (2007). Gene and protein expression of galectin-3 and galectin-9 in experimental pneumococcal meningitis. Neurobiol Dis **28**, 175-183.

Bentley, S. D., Vernikos, G. S., Snyder, L. A. & other authors (2007). Meningococcal genetic variation mechanisms viewed through comparative analysis of serogroup C strain FAM18. PLoS Genet **3**, e23.

Bilukha, O. O. & Rosenstein, N. (2005). Prevention and control of meningococcal disease. Recommendations of the Advisory Committee on Immunization Practices (ACIP). MMWR Recomm Rep **54**, 1-21.

Bogdan, J. A., Minetti, C. A. & Blake, M. S. (2002). A one-step method for genetic transformation of non-piliated Neisseria meningitidis. J Microbiol Methods **49**, 97-101.

Bondarenko, E. I., Protopopova, E. V., Konovalova, S. N., Sorokin, A. V., Kachko, A. V., Surovtsev, I. V. & Loktev, V. B. (2003). [Laminin-binding protein (LBP) as a cellular receptor for the virus of Venezuelan equine encephalomyelitis (VEE): Part 1. A study of the interaction between VEE virus virions and the human recombinant LBP]. Mol Gen Mikrobiol Virusol, 36-39.

Bourke, T. W., Fairley, D. J. & Shields, M. D. (2010). Rapid diagnosis of meningococcal disease. Expert Rev Anti Infect Ther **8**, 1321-1323.

Bradley, C. J., Griffiths, N. J., Rowe, H. A., Heyderman, R. S. & Virji, M. (2005). Critical determinants of the interactions of capsule-expressing Neisseria meningitidis with host cells: the role of receptor density in increased cellular targeting via the outer membrane Opa proteins. Cell Microbiol **7**, 1490-1503.

Brandtzaeg, P., Kierulf, P., Gaustad, P., Skulberg, A., Bruun, J. N., Halvorsen, S. & Sorensen, E. (1989). Plasma endotoxin as a predictor of multiple organ failure and death in systemic meningococcal disease. J Infect Dis **159**, 195-204.

Brandtzaeg, P., Halstensen, A., Kierulf, P., Espevik, T. & Waage, A. (1992a). Molecular mechanisms in the compartmentalized inflammatory response presenting as meningococcal meningitis or septic shock. Microb Pathog **13**, 423-431.

Brandtzaeg, P., Ovsteboo, R. & Kierulf, P. (1992b). Compartmentalization of lipopolysaccharide production correlates with clinical presentation in meningococcal disease. J Infect Dis **166**, 650-652.

Brandtzaeg, P., Bjerre, A., Ovstebo, R., Brusletto, B., Joo, G. B. & Kierulf, P. (2001). Neisseria meningitidis lipopolysaccharides in human pathology. J Endotoxin Res **7**, 401-420.

Braun, J. M., Blackwell, C. C., Poxton, I. R., El Ahmer, O., Gordon, A. E., Madani, O. M., Weir, D. M., Giersen, S. & Beuth, J. (2002). Proinflammatory responses to lipo-oligosaccharide of Neisseria meningitidis immunotype strains in relation to virulence and disease. J Infect Dis **185**, 1431-1438.

Brehony, C., Jolley, K. A. & Maiden, M. C. (2007). Multilocus sequence typing for global surveillance of meningococcal disease. FEMS Microbiol Rev **31**, 15-26.

Brouwer, M. C., Read, R. C. & van de Beek, D. (2010). Host genetics and outcome in meningococcal disease: a systematic review and meta-analysis. Lancet Infect Dis **10**, 262-274.

Buto, S., Tagliabue, E., Ardini, E. & other authors (1998). Formation of the 67-kDa laminin receptor by acylation of the precursor. J Cell Biochem **69**, 244-251.

Capecchi, B., Adu-Bobie, J., Di Marcello, F., Ciucchi, L., Masignani, V., Taddei, A., Rappuoli, R., Pizza, M. & Arico, B. (2005). Neisseria meningitidis NadA is a new invasin which promotes bacterial adhesion to and penetration into human epithelial cells. Mol Microbiol **55**, 687-698.

Carbonnelle, E., Helaine, S., Nassif, X. & Pelicic, V. (2006). A systematic genetic analysis in Neisseria meningitidis defines the Pil proteins required for assembly, functionality, stabilization and export of type IV pili. Mol Microbiol **61**, 1510-1522.

Carbonnelle, E., Hill, D. J., Morand, P., Griffiths, N. J., Bourdoulous, S., Murillo, I., Nassif, X. & Virji, M. (2009). Meningococcal interactions with the host. Vaccine **27 Suppl 2**, B78-89.

Carrol, E. D., Thomson, A. P., Shears, P., Gray, S. J., Kaczmarski, E. B. & Hart, C. A. (2000). Performance characteristics of the polymerase chain reaction assay to confirm clinical meningococcal disease. Arch Dis Child **83**, 271-273.

Cartwright, K. A. & Ala'Aldeen, D. A. (1997). Neisseria meningitidis: clinical aspects. J Infect **34**, 15-19.

Castronovo, V., Claysmith, A. P., Barker, K. T., Cioce, V., Krutzsch, H. C. & Sobel, M. E. (1991a). Biosynthesis of the 67 kDa high affinity laminin receptor. Biochem Biophys Res Commun **177**, 177-183.

Castronovo, V., Taraboletti, G. & Sobel, M. E. (1991b). Functional domains of the 67-kDa laminin receptor precursor. J Biol Chem **266**, 20440-20446.

Castronovo, V., Luyten, F., van den Brule, F. & Sobel, M. E. (1992). Identification of a 14-kDa laminin binding protein (HLBP14) in human melanoma cells that is identical to the 14-kDa galactoside binding lectin. Arch Biochem Biophys **297**, 132-138.

Castronovo, V. (1993). Laminin receptors and laminin-binding proteins during tumor invasion and metastasis. Invasion Metastasis **13**, 1-30.

CDC (2009). Centers for Disease Control and Prevention. Active bacterial core surveillance
(ABCs): surveillance reports Neisseria meningitidis.

Cehovin, A., Winterbotham, M., Lucidarme, J., Borrow, R., Tang, C. M., Exley, R. M. & Pelicic, V. (2010). Sequence conservation of pilus subunits in Neisseria meningitidis. Vaccine **28**, 4817-4826.

Cerliani, J. P., Stowell, S. R., Mascanfroni, I. D., Arthur, C. M., Cummings, R. D. & Rabinovich, G. A. (2011). Expanding the universe of cytokines and pattern recognition receptors: galectins and glycans in innate immunity. J Clin Immunol **31**, 10-21.

Cerra, R. F., Gitt, M. A. & Barondes, S. H. (1985). Three soluble rat beta-galactoside-binding lectins. J Biol Chem **260**, 10474-10477.

Chamot-Rooke, J., Rousseau, B., Lanternier, F. & other authors (2007). Alternative Neisseria spp. type IV pilin glycosylation with a glyceramido acetamido trideoxyhexose residue. Proc Natl Acad Sci U S A **104**, 14783-14788.

Chamot-Rooke, J., Mikaty, G., Malosse, C. & other authors (2011). Posttranslational modification of pili upon cell contact triggers N. meningitidis dissemination. Science **331**, 778-782.

Chaudhuri, A., Martinez-Martin, P., Kennedy, P. G., Andrew Seaton, R., Portegies, P., Bojar, M. & Steiner, I. (2008). EFNS guideline on the management of community-acquired bacterial meningitis: report of an EFNS Task Force on acute bacterial meningitis in older children and adults. Eur J Neurol **15**, 649-659.

Chauhan, V. S., Sterka, D. G., Jr., Gray, D. L., Bost, K. L. & Marriott, I. (2008). Neurogenic Exacerbation of Microglial and Astrocyte Responses to Neisseria meningitidis and Borrelia burgdorferi. J Immunol **180**, 8241-8249.

Chow, J. C., Young, D. W., Golenbock, D. T., Christ, W. J. & Gusovsky, F. (1999). Toll-like receptor-4 mediates lipopolysaccharide-induced signal transduction. J Biol Chem **274**, 10689-10692.

Chung, J. W., Hong, S. J., Kim, K. J., Goti, D., Stins, M. F., Shin, S., Dawson, V. L., Dawson, T. M. & Kim, K. S. (2003). 37-kDa Laminin Receptor Precursor Modulates Cytotoxic Necrotizing Factor 1-mediated RhoA Activation and Bacterial Uptake. J Biol Chem **278**, 16857-16862.

Coimbra, R. S., Voisin, V., de Saizieu, A. B., Lindberg, R. L., Wittwer, M., Leppert, D. & Leib, S. L. (2006). Gene expression in cortex and hippocampus during acute pneumococcal meningitis. BMC Biol **4**, 15.

Collins, R. F., Frye, S. A., Kitmitto, A., Ford, R. C., Tonjum, T. & Derrick, J. P. (2004). Structure of the Neisseria meningitidis outer membrane PilQ secretin complex at 12 A resolution. J Biol Chem **279**, 39750-39756.

Comanducci, M., Bambini, S., Caugant, D. A., Mora, M., Brunelli, B., Capecchi, B., Ciucchi, L., Rappuoli, R. & Pizza, M. (2004). NadA diversity and carriage in Neisseria meningitidis. Infect Immun **72**, 4217-4223.

Cooper, D. N. (2002). Galectinomics: finding themes in complexity. Biochim Biophys Acta **1572**, 209-231.

Corbett MJ, B. J., Wilde CE. (1988). Antibodies to outer-membrane protein–macromolecular complex (OMP-MC) are bactericidal for serum-resistant gonococci. In In Gonococci and Meningococci, pp. pp. 685–691. Edited by H. C. Z. Edited by J. T. Poolmann, T. F. Meyer, J. E. Heckel, P. R. H. Makela, H. Smith & E. C. Beuvery. : Dordrecht, The Netherlands: Kluwer.

Coureuil, M., Mikaty, G., Miller, F. & other authors (2009). Meningococcal type IV pili recruit the polarity complex to cross the brain endothelium. Science **325**, 83-87.

Coureuil, M., Lecuyer, H., Scott, M. G. & other authors (2010). Meningococcus Hijacks a beta2-adrenoceptor/beta-Arrestin pathway to cross brain microvasculature endothelium. Cell **143**, 1149-1160.

Coureuil, M., Join-Lambert, O., Lecuyer, H., Bourdoulous, S., Marullo, S. & Nassif, X. (2012). Mechanism of meningeal invasion by Neisseria meningitidis. Virulence **3**, 164-172.

Cowles, E. A., Agrwal, N., Anderson, R. L. & Wang, J. L. (1990). Carbohydrate-binding protein 35. Isoelectric points of the polypeptide and a phosphorylated derivative. J Biol Chem **265**, 17706-17712.

Craig, L., Volkmann, N., Arvai, A. S., Pique, M. E., Yeager, M., Egelman, E. H. & Tainer, J. A. (2006). Type IV pilus structure by cryo-electron microscopy and crystallography: implications for pilus assembly and functions. Mol Cell **23**, 651-662.

Craig, L. & Li, J. (2008). Type IV pili: paradoxes in form and function. Curr Opin Struct Biol **18**, 267-277.

Crocker, P. R. & Redelinghuys, P. (2008). Siglecs as positive and negative regulators of the immune system. Biochem Soc Trans **36**, 1467-1471.

D. Halliwell, S. A. F., S. Taylor, A. Flockhart, M. Finney and K. Reddin, et al. (2004). Immunisation with the meningococcal PilQ complex is protective in a mouse model of meningococcal disease and elicits bactericidal and opsonic antibodies In 14th international pathogenic Neisseria conference pp. p. 161. Milwaukee, Wisconsin, USA,.

Dagher, S. F., Wang, J. L. & Patterson, R. J. (1995). Identification of galectin-3 as a factor in pre-mRNA splicing. Proc Natl Acad Sci U S A **92**, 1213-1217.

Darton, T., Guiver, M., Naylor, S., Jack, D. L., Kaczmarski, E. B., Borrow, R. & Read, R. C. (2009). Severity of meningococcal disease associated with genomic bacterial load. Clin Infect Dis **48**, 587-594.

Dawson, K. G., Emerson, J. C. & Burns, J. L. (1999). Fifteen years of experience with bacterial meningitis. The Pediatric Infectious Disease Journal **18**, 816-822.

De Giusti, C. J., Alberdi, L., Frik, J., Ferrer, M. F., Scharrig, E., Schattner, M. & Gomez, R. M. (2011). Galectin-3 is upregulated in activated glia during Junin virus-induced murine encephalitis. Neurosci Lett **501**, 163-166.

de Souza, A. L. & Seguro, A. C. (2008). Two centuries of meningococcal infection: from Vieusseux to the cellular and molecular basis of disease. J Med Microbiol **57**, 1313-1321.

Debierre-Grockiego, F., Niehus, S., Coddeville, B. & other authors (2010). Binding of Toxoplasma gondii glycosylphosphatidylinositols to galectin-3 is required for their recognition by macrophages. J Biol Chem **285**, 32744-32750.

Deghmane, A. E., Giorgini, D., Larribe, M., Alonso, J. M. & Taha, M. K. (2002). Down-regulation of pili and capsule of Neisseria meningitidis upon contact with epithelial cells is mediated by CrgA regulatory protein. Mol Microbiol **43**, 1555-1564.

Delacour, D., Greb, C., Koch, A., Salomonsson, E., Leffler, H., Le Bivic, A. & Jacob, R. (2007). Apical sorting by galectin-3-dependent glycoprotein clustering. Traffic **8**, 379-388.

Derrick, J. P., Urwin, R., Suker, J., Feavers, I. M. & Maiden, M. C. (1999). Structural and evolutionary inference from molecular variation in Neisseria porins. Infect Immun **67**, 2406-2413.

Devoe, I. W. & Gilchrist, J. E. (1973). Release of endotoxin in the form of cell wall blebs during in vitro growth of Neisseria meningitidis. J Exp Med **138**, 1156-1167.

Diaz Romero, J. & Outschoorn, I. M. (1994). Current status of meningococcal group B vaccine candidates: capsular or noncapsular? Clin Microbiol Rev **7**, 559-575.

Doulet, N., Donnadieu, E., Laran-Chich, M. P., Niedergang, F., Nassif, X., Couraud, P. O. & Bourdoulous, S. (2006). Neisseria meningitidis infection of human endothelial cells interferes with leukocyte transmigration by preventing the formation of endothelial docking structures. J Cell Biol **173**, 627-637.

Drake, S. L. & Koomey, M. (1995). The product of the pilQ gene is essential for the biogenesis of type IV pili in Neisseria gonorrhoeae. Mol Microbiol **18**, 975-986.

Duenas S, Pajon R, Delgado M, Nogueiras E, A, M. & . (1998). Electroporation of Neisseria meningitidis with plasmid DNA. Biotecnol Aplicada **15**, 247-249.

Dumic, J., Dabelic, S. & Flogel, M. (2006). Galectin-3: an open-ended story. Biochim Biophys Acta **1760**, 616-635.

Dunn, K. L., Virji, M. & Moxon, E. R. (1995). Investigations into the molecular basis of meningococcal toxicity for human endothelial and epithelial cells: the synergistic effect of LPS and pili. Microb Pathog **18**, 81-96.

Elad-Sfadia, G., Haklai, R., Balan, E. & Kloog, Y. (2004). Galectin-3 augments K-Ras activation and triggers a Ras signal that attenuates ERK but not phosphoinositide 3-kinase activity. J Biol Chem **279**, 34922-34930.

Estabrook, M. M., Griffiss, J. M. & Jarvis, G. A. (1997). Sialylation of Neisseria meningitidis lipooligosaccharide inhibits serum bactericidal activity by masking lacto-N-neotetraose. Infect Immun **65**, 4436-4444.

Estabrook, M. M., Jack, D. L., Klein, N. J. & Jarvis, G. A. (2004). Mannose-binding lectin binds to two major outer membrane proteins, opacity protein and porin, of Neisseria meningitidis. J Immunol **172**, 3784-3792.

Esteban, A., Popp, M. W., Vyas, V. K., Strijbis, K., Ploegh, H. L. & Fink, G. R. (2011). Fungal recognition is mediated by the association of dectin-1 and galectin-3 in macrophages. Proc Natl Acad Sci U S A **108**, 14270-14275.

Eugene, E., Hoffmann, I., Pujol, C., Couraud, P. O., Bourdoulous, S. & Nassif, X. (2002). Microvilli-like structures are associated with the internalization of virulent capsulated Neisseria meningitidis into vascular endothelial cells. J Cell Sci **115**, 1231-1241.

Farnworth, S. L., Henderson, N. C., Mackinnon, A. C. & other authors (2008). Galectin-3 reduces the severity of pneumococcal pneumonia by augmenting neutrophil function. Am J Pathol **172**, 395-405.

Feavers, I. M. & Maiden, M. C. (1998). A gonococcal porA pseudogene: implications for understanding the evolution and pathogenicity of Neisseria gonorrhoeae. Mol Microbiol **30**, 647-656.

Fitch, M. T. & van de Beek, D. (2007). Emergency diagnosis and treatment of adult meningitis. Lancet Infect Dis **7**, 191-200.

Foster, L. J., De Hoog, C. L. & Mann, M. (2003). Unbiased quantitative proteomics of lipid rafts reveals high specificity for signaling factors. Proc Natl Acad Sci U S A **100**, 5813-5818.

Fowler, M., Thomas, R. J., Atherton, J., Roberts, I. S. & High, N. J. (2006). Galectin-3 binds to Helicobacter pylori O-antigen: it is upregulated and rapidly secreted by gastric epithelial cells in response to H. pylori adhesion. Cell Microbiol **8**, 44-54.

Fradin, C., Jouault, T., Mallet, A., Mallet, J. M., Camus, D., Sinay, P. & Poulain, D. (1996). Beta-1,2-linked oligomannosides inhibit Candida albicans binding to murine macrophage. J Leukoc Biol **60**, 81-87.

Franzoso, S., Mazzon, C., Sztukowska, M., Cecchini, P., Kasic, T., Capecchi, B., Tavano, R. & Papini, E. (2008). Human monocytes/macrophages are a target of Neisseria meningitidis Adhesin A (NadA). J Leukoc Biol **83**, 1100-1110.

Frasch, C. E., Zollinger, W. D. & Poolman, J. T. (1985). Serotype antigens of Neisseria meningitidis and a proposed scheme for designation of serotypes. Rev Infect Dis **7**, 504-510.

Fredriksen, J. H., Rosenqvist, E., Wedege, E. & other authors (1991). Production, characterization and control of MenB-vaccine "Folkehelsa": an outer membrane vesicle vaccine against group B meningococcal disease. NIPH Ann **14**, 67-79; discussion 79-80.

Frosch, M., Weisgerber, C. & Meyer, T. F. (1989). Molecular characterization and expression in Escherichia coli of the gene complex encoding the polysaccharide capsule of Neisseria meningitidis group B. Proc Natl Acad Sci U S A **86**, 1669-1673.

Frye, S. A., Assalkhou, R., Collins, R. F., Ford, R. C., Petersson, C., Derrick, J. P. & Tonjum, T. (2006). Topology of the outer-membrane secretin PilQ from Neisseria meningitidis. Microbiology **152**, 3751-3764.

Fujimura, Y., Yamada, K. & Tachibana, H. (2005). A lipid raft-associated 67 kDa laminin receptor mediates suppressive effect of epigallocatechin-3-O-gallate on Fc[epsilon]RI expression. Biochemical and Biophysical Research Communications **336**, 674-681.

Fujimura, Y., Sumida, M., Sugihara, K., Tsukamoto, S., Yamada, K. & Tachibana, H. (2012). Green tea polyphenol EGCG sensing motif on the 67-kDa laminin receptor. PLoS One **7**, e37942.

Fukumori, T., Takenaka, Y., Yoshii, T., Kim, H. R., Hogan, V., Inohara, H., Kagawa, S. & Raz, A. (2003). CD29 and CD7 mediate galectin-3-induced type II T-cell apoptosis. Cancer Res **63**, 8302-8311.

Fukumori, T., Takenaka, Y., Oka, N., Yoshii, T., Hogan, V., Inohara, H., Kanayama, H. O., Kim, H. R. & Raz, A. (2004). Endogenous galectin-3 determines the routing of CD95 apoptotic signaling pathways. Cancer Res **64**, 3376-3379.

Fukushi, J., Makagiansar, I. T. & Stallcup, W. B. (2004). NG2 proteoglycan promotes endothelial cell motility and angiogenesis via engagement of galectin-3 and alpha3beta1 integrin. Mol Biol Cell **15**, 3580-3590.

Gardner, P. (2006). Clinical practice. Prevention of meningococcal disease. N Engl J Med **355**, 1466-1473.

Gasparini, R. & Panatto, D. (2011). Meningococcal glycoconjugate vaccines. Hum Vaccin **7**, 170-182.

Gauczynski, S., Peyrin, J. M., Haik, S. & other authors (2001). The 37-kDa/67-kDa laminin receptor acts as the cell-surface receptor for the cellular prion protein. EMBO J **20**, 5863-5875.

Gauczynski, S., Nikles, D., El-Gogo, S., Papy-Garcia, D., Rey, C., Alban, S., Barritault, D., Lasmezas, C. I. & Weiss, S. (2006). The 37-kDa/67-kDa laminin receptor acts as a receptor for infectious prions and is inhibited by polysulfated glycanes. J Infect Dis **194**, 702-709.

Genin, S. & Boucher, C. A. (1994). A superfamily of proteins involved in different secretion pathways in gram-negative bacteria: modular structure and specificity of the N-terminal domain. Mol Gen Genet **243**, 112-118.

Gilbert, M., Watson, D. C., Cunningham, A. M., Jennings, M. P., Young, N. M. & Wakarchuk, W. W. (1996). Cloning of the lipooligosaccharide alpha-2,3-sialyltransferase from the bacterial pathogens Neisseria meningitidis and Neisseria gonorrhoeae. J Biol Chem **271**, 28271-28276.

Girard, M. P., Preziosi, M.-P., Aguado, M.-T. & Kieny, M. P. (2006). A review of vaccine research and development: Meningococcal disease. Vaccine **24**, 4692-4700.

Giuliani, M. M., Adu-Bobie, J., Comanducci, M. & other authors (2006). A universal vaccine for serogroup B meningococcus. Proc Natl Acad Sci U S A **103**, 10834-10839.

Gold, R., Lepow, M. L., Goldschneider, I. & Gotschlich, E. C. (1977). Immune Response of human infants of polysaccharide vaccines of group A and C Neisseria meningitidis. J Infect Dis **136 Suppl**, S31-35.

Gong, H. C., Honjo, Y., Nangia-Makker, P., Hogan, V., Mazurak, N., Bresalier, R. S. & Raz, A. (1999). The NH2 terminus of galectin-3 governs cellular compartmentalization and functions in cancer cells. Cancer Res **59**, 6239-6245.

Gotschlich, E. C., Goldschneider, I. & Artenstein, M. S. (1969). Human immunity to the meningococcus. IV. Immunogenicity of group A and group C meningococcal polysaccharides in human volunteers. J Exp Med **129**, 1367-1384.

Granoff MD, H. L., Borrow R. (2008). Meningococcal Vaccines. In Vaccines, pp. 399-434. Edited by O. W. Plotkin SA, Offit PA, Eds. Philadelphia: Saunders

Greco, C., Vona, R., Cosimelli, M. & other authors (2004). Cell surface overexpression of galectin-3 and the presence of its ligand 90k in the blood plasma as determinants in colon neoplastic lesions. Glycobiology **14**, 783-792.

Griffiths, N. J., Bradley, C. J., Heyderman, R. S. & Virji, M. (2007). IFN-gamma amplifies NFkappaB-dependent Neisseria meningitidis invasion of epithelial cells via specific upregulation of CEA-related cell adhesion molecule 1. Cell Microbiol **9**, 2968-2983.

Grimwood, K., Anderson, P., Anderson, V., Tan, L. & Nolan, T. (2000). Twelve year outcomes following bacterial meningitis: further evidence for persisting effects. Arch Dis Child **83**, 111-116.

Gupta, S. K., Masinick, S., Garrett, M. & Hazlett, L. D. (1997). Pseudomonas aeruginosa lipopolysaccharide binds galectin-3 and other human corneal epithelial proteins. Infect Immun **65**, 2747-2753.

Haghi, F., Peerayeh, S. N., Siadat, S. D. & Zeighami, H. (2012). Recombinant outer membrane secretin PilQ(406-770) as a vaccine candidate for serogroup B Neisseria meningitidis. Vaccine **30**, 1710-1714.

Hamadeh, R. M., Estabrook, M. M., Zhou, P., Jarvis, G. A. & Griffiss, J. M. (1995). Anti-Gal binds to pili of Neisseria meningitidis: the immunoglobulin A isotype blocks complement-mediated killing. Infect Immun **63**, 4900-4906.

Hammerschmidt, S., Muller, A., Sillmann, H. & other authors (1996). Capsule phase variation in Neisseria meningitidis serogroup B by slipped-strand mispairing in the polysialyltransferase gene (siaD): correlation with bacterial invasion and the outbreak of meningococcal disease. Mol Microbiol **20**, 1211-1220.

Hansen, M. V. & Wilde, C. E., 3rd (1984). Conservation of peptide structure of outer membrane protein-macromolecular complex from Neisseria gonorrhoeae. Infect Immun **43**, 839-845.

Harrison, L. H., Trotter, C. L. & Ramsay, M. E. (2009). Global epidemiology of meningococcal disease. Vaccine **27 Suppl 2**, B51-63.

Hart, C. A. & Thomson, A. P. (2006). Meningococcal disease and its management in children. BMJ **333**, 685-690.

Hegge, F. T., Hitchen, P. G., Aas, F. E. & other authors (2004). Unique modifications with phosphocholine and phosphoethanolamine define alternate antigenic forms of Neisseria gonorrhoeae type IV pili. Proc Natl Acad Sci U S A **101**, 10798-10803.

Helaine, S., Carbonnelle, E., Prouvensier, L., Beretti, J. L., Nassif, X. & Pelicic, V. (2005). PilX, a pilus-associated protein essential for bacterial aggregation, is a key to pilus-facilitated attachment of Neisseria meningitidis to human cells. Mol Microbiol **55**, 65-77.

Henderson, N. C. & Sethi, T. (2009). The regulation of inflammation by galectin-3. Immunol Rev **230**, 160-171.

Herrmann, J., Turck, C. W., Atchison, R. E., Huflejt, M. E., Poulter, L., Gitt, M. A., Burlingame, A. L., Barondes, S. H. & Leffler, H. (1993). Primary structure of the soluble lactose binding lectin L-29 from rat and dog and interaction of its non-collagenous proline-, glycine-, tyrosine-rich sequence with bacterial and tissue collagenase. J Biol Chem **268**, 26704-26711.

Hill, D. J., Griffiths, N. J., Borodina, E. & Virji, M. (2010). Cellular and molecular biology of Neisseria meningitidis colonization and invasive disease. Clin Sci (Lond) **118**, 547-564.

Ho, M. K. & Springer, T. A. (1982). Mac-2, a novel 32,000 Mr mouse macrophage subpopulation-specific antigen defined by monoclonal antibodies. J Immunol **128**, 1221-1228.

Hoffmann, I., Eugene, E., Nassif, X., Couraud, P. O. & Bourdoulous, S. (2001). Activation of ErbB2 receptor tyrosine kinase supports invasion of endothelial cells by Neisseria meningitidis. J Cell Biol **155**, 133-143.

Holst, J., Martin, D., Arnold, R., Huergo, C. C., Oster, P., O'Hallahan, J. & Rosenqvist, E. (2009). Properties and clinical performance of vaccines containing outer membrane vesicles from Neisseria meningitidis. Vaccine **27 Suppl 2**, B3-12.

Hsu, D. K., Chernyavsky, A. I., Chen, H. Y., Yu, L., Grando, S. A. & Liu, F. T. (2009). Endogenous galectin-3 is localized in membrane lipid rafts and regulates migration of dendritic cells. J Invest Dermatol **129**, 573-583.

Hu, C. D., Chinenov, Y. & Kerppola, T. K. (2002). Visualization of interactions among bZIP and Rel family proteins in living cells using bimolecular fluorescence complementation. Mol Cell **9**, 789-798.

Huflejt, M. E., Turck, C. W., Lindstedt, R., Barondes, S. H. & Leffler, H. (1993). L-29, a soluble lactose-binding lectin, is phosphorylated on serine 6 and serine 12 in vivo and by casein kinase I. J Biol Chem **268**, 26712-26718.

Hug, I. & Feldman, M. F. (2011). Analogies and homologies in lipopolysaccharide and glycoprotein biosynthesis in bacteria. Glycobiology **21**, 138-151.

Hughes, R. C. (1999). Secretion of the galectin family of mammalian carbohydrate-binding proteins. Biochim Biophys Acta **1473**, 172-185.

Inohara, H., Akahani, S., Koths, K. & Raz, A. (1996). Interactions between galectin-3 and Mac-2-binding protein mediate cell-cell adhesion. Cancer Res **56**, 4530-4534.

Jamieson, K. V., Wu, J., Hubbard, S. R. & Meruelo, D. (2008). Crystal structure of the human laminin receptor precursor. J Biol Chem **283**, 3002-3005.

Jan T. Poolman, P. D., Christiane Feron, Karine Goraj, Vincent Weynants (2006). Outer membrane vesicle-based meningococcal vaccines. In Handbook of meningococcal disease, pp. 371–390. Edited by M. C. J. M. Matthias Frosch: Weinheim:Wiley-VCH.

Jarva, H., Ram, S., Vogel, U., Blom, A. M. & Meri, S. (2005). Binding of the complement inhibitor C4bp to serogroup B Neisseria meningitidis. J Immunol **174**, 6299-6307.

Jennings, M. P., Hood, D. W., Peak, I. R., Virji, M. & Moxon, E. R. (1995). Molecular analysis of a locus for the biosynthesis and phase-variable expression of the lacto-N-neotetraose terminal lipopolysaccharide structure in Neisseria meningitidis. Mol Microbiol **18**, 729-740.

Jennings, M. P., Srikhanta, Y. N., Moxon, E. R., Kramer, M., Poolman, J. T., Kuipers, B. & van der Ley, P. (1999). The genetic basis of the phase variation repertoire of lipopolysaccharide immunotypes in Neisseria meningitidis. Microbiology **145 (Pt 11)**, 3013-3021.

Jennings, M. P., Jen, F. E., Roddam, L. F., Apicella, M. A. & Edwards, J. L. (2011). Neisseria gonorrhoeae pilin glycan contributes to CR3 activation during challenge of primary cervical epithelial cells. Cell Microbiol **13**, 885-896.

Jeon, S. B., Yoon, H. J., Chang, C. Y., Koh, H. S., Jeon, S. H. & Park, E. J. (2010). Galectin-3 exerts cytokine-like regulatory actions through the JAK-STAT pathway. J Immunol **185**, 7037-7046.

Johansson, L., Rytkonen, A., Bergman, P., Albiger, B., Kallstrom, H., Hokfelt, T., Agerberth, B., Cattaneo, R. & Jonsson, A. B. (2003). CD46 in meningococcal disease. Science **301**, 373-375.

Johansson, L., Rytkonen, A., Wan, H., Bergman, P., Plant, L., Agerberth, B., Hokfelt, T. & Jonsson, A. B. (2005). Human-like immune responses in CD46 transgenic mice. J Immunol **175**, 433-440.

John, C. M., Jarvis, G. A., Swanson, K. V., Leffler, H., Cooper, M. D., Huflejt, M. E. & Griffiss, J. M. (2002). Galectin-3 binds lactosaminylated lipooligosaccharides from Neisseria gonorrhoeae and is selectively expressed by mucosal epithelial cells that are infected. Cell Microbiol **4**, 649-662.

Join-Lambert, O., Morand, P. C., Carbonnelle, E., Coureuil, M., Bille, E., Bourdoulous, S. & Nassif, X. (2010). Mechanisms of meningeal invasion by a bacterial extracellular pathogen, the example of Neisseria meningitidis. Prog Neurobiol **91**, 130-139.

Jonsson, A. B., Rahman, M. & Normark, S. (1995). Pilus biogenesis gene, pilC, of Neisseria gonorrhoeae: pilC1 and pilC2 are each part of a larger duplication of the gonococcal genome and share upstream and downstream homologous sequences with opa and pil loci. Microbiology **141 (Pt 10)**, 2367-2377.

Jouault, T., El Abed-El Behi, M., Martinez-Esparza, M., Breuilh, L., Trinel, P. A., Chamaillard, M., Trottein, F. & Poulain, D. (2006). Specific recognition of Candida albicans by macrophages requires galectin-3 to discriminate Saccharomyces cerevisiae and needs association with TLR2 for signaling. J Immunol **177**, 4679-4687.

Kahler, C. M. & Stephens, D. S. (1998). Genetic basis for biosynthesis, structure, and function of meningococcal lipooligosaccharide (endotoxin). Crit Rev Microbiol **24**, 281-334.

Kahler, C. M., Martin, L. E., Tzeng, Y. L., Miller, Y. K., Sharkey, K., Stephens, D. S. & Davies, J. K. (2001). Polymorphisms in pilin glycosylation Locus of Neisseria meningitidis expressing class II pili. Infect Immun **69**, 3597-3604.

Kallstrom, H., Liszewski, M. K., Atkinson, J. P. & Jonsson, A. B. (1997). Membrane cofactor protein (MCP or CD46) is a cellular pilus receptor for pathogenic Neisseria. Mol Microbiol **25**, 639-647.

Kallstrom, H., Islam, M. S., Berggren, P. O. & Jonsson, A. B. (1998). Cell signaling by the type IV pili of pathogenic Neisseria. J Biol Chem **273**, 21777-21782.

Kellogg, D. S., Jr., Cohen, I. R., Norins, L. C., Schroeter, A. L. & Reising, G. (1968). Neisseria gonorrhoeae. II. Colonial variation and pathogenicity during 35 months in vitro. J Bacteriol **96**, 596-605.

Kerppola, T. K. (2006). Visualization of molecular interactions by fluorescence complementation. Nat Rev Mol Cell Biol **7**, 449-456.

Kerppola, T. K. (2008). Bimolecular fluorescence complementation: visualization of molecular interactions in living cells. Methods Cell Biol **85**, 431-470.

Kilpatrick, L. E., Briddon, S. J., Hill, S. J. & Holliday, N. D. (2010). Quantitative analysis of neuropeptide Y receptor association with -arrestin2 measured by bimolecular fluorescence complementation. British Journal of Pharmacology **160**, 892-906.

Kim, K. J., Chung, J. W. & Kim, K. S. (2005). 67-kDa laminin receptor promotes internalization of cytotoxic necrotizing factor 1-expressing Escherichia coli K1 into human brain microvascular endothelial cells. J Biol Chem **280**, 1360-1368.

Kim, K. S. (2006). Microbial translocation of the blood-brain barrier. Int J Parasitol **36**, 607-614.

Kim, K. S. (2008). Mechanisms of microbial traversal of the blood-brain barrier. Nat Rev Micro **6**, 625-634.

Kinoshita, K., Kaneda, Y., Sato, M., Saeki, Y., Wataya-Kaneda, M. & Hoffmann, A. (1998). LBP-p40 binds DNA tightly through associations with histones H2A, H2B, and H4. Biochem Biophys Res Commun **253**, 277-282.

Kirchner, M., Heuer, D. & Meyer, T. F. (2005). CD46-independent binding of neisserial type IV pili and the major pilus adhesin, PilC, to human epithelial cells. Infect Immun **73**, 3072-3082.

Kirsch, E. A., Barton, R. P., Kitchen, L. & Giroir, B. P. (1996). Pathophysiology, treatment and outcome of meningococcemia: a review and recent experience. Pediatr Infect Dis J **15**, 967-978; quiz 979.

Kleshchenko, Y. Y., Moody, T. N., Furtak, V. A., Ochieng, J., Lima, M. F. & Villalta, F. (2004). Human galectin-3 promotes Trypanosoma cruzi adhesion to human coronary artery smooth muscle cells. Infect Immun **72**, 6717-6721.

Kohatsu, L., Hsu, D. K., Jegalian, A. G., Liu, F. T. & Baum, L. G. (2006). Galectin-3 induces death of Candida species expressing specific beta-1,2-linked mannans. J Immunol **177**, 4718-4726.

Koomey, M. (1995). Prepilin-like molecules in type 4 pilus biogenesis: minor subunits, chaperones or mediators of organelle translocation? Trends Microbiol **3**, 409-410; discussion 411-403.

Kowarik, M., Young, N. M., Numao, S. & other authors (2006). Definition of the bacterial N-glycosylation site consensus sequence. EMBO J **25**, 1957-1966.

Ku, S. C., Schulz, B. L., Power, P. M. & Jennings, M. P. (2009). The pilin O-glycosylation pathway of pathogenic Neisseria is a general system that glycosylates AniA, an outer membrane nitrite reductase. Biochem Biophys Res Commun **378**, 84-89.

Lambotin, M., Hoffmann, I., Laran-Chich, M. P., Nassif, X., Couraud, P. O. & Bourdoulous, S. (2005). Invasion of endothelial cells by Neisseria

meningitidis requires cortactin recruitment by a phosphoinositide-3-kinase/Rac1 signalling pathway triggered by the lipo-oligosaccharide. J Cell Sci **118**, 3805-3816.

Landowski, T. H., Dratz, E. A. & Starkey, J. R. (1995). Studies of the structure of the metastasis-associated 67 kDa laminin binding protein: fatty acid acylation and evidence supporting dimerization of the 32 kDa gene product to form the mature protein. Biochemistry **34**, 11276-11287.

Lecuyer, H., Nassif, X. & Coureuil, M. (2012). Two strikingly different signaling pathways are induced by meningococcal type IV pili on endothelial and epithelial cells. Infect Immun **80**, 175-186.

Lee, M. Y., Park, E. G., Choi, J. Y., Cheong, H. S., Chung, D. R., Peck, K. R., Song, J. H. & Ko, K. S. (2010). 'Neisseria skkuensis' sp. nov., isolated from the blood of a diabetic patient with a foot ulcer. J Med Microbiol **59**, 856-859.

Leffler, H., Carlsson, S., Hedlund, M., Qian, Y. & Poirier, F. (2004). Introduction to galectins. Glycoconj J **19**, 433-440.

Lesot, H., Kuhl, U. & Mark, K. (1983). Isolation of a laminin-binding protein from muscle cell membranes. EMBO J **2**, 861-865.

Li, Y., Komai-Koma, M., Gilchrist, D. S., Hsu, D. K., Liu, F. T., Springall, T. & Xu, D. (2008). Galectin-3 is a negative regulator of lipopolysaccharide-mediated inflammation. J Immunol **181**, 2781-2789.

Lin, H. M., Pestell, R. G., Raz, A. & Kim, H. R. (2002). Galectin-3 enhances cyclin D(1) promoter activity through SP1 and a cAMP-responsive element in human breast epithelial cells. Oncogene **21**, 8001-8010.

Liu, F. T. & Orida, N. (1984). Synthesis of surface immunoglobulin E receptor in Xenopus oocytes by translation of mRNA from rat basophilic leukemia cells. J Biol Chem **259**, 10649-10652.

Liu, L., Sakai, T., Sano, N. & Fukui, K. (2004). Nucling mediates apoptosis by inhibiting expression of galectin-3 through interference with nuclear factor kappaB signalling. Biochem J **380**, 31-41.

Livak, K. J. & Schmittgen, T. D. (2001). Analysis of relative gene expression data using real-time quantitative PCR and the 2(-Delta Delta C(T)) Method. Methods **25**, 402-408.

Lopez, E., del Pozo, V., Miguel, T. & other authors (2006). Inhibition of chronic airway inflammation and remodeling by galectin-3 gene therapy in a murine model. J Immunol **176**, 1943-1950.

Ludewigs, H., Zuber, C., Vana, K., Nikles, D., Zerr, I. & Weiss, S. (2007). Therapeutic approaches for prion disorders. Expert Review of Anti-infective Therapy **5**, 613-630.

Ludwig, G. V., Kondig, J. P. & Smith, J. F. (1996). A putative receptor for Venezuelan equine encephalitis virus from mosquito cells. J Virol **70**, 5592-5599.

Lysenko, E. S., Gould, J., Bals, R., Wilson, J. M. & Weiser, J. N. (2000). Bacterial phosphorylcholine decreases susceptibility to the antimicrobial peptide LL-37/hCAP18 expressed in the upper respiratory tract. Infect Immun **68**, 1664-1671.

Madico, G., Welsch, J. A., Lewis, L. A. & other authors (2006). The meningococcal vaccine candidate GNA1870 binds the complement regulatory protein factor H and enhances serum resistance. J Immunol **177**, 501-510.

Mahdavi, J., Sonden, B., Hurtig, M. & other authors (2002). Helicobacter pylori SabA adhesin in persistent infection and chronic inflammation. Science **297**, 573-578.

Maiden, M. C., Ibarz-Pavon, A. B., Urwin, R. & other authors (2008). Impact of meningococcal serogroup C conjugate vaccines on carriage and herd immunity. J Infect Dis **197**, 737-743.

Mairey, E., Genovesio, A., Donnadieu, E. & other authors (2006). Cerebral microcirculation shear stress levels determine Neisseria meningitidis attachment sites along the blood-brain barrier. J Exp Med **203**, 1939-1950.

Malinoff, H. L. & Wicha, M. S. (1983). Isolation of a cell surface receptor protein for laminin from murine fibrosarcoma cells. J Cell Biol **96**, 1475-1479.

Malorny, B., Morelli, G., Kusecek, B., Kolberg, J. & Achtman, M. (1998). Sequence diversity, predicted two-dimensional protein structure, and epitope mapping of neisserial Opa proteins. J Bacteriol **180**, 1323-1330.

Mandrell, R. E. & Zollinger, W. D. (1977). Lipopolysaccharide serotyping of Neisseria meningitidis by hemagglutination inhibition. Infect Immun **16**, 471-475.

Marceau, M., Forest, K., Beretti, J. L., Tainer, J. & Nassif, X. (1998). Consequences of the loss of O-linked glycosylation of meningococcal type IV pilin on piliation and pilus-mediated adhesion. Mol Microbiol **27**, 705-715.

Markowska, A. I., Jefferies, K. C. & Panjwani, N. (2011). Galectin-3 protein modulates cell surface expression and activation of vascular endothelial growth factor receptor 2 in human endothelial cells. J Biol Chem **286**, 29913-29921.

Martignone, S., Pellegrini, R., Villa, E., Tandon, N. N., Mastroianni, A., Tagliabue, E., Menard, S. & Colnaghi, M. I. (1992). Characterization of two monoclonal antibodies directed against the 67 kDa high affinity laminin receptor and application for the study of breast carcinoma progression. Clin Exp Metastasis **10**, 379-386.

Massari, P., Ho, Y. & Wetzler, L. M. (2000). Neisseria meningitidis porin PorB interacts with mitochondria and protects cells from apoptosis. Proc Natl Acad Sci U S A **97**, 9070-9075.

Massari, P., Henneke, P., Ho, Y., Latz, E., Golenbock, D. T. & Wetzler, L. M. (2002). Cutting edge: Immune stimulation by neisserial porins is toll-like receptor 2 and MyD88 dependent. J Immunol **168**, 1533-1537.

Mattick, J. S. (2002). Type IV pili and twitching motility. Annu Rev Microbiol **56**, 289-314.

Mazurek, N., Conklin, J., Byrd, J. C., Raz, A. & Bresalier, R. S. (2000). Phosphorylation of the beta-galactoside-binding protein galectin-3 modulates binding to its ligands. J Biol Chem **275**, 36311-36315.

Mazurek, N., Byrd, J. C., Sun, Y., Hafley, M., Ramirez, K., Burks, J. & Bresalier, R. S. (2012). Cell-surface galectin-3 confers resistance to TRAIL by impeding trafficking of death receptors in metastatic colon adenocarcinoma cells. Cell Death Differ **19**, 523-533.

Menard, S., Castronovo, V., Tagliabue, E. & Sobel, M. E. (1997). New insights into the metastasis-associated 67 kD laminin receptor. J Cell Biochem **67**, 155-165.

Menon, R. P. & Hughes, R. C. (1999). Determinants in the N-terminal domains of galectin-3 for secretion by a novel pathway circumventing the endoplasmic reticulum-Golgi complex. Eur J Biochem **264**, 569-576.

Mercier, S., St-Pierre, C., Pelletier, I., Ouellet, M., Tremblay, M. J. & Sato, S. (2008). Galectin-1 promotes HIV-1 infectivity in macrophages through stabilization of viral adsorption. Virology **371**, 121-129.

Merz, A. J., Enns, C. A. & So, M. (1999). Type IV pili of pathogenic Neisseriae elicit cortical plaque formation in epithelial cells. Mol Microbiol **32**, 1316-1332.

Merz, A. J. & So, M. (2000). Interactions of pathogenic neisseriae with epithelial cell membranes. Annu Rev Cell Dev Biol **16**, 423-457.

Mey, A., Leffler, H., Hmama, Z., Normier, G. & Revillard, J. P. (1996). The animal lectin galectin-3 interacts with bacterial lipopolysaccharides via two independent sites. J Immunol **156**, 1572-1577.

Mikaty, G., Soyer, M., Mairey, E. & other authors (2009). Extracellular bacterial pathogen induces host cell surface reorganization to resist shear stress. PLoS Pathog **5**, e1000314.

Miller, E., Salisbury, D. & Ramsay, M. (2001). Planning, registration, and implementation of an immunisation campaign against meningococcal serogroup C disease in the UK: a success story. Vaccine **20 Suppl 1**, S58-67.

Minetti, C. A., Tai, J. Y., Blake, M. S., Pullen, J. K., Liang, S. M. & Remeta, D. P. (1997). Structural and functional characterization of a recombinant PorB class 2 protein from Neisseria meningitidis. Conformational stability and porin activity. J Biol Chem **272**, 10710-10720.

Minetti, C. A., Blake, M. S. & Remeta, D. P. (1998). Characterization of the structure, function, and conformational stability of PorB class 3 protein from Neisseria meningitidis. A porin with unusual physicochemical properties. J Biol Chem **273**, 25329-25338.

Miyawaki, A., Llopis, J., Heim, R., McCaffery, J. M., Adams, J. A., Ikura, M. & Tsien, R. Y. (1997). Fluorescent indicators for Ca2+ based on green fluorescent proteins and calmodulin. Nature **388**, 882-887.

Mok, S. W., Riemer, C., Madela, K., Hsu, D. K., Liu, F. T., Gultner, S., Heise, I. & Baier, M. (2007). Role of galectin-3 in prion infections of the CNS. Biochem Biophys Res Commun **359**, 672-678.

Molyneux, E. M., Walsh, A. L., Forsyth, H. & other authors (2002). Dexamethasone treatment in childhood bacterial meningitis in Malawi: a randomised controlled trial. Lancet **360**, 211-218.

Moody, T. N., Ochieng, J. & Villalta, F. (2000). Novel mechanism that Trypanosoma cruzi uses to adhere to the extracellular matrix mediated by human galectin-3. FEBS Lett **470**, 305-308.

Moore, J., Bailey, S. E., Benmechernene, Z., Tzitzilonis, C., Griffiths, N. J., Virji, M. & Derrick, J. P. (2005). Recognition of saccharides by the OpcA, OpaD, and OpaB outer membrane proteins from Neisseria meningitidis. J Biol Chem **280**, 31489-31497.

Morand, P. C., Drab, M., Rajalingam, K., Nassif, X. & Meyer, T. F. (2009). Neisseria meningitidis differentially controls host cell motility through PilC1 and PilC2 components of type IV Pili. PLoS One **4**, e6834.

Morris, S., Ahmad, N., Andre, S., Kaltner, H., Gabius, H. J., Brenowitz, M. & Brewer, F. (2004). Quaternary solution structures of galectins-1, -3, and -7. Glycobiology **14**, 293-300.

Moszynski, P. (2010). New meningitis A vaccine is a "breakthrough" for 430 million people at risk. BMJ **341**, c3552.

Mrkic, B., Pavlovic, J., Rulicke, T., Volpe, P., Buchholz, C. J., Hourcade, D., Atkinson, J. P., Aguzzi, A. & Cattaneo, R. (1998). Measles virus spread and pathogenesis in genetically modified mice. J Virol **72**, 7420-7427.

Mumby, S. M., Kleuss, C. & Gilman, A. G. (1994). Receptor regulation of G-protein palmitoylation. Proc Natl Acad Sci U S A **91**, 2800-2804.

Nadel, S. & Kroll, J. S. (2007). Diagnosis and management of meningococcal disease: the need for centralized care. FEMS Microbiol Rev **31**, 71-83.

Nagai, T., Ibata, K., Park, E. S., Kubota, M., Mikoshiba, K. & Miyawaki, A. (2002). A variant of yellow fluorescent protein with fast and efficient maturation for cell-biological applications. Nat Biotech **20**, 87-90.

Nakahara, S., Hogan, V., Inohara, H. & Raz, A. (2006). Importin-mediated nuclear translocation of galectin-3. J Biol Chem **281**, 39649-39659.

Nangia-Makker, P., Raz, T., Tait, L., Hogan, V., Fridman, R. & Raz, A. (2007). Galectin-3 cleavage: a novel surrogate marker for matrix metalloproteinase activity in growing breast cancers. Cancer Res **67**, 11760-11768.

Nassif, X., Beretti, J. L., Lowy, J., Stenberg, P., O'Gaora, P., Pfeifer, J., Normark, S. & So, M. (1994). Roles of pilin and PilC in adhesion of Neisseria meningitidis to human epithelial and endothelial cells. Proc Natl Acad Sci U S A **91**, 3769-3773.

Nassif, X. (1999). Interactions between encapsulated Neisseria meningitidis and host cells. Int Microbiol **2**, 133-136.

Nassif, X., Pujol, C., Morand, P. & Eugene, E. (1999). Interactions of pathogenic Neisseria with host cells. Is it possible to assemble the puzzle? Mol Microbiol **32**, 1124-1132.

Nassif, X., Bourdoulous, S., Eugene, E. & Couraud, P. O. (2002). How do extracellular pathogens cross the blood-brain barrier? Trends Microbiol **10**, 227-232.

Nelson, J., McFerran, N. V., Pivato, G. r., Chambers, E., Doherty, C., Steele, D. & Timson, D. J. (2008). The 67 kDa laminin receptor: structure, function and role in disease. Biosience Reports **028**, 33-48.

Newlaczyl, A. U. & Yu, L. G. (2011). Galectin-3--a jack-of-all-trades in cancer. Cancer Lett **313**, 123-128.

Nieminen, J., Kuno, A., Hirabayashi, J. & Sato, S. (2007). Visualization of galectin-3 oligomerization on the surface of neutrophils and endothelial cells using fluorescence resonance energy transfer. J Biol Chem **282**, 1374-1383.

Nikles, D., Vana, K., Gauczynski, S., Knetsch, H., Ludewigs, H. & Weiss, S. (2008). Subcellular localization of prion proteins and the 37 kDa/67 kDa laminin receptor fused to fluorescent proteins. Biochim Biophys Acta **1782**, 335-340.

Nikulin, J., Panzner, U., Frosch, M. & Schubert-Unkmeir, A. (2006). Intracellular survival and replication of Neisseria meningitidis in human brain microvascular endothelial cells. Int J Med Microbiol **296**, 553-558.

Nothaft, H. & Szymanski, C. M. (2010). Protein glycosylation in bacteria: sweeter than ever. Nat Rev Microbiol **8**, 765-778.

Ochieng, J., Green, B., Evans, S., James, O. & Warfield, P. (1998). Modulation of the biological functions of galectin-3 by matrix metalloproteinases. Biochim Biophys Acta **1379**, 97-106.

Ochieng, J., Furtak, V. & Lukyanov, P. (2004). Extracellular functions of galectin-3. Glycoconj J **19**, 527-535.

Okumura, C. Y., Baum, L. G. & Johnson, P. J. (2008). Galectin-1 on cervical epithelial cells is a receptor for the sexually transmitted human parasite Trichomonas vaginalis. Cell Microbiol **10**, 2078-2090.

Orihuela, C. J., Mahdavi, J., Thornton, J. & other authors (2009). Laminin receptor initiates bacterial contact with the blood brain barrier in experimental meningitis models. J Clin Invest **119**, 1638-1646.

Osterhues, A., Liebmann, S., Schmid, M., Buk, D., Huss, R., Graeve, L. & Zeindl-Eberhart, E. (2006). Stem cells and experimental leukemia can be distinguished by lipid raft protein composition. Stem Cells Dev **15**, 677-686.

Pace, D. & Pollard, A. J. (2012). Meningococcal disease: Clinical presentation and sequelae. Vaccine **30 Suppl 2**, B3-9.

Paola Quattroni, Y. L., Davide Lucchesi, Sebastian Lucas, Derek W. Hood, Martin Herrmann, Hans-Joachim Gabius, Christoph M. Tang and Rachel M. Exley. (2010). Binding of Neisseria meningitidis to Galectin-3. In 17th international pathogenic Neisseria conference. Banff, Canada.

Park, J. W., Voss, P. G., Grabski, S., Wang, J. L. & Patterson, R. J. (2001). Association of galectin-1 and galectin-3 with Gemin4 in complexes containing the SMN protein. Nucleic Acids Res **29**, 3595-3602.

Parkhill, J., Achtman, M., James, K. D. & other authors (2000). Complete DNA sequence of a serogroup A strain of Neisseria meningitidis Z2491. Nature **404**, 502-506.

Pathan, N., Faust, S. N. & Levin, M. (2003). Pathophysiology of meningococcal meningitis and septicaemia. Arch Dis Child **88**, 601-607.

Paz, I., Sachse, M., Dupont, N. & other authors (2010). Galectin-3, a marker for vacuole lysis by invasive pathogens. Cell Microbiol **12**, 530-544.

Pelicic, V. (2008). Type IV pili: e pluribus unum? Mol Microbiol **68**, 827-837.

Pelletier, I. & Sato, S. (2002). Specific recognition and cleavage of galectin-3 by Leishmania major through species-specific polygalactose epitope. J Biol Chem **277**, 17663-17670.

Pepe, J. C. & Lory, S. (1998). Amino acid substitutions in PilD, a bifunctional enzyme of Pseudomonas aeruginosa. Effect on leader peptidase and N-methyltransferase activities in vitro and in vivo. J Biol Chem **273**, 19120-19129.

Pepinsky, R. B., Zeng, C., Wen, D. & other authors (1998). Identification of a palmitic acid-modified form of human Sonic hedgehog. J Biol Chem **273**, 14037-14045.

Perea-Milla, E., Olalla, J., Sanchez-Cantalejo, E., Martos, F., Matute-Cruz, P., Carmona-Lopez, G., Fornieles, Y., Cayuela, A. & Garcia-Alegria, J. (2009). Pre-hospital antibiotic treatment and mortality caused by invasive meningococcal disease, adjusting for indication bias. BMC Public Health **9**, 95.

Philippe C morand, T. R. (2006). Genetics, structure and function of pili. In Handbook of meningococcal disease, pp. 235-254. Edited by M. C. J. M. Matthias Frosch: Weinheim:Wiley-VCH.

Pizza, M., Scarlato, V., Masignani, V. & other authors (2000). Identification of vaccine candidates against serogroup B meningococcus by whole-genome sequencing. Science **287**, 1816-1820.

Pollard, A. J., Perrett, K. P. & Beverley, P. C. (2009). Maintaining protection against invasive bacteria with protein-polysaccharide conjugate vaccines. Nat Rev Immunol **9**, 213-220.

Poolman, J. T., Hopman, C. T. & Zanen, H. C. (1983). Immunogenicity of meningococcal antigens as detected in patient sera. Infect Immun **40**, 398-406.

Post, D. M., Zhang, D., Eastvold, J. S., Teghanemt, A., Gibson, B. W. & Weiss, J. P. (2005). Biochemical and functional characterization of membrane blebs purified from Neisseria meningitidis serogroup B. J Biol Chem **280**, 38383-38394.

Power, P. M., Roddam, L. F., Dieckelmann, M., Srikhanta, Y. N., Tan, Y. C., Berrington, A. W. & Jennings, M. P. (2000). Genetic characterization of pilin glycosylation in Neisseria meningitidis. Microbiology **146 (Pt 4)**, 967-979.

Power, P. M., Roddam, L. F., Rutter, K., Fitzpatrick, S. Z., Srikhanta, Y. N. & Jennings, M. P. (2003). Genetic characterization of pilin glycosylation and phase variation in Neisseria meningitidis. Mol Microbiol **49**, 833-847.

Power, P. M., Seib, K. L. & Jennings, M. P. (2006). Pilin glycosylation in Neisseria meningitidis occurs by a similar pathway to wzy-dependent O-antigen biosynthesis in Escherichia coli. Biochemical and Biophysical Research Communications **347**, 904-908.

Prasher, D. C., Eckenrode, V. K., Ward, W. W., Prendergast, F. G. & Cormier, M. J. (1992). Primary structure of the Aequorea victoria green-fluorescent protein. Gene **111**, 229-233.

Preston, A., Mandrell, R. E., Gibson, B. W. & Apicella, M. A. (1996). The lipooligosaccharides of pathogenic gram-negative bacteria. Crit Rev Microbiol **22**, 139-180.

Prince, S. M., Feron, C., Janssens, D., Lobet, Y., Achtman, M., Kusecek, B., Bullough, P. A. & Derrick, J. P. (2001). Expression, refolding and crystallization of the OpcA invasin from Neisseria meningitidis. Acta Crystallogr D Biol Crystallogr **57**, 1164-1166.

Pujol, C., Eugene, E., de Saint Martin, L. & Nassif, X. (1997). Interaction of Neisseria meningitidis with a polarized monolayer of epithelial cells. Infect Immun **65**, 4836-4842.

Pujol, C., Eugene, E., Marceau, M. & Nassif, X. (1999). The meningococcal PilT protein is required for induction of intimate attachment to epithelial cells following pilus-mediated adhesion. Proc Natl Acad Sci U S A **96**, 4017-4022.

Quattroni, P., Li, Y., Lucchesi, D., Lucas, S., Hood, D. W., Herrmann, M., Gabius, H. J., Tang, C. M. & Exley, R. M. (2012). Galectin-3 binds Neisseria meningitidis and increases interaction with phagocytic cells. Cell Microbiol.

Rao, C. N., Castronovo, V., Schmitt, M. C., Wewer, U. M., Claysmith, A. P., Liotta, L. A. & Sobel, M. E. (1989). Evidence for a precursor of the high-affinity metastasis-associated murine laminin receptor. Biochemistry **28**, 7476-7486.

Rao, N. C., Barsky, S. H., Terranova, V. P. & Liotta, L. A. (1983). Isolation of a tumor cell laminin receptor. Biochem Biophys Res Commun **111**, 804-808.

Rappuoli, R. & Covacci, A. (2003). Reverse vaccinology and genomics. Science **302**, 602.

Raz, A., Avivi, A., Pazerini, G. & Carmi, P. (1987). Cloning and expression of cDNA for two endogenous UV-2237 fibrosarcoma lectin genes. Exp Cell Res **173**, 109-116.

Reichert, F. & Rotshenker, S. (1999). Galectin-3/MAC-2 in experimental allergic encephalomyelitis. Exp Neurol **160**, 508-514.

Resh, M. D. (1999). Fatty acylation of proteins: new insights into membrane targeting of myristoylated and palmitoylated proteins. Biochim Biophys Acta **1451**, 1-16.

Robertson, B. D., Frosch, M. & van Putten, J. P. (1993). The role of galE in the biosynthesis and function of gonococcal lipopolysaccharide. Mol Microbiol **8**, 891-901.

Robida, A. M. & Kerppola, T. K. (2009). Bimolecular fluorescence complementation analysis of inducible protein interactions: effects of factors affecting protein folding on fluorescent protein fragment association. J Mol Biol **394**, 391-409.

Robinson, K., Taraktsoglou, M., Rowe, K. S., Wooldridge, K. G. & Ala'Aldeen, D. A. (2004). Secreted proteins from Neisseria meningitidis mediate differential human gene expression and immune activation. Cell Microbiol **6**, 927-938.

Roff, C. F. & Wang, J. L. (1983). Endogenous lectins from cultured cells. Isolation and characterization of carbohydrate-binding proteins from 3T3 fibroblasts. J Biol Chem **258**, 10657-10663.

Romanov, V., Sobel, M. E., pinto da Silva, P., Menard, S. & Castronovo, V. (1994). Cell localization and redistribution of the 67 kD laminin receptor and alpha 6 beta 1 integrin subunits in response to laminin stimulation: an immunogold electron microscopy study. Cell Adhes Commun **2**, 201-209.

Romanov, V. I., Wrathall, L. S., Simmons, T. D., Pinto da Silva, P. & Sobel, M. E. (1995). Protein synthesis is required for laminin-induced expression of the 67-kDa laminin receptor and its 37-kDa precursor. Biochem Biophys Res Commun **208**, 637-643.

Rose, R. H., Briddon, S. J. & Holliday, N. D. (2010). Bimolecular fluorescence complementation: lighting up seven transmembrane domain receptor signalling networks. Br J Pharmacol **159**, 738-750.

Rowe, H. A., Griffiths, N. J., Hill, D. J. & Virji, M. (2007). Co-ordinate action of bacterial adhesins and human carcinoembryonic antigen receptors in enhanced cellular invasion by capsulate serum resistant Neisseria meningitidis. Cell Microbiol **9**, 154-168.

Rubin, L. L. & Staddon, J. M. (1999). The cell biology of the blood-brain barrier. Annu Rev Neurosci **22**, 11-28.

Rudel, T., Scheurerpflug, I. & Meyer, T. F. (1995). Neisseria PilC protein identified as type-4 pilus tip-located adhesin. Nature **373**, 357-359.

Ryll, R. R., Rudel, T., Scheuerpflug, I., Barten, R. & Meyer, T. F. (1997). PilC of Neisseria meningitidis is involved in class II pilus formation and restores pilus assembly, natural transformation competence and adherence to epithelial cells in PilC-deficient gonococci. Mol Microbiol **23**, 879-892.

Saint-Lu, N., Oortwijn, B. D., Pegon, J. N., Odouard, S., Christophe, O. D., de Groot, P. G., Denis, C. V. & Lenting, P. J. (2012). Identification of galectin-1 and galectin-3 as novel partners for von Willebrand factor. Arterioscler Thromb Vasc Biol **32**, 894-901.

Sakoonwatanyoo, P., Boonsanay, V. & Smith, D. R. (2006). Growth and production of the dengue virus in C6/36 cells and identification of a laminin-binding protein as a candidate serotype 3 and 4 receptor protein. Intervirology **49**, 161-172.

Sandbu, S., Feiring, B., Oster, P. & other authors (2007). Immunogenicity and safety of a combination of two serogroup B meningococcal outer membrane vesicle vaccines. Clin Vaccine Immunol **14**, 1062-1069.

Sano, H., Hsu, D. K., Yu, L., Apgar, J. R., Kuwabara, I., Yamanaka, T., Hirashima, M. & Liu, F. T. (2000). Human galectin-3 is a novel chemoattractant for monocytes and macrophages. J Immunol **165**, 2156-2164.

Sarkari, J., Pandit, N., Moxon, E. R. & Achtman, M. (1994). Variable expression of the Opc outer membrane protein in Neisseria meningitidis is caused by size variation of a promoter containing poly-cytidine. Mol Microbiol **13**, 207-217.

Sato, S. & Hughes, R. C. (1992). Binding specificity of a baby hamster kidney lectin for H type I and II chains, polylactosamine glycans, and appropriately glycosylated forms of laminin and fibronectin. J Biol Chem **267**, 6983-6990.

Sato, S. & Hughes, R. C. (1994). Regulation of secretion and surface expression of Mac-2, a galactoside-binding protein of macrophages. J Biol Chem **269**, 4424-4430.

Sato, S., Ouellet, N., Pelletier, I., Simard, M., Rancourt, A. & Bergeron, M. G. (2002). Role of galectin-3 as an adhesion molecule for neutrophil extravasation during streptococcal pneumonia. J Immunol **168**, 1813-1822.

Sato, S. & Nieminen, J. (2004). Seeing strangers or announcing "danger": galectin-3 in two models of innate immunity. Glycoconj J **19**, 583-591.

Sato, S., St-Pierre, C., Bhaumik, P. & Nieminen, J. (2009). Galectins in innate immunity: dual functions of host soluble beta-galactoside-binding lectins as damage-associated molecular patterns (DAMPs) and as receptors for pathogen-associated molecular patterns (PAMPs). Immunol Rev **230**, 172-187.

Saukkonen, K., Leinonen, M., Abdillahi, H. & Poolman, J. T. (1989). Comparative evaluation of potential components for group B meningococcal vaccine by passive protection in the infant rat and in vitro bactericidal assay. Vaccine **7**, 325-328.

Scarborough, M., Gordon, S. B., Whitty, C. J., French, N., Njalale, Y., Chitani, A., Peto, T. E., Lalloo, D. G. & Zijlstra, E. E. (2007). Corticosteroids for bacterial meningitis in adults in sub-Saharan Africa. N Engl J Med **357**, 2441-2450.

Scarselli, M., Serruto, D., Montanari, P., Capecchi, B., Adu-Bobie, J., Veggi, D., Rappuoli, R., Pizza, M. & Arico, B. (2006). Neisseria meningitidis NhhA is a multifunctional trimeric autotransporter adhesin. Mol Microbiol **61**, 631-644.

Schaechter, M. (2009). Desk Encyclopedia of Microbiology. In Pili, Fimbriae.

Scheuerpflug, I., Rudel, T., Ryll, R., Pandit, J. & Meyer, T. F. (1999). Roles of PilC and PilE proteins in pilus-mediated adherence of Neisseria gonorrhoeae and Neisseria meningitidis to human erythrocytes and endothelial and epithelial cells. Infect Immun **67**, 834-843.

Schoen, C., Joseph, B., Claus, H., Vogel, U. & Frosch, M. (2007). Living in a changing environment: insights into host adaptation in Neisseria meningitidis from comparative genomics. Int J Med Microbiol **297**, 601-613.

Scholten, R. J., Kuipers, B., Valkenburg, H. A., Dankert, J., Zollinger, W. D. & Poolman, J. T. (1994). Lipo-oligosaccharide immunotyping of Neisseria meningitidis by a whole-cell ELISA with monoclonal antibodies. J Med Microbiol **41**, 236-243.

Schroder, H. C., Ushijima, H., Theis, C., Seve, A. P., Hubert, J. & Muller, W. E. (1995). Expression of nuclear lectin carbohydrate-binding protein 35 in human immunodeficiency virus type 1-infected Molt-3 cells. J Acquir Immune Defic Syndr Hum Retrovirol **9**, 340-348.

Seetharaman, J., Kanigsberg, A., Slaaby, R., Leffler, H., Barondes, S. H. & Rini, J. M. (1998). X-ray crystal structure of the human galectin-3 carbohydrate recognition domain at 2.1-A resolution. J Biol Chem **273**, 13047-13052.

Segal, E., Hagblom, P., Seifert, H. S. & So, M. (1986). Antigenic variation of gonococcal pilus involves assembly of separated silent gene segments. Proc Natl Acad Sci U S A **83**, 2177-2181.

Serino, L. & Virji, M. (2002). Genetic and functional analysis of the phosphorylcholine moiety of commensal Neisseria lipopolysaccharide. Mol Microbiol **43**, 437-448.

Serruto, D., Adu-Bobie, J., Scarselli, M., Veggi, D., Pizza, M., Rappuoli, R. & Arico, B. (2003). Neisseria meningitidis App, a new adhesin with autocatalytic serine protease activity. Mol Microbiol **48**, 323-334.

Shalom-Feuerstein, R., Plowman, S. J., Rotblat, B., Ariotti, N., Tian, T., Hancock, J. F. & Kloog, Y. (2008). K-ras nanoclustering is subverted by overexpression of the scaffold protein galectin-3. Cancer Res **68**, 6608-6616.

Shaner, N. C., Campbell, R. E., Steinbach, P. A., Giepmans, B. N., Palmer, A. E. & Tsien, R. Y. (2004). Improved monomeric red, orange and yellow fluorescent proteins derived from Discosoma sp. red fluorescent protein. Nat Biotechnol **22**, 1567-1572.

Shimura, T., Takenaka, Y., Tsutsumi, S., Hogan, V., Kikuchi, A. & Raz, A. (2004). Galectin-3, a novel binding partner of beta-catenin. Cancer Res **64**, 6363-6367.

Shimura, T., Takenaka, Y., Fukumori, T., Tsutsumi, S., Okada, K., Hogan, V., Kikuchi, A., Kuwano, H. & Raz, A. (2005). Implication of galectin-3 in Wnt signaling. Cancer Res **65**, 3535-3537.

Shyu, Y. J., Liu, H., Deng, X. & Hu, C. D. (2006). Identification of new fluorescent protein fragments for bimolecular fluorescence complementation analysis under physiological conditions. Biotechniques **40**, 61-66.

Siddique, A., Buisine, N. & Chalmers, R. (2011). The transposon-like Correia elements encode numerous strong promoters and provide a potential new mechanism for phase variation in the meningococcus. PLoS Genet **7**, e1001277.

Simona Butò, E. T. E. A. A. M. C. G. F. v. d. B. V. C. M. I. C. M. E. S. S. M. (1998). Formation of the 67-kDa laminin receptor by acylation of the precursor. Journal of Cellular Biochemistry **69**, 244-251.

Smedley, J. G., 3rd, Jewell, E., Roguskie, J., Horzempa, J., Syboldt, A., Stolz, D. B. & Castric, P. (2005). Influence of pilin glycosylation on Pseudomonas aeruginosa 1244 pilus function. Infect Immun **73**, 7922-7931.

Somand, D. & Meurer, W. (2009). Central nervous system infections. Emerg Med Clin North Am **27**, 89-100, ix.

Sparrow, C. P., Leffler, H. & Barondes, S. H. (1987). Multiple soluble beta-galactoside-binding lectins from human lung. J Biol Chem **262**, 7383-7390.

St-Pierre, C., Manya, H., Ouellet, M., Clark, G. F., Endo, T., Tremblay, M. J. & Sato, S. (2011). Host-soluble galectin-1 promotes HIV-1 replication through a direct interaction with glycans of viral gp120 and host CD4. J Virol **85**, 11742-11751.

St. Jude Children's Research Hospital, a. (2008). Synthetic Streptococcus pnuemonia vaccine patent

Stein, K. E. (1992). Thymus-independent and thymus-dependent responses to polysaccharide antigens. J Infect Dis **165 Suppl 1**, S49-52.

Stephens, D. S. & Farley, M. M. (1991). Pathogenic events during infection of the human nasopharynx with Neisseria meningitidis and Haemophilus influenzae. Rev Infect Dis **13**, 22-33.

Stephens, D. S., Greenwood, B. & Brandtzaeg, P. (2007). Epidemic meningitis, meningococcaemia, and Neisseria meningitidis. Lancet **369**, 2196-2210.

Stephens, D. S. (2009). Biology and pathogenesis of the evolutionarily successful, obligate human bacterium Neisseria meningitidis. Vaccine **27 Suppl 2**, B71-77.

Stimson, E., Virji, M., Makepeace, K. & other authors (1995). Meningococcal pilin: a glycoprotein substituted with digalactosyl 2,4-diacetamido-2,4,6-trideoxyhexose. Mol Microbiol **17**, 1201-1214.

Stowell, S. R., Arthur, C. M., Dias-Baruffi, M. & other authors (2010). Innate immune lectins kill bacteria expressing blood group antigen. Nat Med **16**, 295-301.

Strom, M. S. & Lory, S. (1993). Structure-function and biogenesis of the type IV pili. Annu Rev Microbiol **47**, 565-596.

Svanborg Eden, C., Gotschlich, E. C., Korhonen, T. K., Leffler, H. & Schoolnik, G. (1983). Aspects on structure and function of pili on uropathogenic Escherichia coli. Prog Allergy **33**, 189-202.

Sylvie, M., Vincent, C., Elda, T. & Mark, E. S. (1997). New insights into the metastasis-associated 67 kD laminin receptor. Journal of Cellular Biochemistry **67**, 155-165.

Tan, L. K., Carlone, G. M. & Borrow, R. (2010). Advances in the development of vaccines against Neisseria meningitidis. N Engl J Med **362**, 1511-1520.

Tappero, J. W., Lagos, R., Ballesteros, A. M. & other authors (1999). Immunogenicity of 2 serogroup B outer-membrane protein meningococcal vaccines: a randomized controlled trial in Chile. JAMA **281**, 1520-1527.

Terranova, V. P., Rao, C. N., Kalebic, T., Margulies, I. M. & Liotta, L. A. (1983). Laminin receptor on human breast carcinoma cells. Proc Natl Acad Sci U S A **80**, 444-448.

Tettelin, H., Saunders, N. J., Heidelberg, J. & other authors (2000). Complete genome sequence of Neisseria meningitidis serogroup B strain MC58. Science **287**, 1809-1815.

Thepparit, C. & Smith, D. R. (2004). Serotype-Specific Entry of Dengue Virus into Liver Cells: Identification of the 37-Kilodalton/67-Kilodalton High-Affinity Laminin Receptor as a Dengue Virus Serotype 1 Receptor. J Virol **78**, 12647-12656.

Thijssen, V. L., Hulsmans, S. & Griffioen, A. W. (2008). The galectin profile of the endothelium: altered expression and localization in activated and tumor endothelial cells. Am J Pathol **172**, 545-553.

Thompson, M. J., Ninis, N., Perera, R., Mayon-White, R., Phillips, C., Bailey, L., Harnden, A., Mant, D. & Levin, M. (2006). Clinical recognition of meningococcal disease in children and adolescents. Lancet **367**, 397-403.

Tonjum, T., Caugant, D. A., Dunham, S. A. & Koomey, M. (1998). Structure and function of repetitive sequence elements associated with a highly

polymorphic domain of the Neisseria meningitidis PilQ protein. Mol Microbiol **29**, 111-124.

Towler, D. A., Gordon, J. I., Adams, S. P. & Glaser, L. (1988). The biology and enzymology of eukaryotic protein acylation. Annu Rev Biochem **57**, 69-99.

Trivedi, K., Tang, C. M. & Exley, R. M. (2011). Mechanisms of meningococcal colonisation. Trends Microbiol **19**, 456-463.

Tsang, R. S., Law, D. K., Tyler, S. D., Stephens, G. S., Bigham, M. & Zollinger, W. D. (2005). Potential capsule switching from serogroup Y to B: The characterization of three such Neisseria meningitidis isolates causing invasive meningococcal disease in Canada. Can J Infect Dis Med Microbiol **16**, 171-174.

Tunkel, A. R., Hartman, B. J., Kaplan, S. L., Kaufman, B. A., Roos, K. L., Scheld, W. M. & Whitley, R. J. (2004). Practice guidelines for the management of bacterial meningitis. Clin Infect Dis **39**, 1267-1284.

Turner, D. P., Marietou, A. G., Johnston, L., Ho, K. K., Rogers, A. J., Wooldridge, K. G. & Ala'Aldeen, D. A. (2006). Characterization of MspA, an immunogenic autotransporter protein that mediates adhesion to epithelial and endothelial cells in Neisseria meningitidis. Infect Immun **74**, 2957-2964.

Umemoto, K., Leffler, H., Venot, A., Valafar, H. & Prestegard, J. H. (2003). Conformational differences in liganded and unliganded states of Galectin-3. Biochemistry **42**, 3688-3695.

University of Nottingham, a. (2009). Laminin receptor binding proteins patent: University of Nottingham.

Unkmeir, A., Latsch, K., Dietrich, G., Wintermeyer, E., Schinke, B., Schwender, S., Kim, K. S., Eigenthaler, M. & Frosch, M. (2002). Fibronectin mediates Opc-dependent internalization of Neisseria meningitidis in human brain microvascular endothelial cells. Mol Microbiol **46**, 933-946.

van de Beek, D., de Gans, J., McIntyre, P. & Prasad, K. (2007). Corticosteroids for acute bacterial meningitis. Cochrane Database Syst Rev, CD004405.

van den Berg, T. K., Honing, H., Franke, N. & other authors (2004). LacdiNAc-glycans constitute a parasite pattern for galectin-3-mediated immune recognition. J Immunol **173**, 1902-1907.

van den Elsen, J., Vandeputte-Rutten, L., Kroon, J. & Gros, P. (1999). Bactericidal antibody recognition of meningococcal PorA by induced fit. Comparison of liganded and unliganded Fab structures. J Biol Chem **274**, 1495-1501.

van der Ley, P., Heckels, J. E., Virji, M., Hoogerhout, P. & Poolman, J. T. (1991). Topology of outer membrane porins in pathogenic Neisseria spp. Infect Immun **59**, 2963-2971.

van Kooyk, Y. & Rabinovich, G. A. (2008). Protein-glycan interactions in the control of innate and adaptive immune responses. Nat Immunol **9**, 593-601.

van Sorge, N. M., Bleumink, N. M., van Vliet, S. J., Saeland, E., van der Pol, W. L., van Kooyk, Y. & van Putten, J. P. (2009). N-glycosylated proteins and distinct lipooligosaccharide glycoforms of Campylobacter jejuni target the human C-type lectin receptor MGL. Cell Microbiol **11**, 1768-1781.

Vasta, G. R. (2009). Roles of galectins in infection. Nat Rev Microbiol **7**, 424-438.

Vermont, C. L., van Dijken, H. H., Kuipers, A. J., van Limpt, C. J., Keijzers, W. C., van der Ende, A., de Groot, R., van Alphen, L. & van den Dobbelsteen, G. P. (2003). Cross-reactivity of antibodies against PorA after vaccination with a meningococcal B outer membrane vesicle vaccine. Infect Immun **71**, 1650-1655.

Virji, M., Heckels, J. E., Potts, W. J., Hart, C. A. & Saunders, J. R. (1989). Identification of epitopes recognized by monoclonal antibodies SM1 and SM2 which react with all pili of Neisseria gonorrhoeae but which differentiate between two structural classes of pili expressed by Neisseria meningitidis and the distribution of their encoding sequences in the genomes of Neisseria spp. J Gen Microbiol **135**, 3239-3251.

Virji, M., Kayhty, H., Ferguson, D. J., Alexandrescu, C., Heckels, J. E. & Moxon, E. R. (1991). The role of pili in the interactions of pathogenic Neisseria with cultured human endothelial cells. Mol Microbiol **5**, 1831-1841.

Virji, M., Makepeace, K., Ferguson, D. J., Achtman, M., Sarkari, J. & Moxon, E. R. (1992). Expression of the Opc protein correlates with invasion of epithelial and endothelial cells by Neisseria meningitidis. Mol Microbiol **6**, 2785-2795.

Virji, M., Makepeace, K., Ferguson, D. J., Achtman, M. & Moxon, E. R. (1993a). Meningococcal Opa and Opc proteins: their role in colonization and invasion of human epithelial and endothelial cells. Mol Microbiol **10**, 499-510.

Virji, M., Saunders, J. R., Sims, G., Makepeace, K., Maskell, D. & Ferguson, D. J. (1993b). Pilus-facilitated adherence of Neisseria meningitidis to human epithelial and endothelial cells: modulation of adherence phenotype occurs concurrently with changes in primary amino acid sequence and the glycosylation status of pilin. Mol Microbiol **10**, 1013-1028.

Virji, M., Makepeace, K. & Moxon, E. R. (1994). Distinct mechanisms of interactions of Opc-expressing meningococci at apical and basolateral surfaces of

human endothelial cells; the role of integrins in apical interactions. Mol Microbiol **14**, 173-184.

Virji, M., Makepeace, K., Peak, I. R., Ferguson, D. J., Jennings, M. P. & Moxon, E. R. (1995). Opc- and pilus-dependent interactions of meningococci with human endothelial cells: molecular mechanisms and modulation by surface polysaccharides. Mol Microbiol **18**, 741-754.

Virji, M., Makepeace, K., Ferguson, D. J. & Watt, S. M. (1996). Carcinoembryonic antigens (CD66) on epithelial cells and neutrophils are receptors for Opa proteins of pathogenic neisseriae. Mol Microbiol **22**, 941-950.

Virji, M. (1997). Post-translational modifications of meningococcal pili. Identification of common substituents: glycans and alpha-glycerophosphate--a review. Gene **192**, 141-147.

Virji, M., Evans, D., Hadfield, A., Grunert, F., Teixeira, A. M. & Watt, S. M. (1999). Critical determinants of host receptor targeting by Neisseria meningitidis and Neisseria gonorrhoeae: identification of Opa adhesiotopes on the N-domain of CD66 molecules. Mol Microbiol **34**, 538-551.

Virji, M. (2009). Pathogenic neisseriae: surface modulation, pathogenesis and infection control. Nat Rev Microbiol **7**, 274-286.

Virji, M. a. G., N. J. (2008). Binding of Opc to vitronectin contributes to increased serum resistance of Neisseria meningitidis isolates. In Sixteenth International
Pathogenic Neisseria Conference pp. P096. Rotterdam, The Netherlands.

Vogel, U., Claus, H., Heinze, G. & Frosch, M. (1997). Functional characterization of an isogenic meningococcal alpha-2,3-sialyltransferase mutant: the role of lipooligosaccharide sialylation for serum resistance in serogroup B meningococci. Med Microbiol Immunol **186**, 159-166.

Vray, B., Camby, I., Vercruysse, V. & other authors (2004). Up-regulation of galectin-3 and its ligands by Trypanosoma cruzi infection with modulation of adhesion and migration of murine dendritic cells. Glycobiology **14**, 647-657.

Wang, K. S., Kuhn, R. J., Strauss, E. G., Ou, S. & Strauss, J. H. (1992). High-affinity laminin receptor is a receptor for Sindbis virus in mammalian cells. J Virol **66**, 4992-5001.

Weiser, J. N., Shchepetov, M. & Chong, S. T. (1997). Decoration of lipopolysaccharide with phosphorylcholine: a phase-variable characteristic of Haemophilus influenzae. Infect Immun **65**, 943-950.

Weiser, J. N., Goldberg, J. B., Pan, N., Wilson, L. & Virji, M. (1998). The phosphorylcholine epitope undergoes phase variation on a 43-kilodalton protein in Pseudomonas aeruginosa and on pili of Neisseria meningitidis and Neisseria gonorrhoeae. Infect Immun **66**, 4263-4267.

Wewer, U. M., Liotta, L. A., Jaye, M. & other authors (1986). Altered levels of laminin receptor mRNA in various human carcinoma cells that have different abilities to bind laminin. Proc Natl Acad Sci U S A **83**, 7137-7141.

Weynants, V. E., Feron, C. M., Goraj, K. K. & other authors (2007). Additive and synergistic bactericidal activity of antibodies directed against minor outer membrane proteins of Neisseria meningitidis. Infect Immun **75**, 5434-5442.

WHO (2001). Epidemics of meningococcal disease. African meningitis belt, 2001. In Wkly Epidemiol Rec, pp. 282-288.

WHO (2004). World health report:changing history: WHO, Geneva.

Winther-Larsen, H. C., Hegge, F. T., Wolfgang, M., Hayes, S. F., van Putten, J. P. & Koomey, M. (2001). Neisseria gonorrhoeae PilV, a type IV pilus-associated protein essential to human epithelial cell adherence. Proc Natl Acad Sci U S A **98**, 15276-15281.

Wolfgang, M., Lauer, P., Park, H. S., Brossay, L., Hebert, J. & Koomey, M. (1998). PilT mutations lead to simultaneous defects in competence for natural transformation and twitching motility in piliated Neisseria gonorrhoeae. Mol Microbiol **29**, 321-330.

Wolfgang, M., van Putten, J. P., Hayes, S. F. & Koomey, M. (1999). The comP locus of Neisseria gonorrhoeae encodes a type IV prepilin that is dispensable for pilus biogenesis but essential for natural transformation. Mol Microbiol **31**, 1345-1357.

Woo, H. J., Shaw, L. M., Messier, J. M. & Mercurio, A. M. (1990). The major non-integrin laminin binding protein of macrophages is identical to carbohydrate binding protein 35 (Mac-2). J Biol Chem **265**, 7097-7099.

Woo, H. J., Lotz, M. M., Jung, J. U. & Mercurio, A. M. (1991). Carbohydrate-binding protein 35 (Mac-2), a laminin-binding lectin, forms functional dimers using cysteine 186. J Biol Chem **266**, 18419-18422.

Wright, V., Hibberd, M. & Levin, M. (2009). Genetic polymorphisms in host response to meningococcal infection: the role of susceptibility and severity genes. Vaccine **27 Suppl 2**, B90-102.

Yamazaki, K., Kawai, A., Kawaguchi, M., Hibino, Y., Li, F., Sasahara, M., Tsukada, K. & Hiraga, K. (2001). Simultaneous induction of galectin-3 phosphorylated on tyrosine residue, p21(WAF1/Cip1/Sdi1), and the proliferating cell nuclear antigen at a distinctive period of repair of hepatocytes injured by CCl4. Biochem Biophys Res Commun **280**, 1077-1084.

Yang, R. Y., Hsu, D. K. & Liu, F. T. (1996). Expression of galectin-3 modulates T-cell growth and apoptosis. Proc Natl Acad Sci U S A **93**, 6737-6742.

Yang, R. Y., Hill, P. N., Hsu, D. K. & Liu, F. T. (1998). Role of the carboxyl-terminal lectin domain in self-association of galectin-3. Biochemistry **37**, 4086-4092.

Yoshii, T., Fukumori, T., Honjo, Y., Inohara, H., Kim, H. R. & Raz, A. (2002). Galectin-3 phosphorylation is required for its anti-apoptotic function and cell cycle arrest. J Biol Chem **277**, 6852-6857.

Zaccone, P., Burton, O., Miller, N., Jones, F. M., Dunne, D. W. & Cooke, A. (2009). Schistosoma mansoni egg antigens induce Treg that participate in diabetes prevention in NOD mice. Eur J Immunol **39**, 1098-1107.

Zhu, L., Pearce, D. & Kim, K. S. (2010). Prevention of Escherichia coli K1 penetration of the blood-brain barrier by counteracting the host cell receptor and signaling molecule involved in E. coli invasion of human brain microvascular endothelial cells. Infect Immun **78**, 3554-3559.

Zhu, P., Morelli, G. & Achtman, M. (1999). The opcA and (psi)opcB regions in Neisseria: genes, pseudogenes, deletions, insertion elements and DNA islands. Mol Microbiol **33**, 635-650.

Zuber, C., Knackmuss, S., Zemora, G. & other authors (2008). Invasion of tumorigenic HT1080 cells is impeded by blocking or downregulating the 37-kDa/67-kDa laminin receptor. J Mol Biol **378**, 530-539.

Zuberi, R. I., Hsu, D. K., Kalayci, O. & other authors (2004). Critical role for galectin-3 in airway inflammation and bronchial hyperresponsiveness in a murine model of asthma. Am J Pathol **165**, 2045-2053.

Appendix B. Formula of commonly used buffers and solutions

Sodium dodecyl sulfate (SDS)-resolving buffer; (18.18 g Tris base, 2 ml 20% SDS, 100 µl 10% NaN3) add deionised water (dH2O) up to 100 ml, pH at 8.8.

SDS-stacking buffer; (6.06 g Tris base, 2 ml 20% SDS, 100 µl 10% NaN3) add dH$_2$O up to 100 ml, pH at 6.8.

SDS running buffer (10 x); (30.3 g Tris base, 144 g Glycine, 1 ml 10% NaN3, 10 g SDS (1%), made up to 1000 ml with dH2O, mix well.

SDS-sample buffer (5 x); 0.62 M Tris-Cl (pH 6.8), 5% SDS, 25% glycerol, 12.5% meracaptoethanol, 0.002% Bromophenol blue, or 7.8125 ml (2 M) Tris-Cl, 1.25 g SDS, 6.25 ml glycerol, 3.125 ml β-meracaptoethanol, tip of pipette Bromophenol blue, made up to 25 ml with dH$_2$O.

SDS-sample buffer (1 x); 2.72 g Tris, 25 ml of 20% SDS, 50% glycerol, 12.5% meracaptoethanol, 0.002% Bromophenol blue and add dH$_2$O up to 100 ml, pH at 6.8.

SDS-sample buffer (2 x); 100mM Tris HCL PH 6.8, 2% SDS, 10% glycerol, 10% DTT, 0.10% Bromophenol blue and add dH$_2$O up to 10 ml, pH at 6.8.

Resolving (separating) gel; 2.5 ml SDS-resolving buffer, 2.52 ml Acrylamide/Bis-Acrylamide (30%), 5 ml dH2O, 20 µl Saturated Ammonium persulfate (APS) and 10 µl Tetramethyl ethylenediamine (TEMED).

Stacking gel; 1.25 ml SDS-stacking buffer, 0.75 ml Acrylamide/Bis-Acrylamide (30%), 3 ml dH$_2$O, 8 µl APS and 10 µl TEMED.

Semi-dry blotting buffer; 5.82 g Tris base, 2.93 g Glycine, 3.75ml 10% SDS, 200 ml methanol and make up to 1000 ml with dH2O.

Phosphate buffered saline solution (PBS); prepared by dissolving 1 tablet of Phosphate buffered saline (Dulbaco A, Oxoid) in 100 ml dH$_2$O and autoclave, this gives sodium chloride 0.16 mol, potassium chloride 0.003 mol, disodium hydrogen phosphate 0.008 mol and potassium dihydrogen phosphate 0.001 mol with a pH value of 7.3.

BSA; (Albumin from bovine serum, Sigma A3912) as lyophilized powder (M W ca. 66 kDa) was prepared in sterile PBS according to the concentration needed.

Buffers for protein purification; 28.2 g Urea, 0.83 g NaH2PO4, 0.07 g Tris base, 60 ml dH$_2$O, mix, adjusts the pH, buffer B at pH 8.0, buffer C at pH 6.3 and buffer E at pH 4.3.

LB (Luria-Bertani) broth; Tryptone 10 g, Yeast extract 5 g and Sodium chloride 10 g for 1000 ml dH$_2$O.

LB (Luria-Bertani) agar; Tryptone 10 g, Yeast extract 5 g, Sodium chloride 10g, Microbial tested agar 15 g for 1000 ml of dH$_2$O, pH 7.0 ± 0.2 at 25°C.

IPTG (Isopropyl-β-D thiogalactopyranoside); (FW 238.8) for 1 M solution, 0.23 g of IPTG dissolve in 1 ml dH$_2$O, sterilize by filtration and store at -20˚C.

LB agar with Amp/IPTG/X-gal; LB agar at 50˚C, 100 μg ml-1 Ampicillin, 40 μg ml-1 IPTG and 50 μg ml-1 X-gal, mix and pour (0.5 mM IPTG and 20 μg ml-1 X-gal).

DNA loading dye (6x); 10 mM Tris-HCl (pH 7.6), 0.03% bromophenol blue, 0.03% xylene cyanol FF, 60% glycerol, 60 mM ethylenediamine tetraacetic acid (EDTA).

TAE buffer (Tris-Acetate-EDTA buffer, 1x); 40 mM Tris base, 40 mM Acetic acid and 1 mM EDTA.

TBS-T (Tris Buffered Saline-Tween, 1 x); 10mM Tris/HCl, pH 7.4, 75mM NaCl, 0.05% Tween-20 (v/v)

Transformation Solution (TS); LB broth with 10% (wt/vol) PEG 8000 + 5% (vol/vol)

DMSO

+ 50 mM (MgCl$_2$) at a final pH of 6.5.

TAE buffer (50 × stock); 242 g Tris base (life technologies), 57.1 ml glacial

acetic acid (Fisher chemicals) 100 ml 500 mM EDTA (pH 8.0) made up to 1 L

with dH$_2$O.

Agarose gel; 1.0 % agarose was prepared by dissolving 1 g of agarose powder

(sigma), 2ml 50 × TAE buffer and made up to 100 ml with dH$_2$O; melt and add 5

µl ethidium bromide (10 mg/ml).

Antibiotics; Antibiotics were purchased from Sigma-Aldrich UK, prepared

according to the manufacturer's recommendations, sterilized by filtration and

store at 4°C.

Ampicillin (100 mg ml^{-1} stock solution prepared in dH$_2$O)

Kanamycin (50 mg ml^{-1} stock solution prepared in dH$_2$O)

Streptomycin (50 mg ml^{-1} stock solution prepared in dH$_2$O)

Erythromycin (100 mg ml^{-1} stock solution prepared in ethanol)